NASA/CR—2003-212205

Smart Structural Components and Simulation Tools for Increased Engine Efficiency, Flight Range, and Safety

Alan Palazzolo, Guangyoung Sun, Randall Tucker, Nikhil Kaushik, Jason Preuss, Andrew Kenny, Lakshmi Subramaniyam, and Andrew Hunt
Texas A&M University College Station, Texas

April 2003

The NASA STI Program Office . . . in Profile

Since its founding, NASA has been dedicated to the advancement of aeronautics and space science. The NASA Scientific and Technical Information (STI) Program Office plays a key part in helping NASA maintain this important role.

The NASA STI Program Office is operated by Langley Research Center, the Lead Center for NASA's scientific and technical information. The NASA STI Program Office provides access to the NASA STI Database, the largest collection of aeronautical and space science STI in the world. The Program Office is also NASA's institutional mechanism for disseminating the results of its research and development activities. These results are published by NASA in the NASA STI Report Series, which includes the following report types:

- TECHNICAL PUBLICATION. Reports of completed research or a major significant phase of research that present the results of NASA programs and include extensive data or theoretical analysis. Includes compilations of significant scientific and technical data and information deemed to be of continuing reference value. NASA's counterpart of peer-reviewed formal professional papers but has less stringent limitations on manuscript length and extent of graphic presentations.

- TECHNICAL MEMORANDUM. Scientific and technical findings that are preliminary or of specialized interest, e.g., quick release reports, working papers, and bibliographies that contain minimal annotation. Does not contain extensive analysis.

- CONTRACTOR REPORT. Scientific and technical findings by NASA-sponsored contractors and grantees.

- CONFERENCE PUBLICATION. Collected papers from scientific and technical conferences, symposia, seminars, or other meetings sponsored or cosponsored by NASA.

- SPECIAL PUBLICATION. Scientific, technical, or historical information from NASA programs, projects, and missions, often concerned with subjects having substantial public interest.

- TECHNICAL TRANSLATION. English-language translations of foreign scientific and technical material pertinent to NASA's mission.

Specialized services that complement the STI Program Office's diverse offerings include creating custom thesauri, building customized databases, organizing and publishing research results . . . even providing videos.

For more information about the NASA STI Program Office, see the following:

- Access the NASA STI Program Home Page at ***http://www.sti.nasa.gov***

- E-mail your question via the Internet to help@sti.nasa.gov

- Fax your question to the NASA Access Help Desk at 301–621–0134

- Telephone the NASA Access Help Desk at 301–621–0390

- Write to:
  NASA Access Help Desk
  NASA Center for AeroSpace Information
  7121 Standard Drive
  Hanover, MD 21076

NASA/CR—2003-212205

Smart Structural Components and Simulation Tools for Increased Engine Efficiency, Flight Range, and Safety

Alan Palazzolo, Guangyoung Sun, Randall Tucker, Nikhil Kaushik, Jason Preuss, Andrew Kenny, Lakshmi Subramaniyam, and Andrew Hunt
Texas A&M University College Station, Texas

Prepared under Cooperative Agreement NCC3–928

National Aeronautics and
Space Administration

Glenn Research Center

April 2003

Contents were reproduced from author-provided presentation materials.

The Propulsion and Power Program at
NASA Glenn Research Center sponsored this work.

Available from

NASA Center for Aerospace Information
7121 Standard Drive
Hanover, MD 21076

National Technical Information Service
5285 Port Royal Road
Springfield, VA 22100

Available electronically at http://gltrs.grc.nasa.gov

Contents

Executive Summary

Task A: High Temperature Magnetic Bearings

A.1
(a) Design of a hyperbolic profile, thrust magnetic bearing for 1,000 lb. force, 30,000 rpm and 1,000 °F service completed.
(b) 2 mil radial press fit required to maintain contact on runner ID at 30,000 rpm and 1,000 °F. This produces Von Mises stress of 56,000 psi (110 percent of Hiperco 1,000 °F yield stress).
(c) Zero press fit produces 40,000 psi peak stress (80 percent of yield).
(d) We recommend light press (line to line) with axial preload and locknut for disc attachment.

A.2
(a) Test rig retrofit concept complete and ready for fab drawing. Concept includes user friendly design for measuring axial actuator force at any speed and temperature.
(b) Fab drawing will be make upon concept approval by NASA.

A.3
(a) Seven high temperature (HT) C cores for a radial MB have been shipped to GRC.
(b) Present C core development focused on terminal post and thermocouple installation as part of C core.

A.4
(a) Dr. Andrew Kenny performed 3D FE magnetic field analysis of HT thrust MB. This is included (A.1).

A.5
(a) HT displacement sensor drive circuit under development. High degree of linearity has been achieved using Bently probe and TAMU circuit.
(b) 3D FE magnetic field modelling employed to aid in design of HT probe.

Task B: Blade Loss Mitigation

B.1
Code developed for predicting stiffness and power loss/drag torque for isolated bearings.

B.2
MATLAB Graphical User Interface (GUI) developed for user friendly operation of code in B.1.

B.3
Dual Rotor Blade Loss Simulation Code developed to integrate high fidelity ball bearing/squeeze film damper model into rotor code. Modelling capabilities will be enhanced to include 3D nonlinear ball bearing model, more rotor and stator levels and more finite element types. Code predicts bearing temperatures and stresses and squeeze film damper pressures along with shaft vibration.

B.4
MATLAB GUI has been developed for user friendly operation of a version of code in B.3.

B.5
Advanced, 3D high fidelity ball bearing model has been developed with independent ball motions and non-linear force deflection capability.

MILESTONE LIST

Task A - High Temperature Magnetic Bearings

The significant milestone list is:

- Year 1:
    * Design and Fabricate High Temp Thrust Mag Brg
    * Develop position Sensor hardware and drive electronics
    * Identify Flight Controller Components
    * Test Expert System on High Temperature Mag. Brg. Test Rig at GRC (HTMBTR)

-Year 2:
    * Test High Temp Thrust Mag. Brg. At Temp & Speed in HTMBTR
    * Design PWM power amplifier
    * Identify components and perform component testing for high temp. catcher brgs.

NASA/CR—2003-212205

* Test position sensors in HTMBTR
* Construct flight ready magnetic suspension controller at GRC

- Year 3:
    * Test PWM power amplifier in HTMBTR
    * Test high temp. catcher bearings in HTMBTR

Timeline / Cost Estimate / Milestones

Timeline

TASK	Year 1 Qtr. 1	2	3	4	Year 2 Qtr. 1	2	3	4	Year 3 Qtr. 1	2	3	4
A												
• High Temp. Thrust Mag. Brg.												
• High Temp. Position Sensor												
• PWM Power Amplifier												
• Flight Ready Controller												
• High Temp Catcher Brgs.												
• Expert System and Redundant Mag. Brgs												

Glenn Research Center

High Temperature Magnetic Bearing - Blade Loss Mitigation
NRA-GRC- 99-02 - 1Year Milestone Review
September 27, 2002, NASA Glenn

Texas A&M Vibration Control and Electromechanics Lab

Task B - Blade Loss Mitigation

The significant milestone list is:

- Year 1:

  * Complete Squeeze film damper and rolling element bearing modules and install in NASA/Boeing code

-Year 2:

  * Finish and test benchmark code

-Year 3:

  * Finish magnetic suspension module and install in NASA/Boeing code.

Timeline / Cost Estimate / Milestones

Timeline

TASK	Year 1 Qtr. 1 2 3 4	Year 2 Qtr. 1 2 3 4	Year 3 Qtr. 1 2 3 4
B			
• Component Models	↔		
• Veracity Benchmark Code		↔	
• Active Shaft Suspension			↔

MILESTONE LIST

Task A - High Temperature Magnetic Bearings

The significant milestone list is:

- Year 1:
  * Design and Fabricate High Temp Thrust Mag Brg
  * Develop position Sensor hardware and drive electronics
  * Identify Flight Controller Components
  * Test Expert System on High Temperature Mag. Brg. Test Rig at GRC (HTMBTR)
- Year 2:
  * Test High Temp Thrust Mag. Brg. At Temp & Speed in HTMBTR
  * Design PWM power amplifier
  * Identify components and perform component testing for high temp. catcher brgs.

Glenn Research Center

High Temperature Magnetic Bearing - Blade Loss Mitigation
NRA-GRC- 99-02 - 1Year Milestone Review
September 27, 2002, NASA Glenn

Texas A&M Vibration Control and Electromechanics Lab

* Test position sensors in HTMBTR
* Construct flight ready magnetic suspension controller at GRC

- Year 3:
  * Test PWM power amplifier in HTMBTR
  * Test high temp. catcher bearings in HTMBTR

Timeline / Cost Estimate / Milestones

Timeline

TASK	Year 1				Year 2				Year 3			
	Qtr. 1	2	3	4	Qtr. 1	2	3	4	Qtr. 1	2	3	4
A												
• High Temp. Thrust Mag. Brg.												
• High Temp. Position Sensor												
• PWM Power Amplifier												
• Flight Ready Controller												
• High Temp Catcher Brgs.												
• Expert System and Redundant Mag. Brgs												

Glenn Research Center

High Temperature Magnetic Bearing - Blade Loss Mitigation
NRA-GRC- 99-02 - 1Year Milestone Review
September 27, 2002, NASA Glenn

Texas A&M Vibration Control and Electromechanics Lab

Task B - Blade Loss Mitigation

The significant milestone list is:

- Year 1:

    * Complete Squeeze film damper and rolling element bearing modules and install in NASA/Boeing code

-Year 2:

    * Finish and test benchmark code

-Year 3:

    * Finish magnetic suspension module and install in NASA/Boeing code.

Timeline / Cost Estimate / Milestones

Timeline

TASK	Year 1 (Qtr. 1 2 3 4)	Year 2 (Qtr. 1 2 3 4)	Year 3 (Qtr. 1 2 3 4)
B			
• Component Models	⟷		
• Veracity Benchmark Code		⟷	
• Active Shaft Suspension			⟷

NASA/CR—2003-212205

A.1: High Temperature Electro-Magnetic Axial Thrust Bearing

By
Waqar Mohiuddin
Dr. Alan B. Palazzolo

Stresses Due to Rotation (Uniform Rotor Disk)

(ID = 2.0 in. and OD = 5.4 in.)

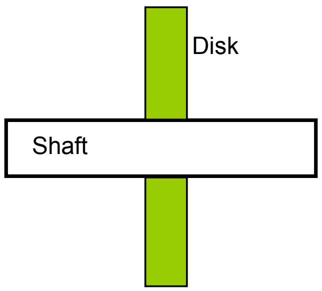

Radius R (in)	Radial Stress (psi)	Tangential Stress (psi)
1.00	0.000000	46357.169
1.17	4929.946	39631.246
1.34	7521.566	34962.251
1.51	8690.042	31435.002
1.68	8912.556	28572.319
1.85	8457.724	26105.584
2.02	7486.143	23874.200
2.19	6098.616	21777.365
2.36	4361.004	19749.218
2.53	2317.814	17745.251
2.70	0.0000000	15734.511

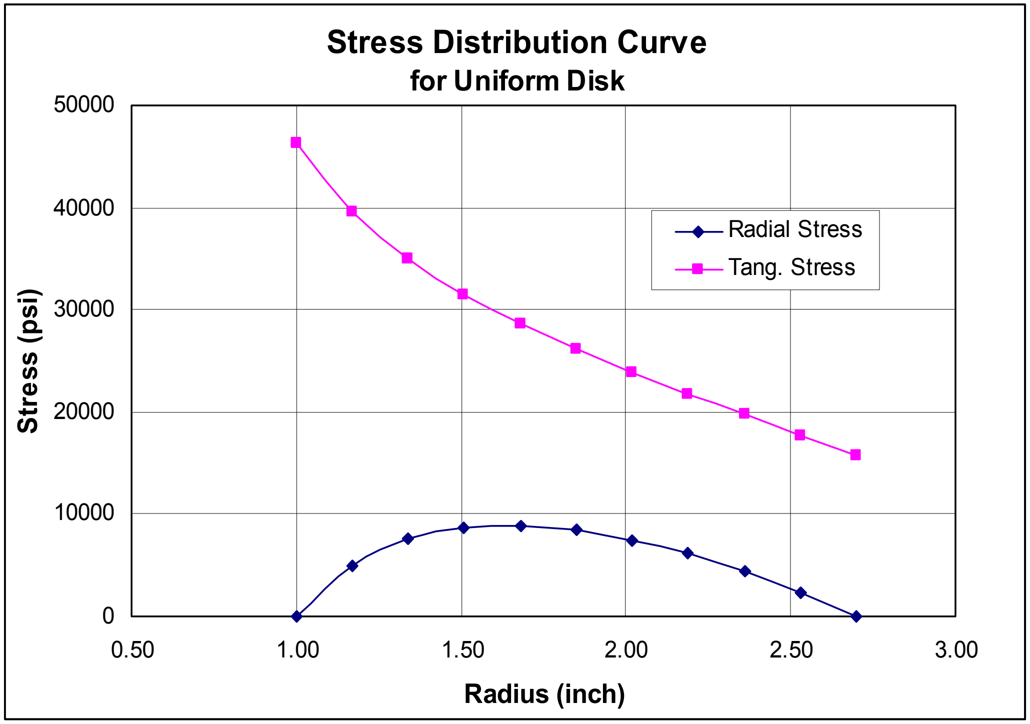

Glenn Research Center

High Temperature Magnetic Bearing - Blade Loss Mitigation
NRA-GRC- 99-02 - 1Year Milestone Review
September 27, 2002, NASA Glenn

Texas A&M Vibration Control and Electromechanics Lab

Stresses Due to Rotation (Tapered Rotor Disk)

(ID = 2.0 in. and OD = 5.4 in.)

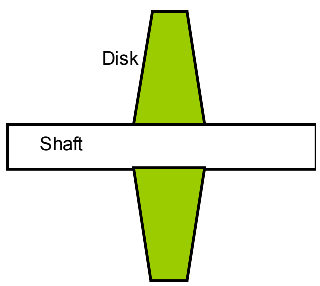

Radius R (in)	Radial Stress (psi)	Tangential Stress (psi)
1	0	39324.232
1.17	3097.531	33547.48
1.34	5488.872	29471.724
1.51	7325.987	26390.13
1.68	8134.329	23916.253
1.85	7664.754	21823.298
2.02	6876.632	19970.536
2.19	5582.173	18266.618
2.36	4361.953	16649.999
2.53	2601.652	15077.901

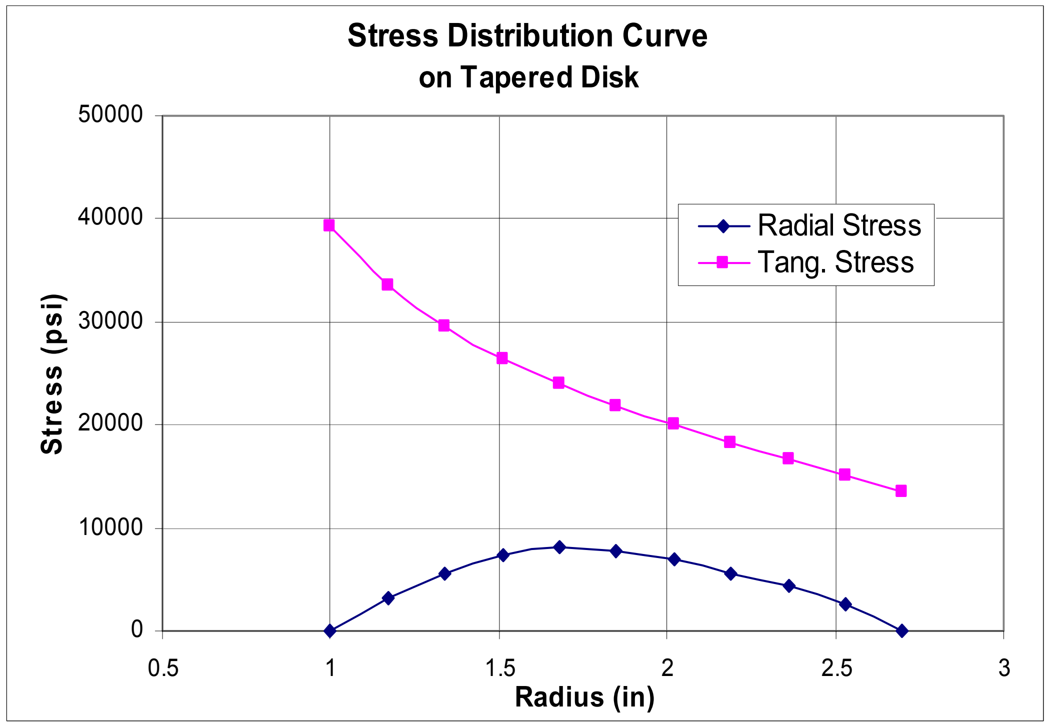

Stresses Due to Rotation (Hyperbolic Rotor Disk)

(ID = 2.0 in. and OD = 5.4 in.)

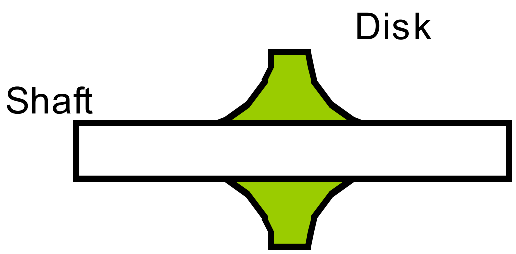

Radius R (in)	Radial Stress (psi)	Tangential Stress (psi)
1.00	0.0000000	37030.064
1.17	3965.799	31662.401
1.34	6354.390	28048.832
1.51	7662.330	25395.096
1.68	8160.346	23276.181
1.85	8007.523	21447.796
2.02	7303.067	19761.450
2.19	6111.910	18122.745
2.36	4478.302	16469.427
2.53	2433.446	14759.170
2.70	0.0000000	12962.449

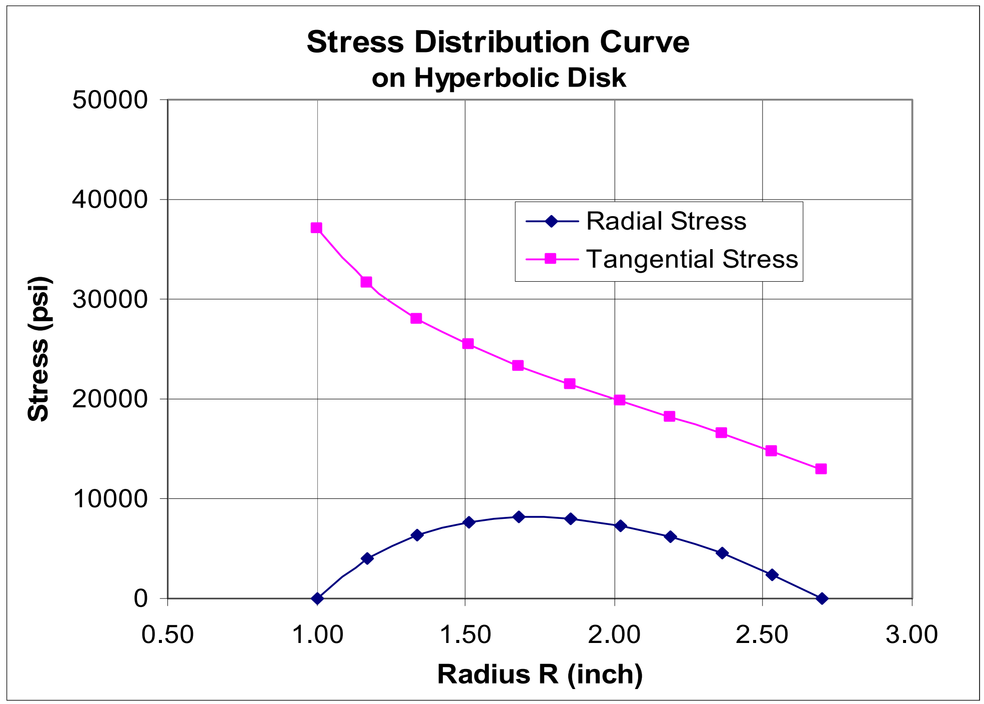

NASA/CR—2003-212205

von Mises Stress in Rotor Disk (Inner Diameter 6 in.)

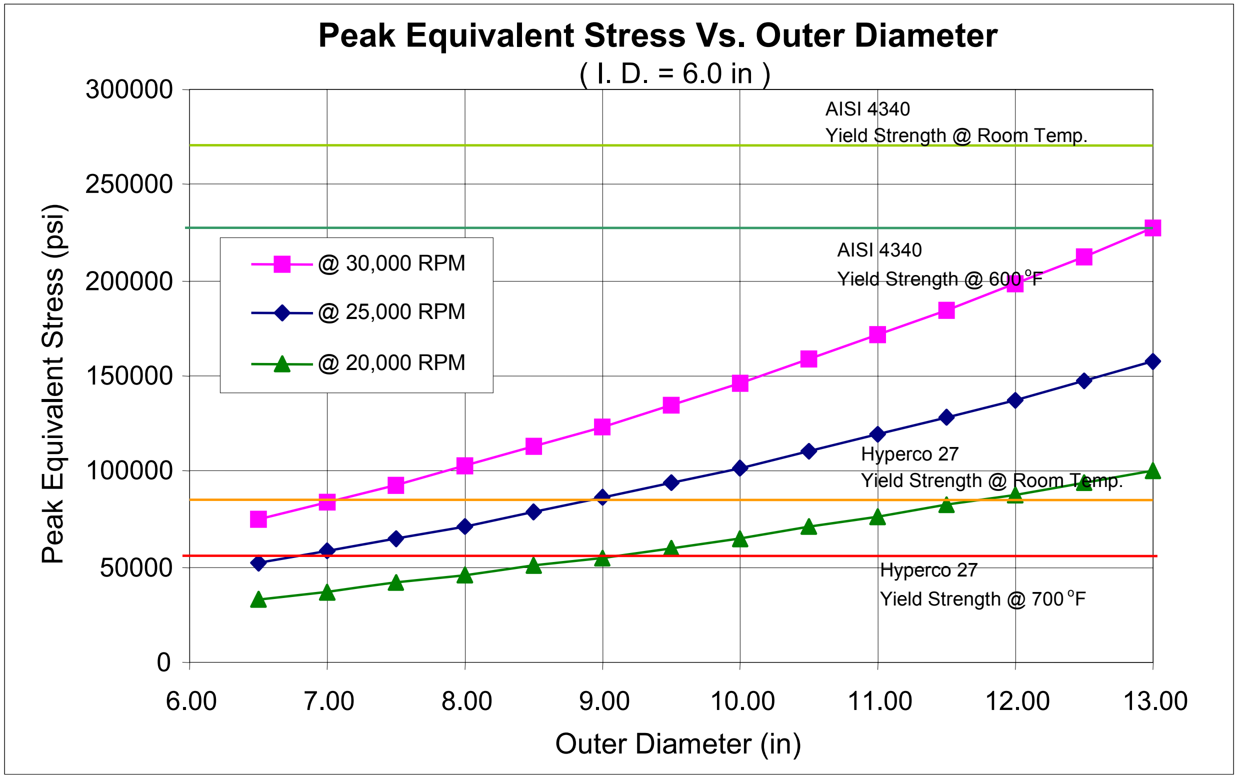

Glenn Research Center

High Temperature Magnetic Bearing - Blade Loss Mitigation
NRA-GRC- 99-02 - 1Year Milestone Review
September 27, 2002, NASA Glenn

Texas A&M Vibration Control and Electromechanics Lab

von Mises Stress in Rotor Disk (Inner Diameter 2 in.)

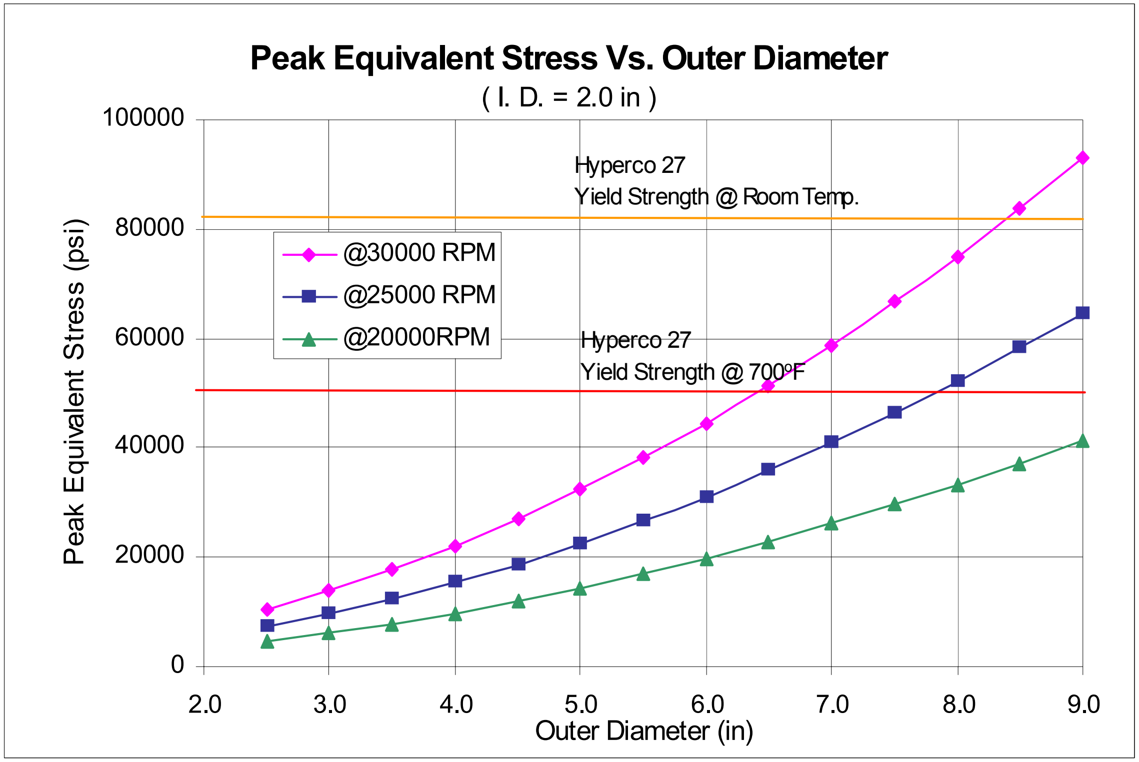

Variation of Outer Diameter with Load Capacity (I. D.= 6 in.)

For AISI 4340 (B_{sat} = 1.5T)	
Load (lb-f)	**O.D.** (in)
1000	10.98
2000	11.52
3000	12.04
4000	12.52
5000	13.00

Variation of Outer Diameter with Load Capacity (I. D.= 2 in.)

For Hyperco 27 (B_{sat} = 2.0T)	
Load (lb-f)	**O.D.** (in)
1000	5.40
2000	6.00
3000	6.54
4000	7.04
5000	7.50

High Temperature Magnetic Bearing - Blade Loss Mitigation
NRA-GRC- 99-02 - 1Year Milestone Review
September 27, 2002, NASA Glenn

Glenn Research Center

Texas A&M Vibration Control and Electromechanics Lab

Comparison between Handbook and ANSYS Approach

For AISI 4340 Hyperbolic Profile (with 6 in. ID Rotor)

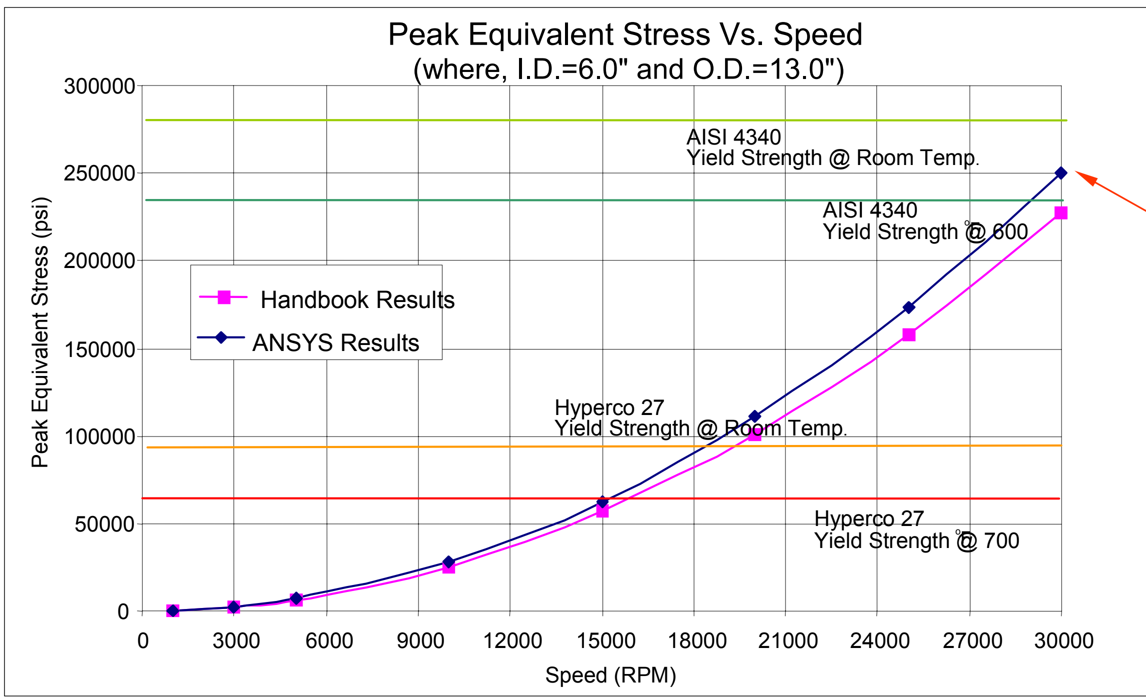

Max. Stress Crossed Yield Stress Limit on ANSYS Simulation

Glenn Research Center

High Temperature Magnetic Bearing - Blade Loss Mitigation
NRA-GRC- 99-02 - 1Year Milestone Review
September 27, 2002, NASA Glenn

Texas A&M Vibration Control and Electromechanics Lab

Effective Force on Hyperbolic Rotor

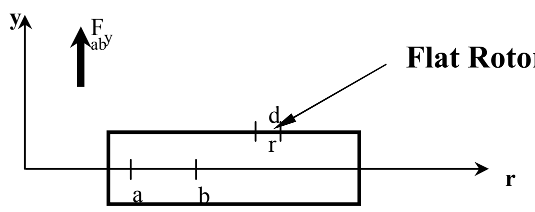

Surface area of a disk with flat profile is

$$A = \int 2\pi r dr = \pi(b^2 - a^2)$$

Force on the surface

$$F_y^{a\to b} = \frac{B^2 A}{2\times\mu_o} = \frac{B^2\times\pi(b^2-a^2)}{2\times\mu_o}$$

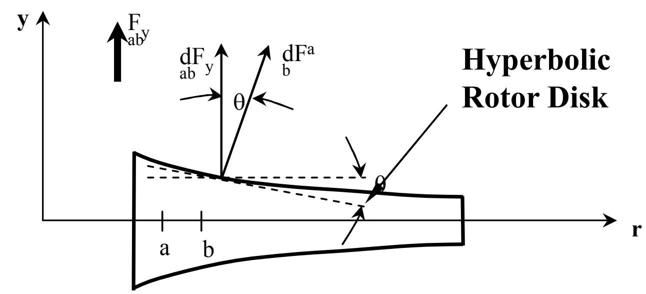

Infinitesimally small surface area dA is

$$dA = 2\pi r.ds$$

Force on the surface

$$dF_y^{a\to b} = \left(\frac{B^2 dA}{2\mu_o}\right) Cos\theta$$

$$F_y^{a\to b} = \int dF_y^{a\to b} = \frac{B^2\pi}{2\mu_o}(b^2 - a^2)$$

In Both Cases, Forces are Same. Therefore, Hyperbolic Shape is NOT Effecting Axial Thrust Loading

Fabrication Drawing of Thrust Rotor

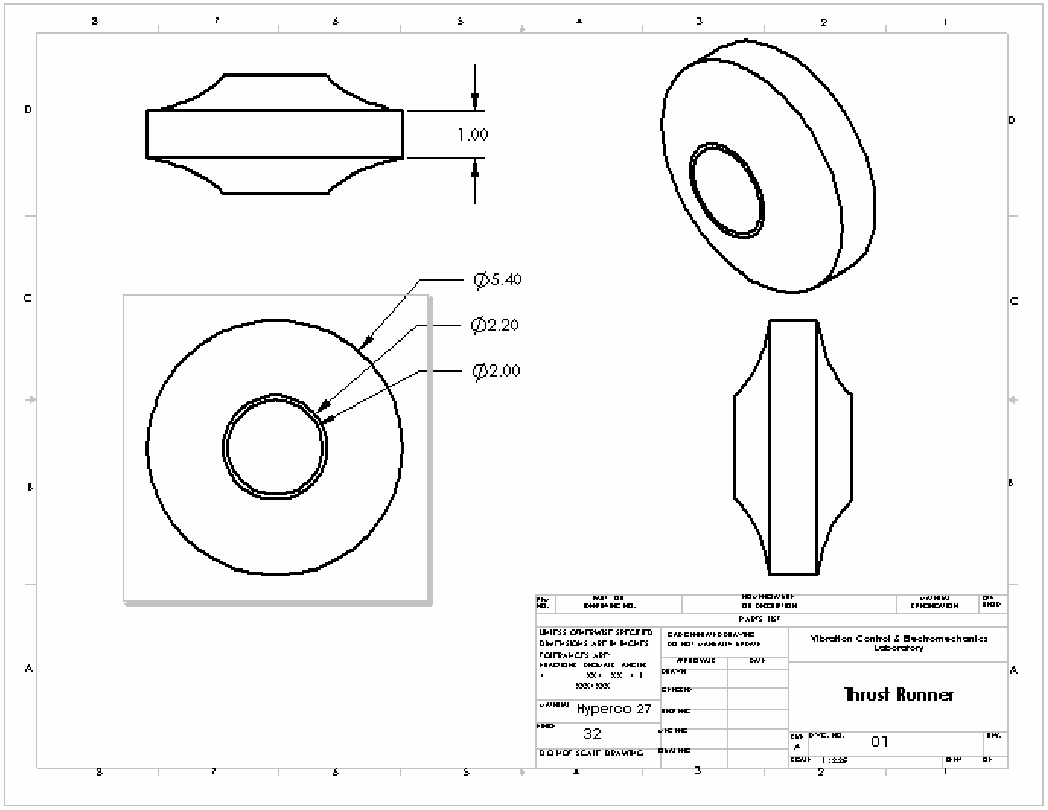

Fabrication Drawing of Thrust Stator

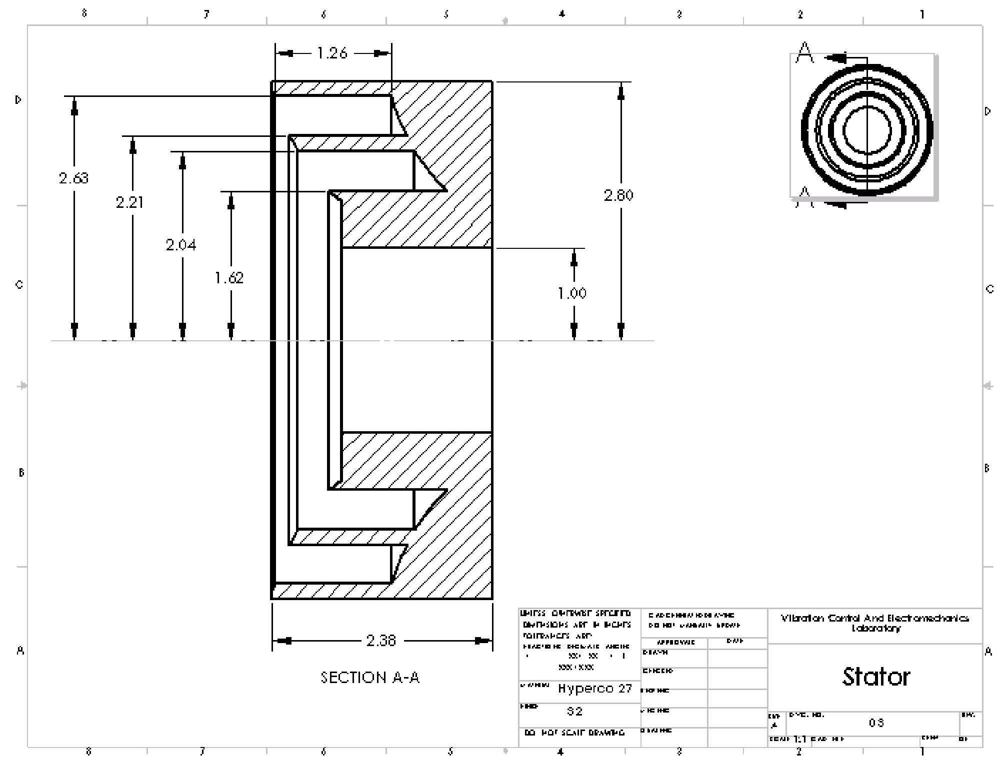

Fabrication Drawing of Thrust Stator

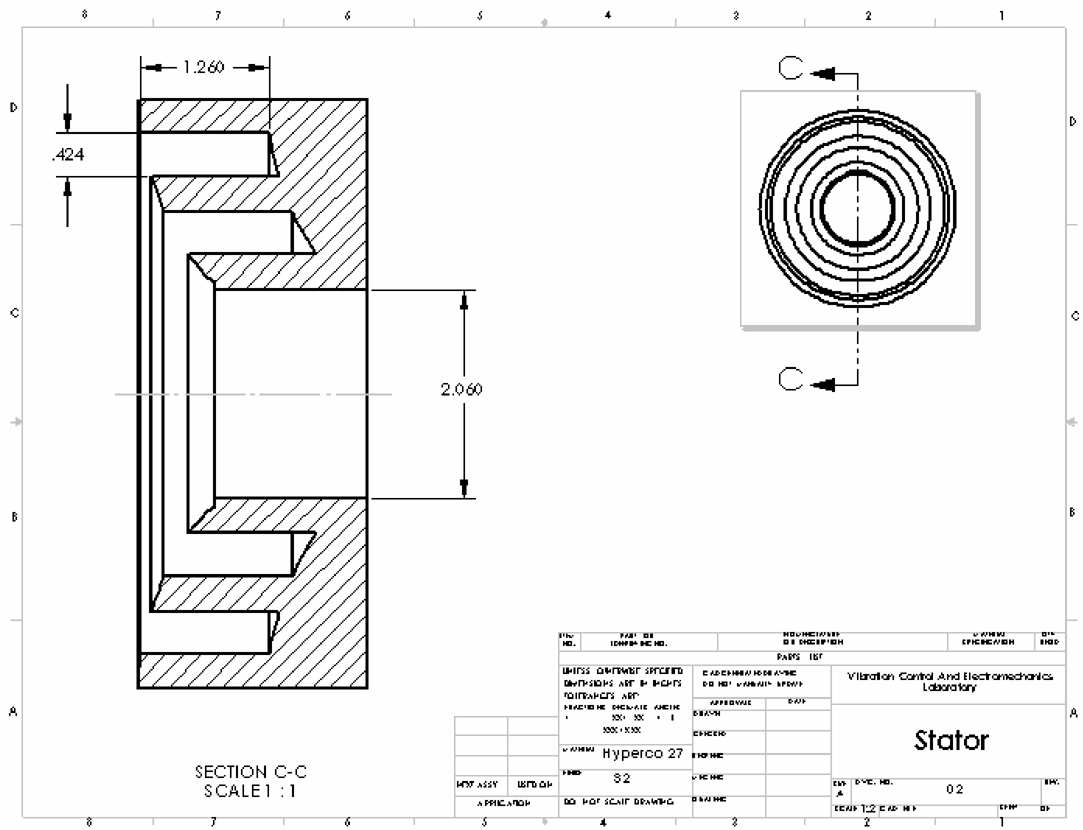

Forged Hyperco 27 Disk

Suggested Materials for Thrust Runner

Alloy	B_{sat}	Yield Strength (ksi)
Aermet 100 Alloy	1.6	> 200
Oil quenched AISI 4340	2.0	100 ~ 200
Hyperco 27	2.3	52.5

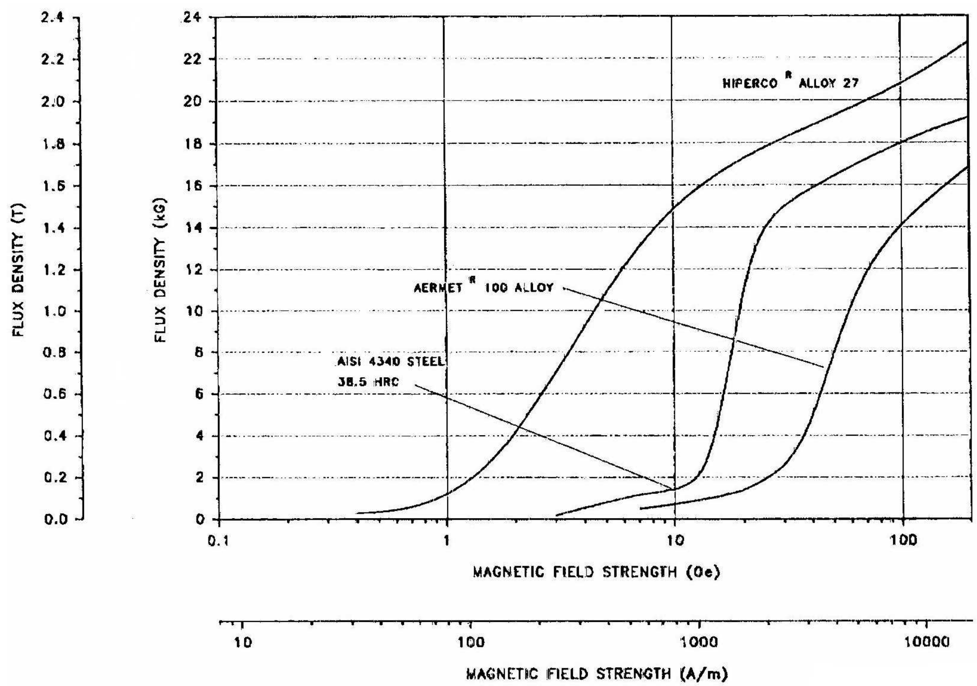

Ref.: Les Harner, Carpenter Technologies Inc.

NASA/CR—2003-212205

DC Magnetization Curve for Hyperco 27

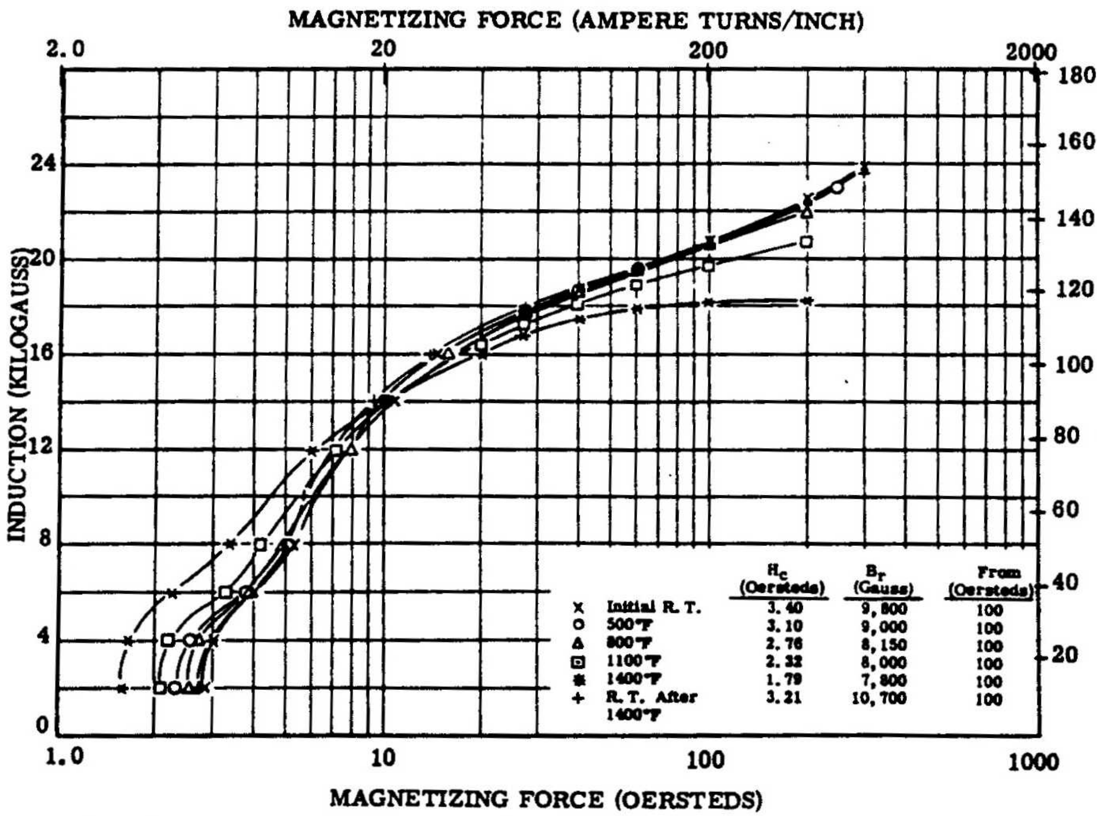

Ref: NASA SP-3083

Tensile Strength of Forged Hyperco 27

(Tested in Air and Argon)

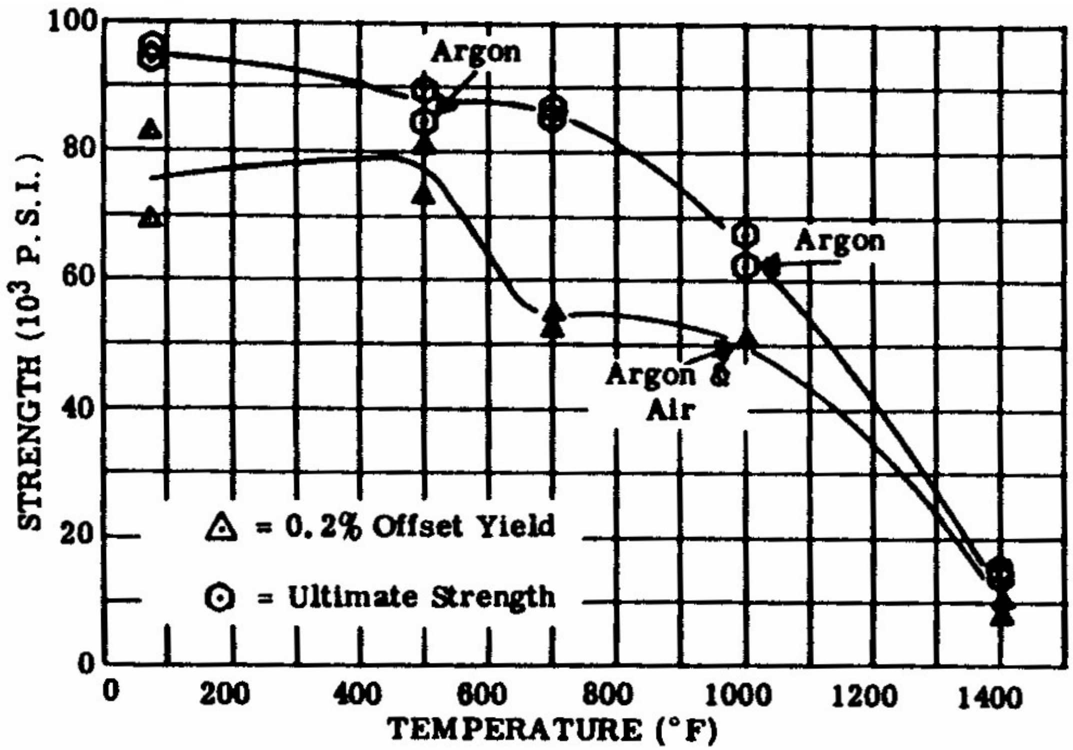

Ref: NASA SP-3083

Block Diagram of AISI 4340 Test Set-up

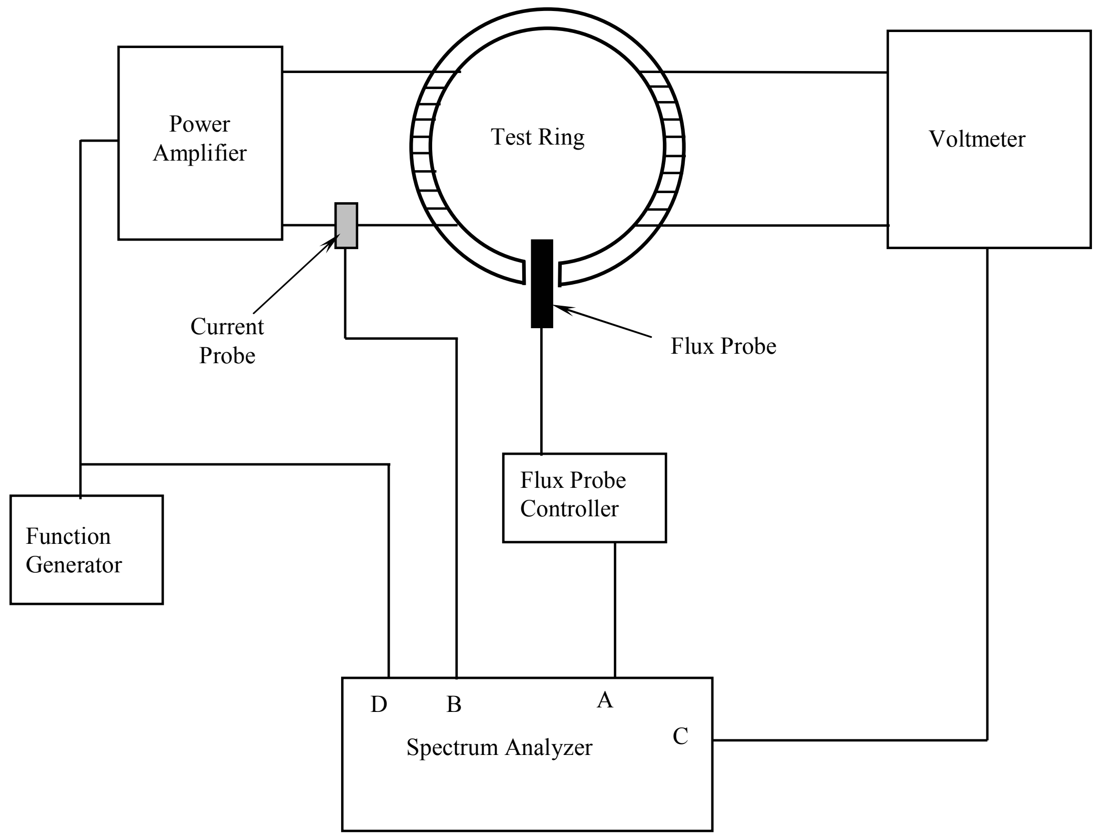

Glenn Research Center

High Temperature Magnetic Bearing - Blade Loss Mitigation
NRA-GRC- 99-02 - 1Year Milestone Review
September 27, 2002, NASA Glenn

Texas A&M Vibration Control and Electromechanics Lab

Flux Probe Inserted into the Gap of the AISI 4340 Ring

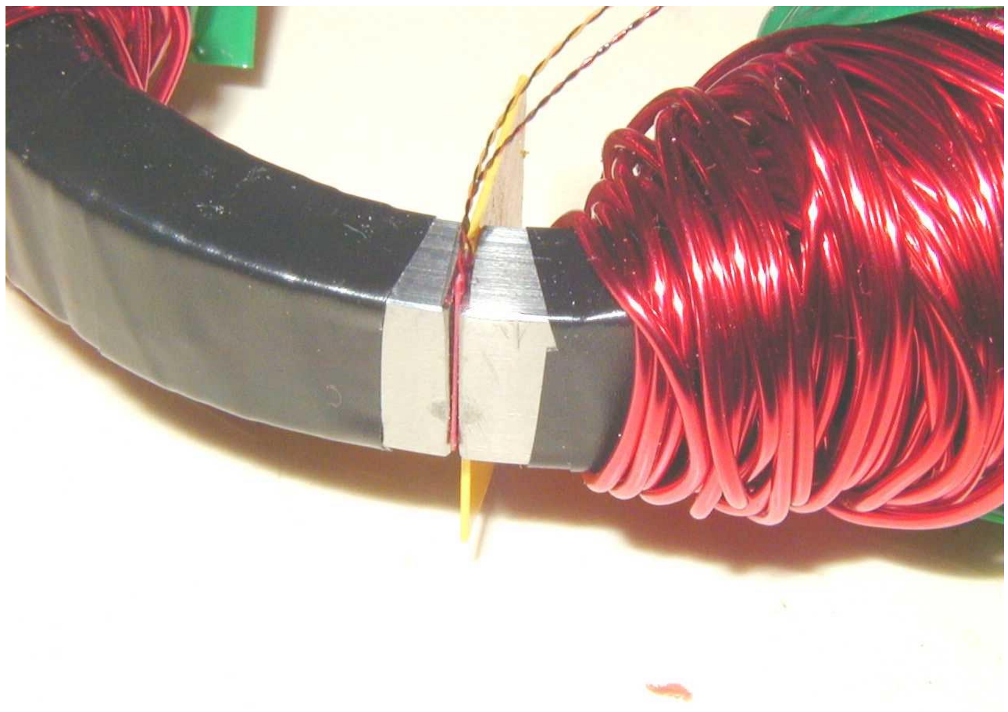

Set-up for Test of Magnetic Properties of AISI 4340

Induced Flux and Voltage with Applied Current

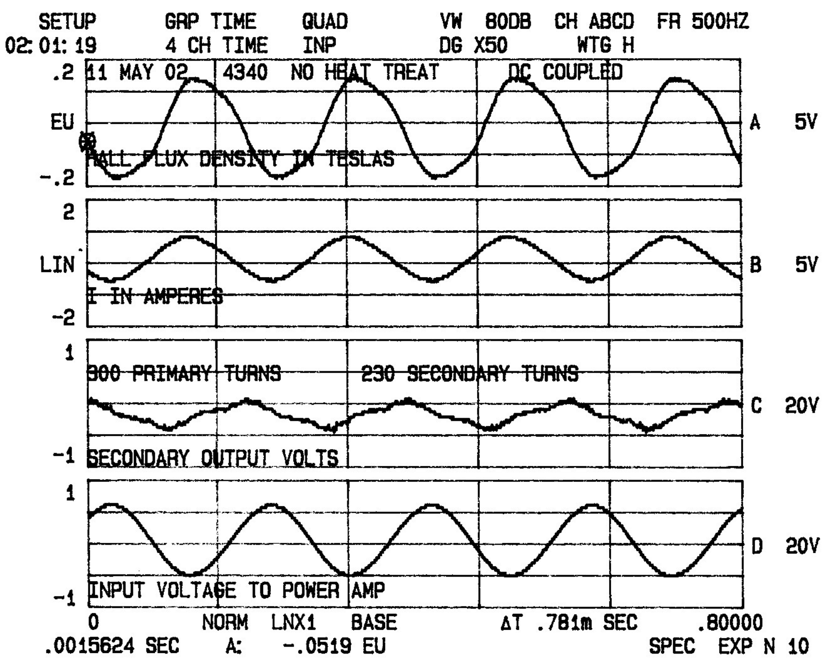

Saturated Flux Density with Applied Current of 3.25 A

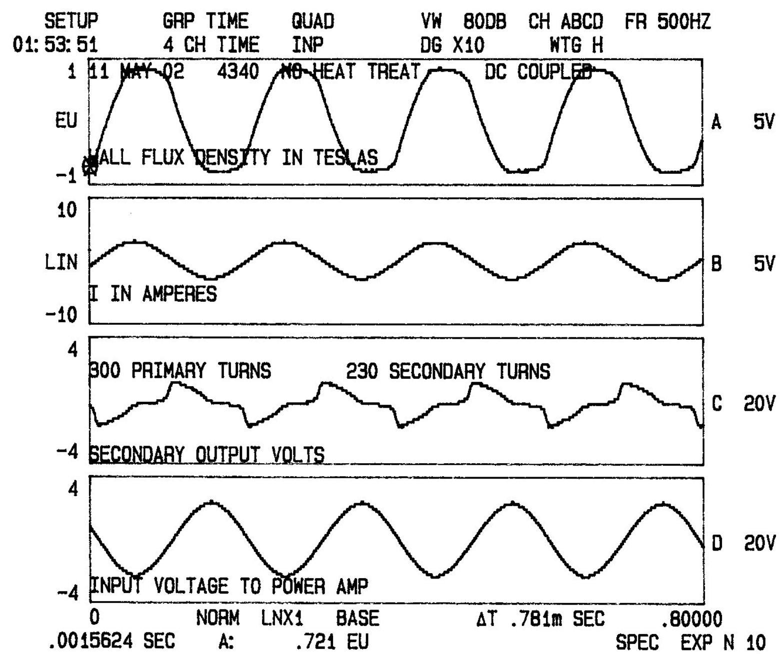

1-D Magnetic Circuit Analysis

- **Saturation Flux Density, B_{sat}= 2.0 T**
  Bias Current, I = 15 Amps
- **Gap between Rotor and Stator, s = 0.02 in.**
- **Number of Turns Required = 110**

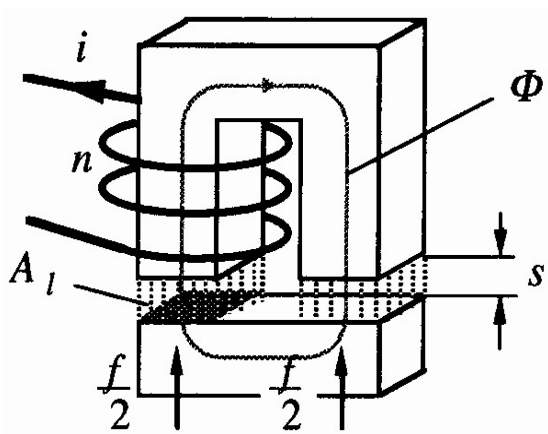

$$B = \mu_o \frac{N.I}{2.s}$$

1-D Magnetic Circuit Analysis

- Shaft Diameter, r = 2.0 in
- For Stator
  - Inner Diameter, r_1= 2.05 in
  - Outer Diameter, r_6= 5.6 in
- For Inner coil
  - Inner Diameter, r_2 = 3.24 in
  - Outer Diameter, r_3 = 4.08 in
- For Outer Coil
  - Inner Diameter, r_4 = 4.42 in
  - Outer Diameter, r_5 = 5.26 in

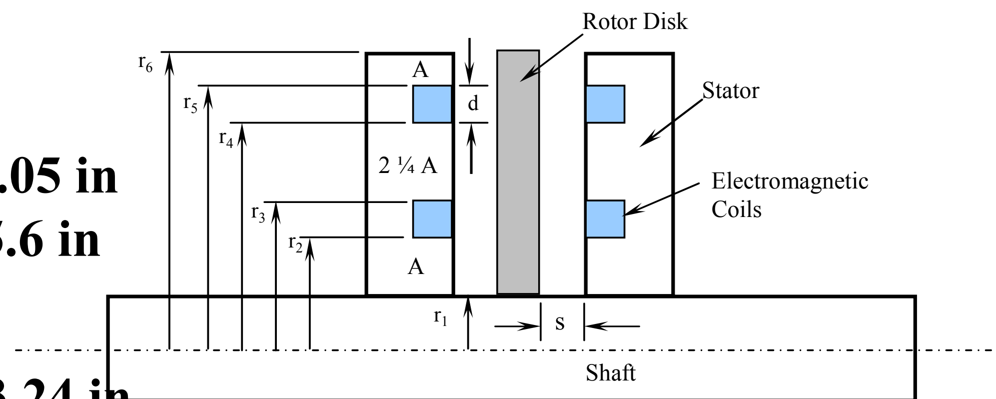

Electromagnetic FEA Simulation of Thrust Bearing

Maximum force on Hyperco27 rotor calculated with nonlinear FEA is 1211 lbs.

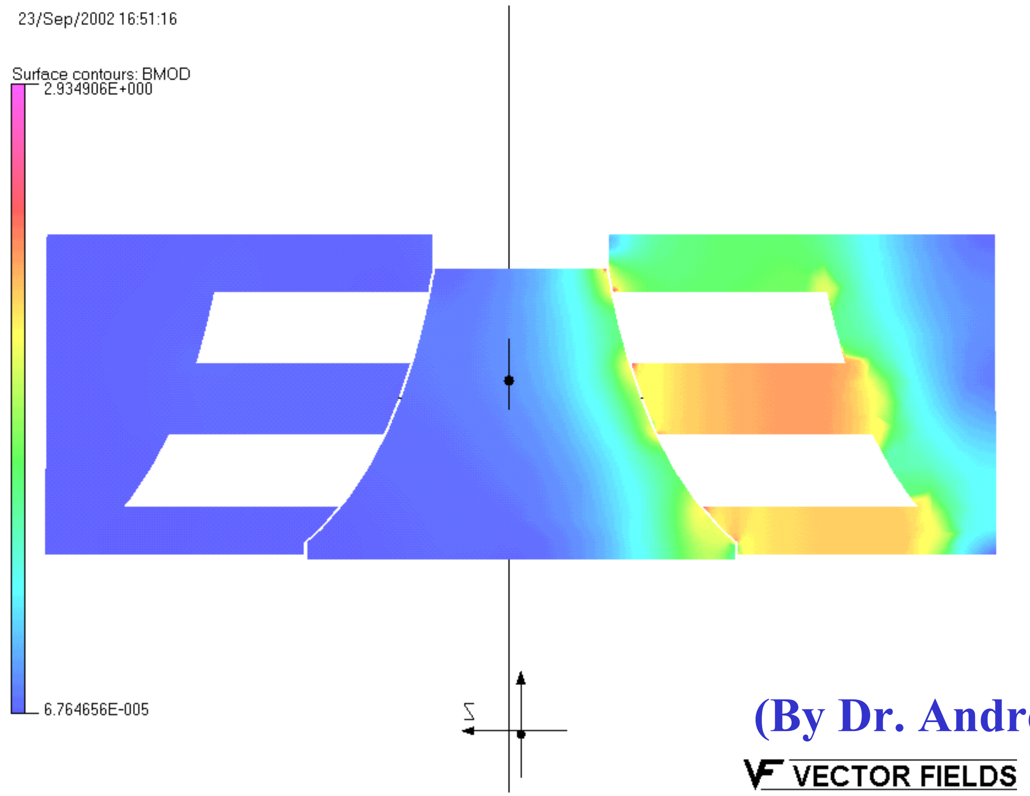

(By Dr. Andrew Kenny)

Eddy Currents Generated By Rotating Thrust Runner

(At 1 rpm.)

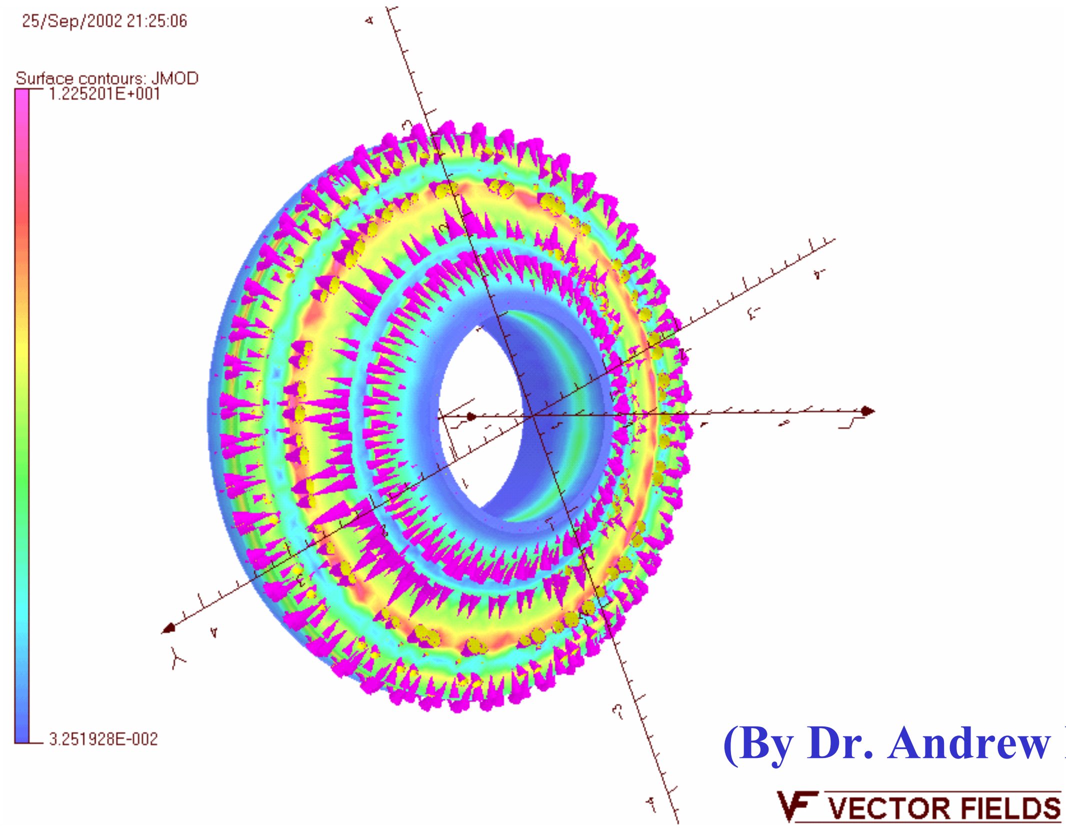

(By Dr. Andrew Kenny)

Specification of Catcher Bearing (ZSB107J)

1. Outside Diameter: 2.4409 in.
2. Width: 1.4 cm 0.5512 in.
3. Diameter of Ball: 0.21875 in.
4. Static Capacity:
   a. Radial Load: 2537 lbf
   b. Thrust Load: 3367 lbf
5. Basic Dynamic Load Rating: 2778 lbf
6. Standard Pre-load:
   a. Light: 30 lbf
   b. Medium: 80 lbf
   c. Heavy: 80 lbf

Campbell Diagram

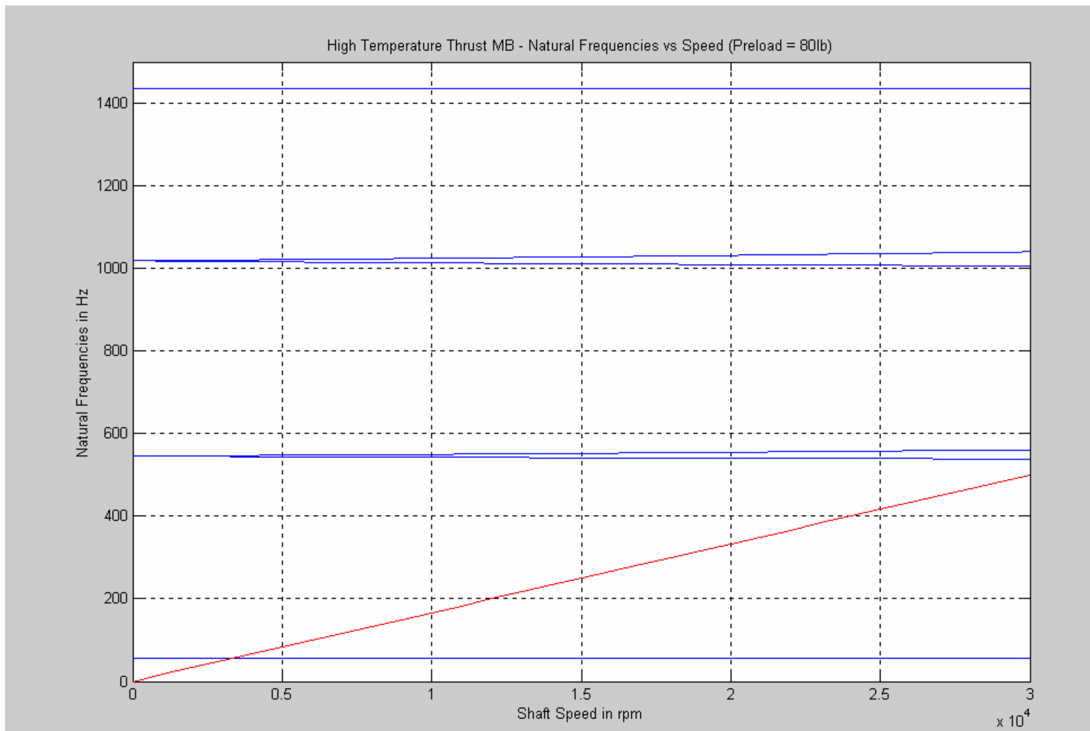

High Temperature Magnetic Bearing - Blade Loss Mitigation
NRA-GRC- 99-02 - 1Year Milestone Review
September 27, 2002, NASA Glenn

N = 538.76 Hz

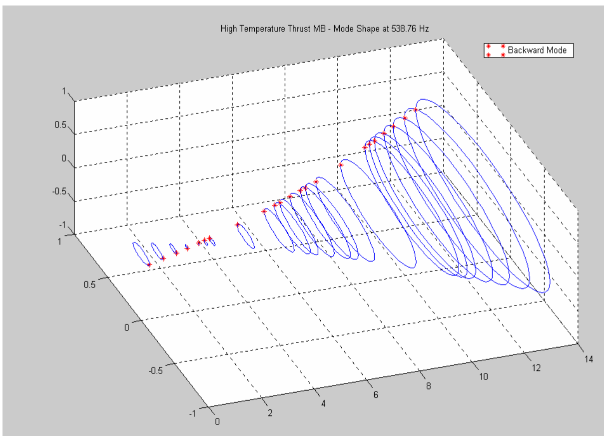

N = 560.99 Hz

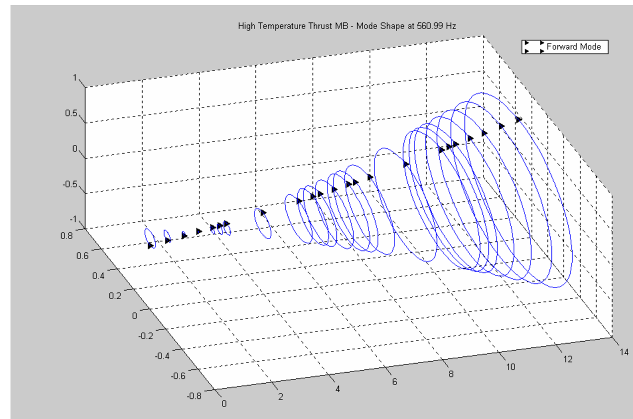

N = 1005.9 Hz

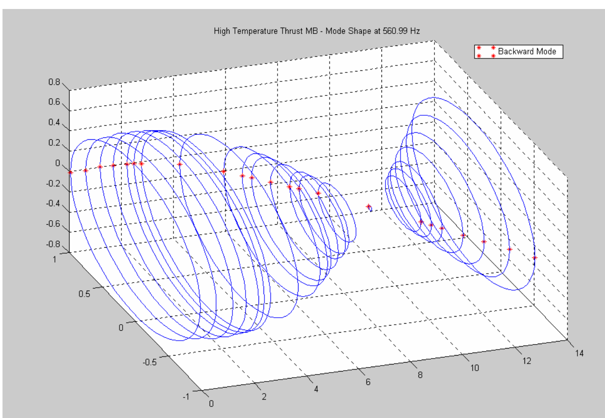

N = 1040.5 Hz

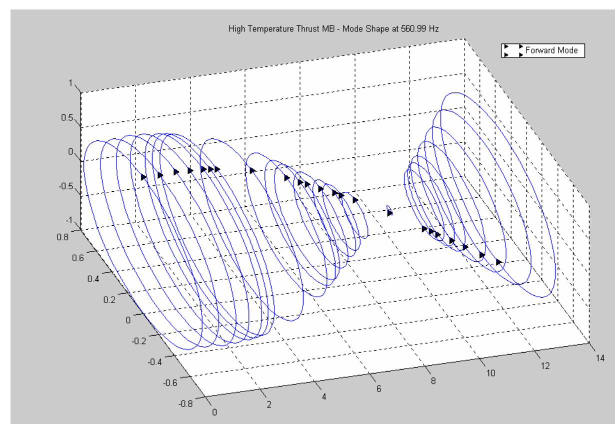

Glenn Research Center

High Temperature Magnetic Bearing - Blade Loss Mitigation
NRA-GRC- 99-02 - 1Year Milestone Review
September 27, 2002, NASA Glenn

Texas A&M Vibration Control and Electromechanics Lab

von Mises Stress in the Stator

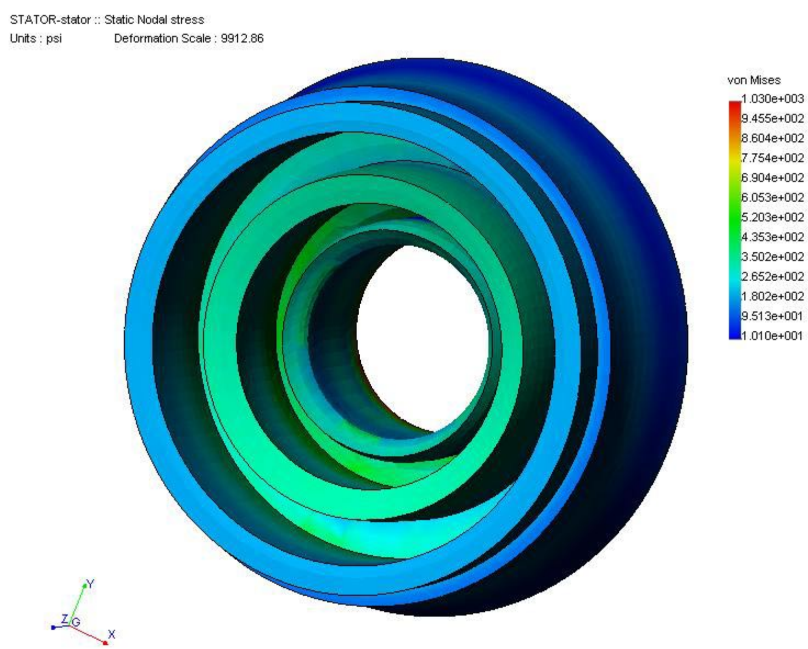

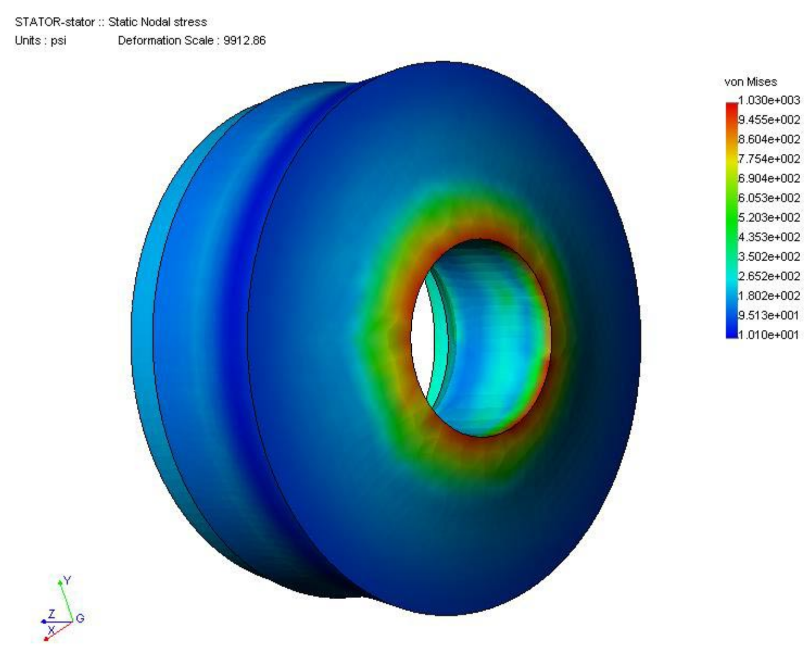

Deflection of Catcher Bearing Web

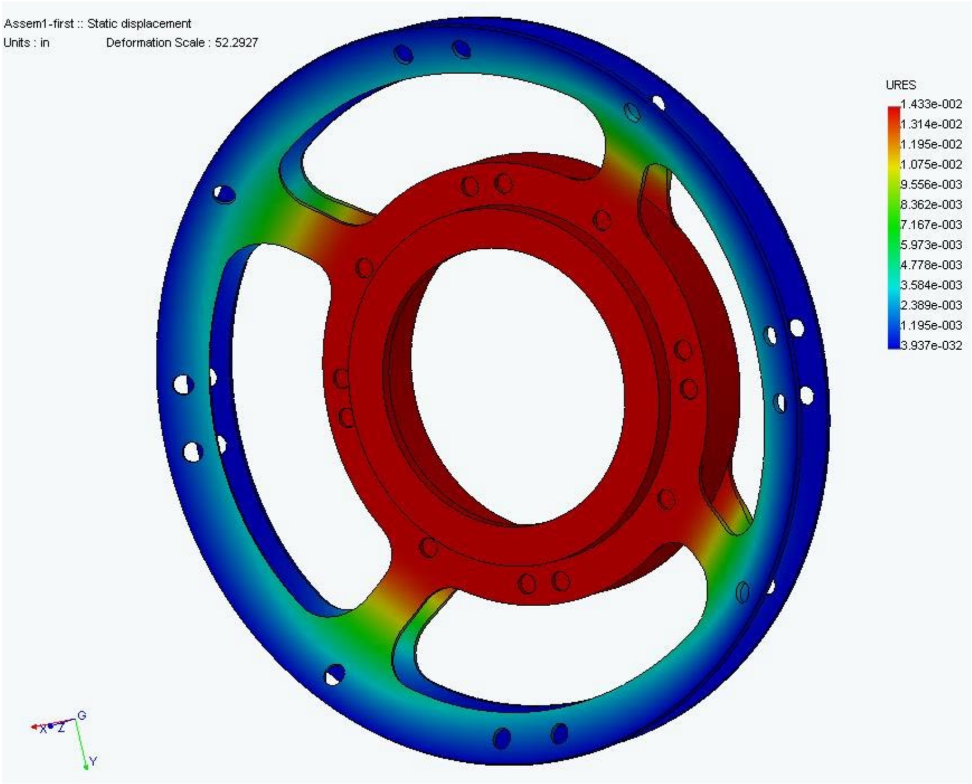

Max. Displacement 14.33 mils

Force Applied 88lb-f

Rotor Containment Vessel Calculation

Polar Moment of Inertia of the Rotor Disk from SolidWorks, J_p

9.93×10^{-3} lb-in-sec²

At 30000 rpm, Total Disk Energy, KE_w

$\frac{1}{2} \cdot I_p \cdot \omega^2$

$= \frac{1}{2} \times 9.93 \times 10^{-3} \times (3141.6)^2$

$=$ 49002.81 lb-in

Transnational Energy, KE_T

$0.22 \times KE_w$

$=$ 10780.62 lb-in

Thickness of the Containment Vessel (from Plot),

0.3 in

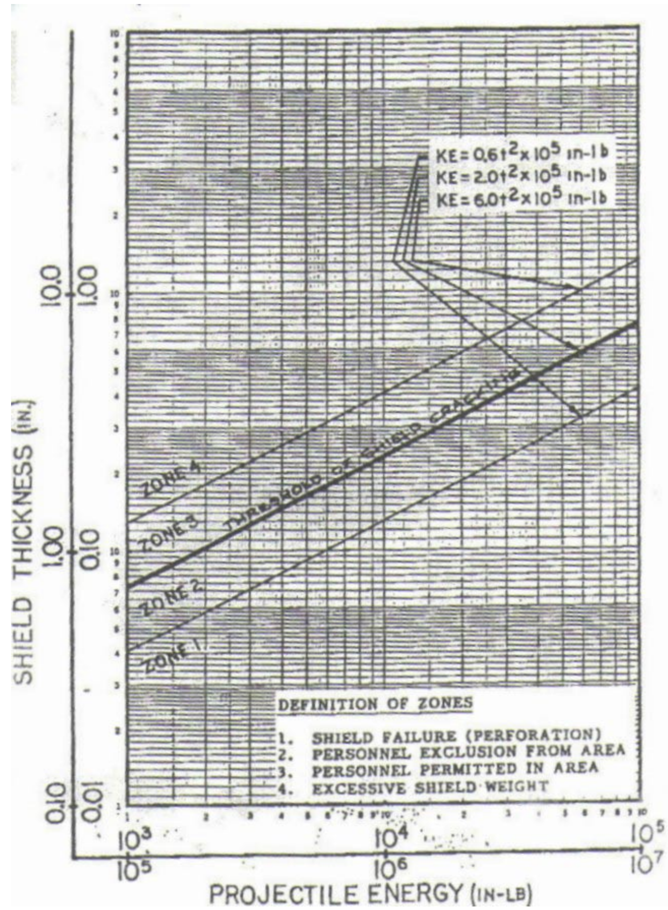

von Mises Stress and Displacement

(Rotor ID=2.0 in., OD=5.4 in.)
Interference fit used between Shaft and Rotor is 0.0013 in.

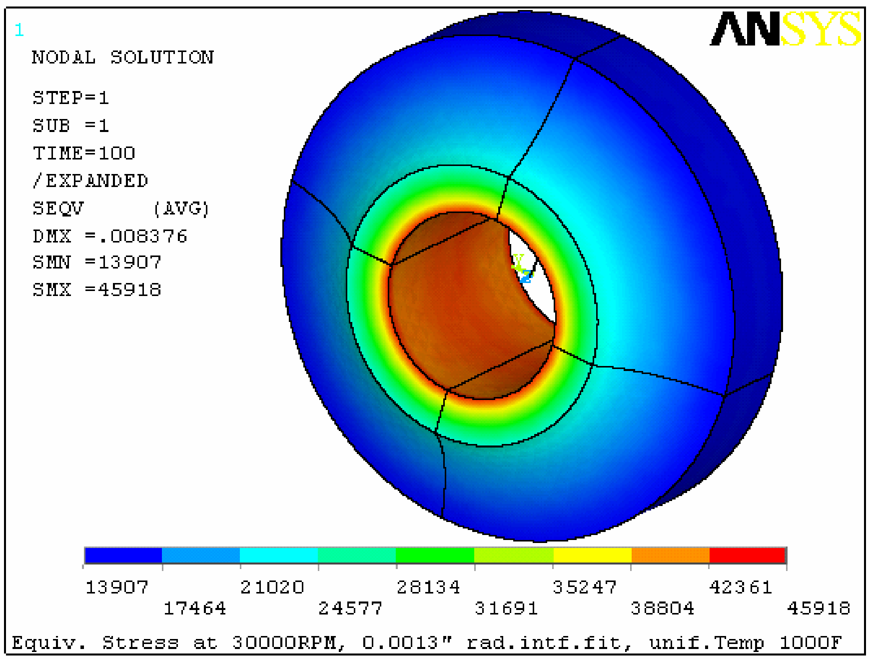

von Mises Stress Developed at 30000 rpm with 1000 lb Axial Thrust Load at 1000°F (Max. Stress 45918 Psi)

Stress Developed with Crowned Interface of 0.0018 in. and 0.002 in. Radial Interference

- The interface between the rotor and shaft were crowned.
- Center of the crown had 0.02 in. gap.
- Rest of the interface were at 0.0018 in. interference fit.

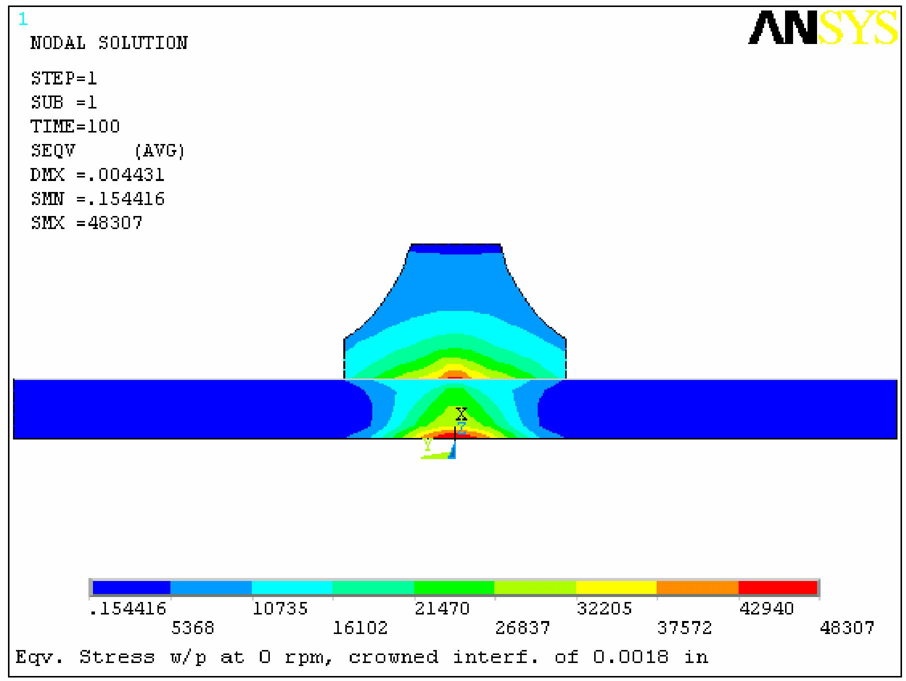

von Mises Stress Developed at ZERO rpm with 1000 lb Axial Thrust Load (Max. Stress 48307 Psi)

Glenn Research Center

High Temperature Magnetic Bearing - Blade Loss Mitigation
NRA-GRC- 99-02 - 1Year Milestone Review
September 27, 2002, NASA Glenn

Texas A&M Vibration Control and Electromechanics Lab

Stress Developed with Crowned Interface of 0.0018 in. and 0.002 in. Radial Interference

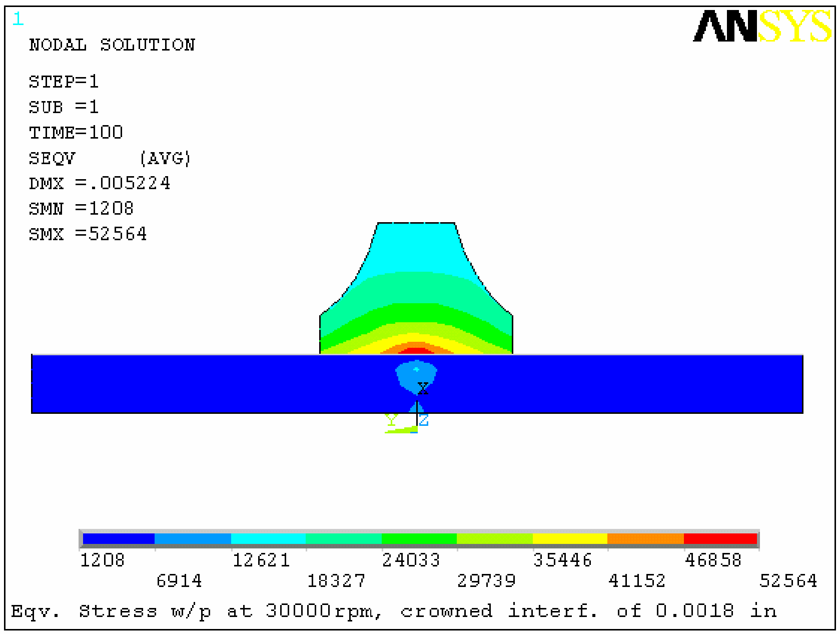

von Mises Stress Developed at 30000 rpm with 1000 lb Axial Thrust Load (Max. Stress 52564 Psi)

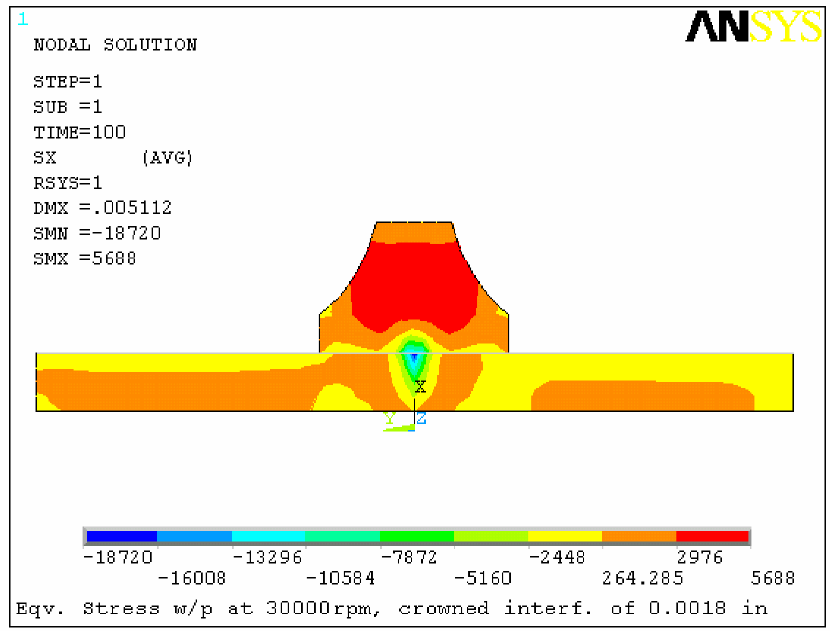

Radial Stress Developed at 30000 rpm with 1000 lb Axial Thrust Load (Max. Stress 5688 Psi)

Stress Developed in Deeply Crowned Rotor

- No interference fit between Rotor and Shaft
- Stress was higher than that of flat interfaced Rotor. (will be shown in the next slide)
- Removal of material from Rotor did not have any positive effect on stress

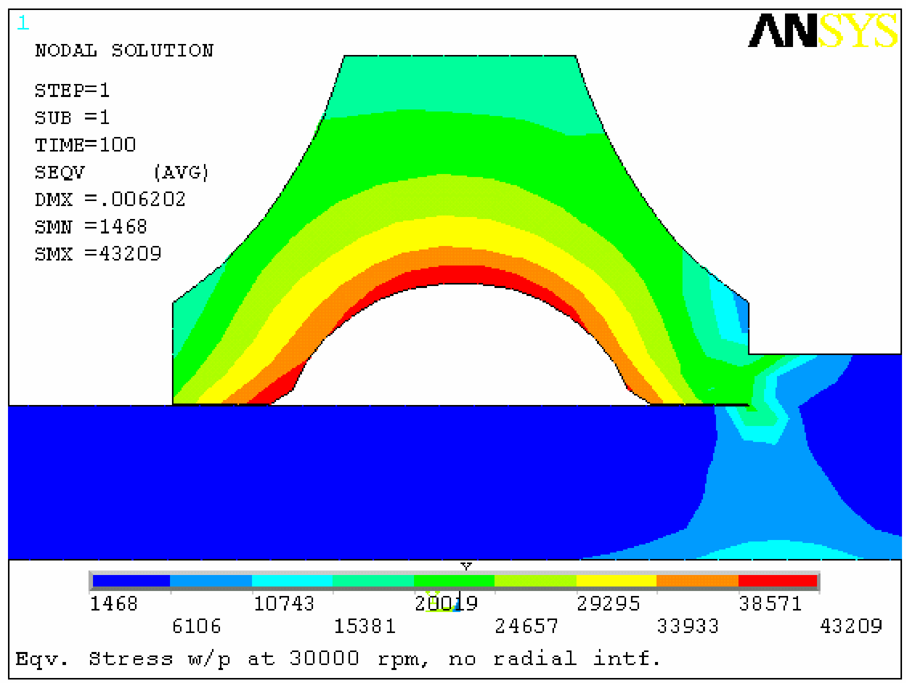

Max. von Mises Stress Developed 43209 Psi, with 1000 lb Axial Thrust rotating at 30000 rpm (Max. Stress 43209 Psi)

Glenn Research Center

High Temperature Magnetic Bearing - Blade Loss Mitigation
NRA-GRC- 99-02 - 1Year Milestone Review
September 27, 2002, NASA Glenn

Texas A&M Vibration Control and Electromechanics Lab

Stress Developed in Rotor with NO Interference Fit (Final)

Have under-cut to counter "Internal Friction" (Shaft not Shown)

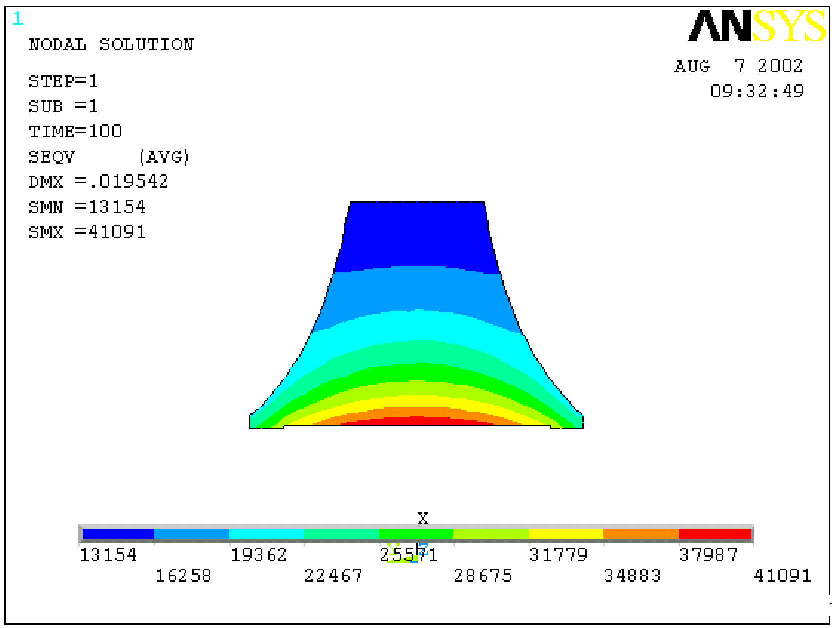

von Mises Stress with 1000 lb thrust at 30000 rpm and room temperature (Max. Stress 41091 Psi)

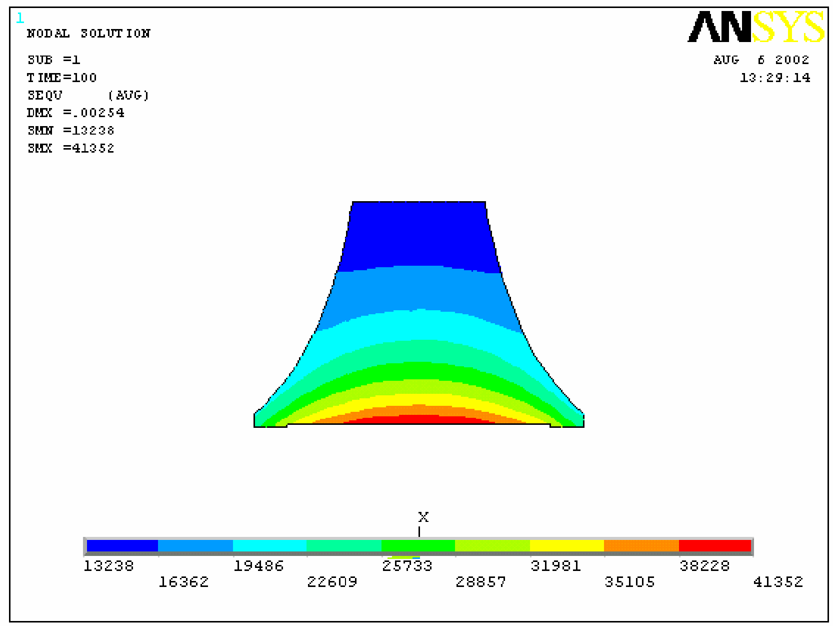

von Mises Stress with 1000 lb thrust at 30000 rpm and 1000°F uniform temp. (Max. Stress 41352 Psi)

Conclusion

- At 30000 rpm and the diameter (9 inches) required for a 1000-lb load capacity, Hyperco 27 disk peak stress (125000Psi) is 70000Psi, which is higher than its yield strength (52000) at 700°F. Hence, it is impractical to use Hyperco 27 for a 6 inches inner diameter thrust runner.

- At 30000 rpm, and with the diameter (11 inches) required for a 1000 lb load capacity, AISI 4340 disk peak stress (170000 Psi) is 70000 Psi less than its yield strength (240000 Psi) at 600°F. Hence, it should be safe to manufacture the thrust runner with AISI 4340 for 1000 lb, 30000 rpm, 700°F application.

Conclusion

- However, in our test B_{sat} was identified as 1.0T. According to the paper published by Les Harner, D. W. Dietrich and M. S. Masteller, "An Overview of Soft Magnetic Material for Magnetic Bearings", the B_{sat} of AISI 4340 is 2.0T. Correspondence with Les Harner did not confirm that 2.0T is realistic.

- The peak stress of Hyperco disk at 6 inches of inner diameter, 20000 rpm, 700°F, and 1000 lb load approximately equals the yield stress. Therefore, Hyperco 27 could be used at 20000 rpm, but that speed was below the required speed. However, safety factor would be 1.0 or less when interference fit stress is included.

DESIGN HIGH TEMPERATURE THRUST MAGNETIC BEARING (TMB) TEST RIG

Dr. A.B. Palazzolo   Waqar Mohiuddin   Randall Tucker

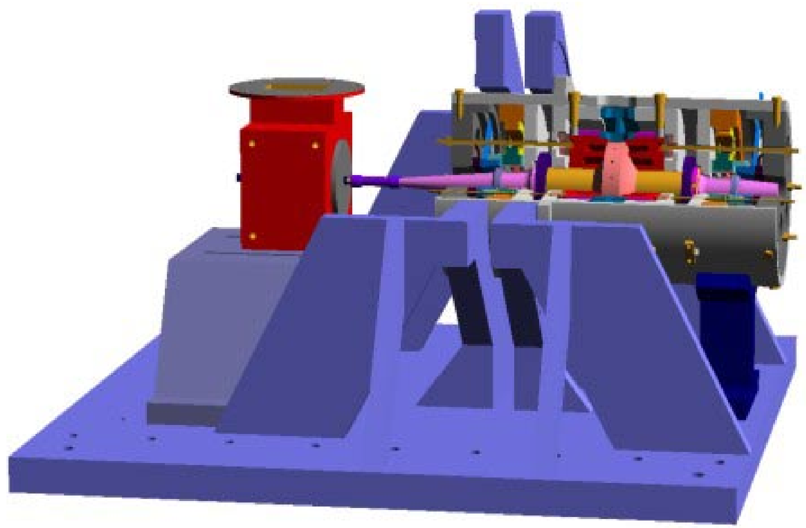

DESIGN OBJECTIVES

Design a system to test new magnetic thrust bearing design.

System will operate at:

- 30,000 RPM
- 1000^{o} F
- 1000 lb axial load

SYSTEM DESIGN REQUIREMENTS

- Provide safe design for electrical, high temperature and high rotor speed operation.
- Ability to set catcher bearing (CB) hot
- Find sensor target voltage hot
- Maintenance friendly
- Modular -- easy assembly/disassembly
- Roller bearing cooling for both inner and outer race
- Measure critical temperatures on TMB
- Measure TMB force while shaft is rotating at speed
- TMB supported on negligible axial spring stiffness from bearing supports

THE EXISTING RIG

- The existing base was designed to test radial bearing systems
- Tests of new systems often require alignment of all sub components at NASA
- New TMB test rig design will ease NASA alignment problems by using a modular design with pre-aligned internal components

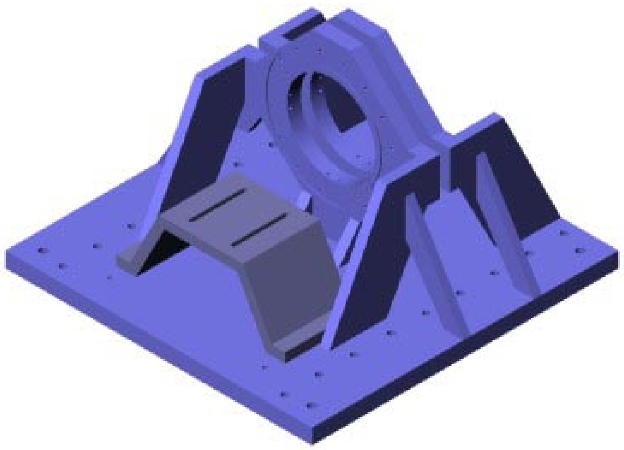

TMB SYSTEM

- TMB rig to be mounted off center to allow easier operation and access to thrust disk
- TMB test rig will simplify alignment because the system will be will be internally pre-aligned and partially tested before delivery

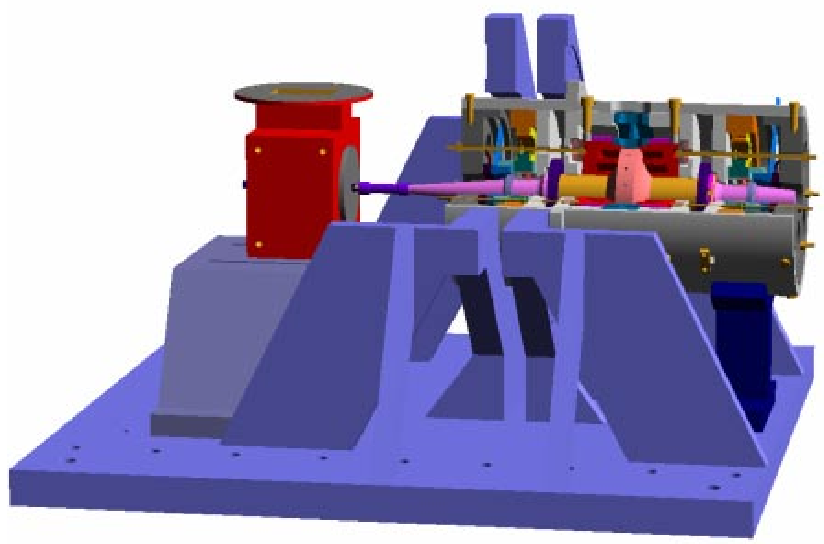

TMB TEST RIG

System consists of:

- 1) TMB rotor and stator
- 2) Shaft
- 3) Catcher bearings
- 4) Load cells
- 5) Axial rotor disk position system
- 6) Containment housing

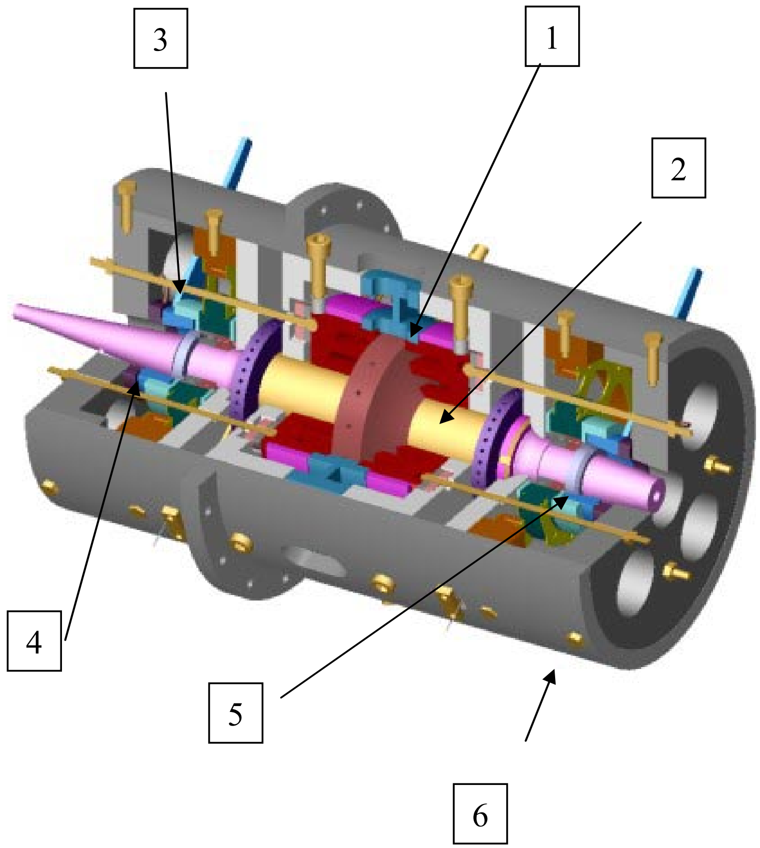

STATOR ADJUSTMENT COMPONENTS

- Aligned hot
- Macor barriers to lower heat from escaping
- Five DOF to adjust stator position

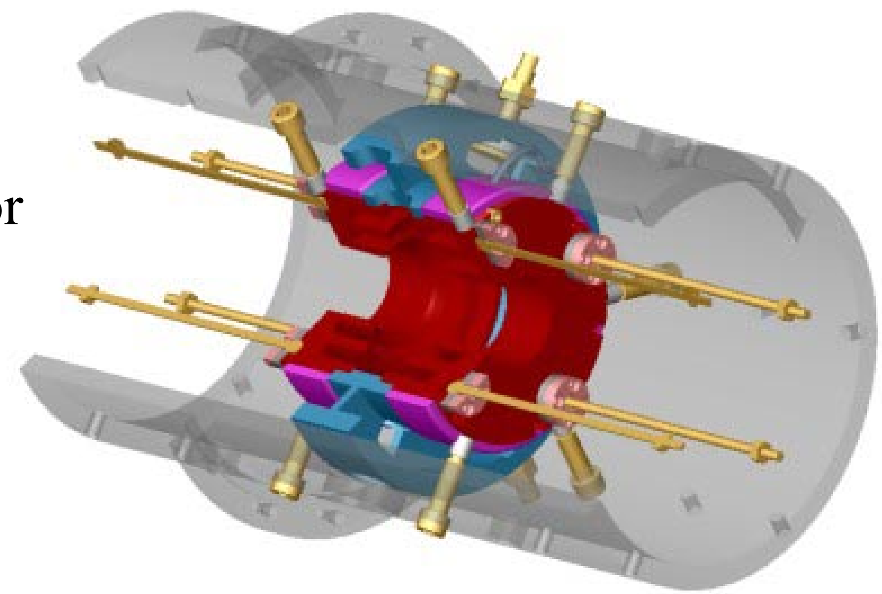

SHAFT ASSEMBLY

- Thrust Disk supported by sleeves to locate shaft axially
- Rotor dynamic analysis complete
- Air blown through hollow shaft lowers temperature of inner races on catcher bearings
- Three balance planes

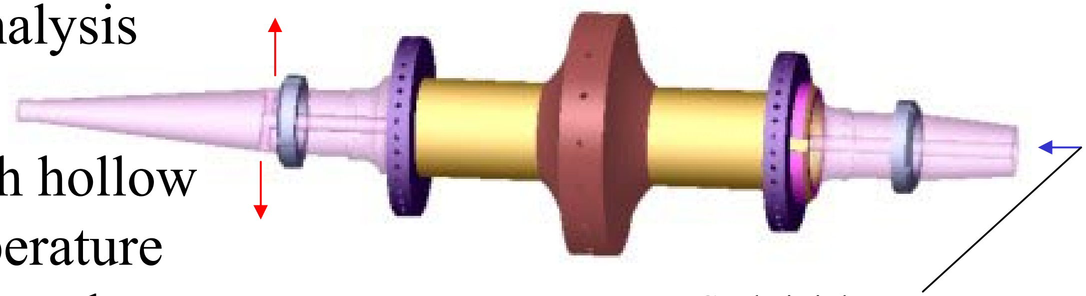

HEATING SYSTEMS

- 1) Watlow band heaters
- 2) High temperature insulation
- 3) Macor insulators
- Air cooling lines (not shown)

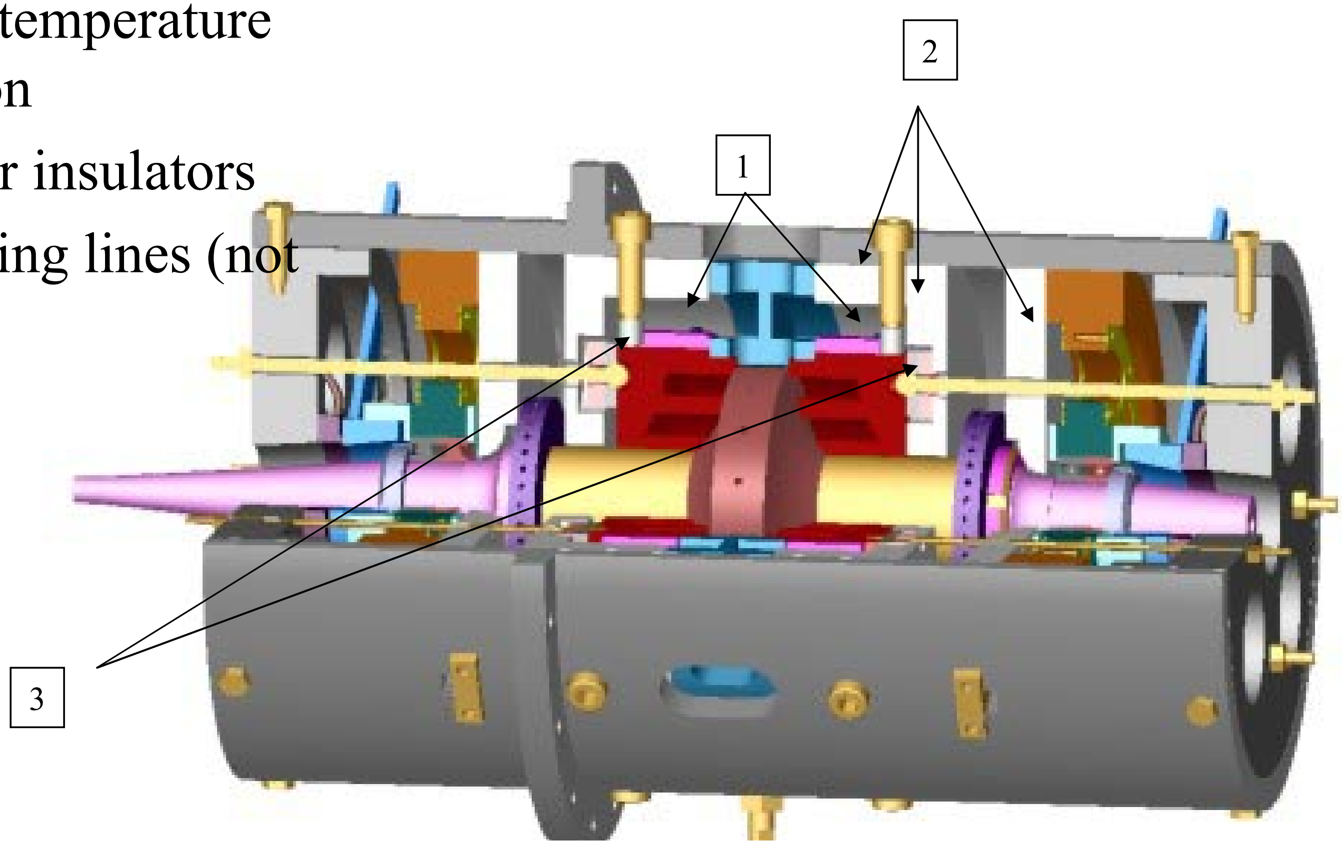

COOLING THE SYSTEM WITH AIR

- 1) Cool air is directed into the shaft on the outboard end and exits the shaft before reaching the shaft coupling
- 2) Cool air is directed into the containment housing
- 3) Heated air is released from the housing at the ends

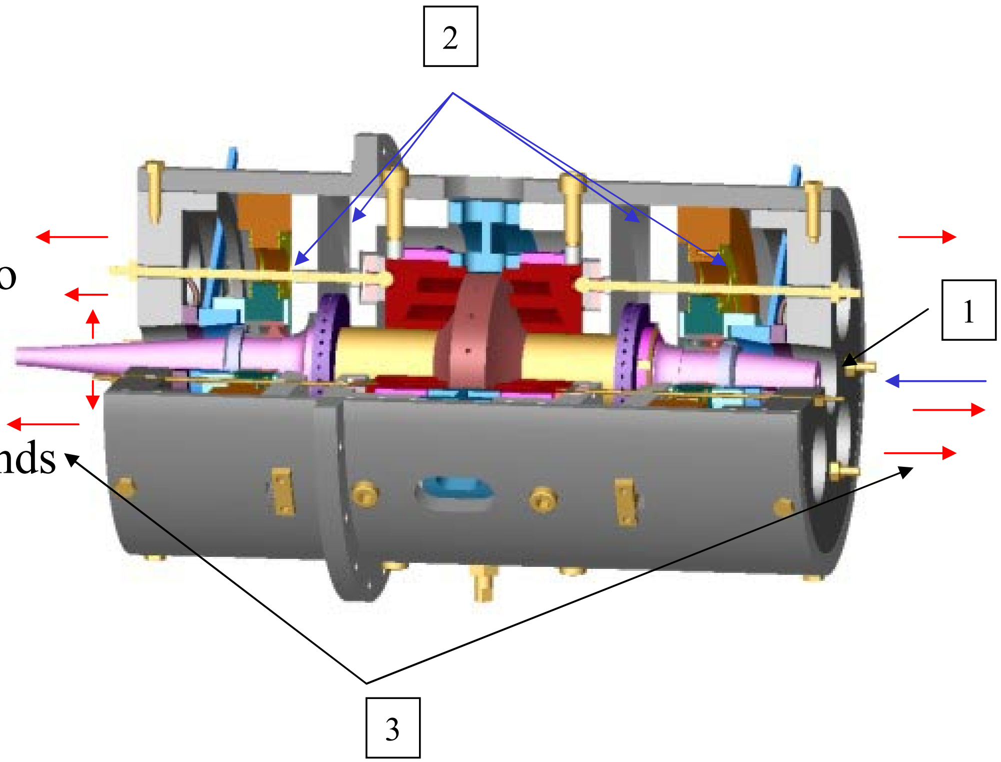

ROTOR POSITIONING SYSTEM

- 1) Rotor Disk Position and catcher bearing is accomplished by threaded nuts that push each end of the shaft through a load cell and bearing housing on each end of the shaft
- By releasing one and advancing another the thrust disk can be accurately positioned
- 2) Positioning arms allow the nuts to be moved from the outside while unit is hot. The arms are then locked in place

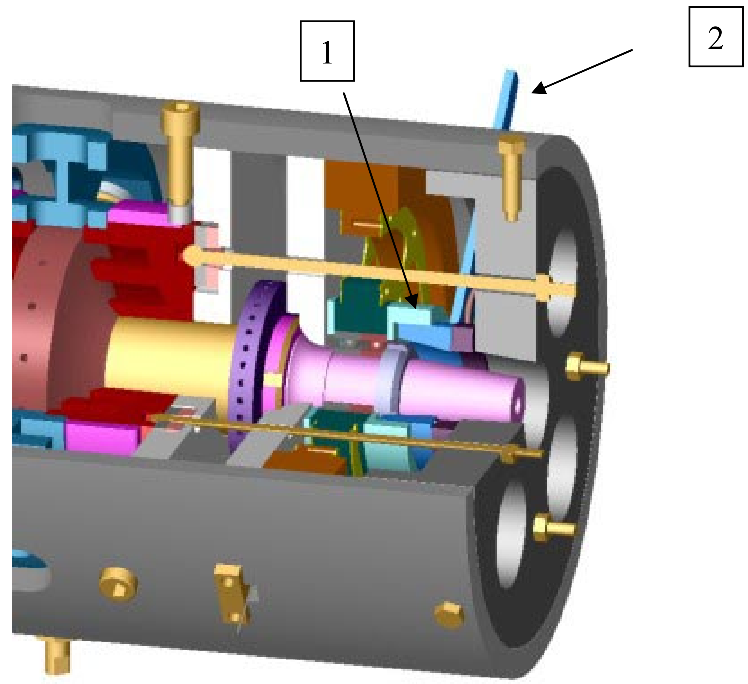

ROTOR POSITIONING CONTINUED

- With view port safety cover removed the gap can been accessed during disk repositioning
- Three ports enable the gap to be accurately set hot.

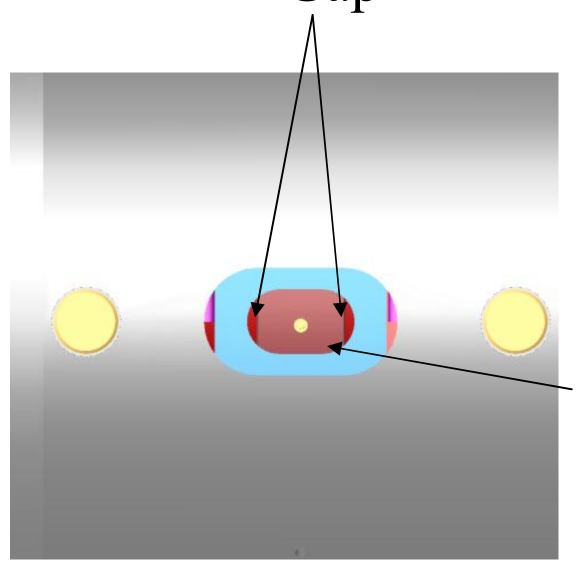

Top view of outer case, rotor disk, and gap

ASSEMBLY

- Components are slid in the containment cylinder from the ends

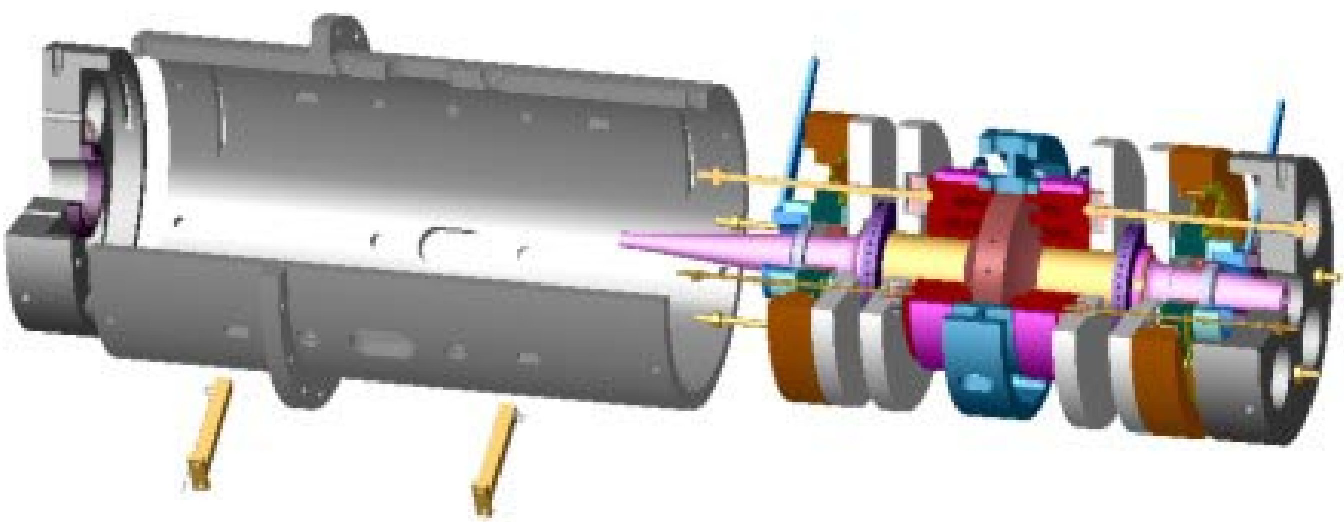

SHAFT POSITIONING CONTINUED

- 1) High temperature sensors directed towards face of balance plane detect changes in position
- 2) Sensor holder is adjustable from the outside
- 3) Sensors can be set under hot (heat soaked) conditions to eliminate thermal growth effects on target position.

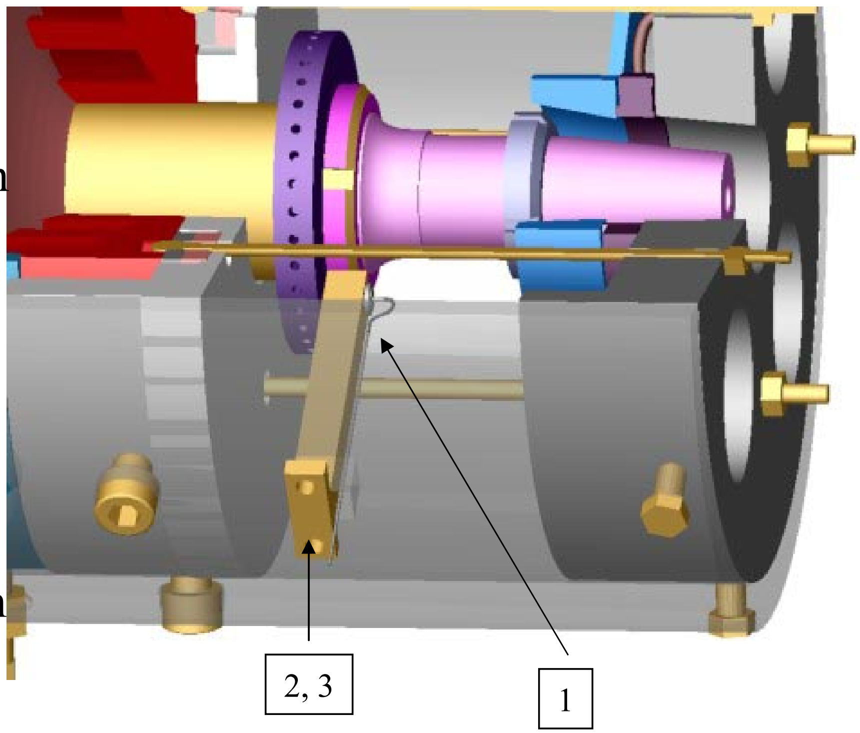

PRIOR TO ASSEMBLY

Before assembly the thrust disk and stator halves are checked cold to insure that they have been manufactured correctly.

- Faces of rotor and stators contact correctly along the pole surfaces
- When the stator halves are mated with the spacer around the thrust disk that there is the proper clearance. (Can check through the port opening and using plastiguage)

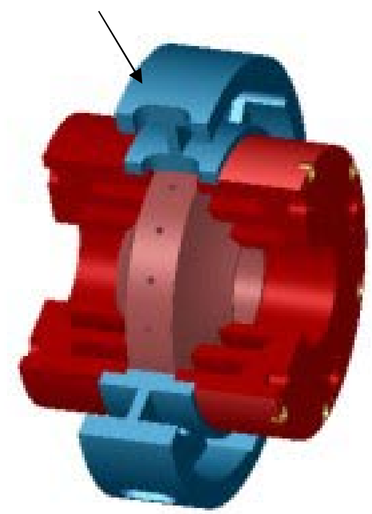

ASSEMBLY PROCEDURE

- Align the shaft/rotor in along the axis using shims to obtain necessary position
- Install spacers to bring the force nuts in light interference with the load cells
- Check for rattles and structure vibration modes near the operating speed

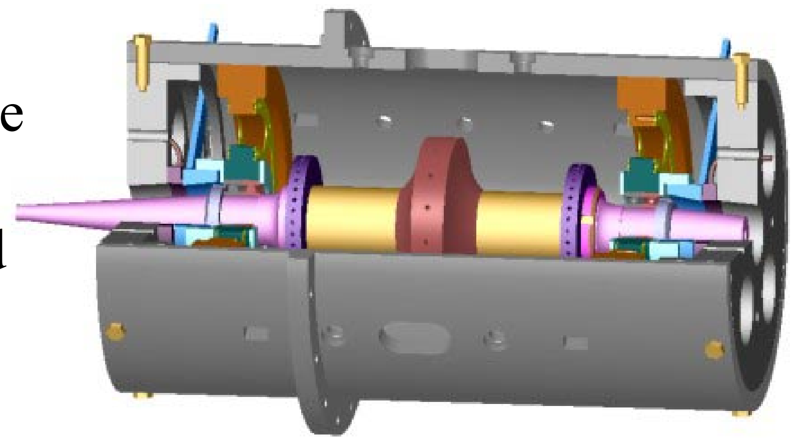

ASSEMBLY PROCEDURE CONTINUED

- Orientation of aligned components are marked on the housing.
- End caps, force nuts, arms and load cells are removed.
- The stator is positioned over the thrust disk.
- The entire assembly is slid into the containment cylinder
- Retaining bolts are then installed.
- Rough position alignment of rotor/stator is confirmed.
- Sensor and other components that are installed from the outside are added.

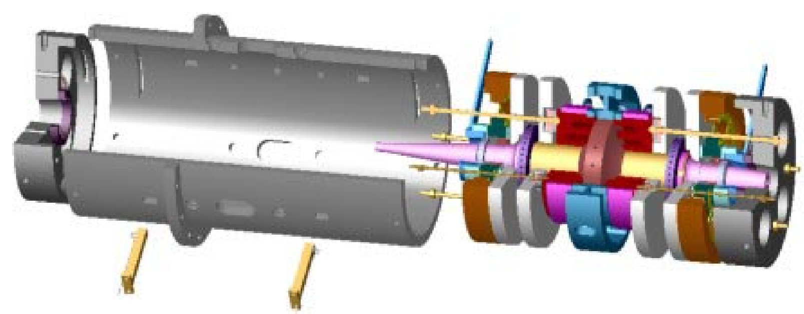

HIGH TEMPERATURE ALIGNMENT PROCEDURE CONTINUED

- After assembly and rough alignment the system is heat soaked and the stator is centered around the thrust disk
- Axial stator tensioning bolts are tightened while maintaining shaft center position using the thrust nuts.
- High temperature position sensors are brought in and checked.
- Shaft is pushed using the force nut arms to pole contact and position sensor values recorded. Scribed marks are made on the force nut arm locks indicating no-go areas.

All work is done with heat soaked conditions from the outside!

TASKS TO BE COMPLETED AT NASA

- 1) Install rig in base unit
- 2) Add end support
- 3) Connect and align turbine shaft
- 4) Three plane balance rotor

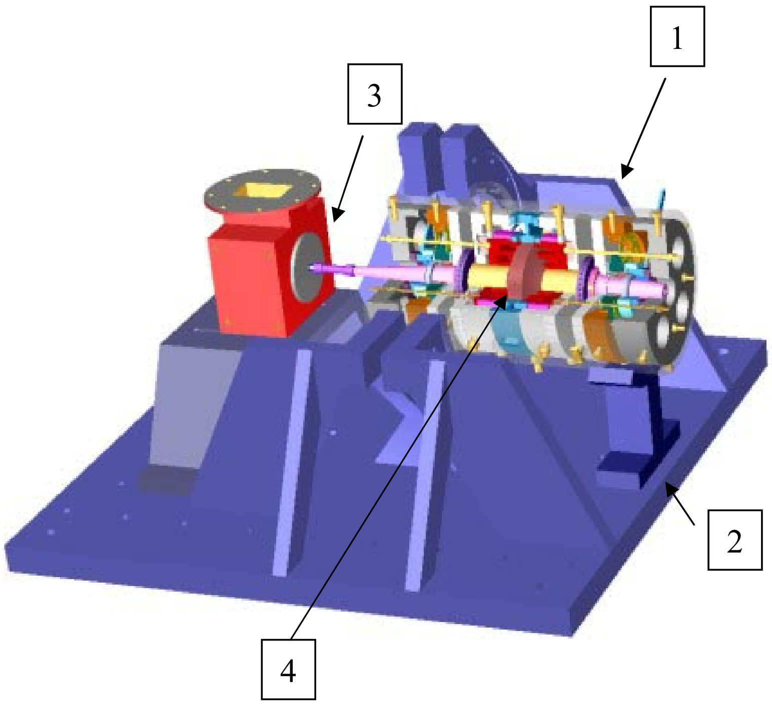

HIGH TEMPERATURE OPERATING PROCEDURE

Two ways the rig can be operated.

- Using only power amplifiers and no controller
- Using a controller

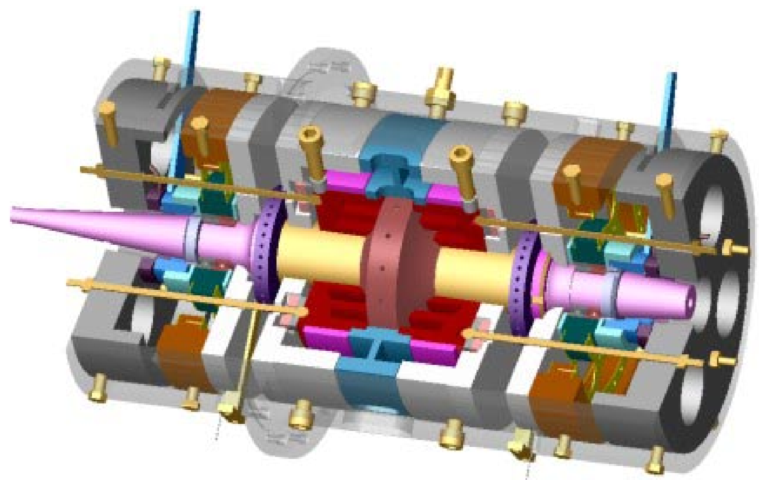

NO CONTROLLER OPERATON

- Unit can be operated in the no-controller mode by holding the thrust disk in the desired position using the thrust nuts.
- No rattle space is produced by clamping the thrust disk in position by both ends. This will even allow for a pre-load that can be added to the force produced by the coils.
- Thrust disk axial position can be varied from the center position to immediately before pole contact.

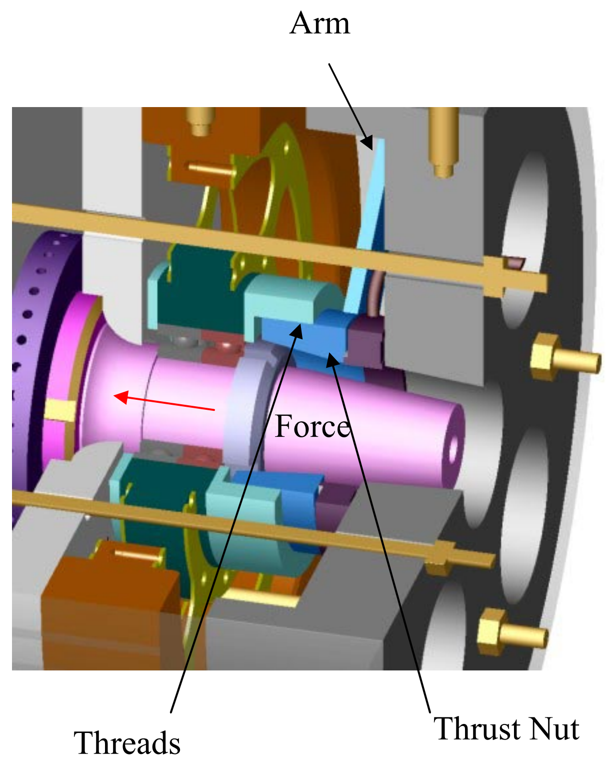

CONTROLLER OPERATON

- For use with a controller the thrust nuts are positioned to allow for a rattle space.
- The thrust nuts are moved to a position that will cause the roller bearings to work as catcher bearings to prevent a rub.
- Catcher bearings can be repositioned to allow controller to apply a force to the load cells that can be recorded.

DESIGN WORK REMAINING

- Add the wiring conduit in the module.
- Add the air cooling lines.
- Check measurements at both NASA and on parts to make sure there are no conflicts.
- Add details to make production drawings

NASA/CR—2003-212205

SUMMARY

- Safe
- Easy operation
- Low maintenance
- Cost effective

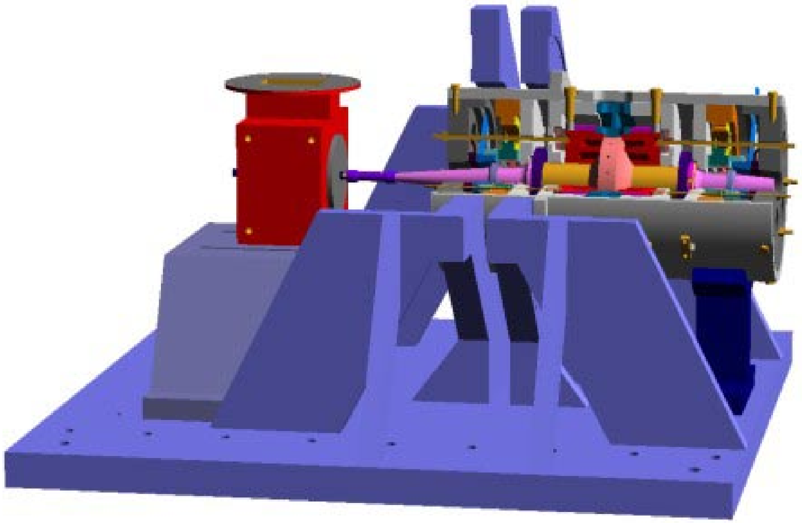

NASA/CR—2003-212205

Task A.3 : Radial High Temperature Magnetic Bearing Coil Progress

By:

Jason Preuss

Andrew Hunt

Randy Tucker

Dr. Alan Palazzolo

Winding and Potting of High Temperature Radial Magnetic Bearing C-Cores

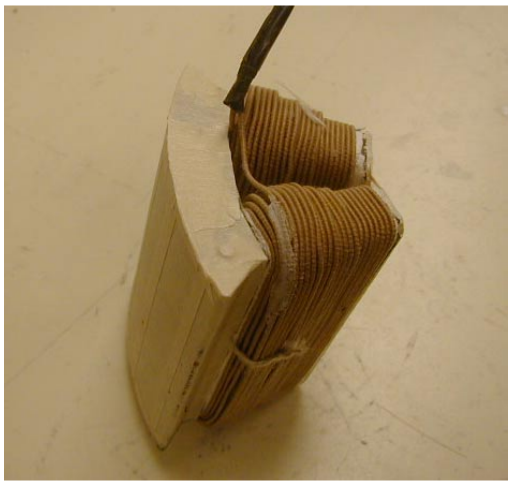

Figure A.3.1: Wound C-Core Prepared for Assembly into Mold

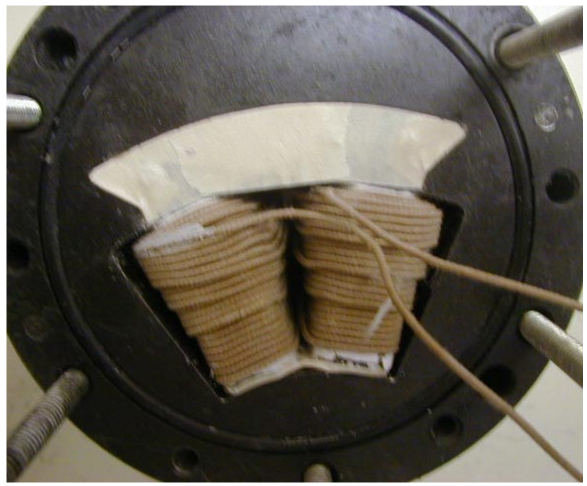

Figure A.3.2: View of Mold Cross Section During Assembly

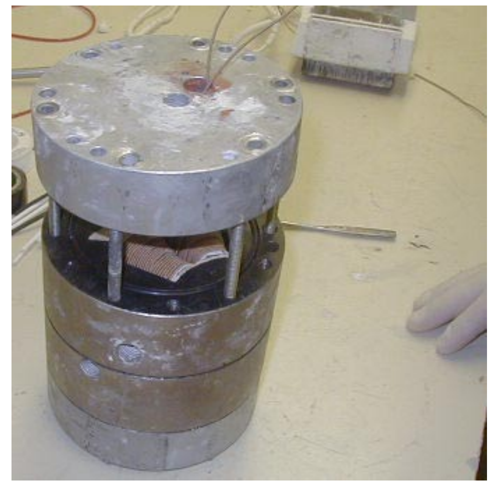

Figure A.3.3: Final Stages of Mold Assembly

Glenn Research Center

High Temperature Magnetic Bearing - Blade Loss Mitigation
NRA-GRC- 99-02 - 1Year Milestone Review
September 27, 2002, NASA Glenn

Texas A&M Vibration Control and Electromechanics Lab

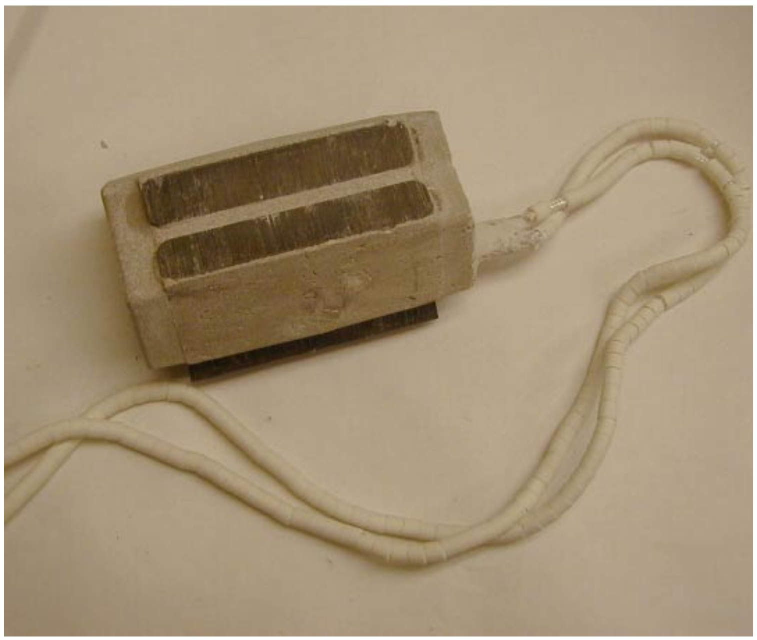

Figure A.3.4: Completed C-Core Ready for 1000F + Service

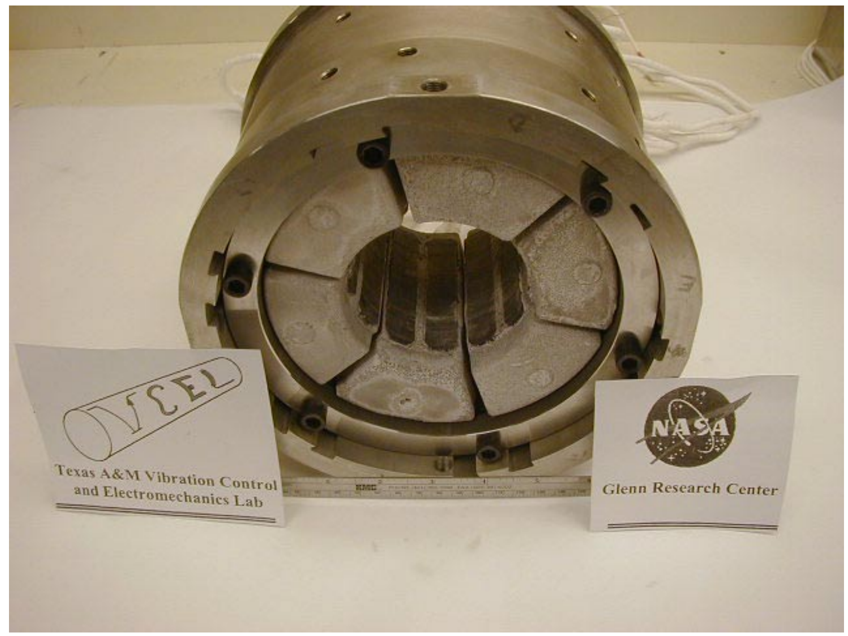

Figure A.3.5: C-Cores Assembled into Bearing Housing

12 Pole, High Temperature Magnetic Bearing Hi Pot Test at Texas A&M University, Coils 1-6: 12/20/01 and Coil 7: 07/01/02

C-Core	DC Voltage (V)	DC Current (micro-amps)	AC* Voltage (V)	AC* Current (micro-amps)	Inductance (mH)**	Q**
1	500	0	500	80	5.02	7.33
2	500	0	500	80	5.19	7.26
3	500	0	500	80	5.10	7.29
4	500	0	500	80	5.22	7.38
5	500	0	500	80	5.20	7.30
6	500	0	500	80	5.25	7.38
7	500	0	500	90	4.74	6.64

*** At 60 Hz**
**** At 120 Hz**
***** For Coils 1-6: Bearing Fully Assembled, No Rotor. Coil 7: Tested Individually**

Figure A.3.6: Typical Plot of Resistance vs. Temperature for High Temperature Radial Magnetic Bearing C-Cores (Data presented here taken from coil #7, fabricated 07/01/02)

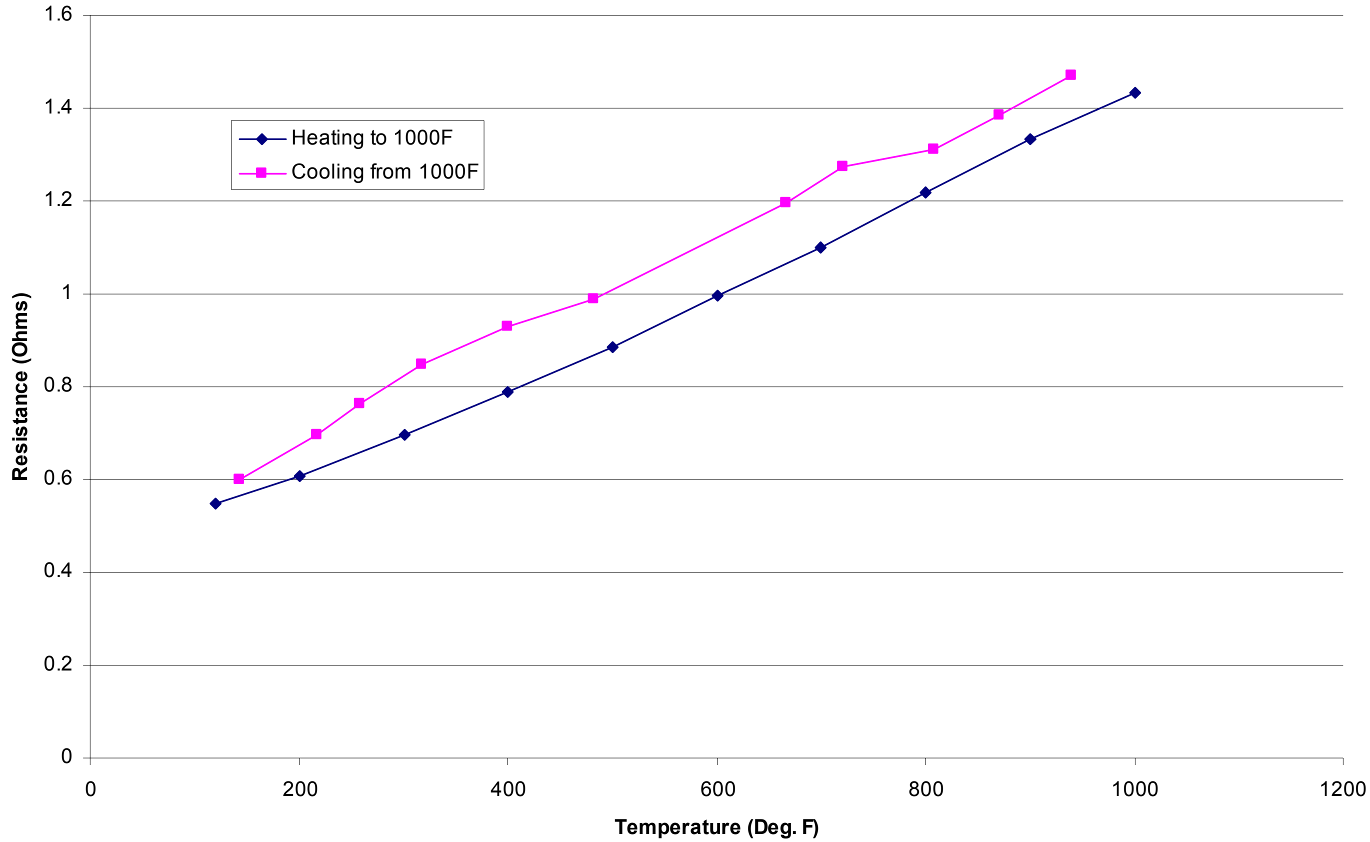

Present Status

- Fabricated replacement c-core for failed coil in Radial HTMB (July 02).
- Fabricating two backup c-cores with the following developments:
  1) Temperature probe embedded into potting for direct measurement of coil temperature.
  2) Electrical connector at wire exit of c-core to help eliminate lost coils due wire fatigue.

Temperature Probe for Direct Measurement of Coil Temperature

Probe Requirements:
1) Embedded and in contact with coils.
2) 1500F + Operating Temperature
(Coils operate above 1000F ambient)
3) Resistant to EMI

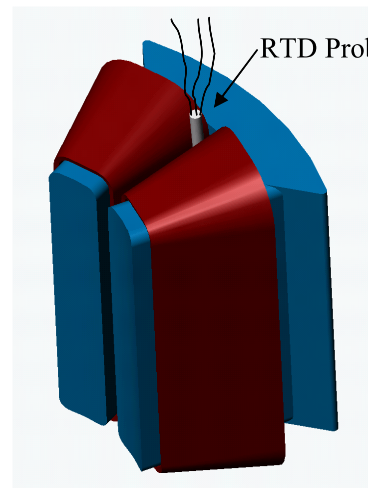

Probe Type : Platinum RTD (Omega)

Probe Specs:
1) Max Temp 1562F
2) Element Potted in Ceramic
3) Class B, 100 ohm, .00385 Curve Elements
4) Better resistance to EMI compared to thermocouple

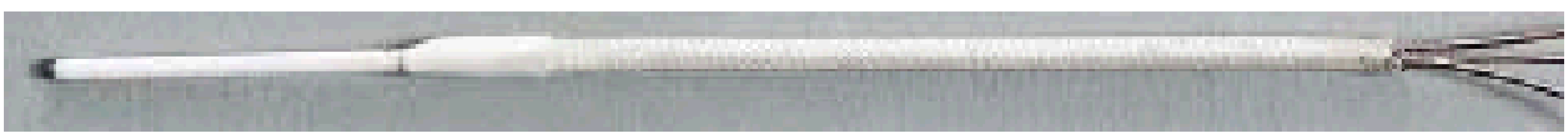

Figure A.1.3.7: High Temperature RTD Probe

High Temperature Electrical Connector

Objective: Provide electrical connector integral with potted c-core to eliminate current problems with fatigue at wire exit.

Current Status:
1) Threaded post arrangement chosen
2) High Temperature Tests to confirm long term electrical connection:
   a) Materials testing: Stainless, Inconel
   b) Gold Plating
3) Machining of mold to accommodate threaded posts during potting.

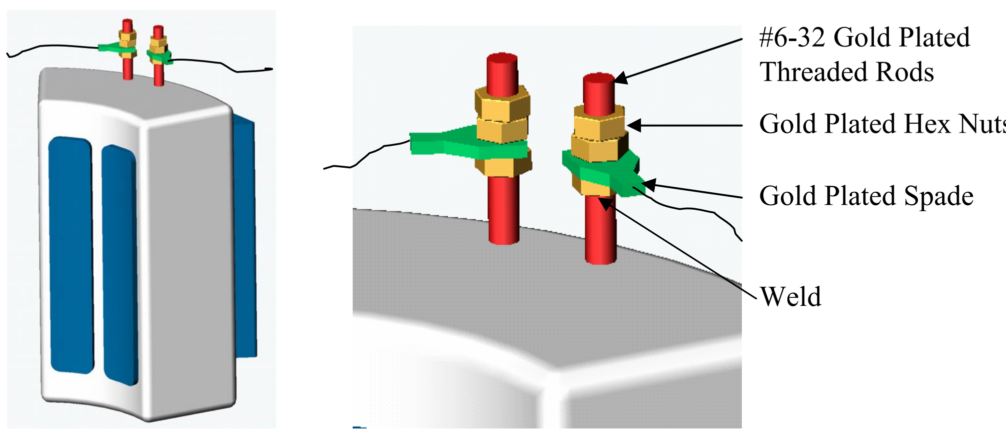

Figure A.1.3.8 : Radial HTMB Electrical Connector

Task A.4: 3D FE of HT Magnetic Thrust Bearing

(See Section A.1)

A.5 HT SENSOR DEVELOPMENT

Erwin Thomas, Dr. Andrew Kenny

&

Dr. Alan Palazzolo

High Temperature Magnetic Bearing - Blade Loss Mitigation
NRA-GRC- 99-02 - 1Year Milestone Review
September 27, 2002, NASA Glenn

Glenn Research Center

Texas A&M Vibration Control and Electromechanics Lab

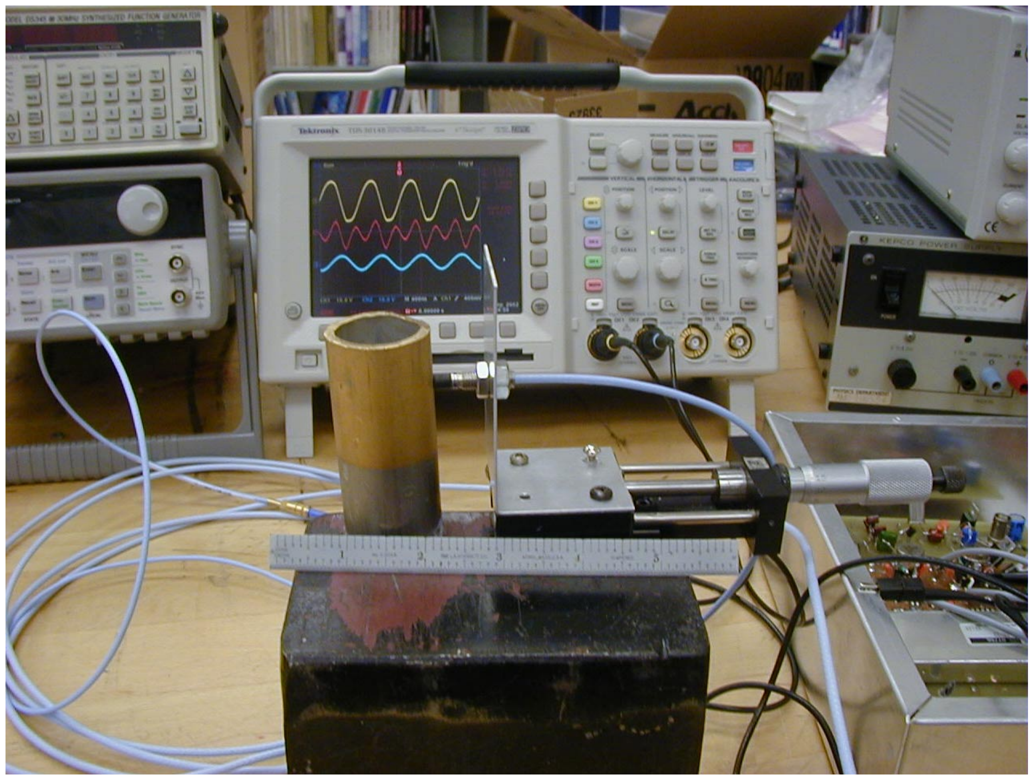

High Temperature Magnetic Bearing - Blade Loss Mitigation
NRA-GRC- 99-02 - 1Year Milestone Review
September 27, 2002, NASA Glenn

Glenn Research Center

Texas A&M Vibration Control and Electromechanics Lab

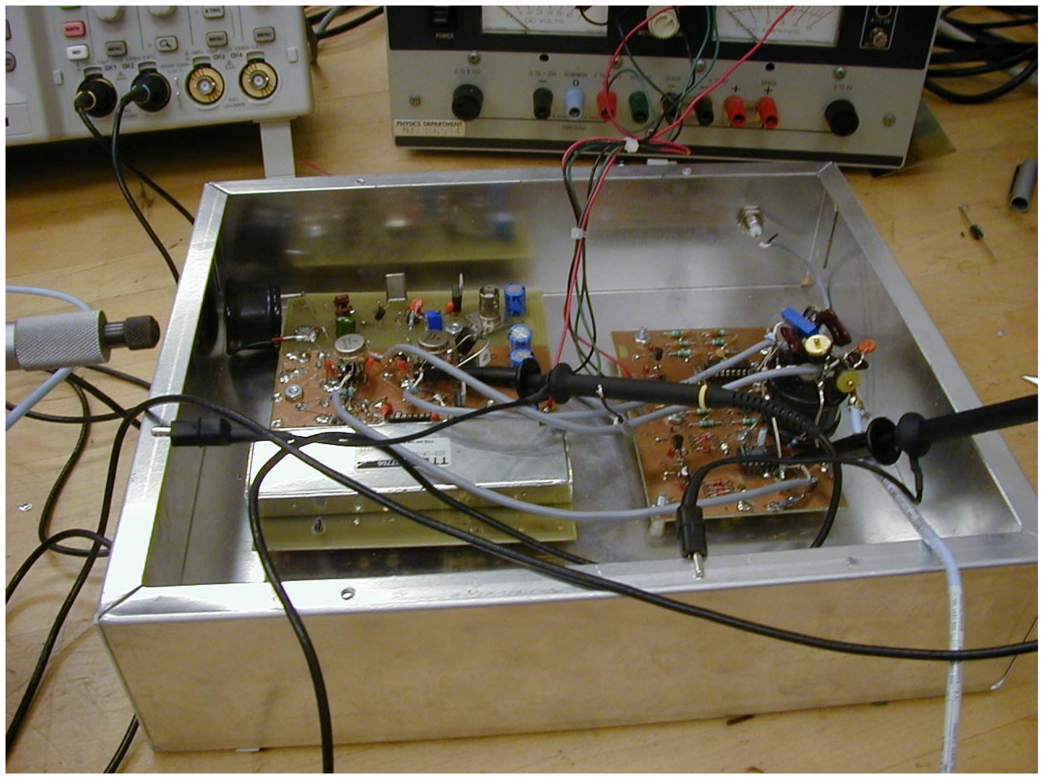

NASA/CR—2003-212205

HT Sensor Development

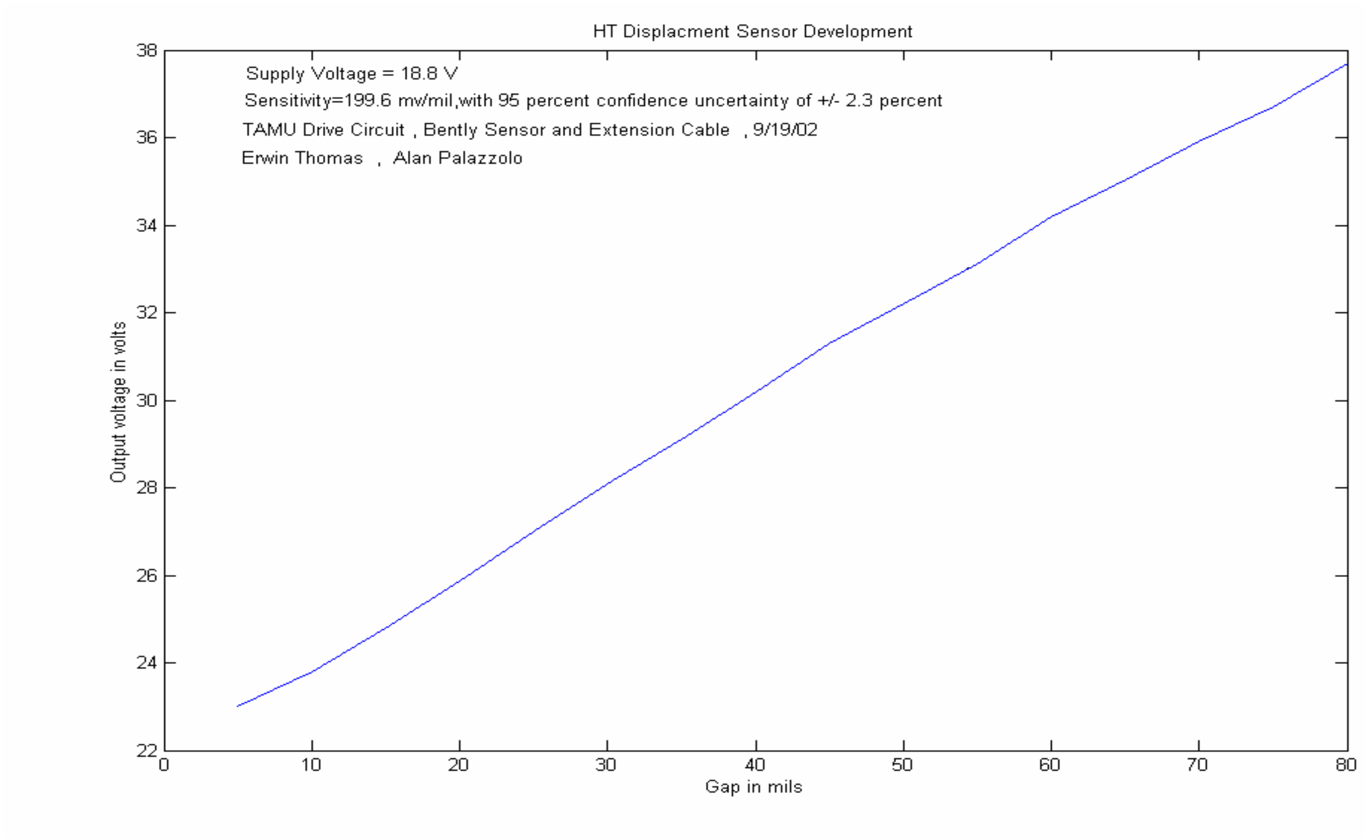

NASA/CR—2003-212205

High Temperature – High Frequency Position Sensor Study

By

Dr. Andrew Kenny

Objective: High ratio of signal to change in distance

Approach: Examine effect of coil parameters on coil inductance at 10 MHz with FEA model

Eddy Currents Generated by 10 MHz Position Sensor

On Rotor Surface

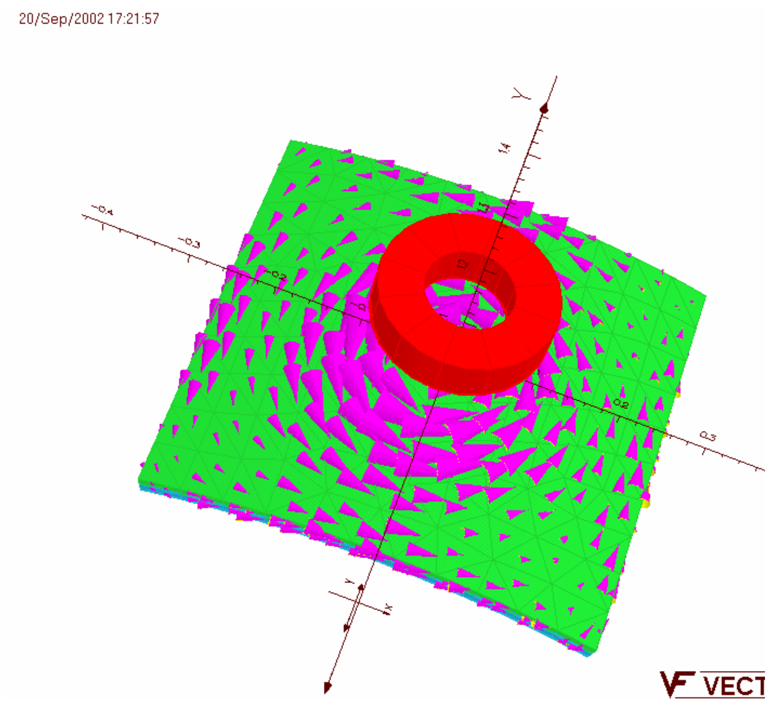

Just Below Rotor Surface

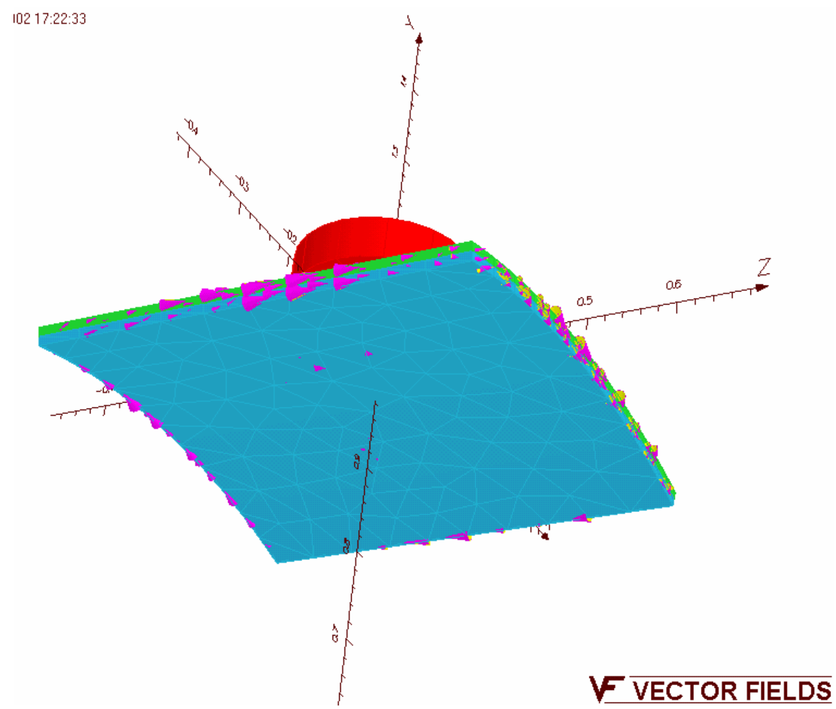

Glenn Research Center

High Temperature Magnetic Bearing - Blade Loss Mitigation
NRA-GRC- 99-02 - 1Year Milestone Review
September 27, 2002, NASA Glenn

Texas A&M Vibration Control and Electromechanics Lab

Bias Flux Density on Rotor Surface

At DC Frequency

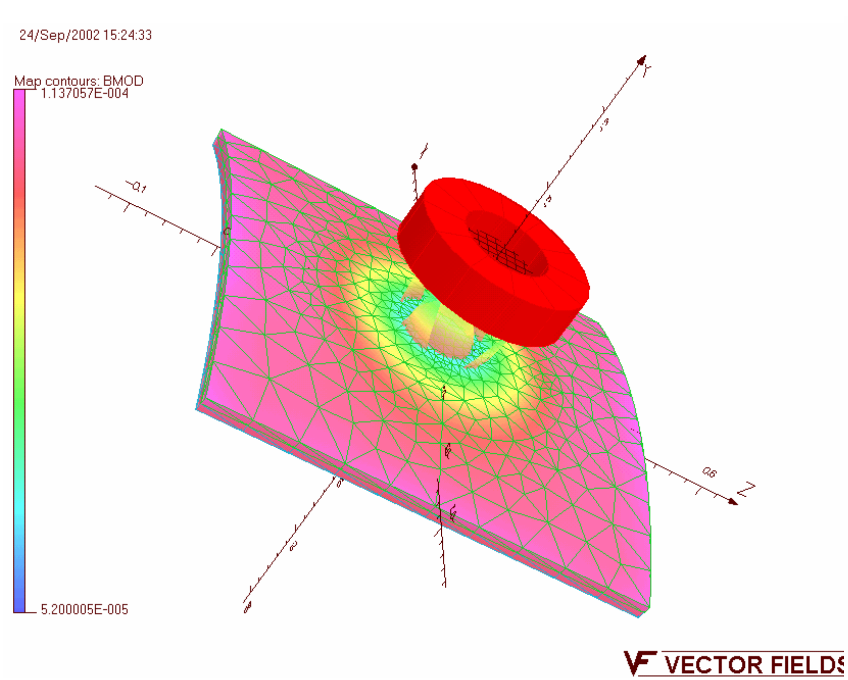

At 10 MHz

(The Field is Completely Reflected)

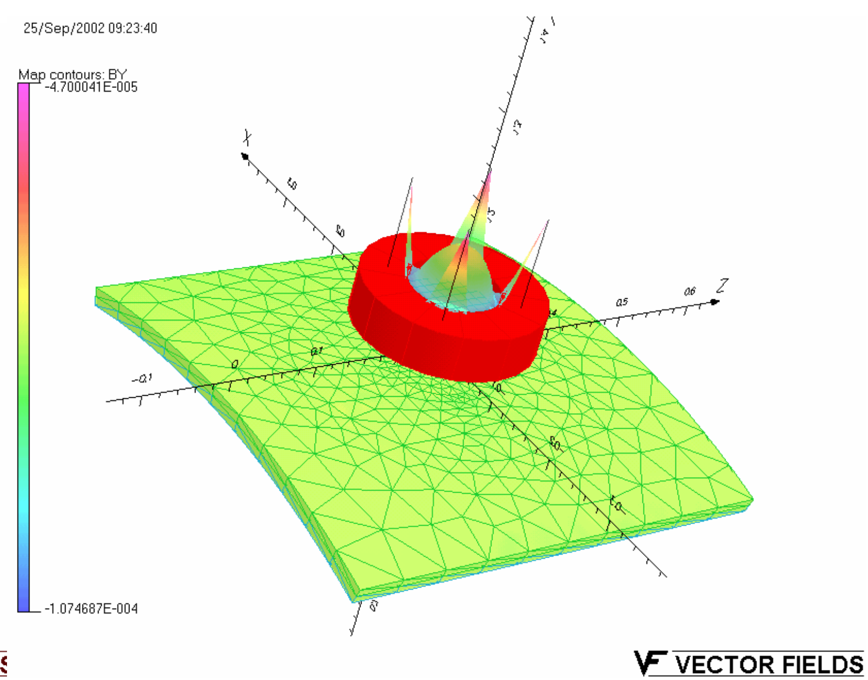

Quantitative Results

(Flux passing thru center hole of coil indicates inductance)

Frequency	Mean Coil Height	Integrated Flux Density Thru Hole
10 MHz	0.125 in	5.981 nWb
10 MHz	0.100 in	5.903 nWb
10 MHz	0.075 in	5.735 nWb
10 MHz	0.050 in	5.290 nWb

Conclusion: This coil configuration is only mildly sensitive to position at this distance.
Summary: Another set of dimensions is being worked out to increase position sensitivity.

NASA/CR—2003-212205

Task B.1: 2D Isolated Ball Bearing Code

by
Guangyoung Sun, Ph.D. Candidate
and
Dr. Alan B. Palazzolo, Professor

Objectives

- A bearing analysis code was developed based on J. M. de Mul's work[1].
- Given bearing information (geometry, material, preload, etc.) from vendors, the code can *predict the stiffness, drag torque and ball whirl rate* for angular contact ball bearing.
- The simulation results can be used in numerical bearing model and in power loss calculation.

1. J. M. de Mul, et al., Jan. 1989, "Equilibrium and Associated Load Distribution in Ball and Roller Bearings Loaded in Five Degrees of Freedom While Neglecting Friction-Part I: General Theory and Application to Ball Bearings", *ASME Journal of Tribology*, Vol.111, pp.142 - 148

Executive Summary

- Radial stiffness from the code is compared to the results from two references: an ASME paper[2], BASDREL (Ball Bearing Stress Deflection Reliability and Life written by Crawford Meek). It shows good match with a little difference.
- Ball whirl rate from the code is compared to the calculation using Barden Brg. BPFO (Ball Pass Frequency Outer). It also shows good match.
- Drag torque from the code is compared to the result from BASDREL. It still shows good match with a little difference.
- The developed code provides reliable analysis for commercial ball bearing model.

2. Bert R. Jorgensen and Yung C. Shin, Oct. 1997, "Dynamics of Machine Tool Spindle/Bearing Systems Under Thermal Gorwth", *ASME Journal of Tribology,* Vol.119, pp.875 - 882

Fig.B.1.1 Generalized Schematic of Ball Bearing

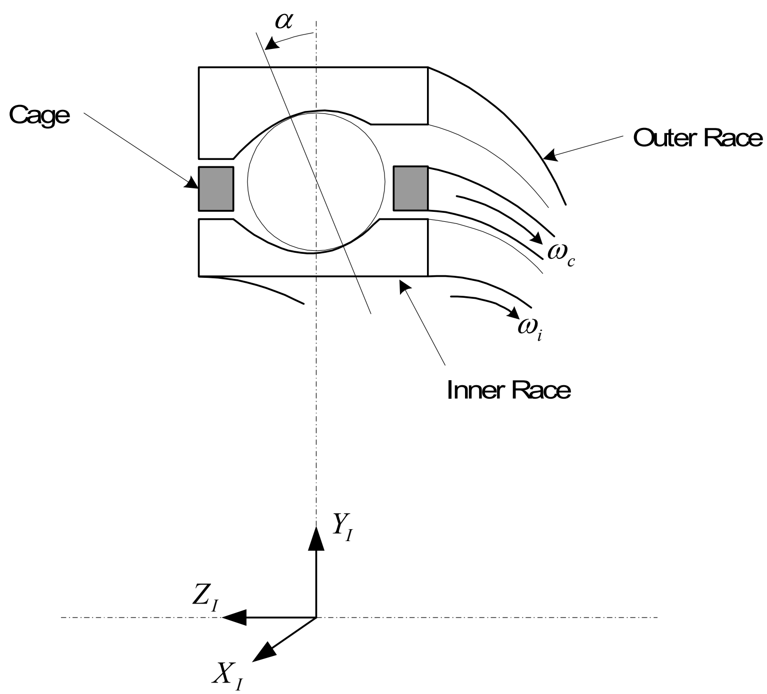

Fig.B.1.2 Inner Race Coordinate Transformation

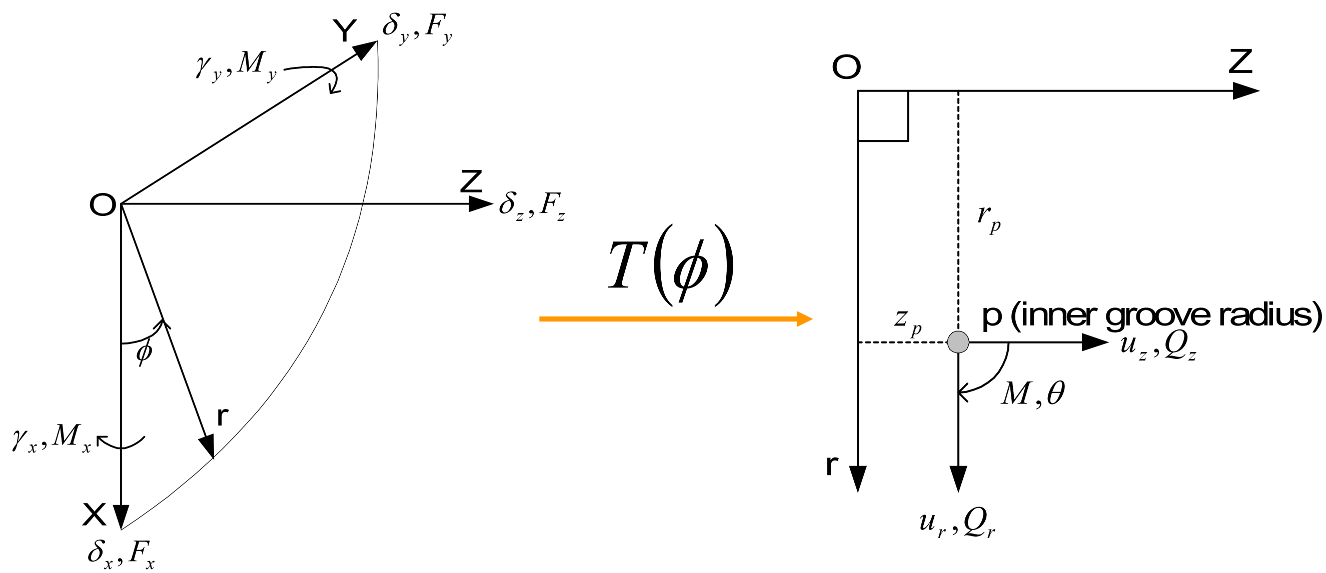

(a) Bearing loads and displacements

(b) Cross section with contact loads

Bearing Load Equilibrium Equations

- It is assumed that outer race is fixed in housing.
- Inner race load equilibrium equations

$$\{F\} + \sum_{j=1}^{n} T'\{Q\}_j = \{0\}$$

where

$\{F\}^T = \{F_x, F_y, F_z, M_x, M_y)$, $\{Q\}^T = \{Q_r, Q_z, M\}$ and

$$T = \begin{bmatrix} \cos\phi & \sin\phi & 0 & -z_p \sin\phi & z_p \cos\phi \\ 0 & 0 & 1 & r_p \sin\phi & -r_p \cos\phi \\ 0 & 0 & 0 & -\sin\phi & \cos\phi \end{bmatrix}$$

NASA/CR—2003-212205

Bearing Load Equilibrium Equations (continued)

- Ball load equilibrium equations

$$\begin{Bmatrix} F_r \\ F_z \end{Bmatrix} = \begin{Bmatrix} Q_i \cos\alpha_i - Q_e \cos\alpha_e + F_c \\ Q_i \sin\alpha_i - Q_e \sin\alpha_e \end{Bmatrix} = \begin{Bmatrix} 0 \\ 0 \end{Bmatrix}$$

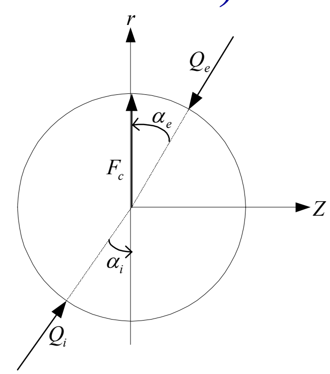

- Linearized equations to use Newton-Raphson method

For inner race,

$$\{F\} + \sum_{j=1}^{n} T'\{Q\}_j + \sum_{j=1}^{n} T'_j \cdot \left[\frac{\partial\{Q\}}{\partial\{u\}^T}\right]_j \cdot T_j\{\Delta\delta\} = \{0\}$$

where $\{u\}^T = \{u_r, u_z, \theta\}$, $\{\delta\}^T = \{x, y, z, \gamma_x, \gamma_y\}$ and $\{u\} = T\{\delta\}$

Bearing Stiffness

For ball,

$$\begin{Bmatrix} F_r \\ F_z \end{Bmatrix} + \begin{bmatrix} \dfrac{\partial F_r}{\partial v_r} & \dfrac{\partial F_r}{\partial v_z} \\ \dfrac{\partial F_z}{\partial v_r} & \dfrac{\partial F_z}{\partial v_z} \end{bmatrix} \cdot \begin{Bmatrix} \Delta v_r \\ \Delta v_z \end{Bmatrix} = \begin{Bmatrix} 0 \\ 0 \end{Bmatrix}$$

where v_r and v_z are ball locations.

- For duplex pair of bearing, the number of rows are multiplied to the obtained radial bearing stiffness to get the total stiffness.

Drag Torque

- From the empirical evaluation by Palmgren[3], the total drag torque $M_f = M_{fl} + M_{f\nu}$ is the sum of

$$M_{fl} = f_1 F_\beta d_m \text{ : due to applied loads}$$

$$M_{f\nu} = 1.42E-5 \cdot f_o (\nu_o N_i)^{2/3} d_m^3 \text{ : due to viscosity and speed}$$

where f_1 and f_o factors depending on bearing type and lubricant, respectively, ν_o is viscosity [cst] of lubricant, N_i is IR spinning speed [rpm], d_m is pitch diameter, and F_β is external loads.

3. Tedric A. Harris, 1984, "Rolling Bearing Analysis", 2nd Version, Wiley-Interscience

Ball Whirl Rate

- The rotational speed of rolling element set is

$$n_c = \frac{1}{2} n_i (1-\gamma) \text{ [rpm]}$$

where n_i = inner race speed, n_o = outer race speed
$\gamma = D\cos\alpha / d_m$ (D: ball diameter, α: contact angle)

- Ball whirl rate from a brg caltalogue can be calculated as

$$n_c = \frac{BPFO}{N_b} n_i$$

where $BPFO$ is Ball Pass Frequency Outer and N_b is the numbers of balls

Model Validation

- The results from the code are compared to three references:

  ASME paper, BASDREL (commercialized bearing analysis code) and Barden brg catalogue.

- Radial stiffness and drag torque

  Brg specs: α_o = 15 deg, d_m= 0.09 m, D = 0.0119 m, N_b = 20

  Loads and viscosity: F_a = 540 N, F_x = 500 N, v = 30 cst

  Ball materials: steel or ceramic

- Ball whirl rate

  Barden brg CZSB103J (brg specs are in result section)

  From brg catalogue, *BPFO* = 6.822

Fig.B.1.3 Radial bearing stiffness

(-: our code, o: ASME paper, Δ: BASDREL)

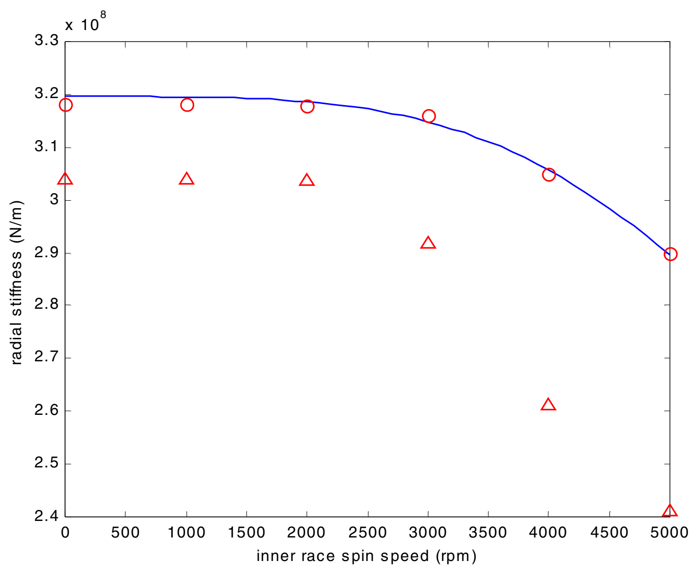

(a) Steel ball bearing

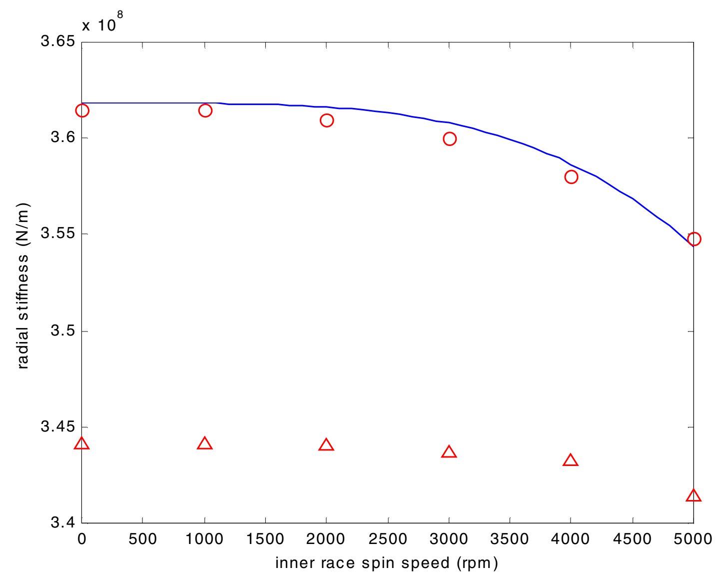

(b) Ceramic ball bearing

Fig.B.1.4 Drag torque and ball whirl rate
(-: our code, o: BASDREL or Barden brg catalogue)

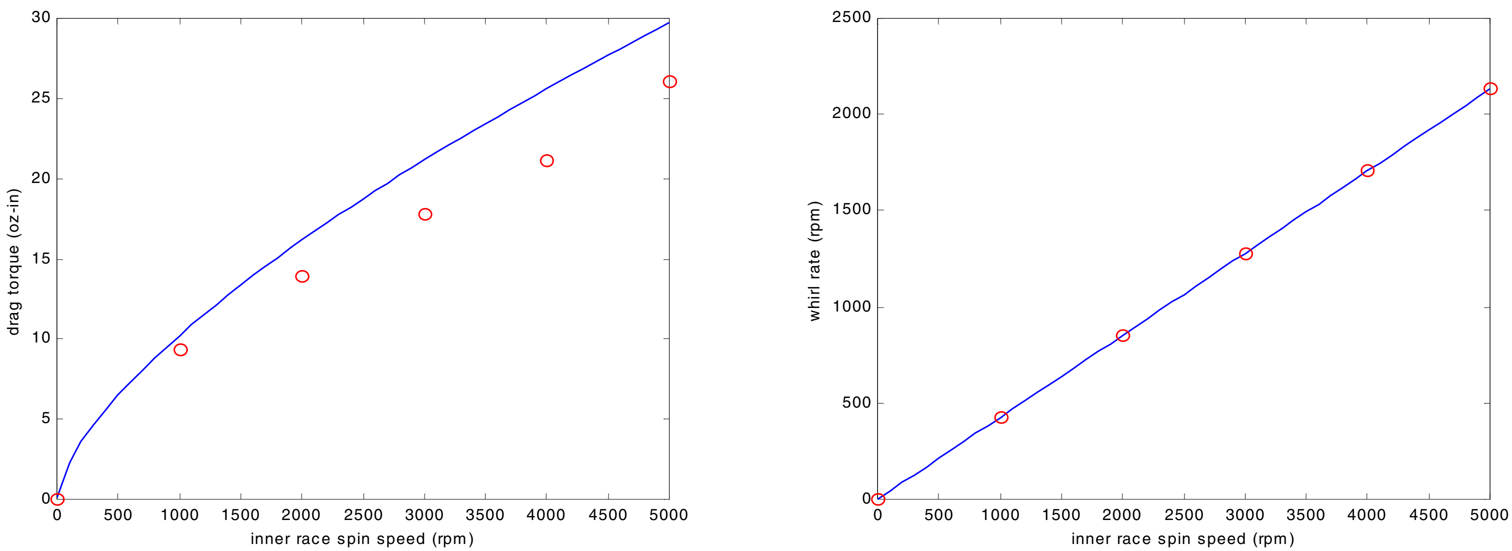

(a) Drag torque

(b) Ball whirl rate

Results

- Bearing analysis is conducted for commercial Barden ball bearing model (model No: CZSB103J)

Property	Specification
Geometry	
Bore diameter, BD	0.6693 [in]
Outside diameter, OD	1.3780 [in]
Width	0.3937 [in]
Inner and outer race groove radius, $r_{i,e}$	0.082 and 0.0844 [in]
Number of balls	16
Diameter of a ball, D	5/32 [in]
Initial contact angle	15 [degree]
Material	
Density of ball	0.11553 [lb/in^3]
Density of inner and outer race	0.2816 [lb/in^3]
Elastic modulus of ball	45E+6 [psi]
Poisson's ratio of ball	0.26
Elastic modulus of inner and outer race	30E+6 [psi]
Poisson's ratio of inner and outer race	0.3
Lubricant viscosity	30 [cst]
Axial prelod	5, 10, 20 [lb]

Fig.B.1.5 Barden ball bearing stiffness for different speeds and preloads

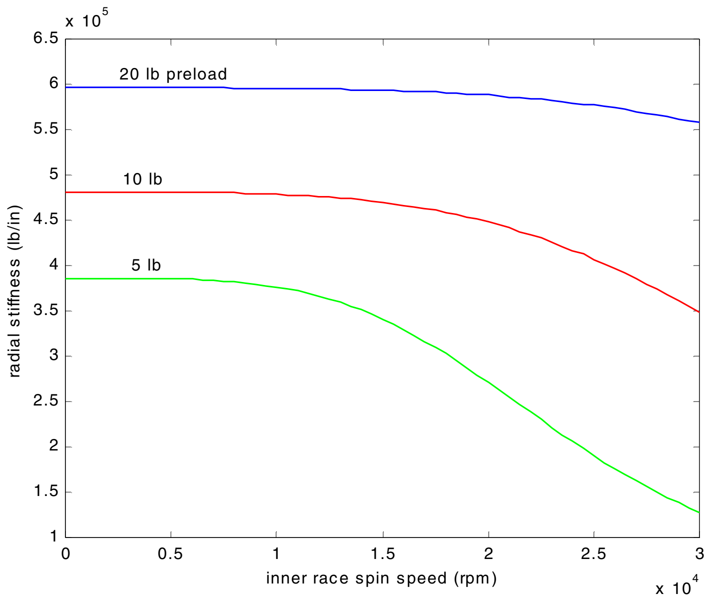

(a) Radial stiffness

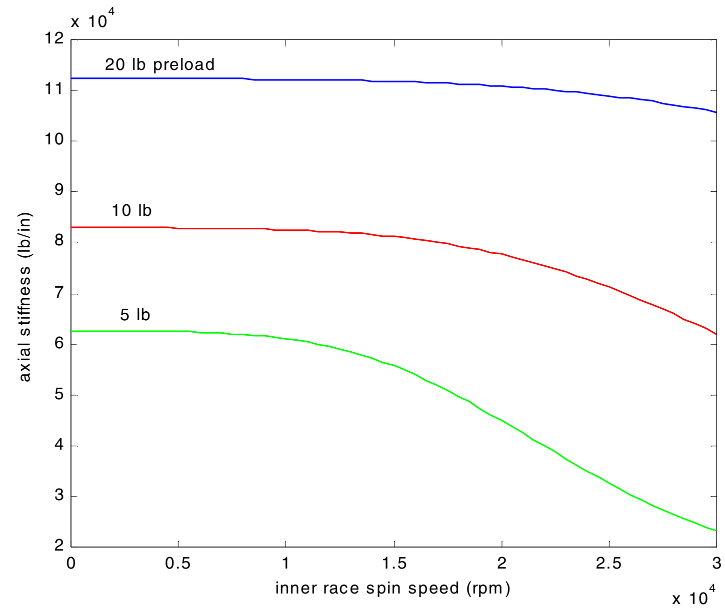

(b) Axial stiffness

Glenn Research Center

High Temperature Magnetic Bearing - Blade Loss Mitigation
NRA-GRC- 99-02 - 1 Year Milestone Review
September 27, 2002, NASA Glenn

Texas A&M Vibration Control and Electromechanics Lab

Fig.B.1.6 Contact angles and loads for different speeds and preloads

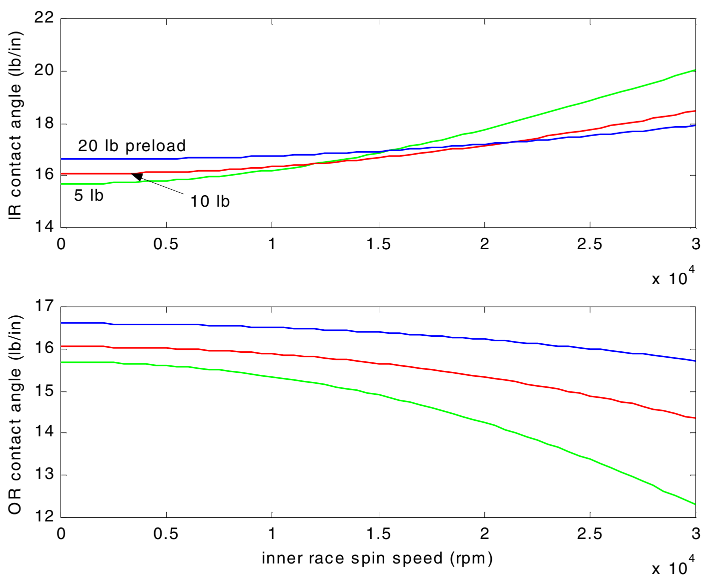

(a) Contact angle

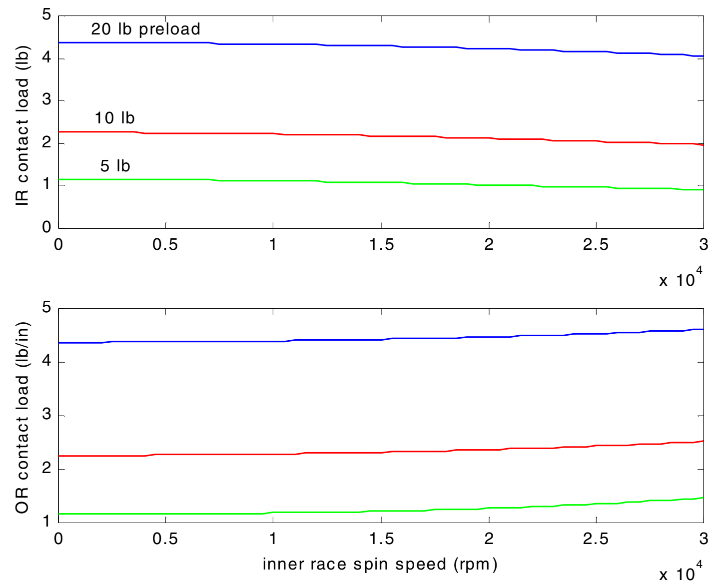

(b) Contact load

Fig.B.1.7 Drag torque and ball whirl rate for different speeds and preloads

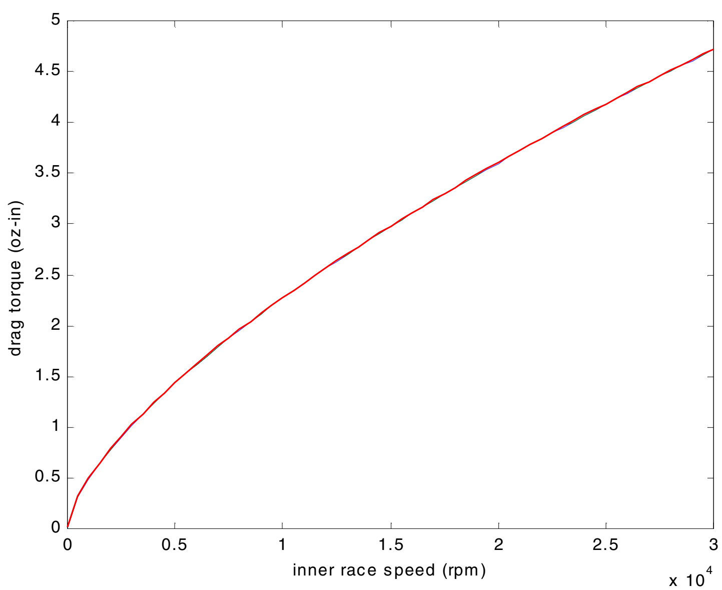

(a) Drag torque for 5, 10, 20 lb

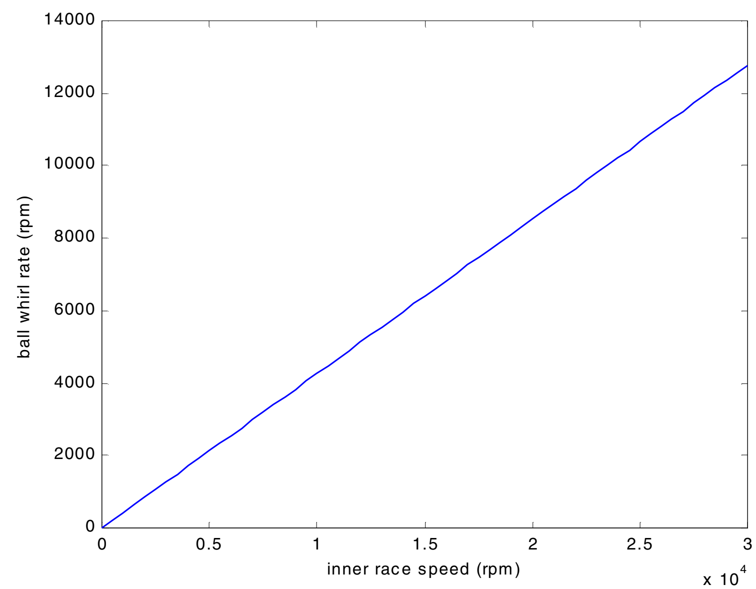

(b) Ball whirl rate

Summary

- The bearing analysis code is developed and validated by the references.
- The code can provide reliable analysis (bearing stiffness, drag torque and ball whirl rate) for commercial ball bearing model.
- The obtained results can be utilized in bearing simulation model and in power loss prediction.

TASK B2 : GUI for 2D Isolated Ball Bearing Code

By

Karthik Ganesan

&

Lakshmi Subramaniyam

EXECUTIVE SUMMARY:

Dedicated code and GUI developed to produce stiffness and power loss estimates for Isolated Ball bearing speed Vs speed and preload

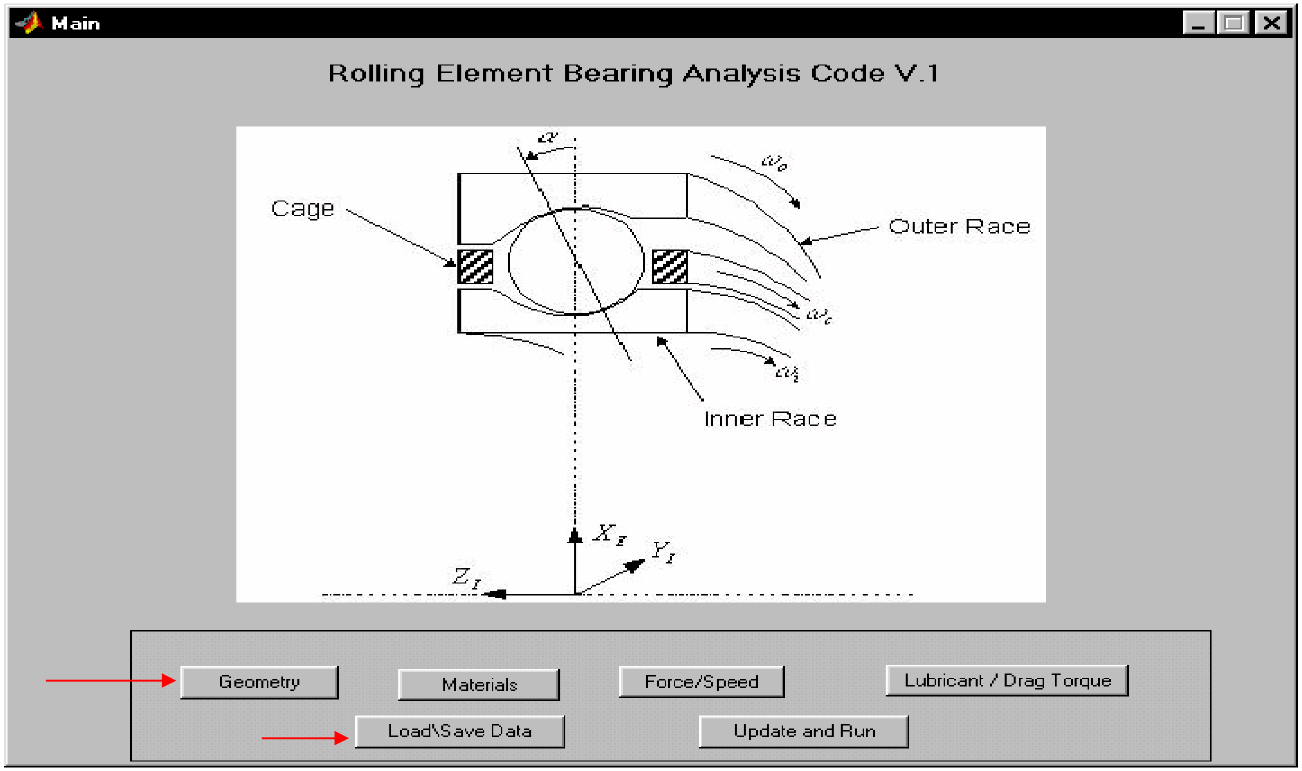

This is the main panel. A user can load previously saved data by clicking on "Load/Save Data" panel or enter a new set of bearing data for four categories (top four panels).

Glenn Research Center

High Temperature Magnetic Bearing - Blade Loss Mitigation
NRA-GRC-99-02 - 1Year Milestone Review
September 27, 2002, NASA Glenn

Texas A&M Vibration Control and Electromechanics Lab

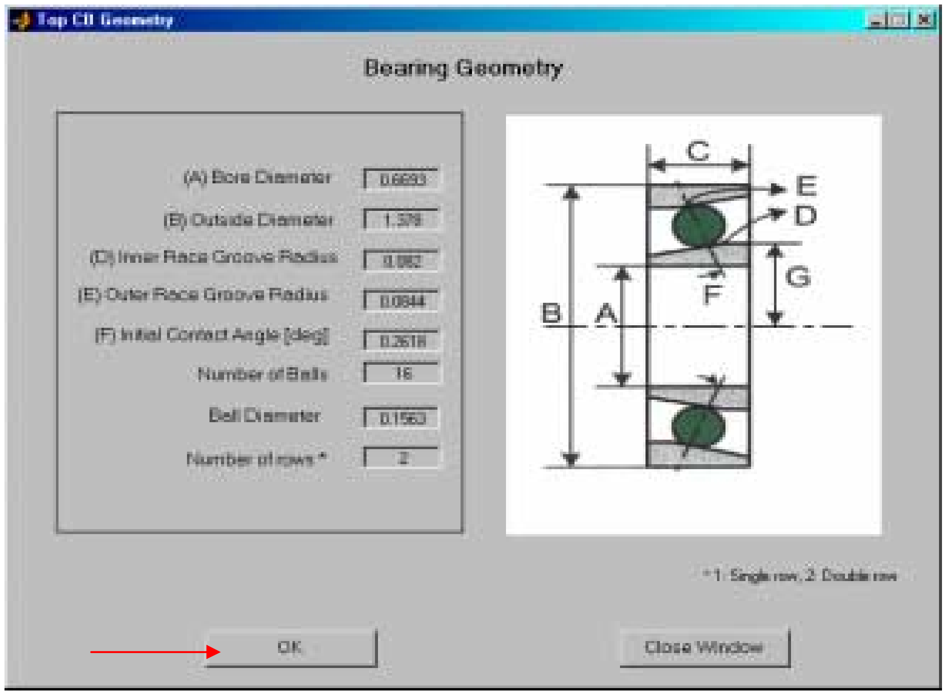

This panel contains all the geometric information of the bearing.
A cutaway diagram is shown indicating the dimensions to the user.
Click on OK after all the geometric data is entered.

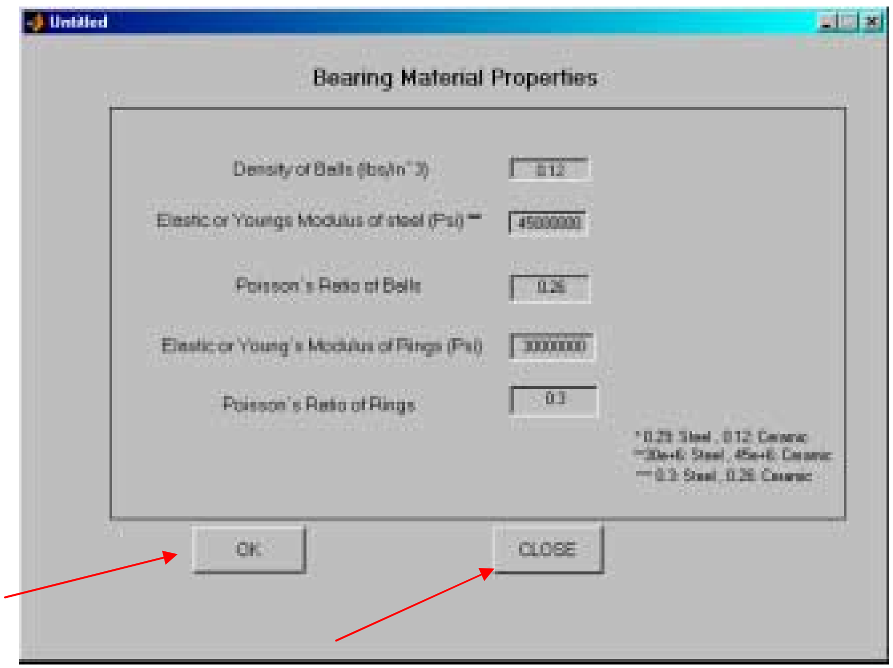

Next panel is "Materials" which is about ball and races materials. The density, Young's modulus and Poisson's ratio for steel and ceramic are referenced in the right side corner. When finished, click OK and Close.

In “Force/Speed” panel, the user inputs axial preload, external forces and moments applied to inner race. There is “Help?” button, which can provide a general information of preload and approximate preload amount according to bearing bore size. The user has to use bracket, [*] when analyzing series of preload amounts and inner race speeds.

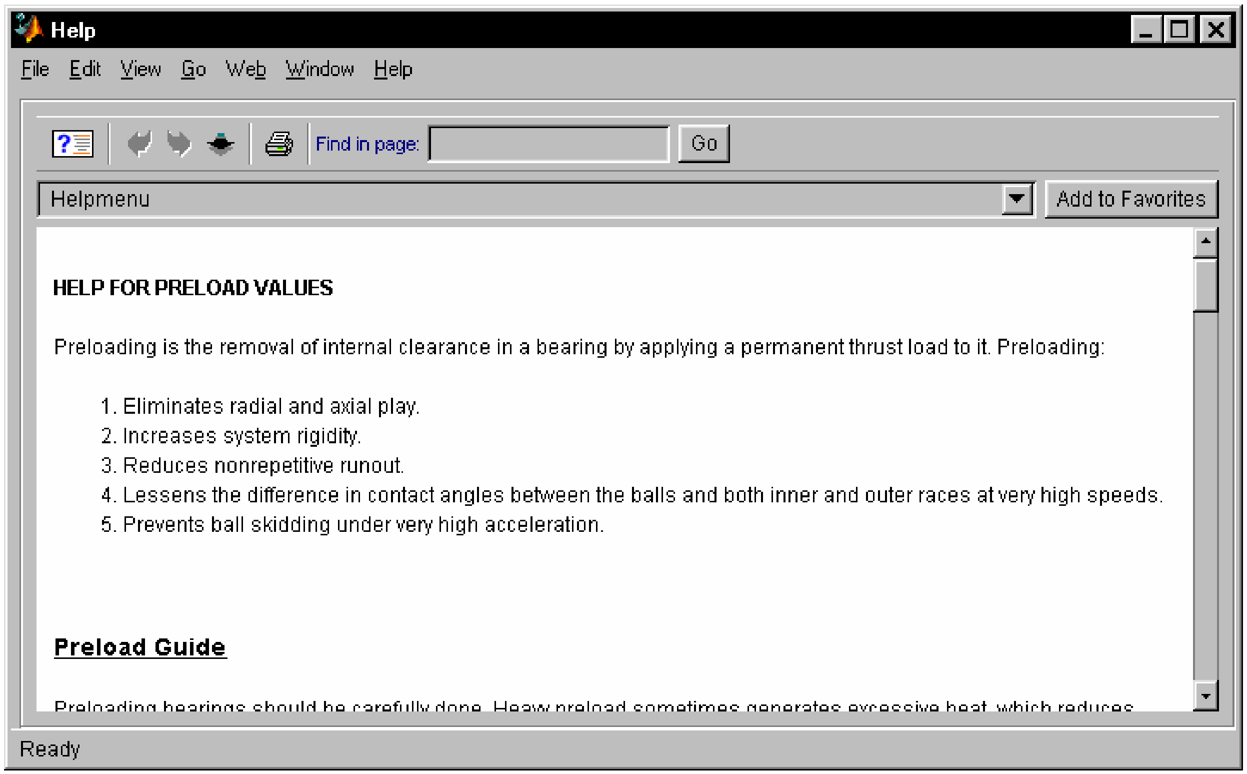

Here we see a Help menu to aid in the selection of preload values for the bearing under consideration.This feature is very helpful to the user.

Glenn Research Center

High Temperature Magnetic Bearing - Blade Loss Mitigation
NRA-GRC-99-02 - 1Year Milestone Review
September 27, 2002, NASA Glenn

Texas A&M Vibration Control and Electromechanics Lab

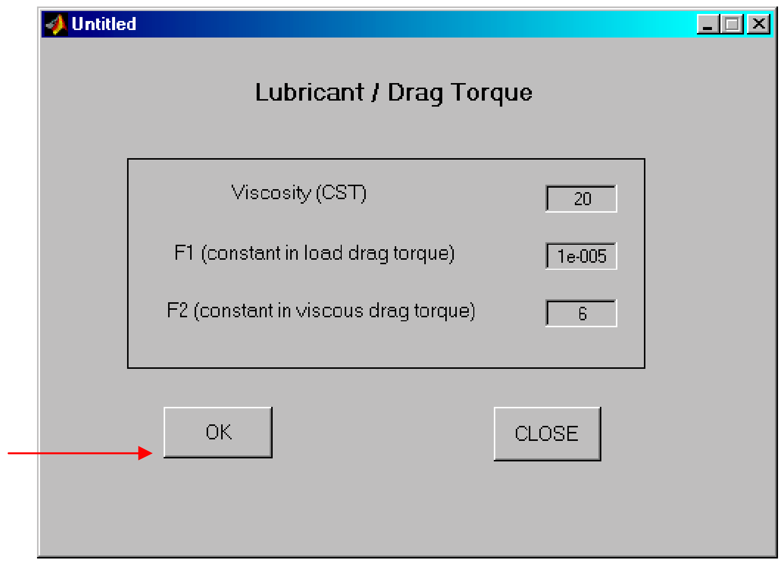

The last panel is for "Lubricant/Drag Torque", which includes viscosity of lubricant, two factors f_1 and f_2 in Palmgren's formula. Click OK and CLOSE when finished.

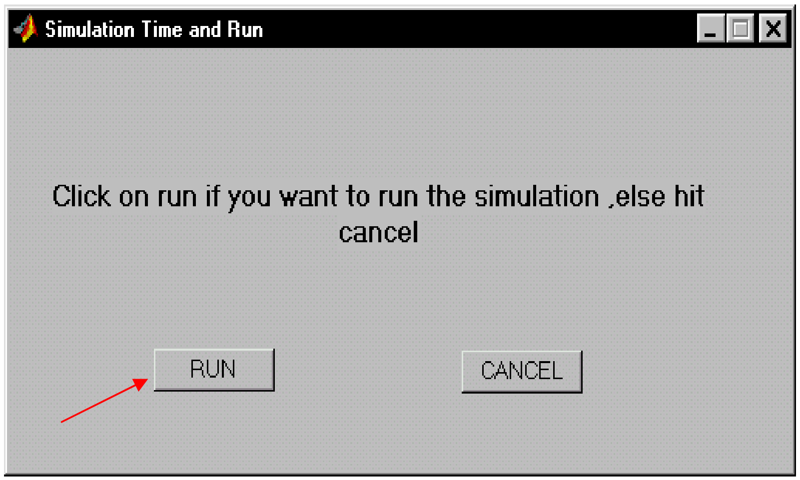

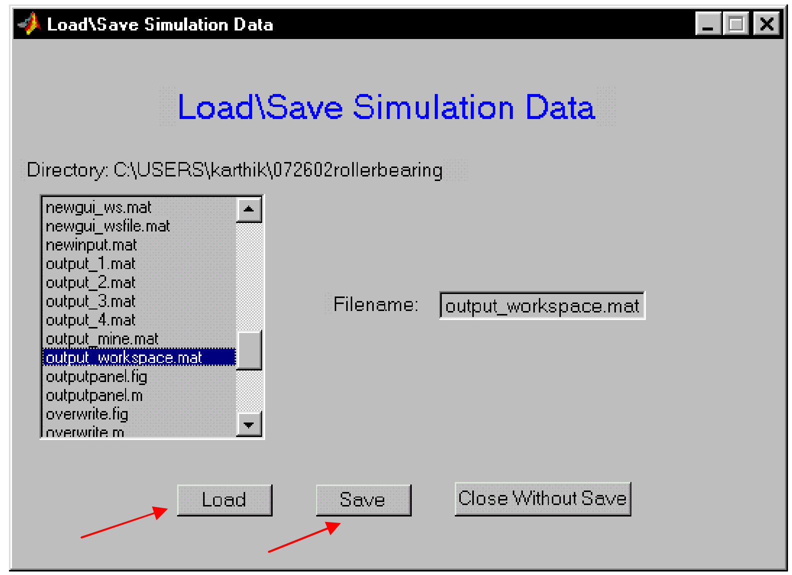

When entering input values is done, go to main panel and click "Update and Run" panel. When the computation is done, "Load/Save Data" panel in the next page is shown up. Find and double click on output_workspace.mat. Rename it and click Save. Click Load and "Output panel" is shown up.

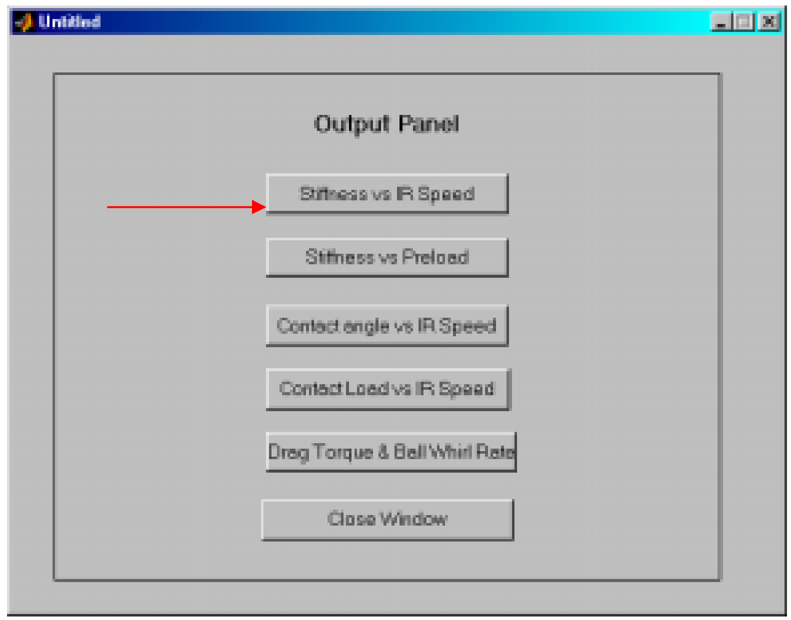

Output results are composed of three categories: bearing stiffness, contact angle/load, and drag torque/ball whirl rate. The user can choose the categories.

Glenn Research Center

High Temperature Magnetic Bearing - Blade Loss Mitigation
NRA-GRC-99-02 - 1Year Milestone Review
September 27, 2002, NASA Glenn

Texas A&M Vibration Control and Electromechanics Lab

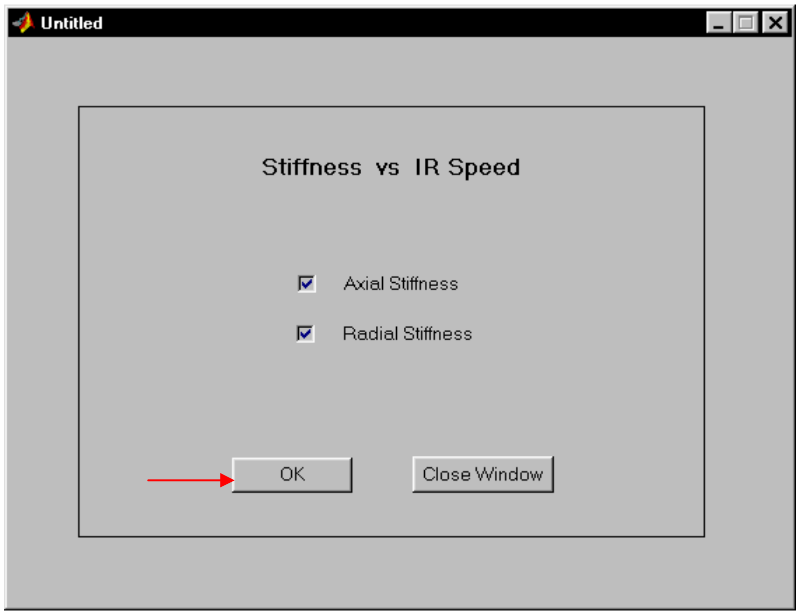

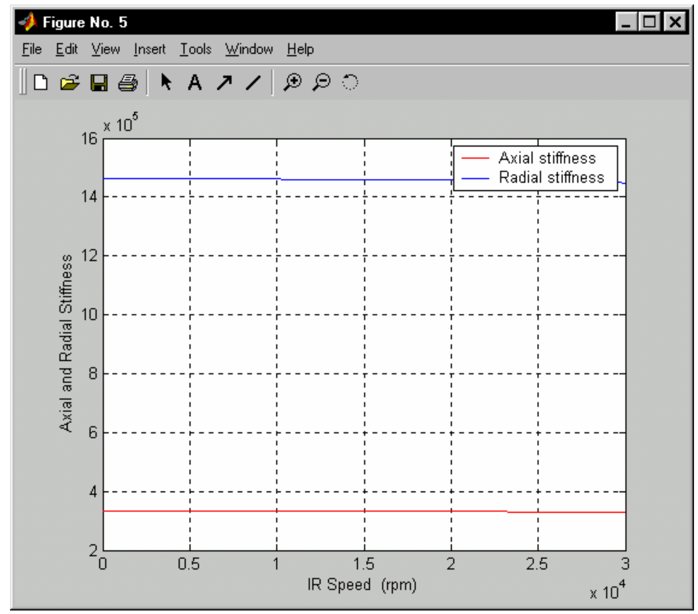

There are sub categories on each panel. For case of Stiffness vs. IR Speed, the user can fill the check boxes for Axial and Radial Stiffness. Click OK and the selected results will be plotted.

Glenn Research Center

High Temperature Magnetic Bearing - Blade Loss Mitigation
NRA-GRC-99-02 - 1Year Milestone Review
September 27, 2002, NASA Glenn

Texas A&M Vibration Control and Electromechanics Lab

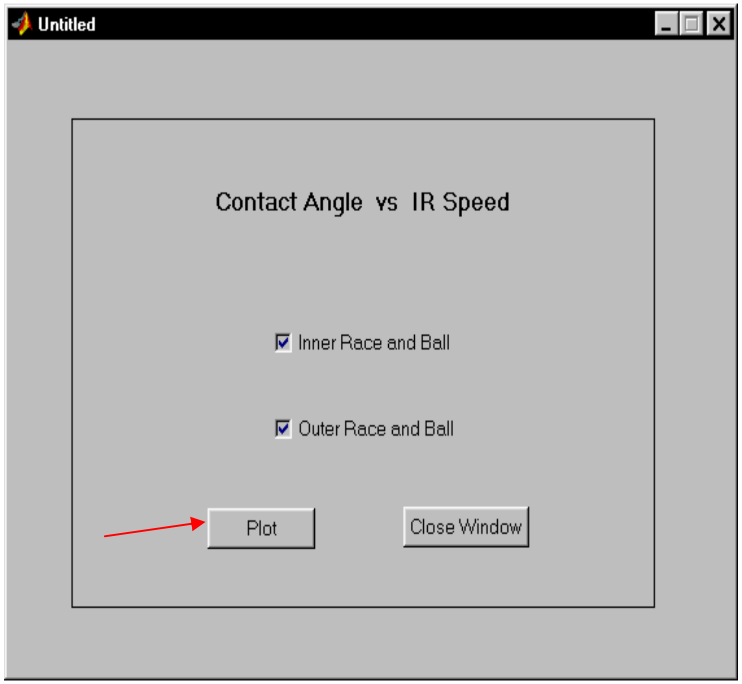

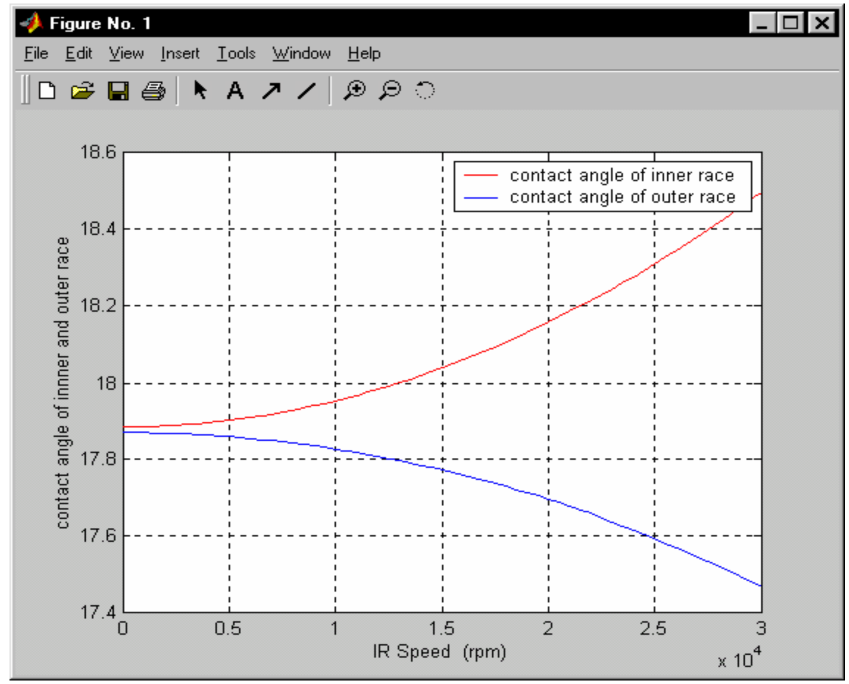

This panel shows the plot of contact angle Vs IR speed for the inner and outer races.

Glenn Research Center

High Temperature Magnetic Bearing - Blade Loss Mitigation
NRA-GRC-99-02 - 1Year Milestone Review
September 27, 2002, NASA Glenn

Texas A&M Vibration Control and Electromechanics Lab

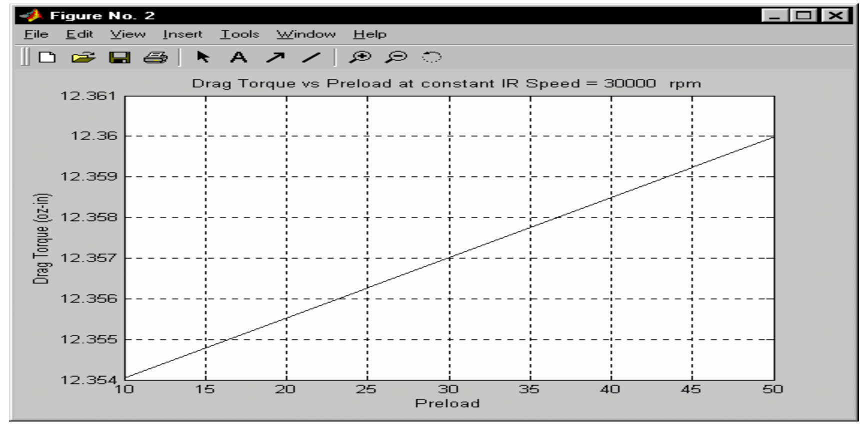

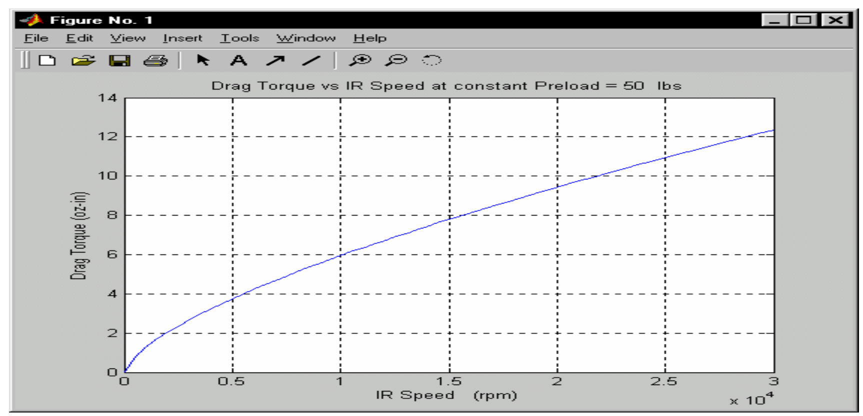

This panel shows the plot of Drag torque Vs IR speed and preload.

Glenn Research Center

High Temperature Magnetic Bearing - Blade Loss Mitigation
NRA-GRC-99-02 - 1Year Milestone Review
September 27, 2002, NASA Glenn

Texas A&M Vibration Control and Electromechanics Lab

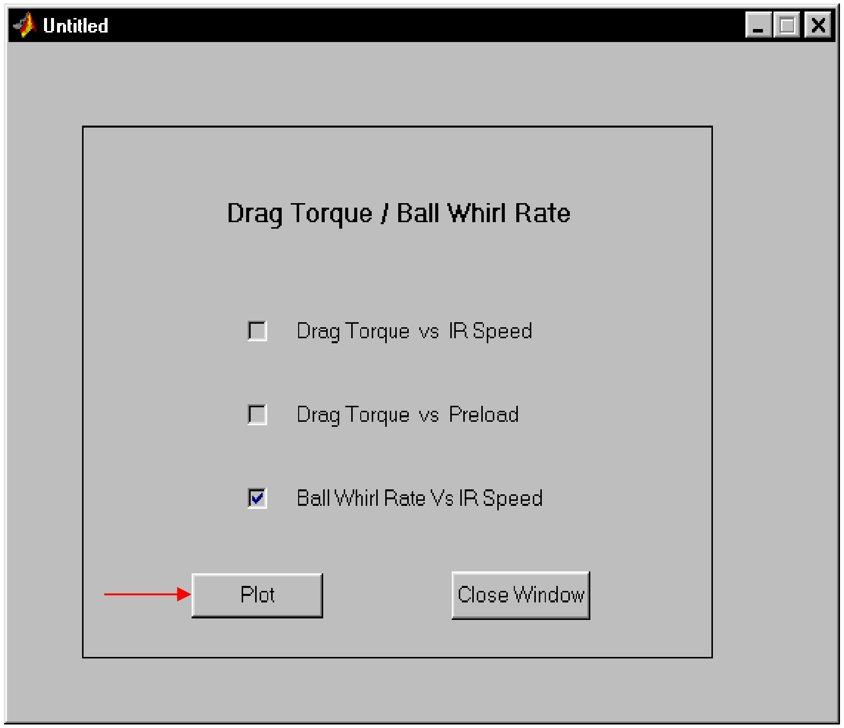

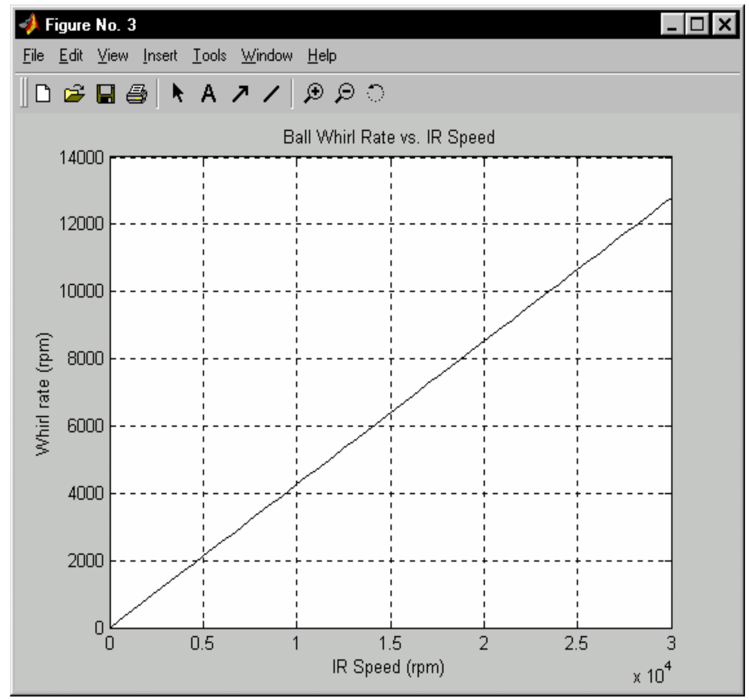

Here we see the plot of Ball Whirl rate Vs IR speed.

NASA/CR—2003-212205

Here we have seen a GUI written for the 2D isolated Bearing Code.

FUTURE WORK :

We will soon add the following to the GUI

- Finite element Squeeze film damper model
- Thermal model
- Thermal Growth model

Glenn Research Center

High Temperature Magnetic Bearing - Blade Loss Mitigation
NRA-GRC-99-02 - 1Year Milestone Review
September 27, 2002, NASA Glenn

Texas A&M Vibration Control and Electromechanics Lab

B.3: Dual Rotor - High Fidelity Bearing - Blade Out Simulation Code (DRBB)

By

Nikhil Kaushik, Guangyoung Sun and Dr. Alan Palazzolo

Objectives

- Provide improved component modeling for the dual rotor system.
- Integrate a detailed force-motion model of the squeeze film damper and rolling element bearing modules into the simulation code.
- Increase computational efficiency for repeated simulation of system dynamics.

Executive Summary

- Version 1 of combined rotor/bearing blade-out code completed. This version includes Timoshenko beam elements and bearings with Hertzian contact stiffness model, temperature prediction, thermal growth, ball loading and Torsional drag features.
- Code capabilities are demonstrated on Gas Turbine Engine Model with Power Turbine and Gas Generator taken from Li, Dennis, 1978, “Dynamic Analysis of Complex Multi-Level Flexible Rotor systems”, University of Virginia.
- Modal Synthesis with all component modes below 2000 Hz included. Reduced run time from 19.13 hrs to 88.48 secs for Li example executing on P3 933 MHz processor.

Bearing and Damper Model

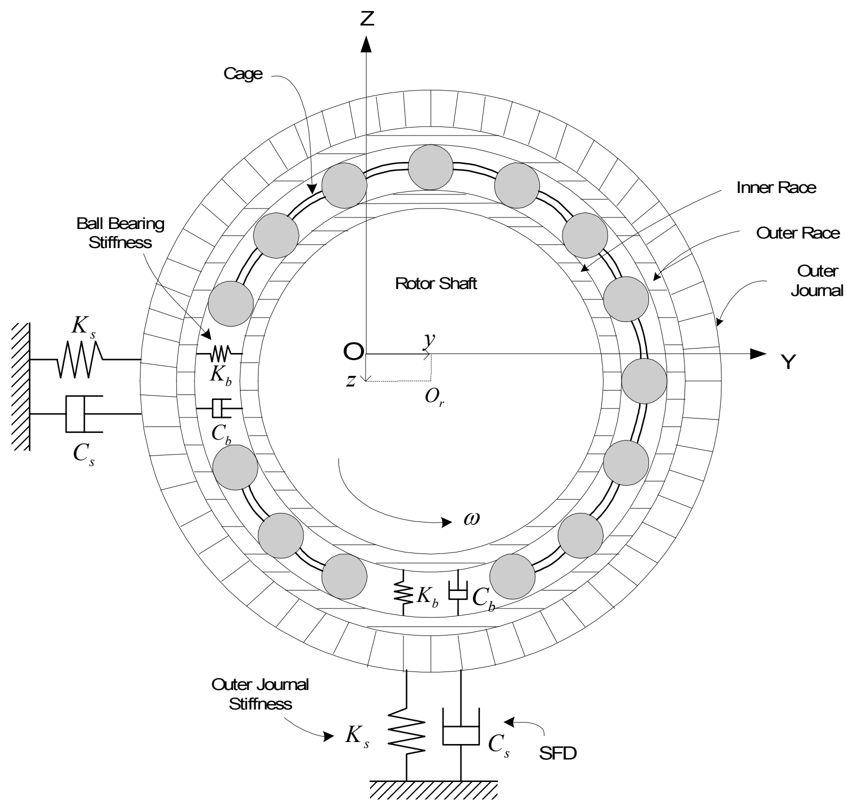

Fig.B.3.1 Jet engine rotor supported on ball bearing with SFD

Bearing Feature Summary

- 2D linearized bearing model
- Detailed squeeze film damper model based on FEM
- Bearing thermal model

1. Power loss in bearing
2. Heat transfer
3. Thermal expansion
4. Thermally Induced load

Bearing and Damper Model
2D Linearized Bearing Model

- From the Jacobian bearing stiffness matrix in Task B.1,

$$K_b = -\sum_{j=1}^{n} T' \cdot \left[\frac{\partial \{Q\}}{\partial \{u\}^T} \right] \cdot T$$ (1, 1): Radial stiffness

$$K_a = -\sum_{j=1}^{n} T' \cdot \left[\frac{\partial \{Q\}}{\partial \{u\}^T} \right] \cdot T$$ (3, 3): Axial stiffness

- The obtained bearing stiffness is used in the dynamic equations of motion.

NASA/CR—2003-212205

Bearing and Damper Model
Contact Stress in Ball Bearing

- For elliptical contact area between ball and races, the stress at the geometric center is

$$\sigma = -\frac{3Q}{2\pi ab}$$

where a and b are the semimajor and semiminor axes of the contact area, Q is the contact load.

- a and b are determined by the contact load, geometric and material characteristics.

Bearing and Damper Model

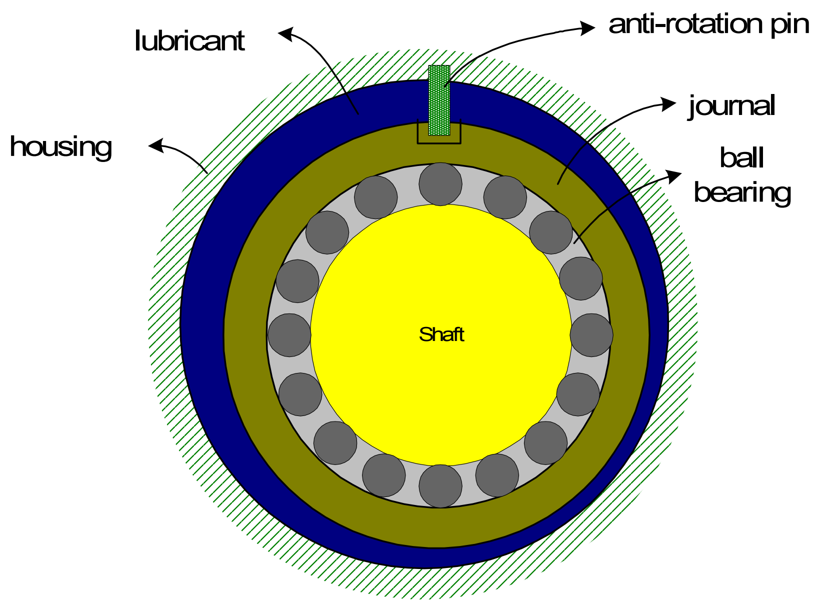

Figure B.3.2 Schematic of Typical SFD

Bearing and Damper Model - FE SFD Model

- Assuming an incompressible Newtonian fluid, Reynold's equation governs characteristics of fluid film between two journals as:

$$\nabla \cdot \left(\frac{\rho h^3}{12\mu} \nabla P \right) = \frac{\partial}{\partial t} (\rho h)$$

where ρ is the density of fluid, h is the film thickness, μ is the viscosity, and P is the fluid pressure.

- The functional[1] corresponding to the Reynold's equation

$$J(P) = \int_A \left\{ \frac{\rho h^3}{24\mu} \nabla P \cdot \nabla P + \frac{\partial}{\partial t} (\rho h) P \right\} dA$$

- Minimize $J\left(P^{(e)}\right)$

$$\left[K^{(e)}\right]\left\{P^{(e)}\right\} = \left\{S^{(e)}\right\}$$

1 Huebner, K.H., 1975, "The Finite Element Method for Engineers", John Wiely & Sons

Bearing and Damper Model

EX1: Two Flat Square Plates with Fluid between

- Conditions:

  L = 1 [m], h = 0.01 [m], $\partial h / \partial t$ = -1 [m/s], μ = 2E-6 [N-s/m^2] and ρ = 12 [kg/m^3]

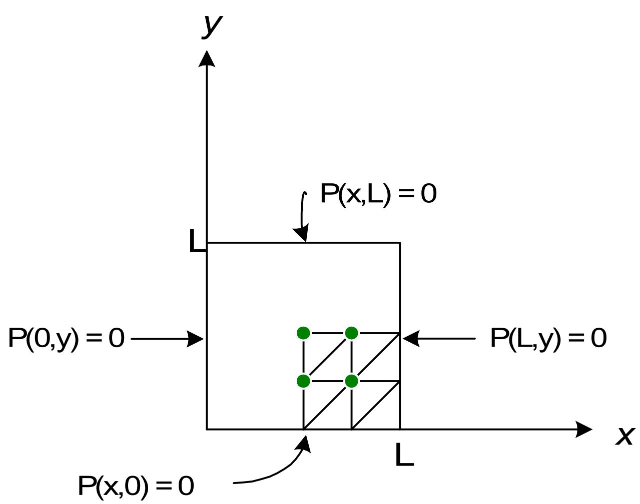

Figure B.3.3 Boundary Conditions

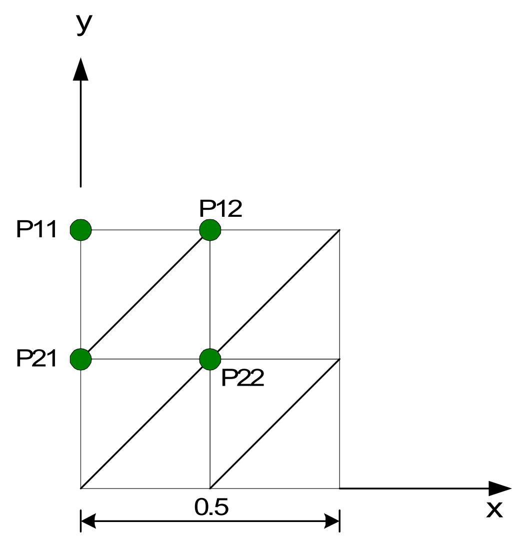

Figure B.3.4 Division of One Quadrant

Bearing and Damper Model

	P_{11}	P_{12}	P_{21}	P_{22}
FEM (32)	1.6875	1.3125	1.3125	1.0312
FEM (128)	1.7468	1.3594	1.3594	1.0719
Exact Sol.	1.7692	1.3767	1.3767	1.0872
E_r (32)	4.6 %	4.7 %	4.7 %	5.15 %
E_r (128)	1.3 %	1.3 %	1.3 %	1.4 %

Table B.3.1 FEM Results and Exact Solution[2]: N/m^2

2 Hays, D.F., March 1963, “Squeeze Films for Rectangular Plates”, Journal of Basic Engineering, Vol.85, No.2, pp. 243-246.

Bearing and Damper Model

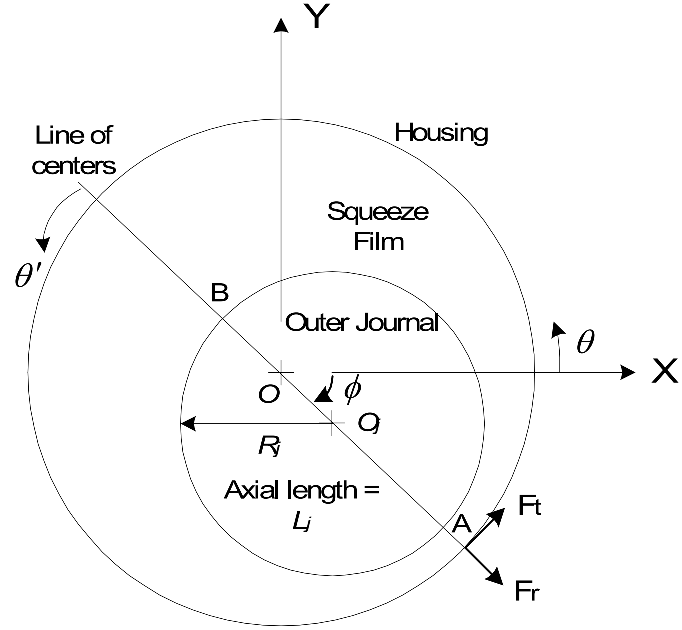

Figure B.3.5 SFD Geometry

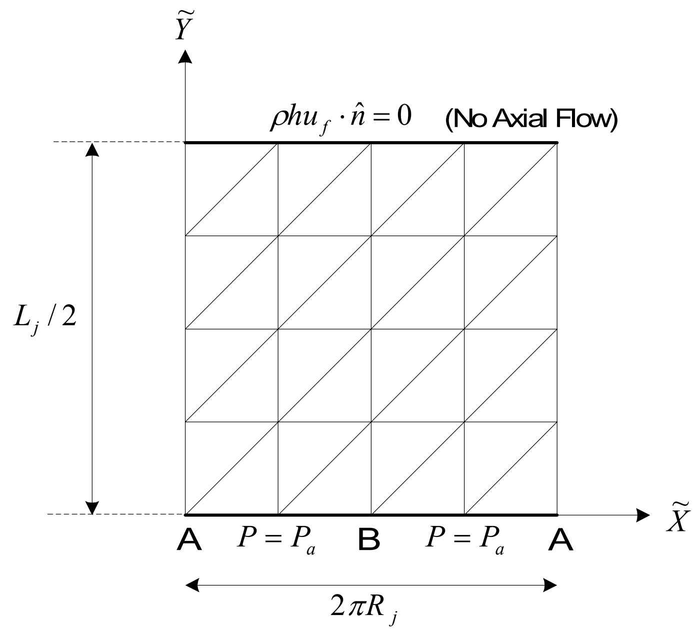

Figure B.3.6 SFD Boundary Conditions

Bearing and Damper Model - FE SFD Model

- Film thickness and its derivative

$$h = c - x\cos\theta - y\sin\theta, \quad \dot{h} = -\dot{x}\cos\theta - \dot{y}\sin\theta$$

- Pressure distribution at each element

$$\left[K^{(e)}\right]\cdot\left\{P^{(e)}\right\} = \left\{S^{(e)}\right\}$$

- SFD forces are

$$F_r = \int_A P\cos\theta' dA\ , \quad F_t = \int_A P\sin\theta' dA$$

- Applying triangular FE model, FE SFD forces are

$$\begin{Bmatrix} F_r \\ F_t \end{Bmatrix} = \frac{2}{3}\sum_{e=1}^{NE}\left(P_1^{(e)} + P_2^{(e)} + P_3^{(e)}\right)\cdot\begin{Bmatrix} \cos\left(\dfrac{\tilde{X}^{(e)}}{R_j} + \pi\right) \\ \sin\left(\dfrac{\tilde{X}^{(e)}}{R_j} + \pi\right) \end{Bmatrix} A^{(e)}$$

Bearing and Damper Model

Thermally Induced Bearing Load Model

- Bearing Seizure (Lockup) Model

  1. Power Losses due to drag torque
  2. Heat Transfer Network
  3. Thermal Expansions
  4. Thermally Induced Bearing Loads

- Since the induced thermal load causes more power loss, this feedback loop can cause premature bearing failure, so-called Thermally Activated Bearing Seizure (Lockup).

Bearing and Damper Model

Power Losses due to Drag Torque

- Modified Friction (Drag) Torque

The loading drag torque is modified from Palmgren's formula to include thermally induced load[3] and dynamic load.

$M_{fl} = f_1(F_\beta + F_{temp} + \alpha \cdot F_{dyn})d_m$: due to applied load

$M_{fv} = 1.42E-5 \cdot f_o(v_o N_i)^{2/3} d_m^3$: due to IR speed and viscosity

where f_1 and f_o factors depending on bearing type and lubricant, v_o is viscosity [cst] of lubricant, N_i is rotor spin speed [rpm], d_m is pitch diameter, F_β is static external loads, F_{temp} is the thermally induced load, F_{dyn} is dynamic loading due to blade loss, and α is derating factor.

3 J. L. Stein and J. F. Tu, Sept. 1994, "A State-Space Model for Monitoring Thermally Induced Preload in Anti-Friction Spindle Bearings of High Speed Machine Tools", *ASME Journal of Dynamic Systems, Measurement, and Control*, Vol.116, pp. 373-386.

NASA/CR—2003-212205

Bearing and Damper Model

Power Losses due to Drag Torque

- Power loss

Power loss can be calculated by

$$H = N_i \cdot \left(M_{fl} + M_{fv}\right) \text{ [lb-in/s]}$$

According to reference [4], the total heat source can be divided as

Heat source at balls: $H_b = 0.5 \cdot H$

Heat source at inner race: $H_i = 0.25 \cdot H$

Heat source at outer race: $H_o = 0.25 \cdot H$

NASA/CR—2003-212205

Bearing and Damper Model

Heat Transfer Network

The following assumptions are used in developing thermal model:

1. 1D radial heat transfer equations
2. Heat generation in a bearing acts on balls, IR and OR only, since contact fluid volume is small.
3. Bearing and rotor are modeled as lumped heat mass elements.
4. Heat mass has the uniform temperature distribution.
5. The temperature nodes outside SFD journal are invariant (T_∞) during transient simulation time.

Bearing and Damper Model

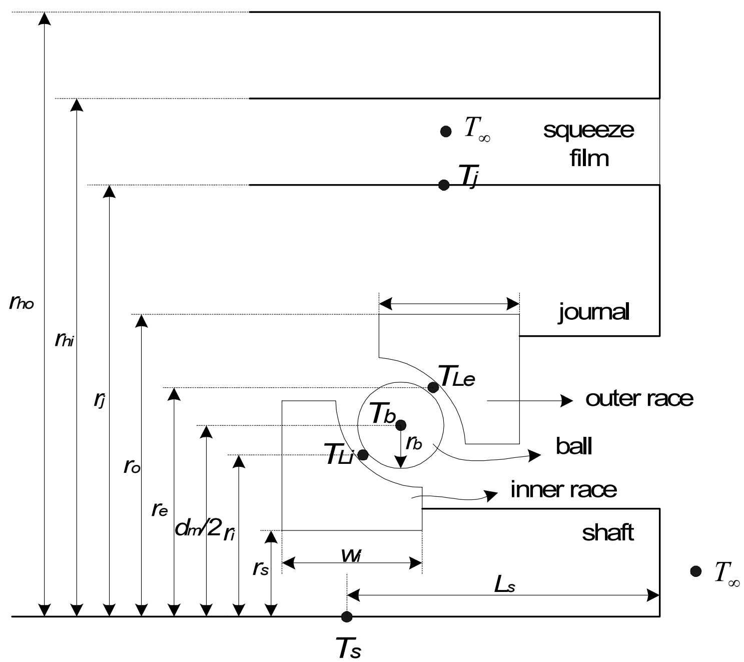

Figure B.3.7 Temperature Nodes of Cross-Sectioned Bearing

Bearing and Damper Model

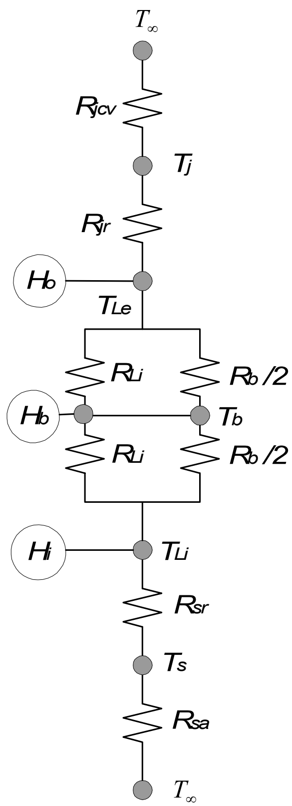

Figure B.3.8 Heat Transfer for Grease-Pack Ball Bearing

Bearing and Damper Model

Table B.3.2 Thermal Resistances of Heat Transfer Network

Ball and Lubricant	Inner Ring and Shaft	Outer Ring and SFD Journal
$R_{Li} \approx \dfrac{nr_b}{k_l(2\pi r_i W_i - \pi n r_b^2)}$	$R_{sr} = \dfrac{\ln\left(r_i / r_s\right)}{2\pi k_i W_i} + \dfrac{1}{k_s \pi W_i}$	$R_{jr} = \dfrac{\ln\left(r_j / r_e\right)}{2\pi k_j W_e}$
$R_{Le} \approx \dfrac{nr_b}{k_l(2\pi r_e W_e - \pi n r_b^2)}$	$R_{sa} = \dfrac{L_s}{k_s \pi r_s^2} + \dfrac{1}{h_s \pi r_s^2}$	$R_{jrcv} = \dfrac{1}{2\pi r_j h_j W_e}$
$R_b \approx \dfrac{1}{n k_b \pi r_b}$		
$R_1 = \dfrac{R_{Li} \cdot R_b/2}{R_{Li} + R_b/2}$		
$R_2 = \dfrac{R_{Le} \cdot R_b/2}{R_{Le} + R_b/2}$		

Bearing and Damper Model

Heat Transfer Network

- Bearing thermal equations are developed by

$$mC_P \frac{dT}{dt} = Q_i - Q_o$$

where m is thermal mass, C_p is specific heat, and $Q_{i,o}$ are heat flow in, out. For example, the thermal equation for the inner race contact T_{Li} is

$$M_i C_{pi} \frac{dT_{Li}}{dt} + \frac{T_{Li} - T_s}{R_{sr}} + \frac{T_{Li} - T_b}{R_1} = H_i$$

- Free convection coefficient is approximated by Tedric A. Harris[4]

$h = 3 \cdot (T - T_\infty)^{0.25}$ [lb-in/s-in^2/°F]

4. Tedric A. Harris, 1984, “Rolling Bearing Analysis”, Wiley-Interscience

Bearing and Damper Model

Thermal Expansions of CB Components

From Timoshenko and Goodier[5],

- For IR and OR, the thermal expansions are determined from

$$\varepsilon_i = \frac{\alpha_d r_i}{3} \cdot (1+\nu_i) \cdot \left(\Delta T_s + \Delta T_{Li}\right)$$

$$\varepsilon_o = \frac{\alpha_d}{3} \cdot \frac{(1+\nu_e)\cdot r_e}{r_e + r_j} \cdot \left(\Delta T_{Le} \cdot (2r_e + r_j) + \Delta T_j \cdot (2r_j + r_e)\right)$$

- For Balls, the thermal expansion is determined from

$$\varepsilon_b = \alpha_d \cdot r_b \cdot \Delta T_b$$

where α_d [in/in-°F] is thermal expansion coeff. and ν is the Poisson's ratio.

5 Timoshenko, S. P. and Goodier, J. N., 1987, "Theory of Elasticity", McGraw-Hill

Bearing and Damper Model

Thermally Induced Bearing Loads

- Assuming only elastic deformation on contact, the thermal load due to interference change is obtained using the principle of Hertzian contact:

$$F_{temp} = k_t \varepsilon_t^{\beta}$$

where k_t is elastic constant of bearing, β is 1.5 for ball bearings.

- The total interference change ε_t

$$\varepsilon_t = \varepsilon_b + \frac{1}{2}(\varepsilon_i - \varepsilon_o)\cos\alpha_o$$

- The induced load feeds back to the thermal heat sources (drag load torque)

Bearing and Damper Model

Fig B.3.9 Temperature effect[6] on rolling element fatigue life of hot-pressured alumina balls in five ball fatigue tester. Maximum Hertz stress,

3.79 Gpa (550 ksi); contact angle 20°

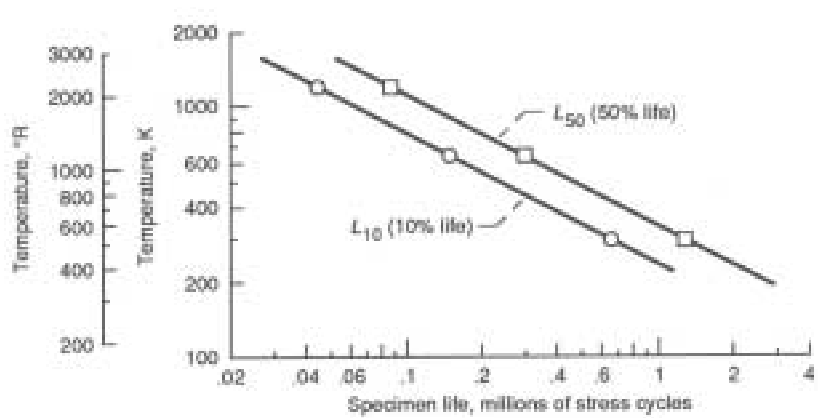

6. Erwin V. Zaretsky, 1992, "STLE Life Factors for Rolling Bearings", STLE Publication

Rotor Model Description
Timoshenko Beam Element[7]

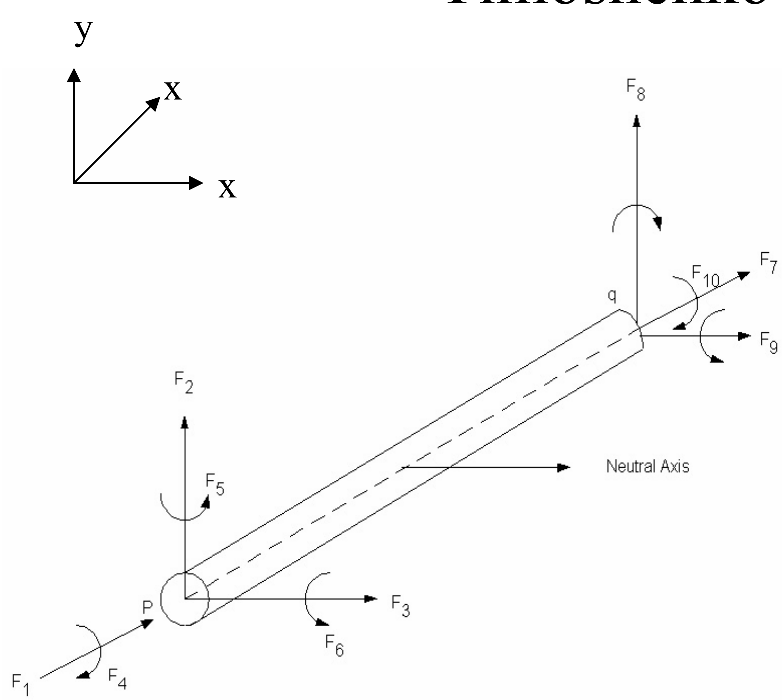

Fig B.3.10 Beam Element

- 6 DOF at each node: Translations in the nodal x, y & z directions ; rotations about the nodal x, y & z axes
- Assumed to be straight bar of uniform cross section capable of resisting axial forces, bending moments about the 2 principal axes in the plane of its cross section, and twisting moments about its centroidal axis.

7. Przemieniecki, J.S., 1968, “Theory of Matrix Structural Analysis”, McGraw-Hill

NASA/CR—2003-212205

Rotor Model Description
Stiffness Matrix

$$
Ke=\begin{bmatrix}
\frac{AE}{L} & 0 & 0 & 0 & 0 & 0 & -\frac{AE}{L} & 0 & 0 & 0 & 0 & 0 \\
0 & az & 0 & 0 & 0 & cz & 0 & bz & 0 & 0 & 0 & cz \\
0 & 0 & ay & 0 & dy & 0 & 0 & 0 & b & 0 & dy & 0 \\
0 & 0 & 0 & \frac{GJ}{L} & 0 & 0 & 0 & 0 & 0 & -\frac{GJ}{L} & 0 & 0 \\
0 & 0 & dy & 0 & ey & 0 & 0 & 0 & cy & 0 & fy & 0 \\
0 & cz & 0 & 0 & 0 & ez & 0 & dz & 0 & 0 & 0 & fz \\
-\frac{AE}{L} & 0 & 0 & 0 & 0 & 0 & \frac{AE}{L} & 0 & 0 & 0 & 0 & 0 \\
0 & bz & 0 & 0 & 0 & dz & 0 & az & 0 & 0 & 0 & dy \\
0 & 0 & b & 0 & cy & 0 & 0 & 0 & ay & 0 & cz & 0 \\
0 & 0 & 0 & -\frac{GJ}{L} & 0 & 0 & 0 & 0 & 0 & \frac{GJ}{L} & 0 & 0 \\
0 & 0 & dy & 0 & fy & 0 & 0 & 0 & cz & 0 & ey & 0 \\
0 & cz & 0 & 0 & 0 & fz & 0 & dy & 0 & 0 & 0 & ez
\end{bmatrix}
$$

A = cross-section area
E = Young's modulus
L = element length
G = shear modulus
J = Torsional Moment of inertia

ai = $\dfrac{12EI}{L^3(1+\Phi)}$

ci = $\dfrac{6EI}{L^2(1+\Phi)}$

ei = $\dfrac{(4+\Phi)EI}{L\,(1+\Phi)}$

fi = $\dfrac{(2-\Phi)EI}{L\,(1+\Phi)}$

$\Phi_y = \dfrac{12EI_z}{GA_z^s L^2}$

$\Phi_z = \dfrac{12EI_y}{GA_y^s L^2}$

I_i = moment of inertia normal to direction i
= shear area normal to direction Ii = A / K_i
Ki = shear co-efficient[8] $= \dfrac{(7+6\mu)(1+(r_i/r_o)^2)^2+(20+12\mu)(r_i/r_o)^2}{6(1+\mu)(1+(r_i/r_o)^2)^2}$

8. Rouch, Keith, 1977, “Finite Element Analysis of Rotor Bearing Systems with Matrix Reduction”, Marquette University

Rotor Model Description
Lumped Mass Matrix

$$
Me = \frac{1}{2}\begin{bmatrix}
Mt & 0 & 0 & 0 & 0 & 0 & 0 & 0 & 0 & 0 & 0 & 0 \\
0 & Mt & 0 & 0 & 0 & 0 & 0 & 0 & 0 & 0 & 0 & 0 \\
0 & 0 & Mt & 0 & 0 & 0 & 0 & 0 & 0 & 0 & 0 & 0 \\
0 & 0 & 0 & Ip & 0 & 0 & 0 & 0 & 0 & 0 & 0 & 0 \\
0 & 0 & 0 & 0 & It & 0 & 0 & 0 & 0 & 0 & 0 & 0 \\
0 & 0 & 0 & 0 & 0 & It & 0 & 0 & 0 & 0 & 0 & 0 \\
0 & 0 & 0 & 0 & 0 & 0 & Mt & 0 & 0 & 0 & 0 & 0 \\
0 & 0 & 0 & 0 & 0 & 0 & 0 & Mt & 0 & 0 & 0 & 0 \\
0 & 0 & 0 & 0 & 0 & 0 & 0 & 0 & Mt & 0 & 0 & 0 \\
0 & 0 & 0 & 0 & 0 & 0 & 0 & 0 & 0 & Ip & 0 & 0 \\
0 & 0 & 0 & 0 & 0 & 0 & 0 & 0 & 0 & 0 & It & 0 \\
0 & 0 & 0 & 0 & 0 & 0 & 0 & 0 & 0 & 0 & 0 & It
\end{bmatrix}
$$

A = cross section area
L = elemental length
$M_t = \rho AL$
I_p = Mass Moment of Inertia in x1 direction
I_t = Mass Moment of Inertia in the x2 or x3 direction

Rotor Model Description
Consistent Mass Matrix

$$
Me=\begin{bmatrix}
\rho AL/3 & & & & & & & & & & & \\
0 & ai & & & & & \text{Symmetric} & & & & & \\
0 & 0 & ai & & & & & & & & & \\
0 & 0 & 0 & \rho JL/3 & & & & & & & & \\
0 & 0 & bi & 0 & ci & & & & & & & \\
0 & bi & 0 & 0 & 0 & ci & & & & & & \\
\rho AL/6 & 0 & 0 & 0 & 0 & 0 & \rho AL/3 & & & & & \\
0 & di & 0 & 0 & 0 & ei & 0 & ai & & & & \\
0 & 0 & di & 0 & ei & 0 & 0 & 0 & ai & & & \\
0 & 0 & 0 & \rho JL/6 & 0 & 0 & 0 & 0 & 0 & \rho JL/3 & & \\
0 & 0 & -ei & 0 & fi & 0 & 0 & 0 & -bi & 0 & ci & \\
0 & -ei & 0 & 0 & 0 & fi & 0 & -bi & 0 & 0 & 0 & ci
\end{bmatrix}
$$

$$ai = \Psi_{mi}^{u} * 156 + \Psi_{mi}^{\theta} * 36$$

$$bi = \Psi_{mi}^{u} * 22L + \Psi_{mi}^{\theta} * 3L$$

$$ci = \Psi_{mi}^{u} * 4L^2 + \Psi_{mi}^{\theta} * 4L^2$$

$$di = \Psi_{mi}^{u} * 54 - \Psi_{mi}^{\theta} * 36$$

$$ei = \Psi_{mi}^{u} * 13L - \Psi_{mi}^{\theta} * 3L$$

$$fi = -\Psi_{mi}^{u} * 3L^2 - \Psi_{mi}^{\theta} * L^2$$

$$\Psi_{mi}^{u} = \rho AL/420$$

$$\Psi_{mi}^{\theta} = \rho I_{xi}/30L$$

in the transverse ith direction

Rotor Model Description
Gyroscopic Damping Matrix

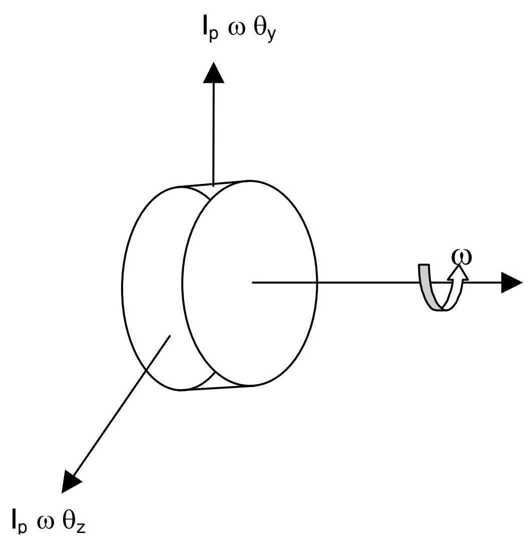

Fig B.3.11 Gyroscopic Moment

$$Cg := \begin{bmatrix} 0 & 0 & 0 & 0 & 0 & 0 \\ 0 & 0 & 0 & 0 & 0 & 0 \\ 0 & 0 & 0 & 0 & 0 & 0 \\ 0 & 0 & 0 & 0 & 0 & 0 \\ 0 & 0 & 0 & 0 & 0 & Ip\ \omega \\ 0 & 0 & 0 & 0 & -Ip\ \omega & 0 \end{bmatrix}$$

I_p = Mass Moment of Inertia in x1 direction

ω = rotation frequency about the positive x axis

Modal Synthesis Description

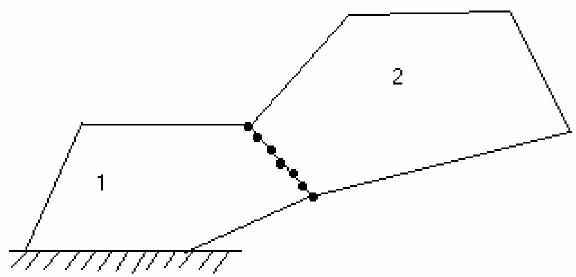

Fig B.3.12
Schematic diagram of a two Component Model of a structure

Definitions:

$X^1_{\phi F}$ = vector of modal coordinates for the undamped system, free vibration modes of component 1, with interface 1-2 fixed in space

$X^2_{\phi F}$ = vector of modal coordinates for the undamped system, free vibration modes of component 2, with interface 1-2 fixed in space

q^1_J = vector of Guyan retained dofs that are in component 1 & on interface 1-2

q^2_J = vector of Guyan retained dofs that are in component 2 & on interface 1-2

q^1_I = vector of interior dofs that are in component 1

q^2_I = vector of interior dofs that are in component 2

Modal Synthesis Description

f_J^1 = vector of reaction forces acting on body 1 at interface 1-2

f_J^2 = vector of reaction forces acting on body 2 at interface 1-2

f_I^1 = vector of external forces acting at interior dofs that are in component 1

f_I^2 = vector of external forces acting at interior dofs that are in component 2

Total number of degrees of freedom in component 1 and 2 is

$N^1 = n_I^1 + n_j$

$N^2 = n_I^2 + n_j$

System equilibrium equations may be written as:

$$\left[\begin{array}{c|c} \underline{M}^1 & \underline{0} \\ \hline \underline{0} & \underline{M}^2 \end{array}\right]\left\{\begin{array}{c} \ddot{\underline{q}}^1 \\ \hline \ddot{\underline{q}}^2 \end{array}\right\} + \left[\begin{array}{c|c} \underline{C}^1 & \underline{0} \\ \hline \underline{0} & \underline{C}^2 \end{array}\right]\left\{\begin{array}{c} \dot{\underline{q}}^1 \\ \hline \dot{\underline{q}}^2 \end{array}\right\} + \left[\begin{array}{c|c} \underline{K}^1 & \underline{0} \\ \hline \underline{0} & \underline{K}^2 \end{array}\right]\left\{\begin{array}{c} \underline{q}^1 \\ \hline \underline{q}^2 \end{array}\right\} = \left\{\begin{array}{c} \underline{f}^1 \\ \hline \underline{f}^2 \end{array}\right\}$$

Modal Synthesis Description

where

$$\underline{q}^1 = \left\{ \begin{array}{c} \underline{q}^1_I \\ \hline \underline{q}^1_J \end{array} \right\}, \quad \underline{q}^2 = \left\{ \begin{array}{c} \underline{q}^2_I \\ \hline \underline{q}^2_J \end{array} \right\}, \quad \underline{f}^1 = \left\{ \begin{array}{c} \underline{f}^1_I \\ \hline \underline{f}^1_J \end{array} \right\}, \quad \underline{f}^2 = \left\{ \begin{array}{c} \underline{f}^2_I \\ \hline \underline{f}^2_J \end{array} \right\}$$

$$\underline{M}^1 = \left[\begin{array}{c|c} M^1_{I,I} & M^1_{I,J} \\ \hline M^1_{J,I} & M^1_{J,J} \end{array} \right], \quad \underline{M}^2 = \left[\begin{array}{c|c} M^2_{I,I} & M^2_{I,J} \\ \hline M^2_{J,I} & M^2_{J,J} \end{array} \right]$$

$$\underline{C}^1 = \left[\begin{array}{c|c} C^1_{I,I} & C^1_{I,J} \\ \hline C^1_{J,I} & C^1_{J,J} \end{array} \right], \quad \underline{C}^2 = \left[\begin{array}{c|c} C^2_{I,I} & C^2_{I,J} \\ \hline C^2_{J,I} & C^2_{J,J} \end{array} \right]$$

$$\underline{K}^1 = \left[\begin{array}{c|c} K^1_{I,I} & K^1_{I,J} \\ \hline K^1_{J,I} & K^1_{J,J} \end{array} \right], \quad \underline{K}^2 = \left[\begin{array}{c|c} K^2_{I,I} & K^2_{I,J} \\ \hline K^2_{J,I} & K^2_{J,J} \end{array} \right]$$

Dependency Relations:

These relations are introduced for two purposes:

- Couple components 1 and 2
- Reduce the number of dofs by Guyan reduction and modal condensation

Modal Synthesis Description

To couple components 1 and 2 use the interface compatibility condition

$$\underline{q}^2_J = \underline{T}_{J12}\, \underline{q}^1_J$$

The T_{J12} matrix has a block diagonal structure with each block being a 2 or 3 dimensional co-ordinate transformation matrix. This transforms the displacements at junction nodes from the convention employed in component 1 to the convention employed in component 2. Since T_{J12} is a block diagonal matrix with each block being an orthogonal matrix,

$$T^{-1}_{J12} = T^{T}_{J12}$$

The component 1 response is a linear combination of the undamped free vibration modes of component 1 with the junction fixed in space, i.e.

$$\underline{q}^1_{(n)} = \begin{Bmatrix} \underline{q}^1_I \\ \underline{q}^1_J \end{Bmatrix}_{(n)} = \begin{bmatrix} \underset{n_I^1 \times n_k^1}{\underline{\Phi}^1_I} \\ \underset{n_J^1 \times n_k^1}{\underline{0}} \end{bmatrix} \begin{Bmatrix} \underset{n_k^1 \times 1}{\underline{\chi}^1_{sF}} \end{Bmatrix} = \underline{\Phi}_1\, \underline{\chi}^1_{sF}$$

where Φ_1 is the modal matrix for component 1 with the junction fixed.

NASA/CR—2003-212205

Modal Synthesis Description

The second part of the component 1 response is a linear combination of the Guyan constraint vectors for retained dofs on the interface.

$$\underline{q}^1_{(b)} = \begin{Bmatrix} \underline{q}^1_I \\ \underline{q}^1_J \end{Bmatrix}_{(b)} = \begin{bmatrix} \underset{n_I \times n_J}{-\left(\underline{K}^1_{I,I}\right)^{-1} \underline{K}^1_{I,J}} \\ \hdashline \underset{n_J \times n_J}{\underline{I}} \end{bmatrix} \begin{Bmatrix} \underset{n_J \times 1}{\underline{q}^1_J} \end{Bmatrix} = \underline{T}^1_{GI}\, \underline{q}^1_J$$

Therefore the deflections in component 1 are approximated by

$$\underline{q}^1 = \underline{q}^1_{(a)} + \underline{q}^1_{(b)} = \begin{Bmatrix} \underset{n_I^1 \times 1}{\underline{q}^1_I} \\ \hdashline \underset{n_J^1 \times 1}{\underline{q}^1_J} \end{Bmatrix} = \left[\begin{array}{c:c} \underset{n_I^1 \times n_k^1}{\underline{\Phi}^1_I} & \underset{n_I^1 \times n_J^1}{\underline{G}^1_J} \\ \hdashline \underset{n_J \times n_k^1}{\underline{0}} & \underset{n_J \times n_J}{\underline{I}} \end{array}\right] \begin{Bmatrix} \underset{n_k^1 \times 1}{\underline{\chi}^1_{\phi r}} \\ \hdashline \underset{n_J^1 \times 1}{\underline{q}^1_J} \end{Bmatrix}$$

where $G^1_J = -(K^1_{I,I})^{-1} K^1_{I,J}$

The uncoupled system displacements is approximated by

$$\underline{q} = \begin{Bmatrix} \underline{q}^1_I \\ \underline{q}^1_J \\ \underline{q}^2_I \\ \underline{q}^2_J \end{Bmatrix} = \left[\begin{array}{c:c:c:c} \underline{\Phi}^1_I & \underline{G}^1_J & \underline{0} & \underline{0} \\ \hdashline \underline{0} & \underline{I}_J & \underline{0} & \underline{0} \\ \hdashline \underline{0} & \underline{0} & \underline{\Phi}^2_I & \underline{G}^2_J \\ \hdashline \underline{0} & \underline{0} & \underline{0} & \underline{I}_J \end{array}\right] \begin{Bmatrix} \underline{\chi}^1_{\phi r} \\ \underline{q}^1_J \\ \underline{\chi}^2_{\phi r} \\ \underline{q}^2_J \end{Bmatrix}$$

Modal Synthesis Description

Inserting the compatibility relationship yields

$$\underline{q} = \begin{Bmatrix} \underline{q}_I^1 \\ \hline \underline{q}_J^1 \\ \hline \underline{q}_I^2 \\ \hline \underline{q}_J^2 \end{Bmatrix} = \left[\begin{array}{c:c:c} \underline{\Phi}_I^1 & \underline{G}_J^1 & \underline{0} \\ \hdashline \underline{0} & \underline{I}_J & \underline{0} \\ \hdashline \underline{0} & \underline{G}_J^2 \underline{T}_{J12} & \underline{\Phi}_I^2 \\ \hdashline \underline{0} & \underline{T}_{J12} & \underline{0} \end{array}\right] \begin{Bmatrix} \underline{\chi}_{st}^1 \\ \hline \underline{q}_J^1 \\ \hline \underline{\chi}_{st}^2 \end{Bmatrix}$$

Or $q = T\,X$

The subspace condensation transformation is substituted into the uncoupled model EOM to obtain

$$\underline{\tilde{M}}\,\ddot{\underline{\chi}} + \underline{\tilde{C}}\,\dot{\underline{\chi}} + \underline{\tilde{K}}\,\underline{\chi} = \underline{\tilde{f}}$$

where

$$\underline{\tilde{M}} = \underline{T}^T \underline{M}\,\underline{T}$$
$$\underline{\tilde{C}} = \underline{T}^T \underline{C}\,\underline{T}$$
$$\underline{\tilde{K}} = \underline{T}^T \underline{K}\,\underline{T}$$
$$\underline{\tilde{f}} = \underline{T}^T \underline{f}$$

Modal Synthesis Description

The force vector f contains the unknown junction forces and hence

$$\underline{f} = \begin{Bmatrix} \underline{f}^1 \\ \underline{f}^2 \end{Bmatrix} = \begin{Bmatrix} \underline{f}^1_I \\ \underline{f}^1_J \\ \underline{f}^2_I \\ \underline{f}^2_J \end{Bmatrix}$$

The unknown junction forces are related by Newton's 3rd Law and the coordinate transformation as

$$f_J^2 = -T_{J12} f_J^1$$

or

$$f_J^1 = -T_{J12}^T f_J^2$$

Modal Synthesis Description

The joined system force vector is

$$
\begin{aligned}
\tilde{\underline{f}} &= \underline{T}^T \underline{f} \\
&= \left[\begin{array}{c:c:c:c}
(\underline{\Phi}_i^1)^T & \underline{0} & \underline{0} & \underline{0} \\
\hdashline
(\underline{G}_j^1)^T & \underline{L}_J & \underline{T}_{J12}^T (\underline{G}_j^2)^T & \underline{T}_{J12}^T \\
\hdashline
\underline{0} & \underline{0} & (\underline{\Phi}_i^2)^T & \underline{0}
\end{array}\right]
\left\{\begin{array}{c}
\underline{f}_i^1 \\ \hdashline \underline{f}_j^1 \\ \hdashline \underline{f}_i^2 \\ \hdashline \underline{f}_j^2
\end{array}\right\} \\
&= \left\{\begin{array}{c}
(\underline{\Phi}_i^1)^T \underline{f}_i^1 \\
\hdashline
(\underline{G}_j^1)^T \underline{f}_i^1 + \underline{f}_j^1 + \underline{T}_{J12}^T (\underline{G}_j^2)^T \underline{f}_i^2 + \underline{T}_{J12}^T \underline{f}_j^2 \\
\hdashline
(\underline{\Phi}_i^2)^T \underline{f}_i^2
\end{array}\right\}
\end{aligned}
$$

Using Newton’s 3rd Law relation,

$$
\tilde{\underline{f}} = \left\{\begin{array}{c}
(\underline{\Phi}_i^1)^T \underline{f}_i^1 \\
\hdashline
(\underline{G}_j^1)^T \underline{f}_i^1 + (\underline{G}_j^2 \underline{T}_{J12})^T \underline{f}_i^2 \\
\hdashline
(\underline{\Phi}_i^2)^T \underline{f}_i^2
\end{array}\right\}
$$

which does not contain the unknown junction force.

Description of Gas Turbine Rotor System

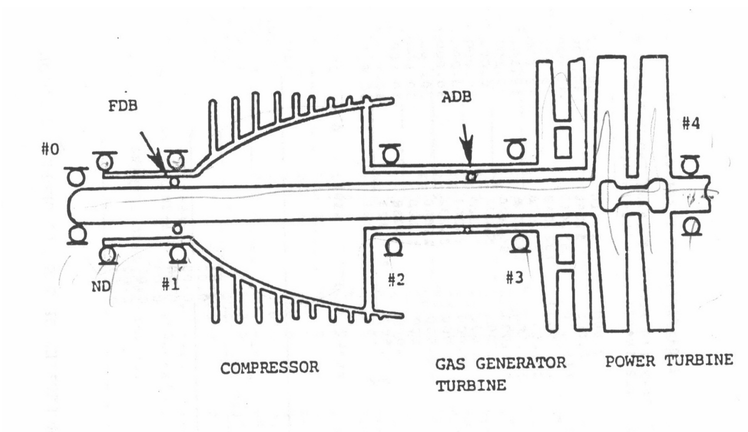

Fig B.3.13 Two Spool Aircraft Turbine Engine with 8 bearings[9]

- Consists of an inner core rotor called the power turbine, supported to ground by 2 main bearings located at the shaft extremities
- 2 intermediate differential bearings connect the core power turbine to the gas generator rotor.
- Gas generator rotor consists of a 2 stage generator turbine which drives an axial compressor. It is supported to ground by rolling element bearings at 4 locations.

9. Li, Dennis, 1978, “Dynamic Analysis of Complex Multi-Level Flexible Rotor Systems”, University of Virginia

Description of FE Model

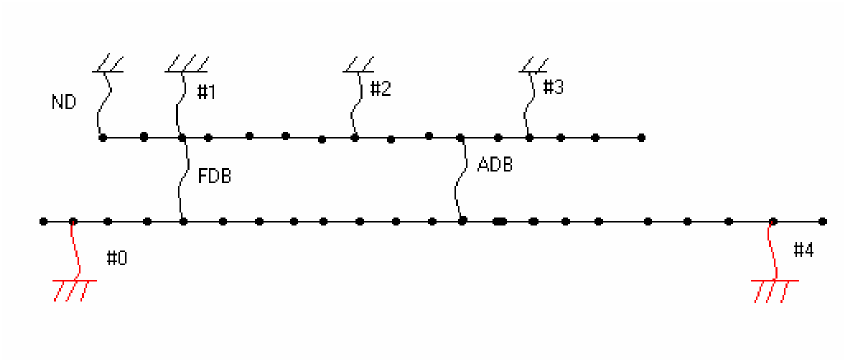

Fig B.3.14 Two Spool Aircraft Turbine Engine Lumped Parameter FE Model

- 38 lumped masses with the power turbine divided into 22 nodes & the gas generator divided into 16 nodes.
- Total System DOF = 228
- Polar moments of inertia in the rotors are considered only at the turbine and compressor stages.
- Bearings #0 and #4 are modeled as High Fidelity Bearings

Physical and Cross-sectional Properties

Station No.	Weight (lb)	Length (in)	Shaft dia out	Shaft dia in	I (in^4)	Ip Lb-in^2	It Lb-in^2	E*10-6 (lb/in^2)
1	0.740	1.3	2.00	1.53	0.52	0.0	0.129	30.0
2	1.539	1.3	2.10	1.53	0.69	0.0	0.297	30.0
3	1.989	3.0	2.10	1.53	0.69	0.0	0.977	30.0
4	1.679	4.3	2.10	1.53	0.69	0.0	2.749	30.0
5	2.082	4.8	2.30	1.80	0.86	0.0	4.623	30.0
6	2.187	4.8	2.30	1.80	0.86	0.0	5.365	30.0
7	1.851	4.4	1.80	1.30	0.38	0.0	4.139	30.0
8	1.516	4.4	1.80	1.30	0.38	0.0	2.913	30.0
9	1.120	2.1	1.80	1.30	0.38	0.0	1.701	30.0
10	0.896	3.1	1.80	1.30	0.38	0.0	0.837	30.0
11	0.896	2.1	1.80	1.30	0.38	0.0	0.837	30.0
12	0.723	2.1	1.80	1.30	0.38	0.0	0.489	30.0
13	1.429	2.0	2.60	1.40	2.05	0.0	1.181	30.0
14	2.187	2.1	2.60	1.40	2.05	0.0	1.959	30.0
15	2.027	1.7	2.60	1.40	2.05	0.0	1.735	30.0
16	1.387	0.9	2.60	1.40	2.05	0.0	1.007	30.0
17	1.173	2.4	2.25	1.57	0.96	0.0	0.953	30.0
18	1.386	2.4	2.25	1.57	0.96	0.0	1.317	30.0
19	26.501	2.8	2.25	1.57	0.96	625.0	314.067	30.0
20	31.028	2.0	1.80	1.50	0.27	704.5	353.257	30.0
21	2.660	1.5	3.30	1.50	5.57	0.0	1.602	30.0
22	1.440	0.0	0.00	0.00	0.00	0.0	1.453	0.0

Table B.3.3 Lumped Parameters and Cross-sectional properties of the Power Turbine Rotor

Physical and Cross-sectional Properties

Station No.	Weight (lb)	Length (in)	Shaft dia outside	Shaft dia inside	I (in^4)	Ip (lb – in^2)	It (lb-in^2)	E*10-6 Lb/in^2
23	0.693	3.0	2.80	2.40	1.39	0.0	1.110	30.0
24	2.270	4.3	3.05	2.45	2.48	0.0	5.048	30.0
25	9.389	4.8	11.00	10.97	7.81	111.0	65.417	30.0
26	13.514	4.8	11.00	10.86	35.90	297.5	182.243	15.0
27	7.600	4.4	11.00	10.79	53.33	301.5	215.078	12.8
28	11.404	4.4	11.00	10.66	35.90	232.0	177.576	19.3
29	3.126	2.1	3.85	2.80	7.77	117.0	86.170	27.3
30	2.691	3.1	3.39	2.90	3.01	0.0	5.078	30.0
31	1.697	2.1	3.60	3.20	3.10	0.0	3.325	30.0
32	1.270	2.1	3.60	3.20	3.10	0.0	2.307	30.0
33	1.239	2.0	3.60	3.20	3.10	0.0	2.232	30.0
34	1.010	2.1	3.60	3.35	2.08	0.0	1.840	30.0
35	0.872	1.7	3.70	3.35	3.02	0.0	1.600	30.0
36	1.108	0.9	4.20	3.35	9.09	0.0	2.039	30.0
37	27.605	2.4	9.40	9.00	61.19	612.5	329.123	30.0
38	26.963	0.0	0.00	0.00	0.00	600.0	321.721	30.0

Table B.3.4 Lumped Parameters and Cross-sectional properties of the Gas Generator Rotor

Description of Analysis

- The model was divided into the following superelements:
  - Power turbine with bearing #0 and #4.
  - Gas Generator with bearings ND, #1, #2 and #3.
- The intermediate shaft bearings were incorporated into the model with 2 junction nodes.
- The component mode reduction was done in each run as described above.

Static Analysis

- The equation of equilibrium for static analysis can be written as:

$$[K]\ \{Q\} = \{F\}$$

[K] = System stiffness matrix

{F} = Static input force vector

{Q} = Static deflection vector for the system

- The following load case was run for the static analysis:
  - 100 lb force acting in the positive y direction at bearing #4
  - 25 lb force acting downwards on the power turbine mid span and the second stage Power turbine.
- The results show the displacement in the y direction.

Static Analysis

Case 1:

Location	Full Model (without reduction) [in]	VCEL Modal Synthesis [in]	Boeing Modal Synthesis [in]
#0 bearing	9.5337e-5	9.5332e-5	9.5332e-5
Rotor Mid span	6.8703e-5	6.8702e-5	6.8720e-5
Second Stage Power Turbine	0.0027	0.0027	0.0027
#4 bearing	0.0030	0.0030	0.0030

Case 2:

Location	Full Model (without reduction) [in]	VCEL Modal Synthesis [in]	Boeing Modal Synthesis [in]
#0 bearing	-6.9808e-5	-7.1694e-5	-7.1009e-5
Rotor Mid span	6.4124e-4	6.3051e-4	6.3552e-4
Second Stage Power Turbine	6.5092e-4	6.5094e-4	6.5094e-4
#4 bearing	6.3262e-4	6.3270e-4	6.3270e-4

Table B.3.5 Static Analysis Displacements (in inches)

NASA/CR—2003-212205

Undamped Modal Analysis

- The undamped normal modal frequencies and mode shapes are extracted using the following equation:

$([K] - \omega^2 [M]) [\Phi] = 0$

[M] = System Mass Matrix

[Φ] = Eigen vector matrix

ω = Normal mode frequencies

- The gyroscopic and damping matrices are ignored for this analysis. The modes of each rotors were obtained independently by omitting the intermediate bearings.
- The undamped normal mode shapes below 2000 Hz were included in the component model.

Undamped Modal Analysis

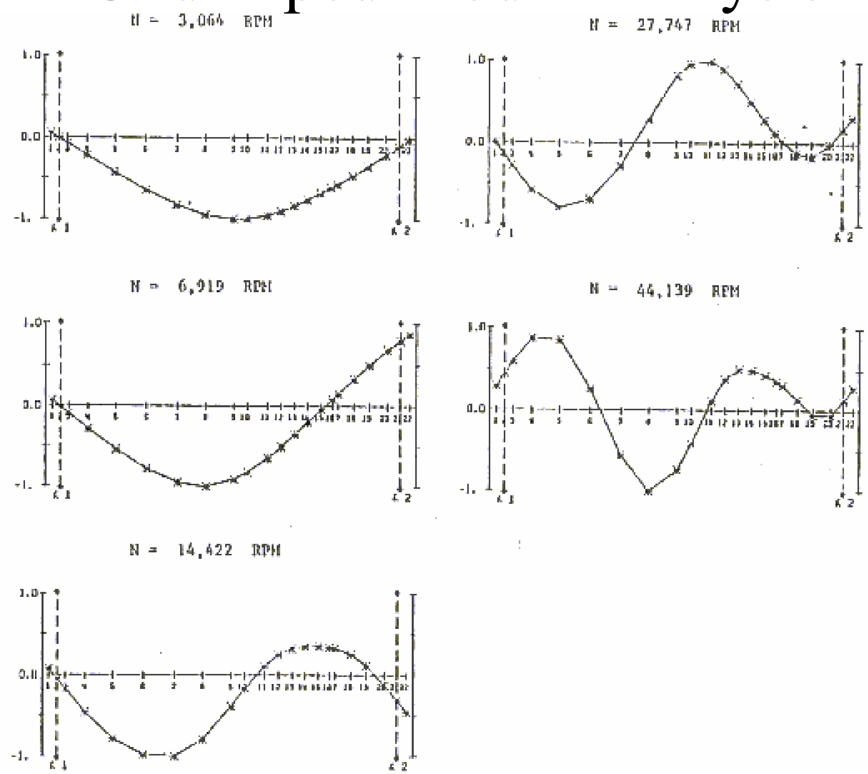

Fig B.3.15 Power Turbine Rotor Undamped Component Mode 1 to 5[10]

10. Li, Dennis, 1978, “Dynamic Analysis of Complex Multi-Level Flexible Rotor Systems”, University of Virginia

Undamped Modal Analysis

N = 3080.2 CPM

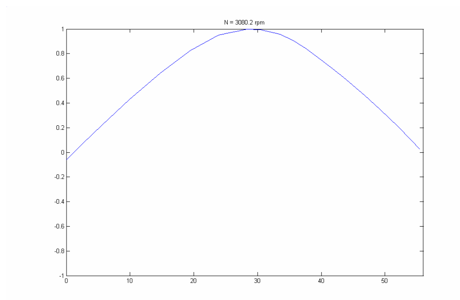

N = 6942.8 CPM

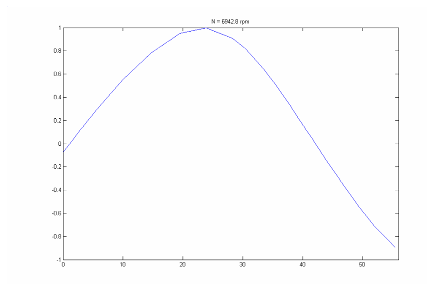

N = 14370 CPM

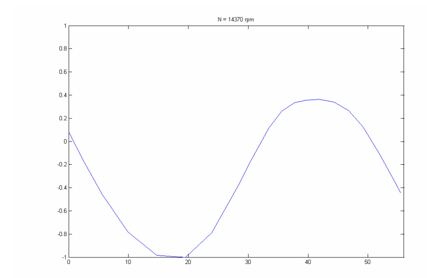

N = 27563 CPM

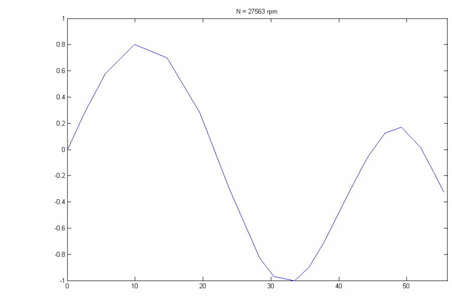

N = 43676 CPM

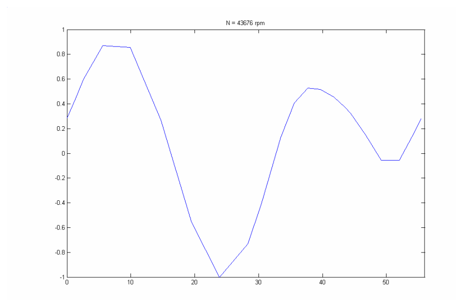

Fig B.3.16 Power Turbine Rotor Undamped Component Mode 1 to 5

NASA/CR—2003-212205

Undamped Modal Analysis

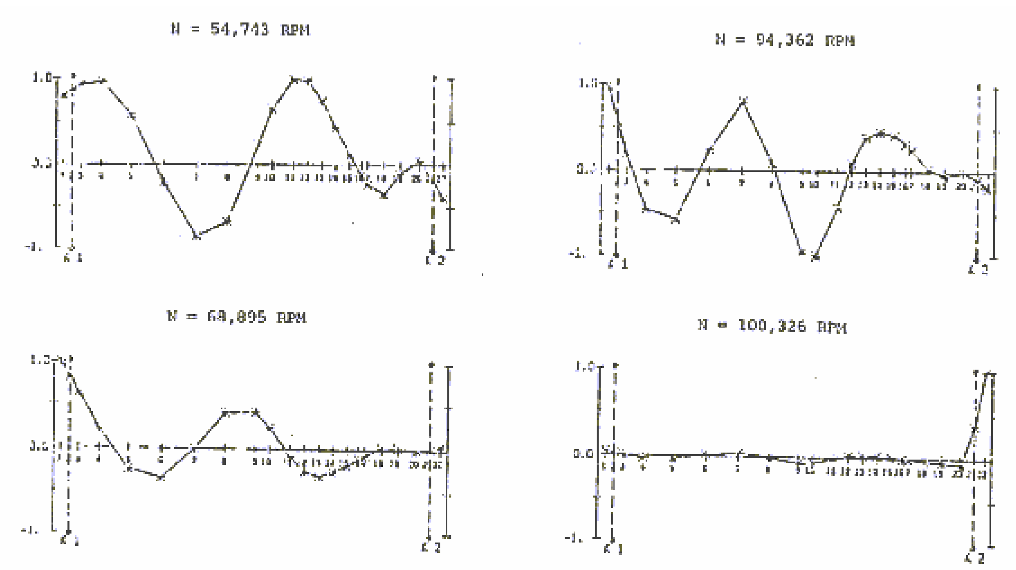

Fig B.3.17 Power Turbine Rotor Undamped Component Mode 6 to 9[11]

11. Li, Dennis, 1978, “Dynamic Analysis of Complex Multi-Level Flexible Rotor Systems”, University of Virginia

Undamped Modal Analysis

N = 54341 CPM

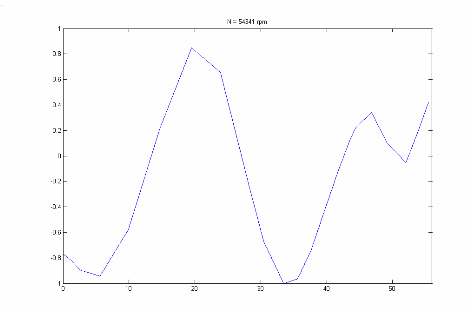

N = 90802 CPM

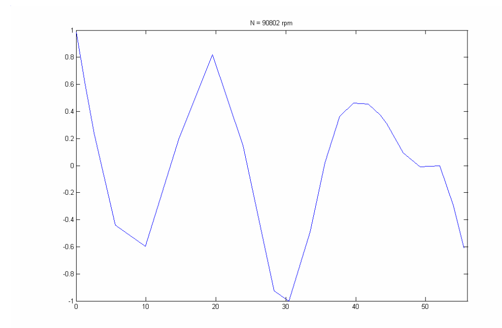

N = 68024 CPM

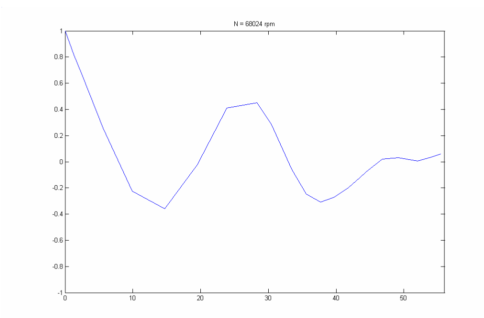

N = 93481 CPM

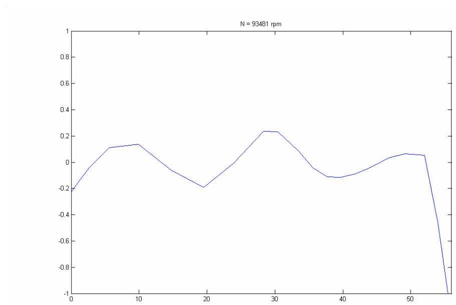

Fig B.3.18 Power Turbine Rotor Undamped Component Mode 6 to 9

NASA/CR—2003-212205

Undamped Modal Analysis

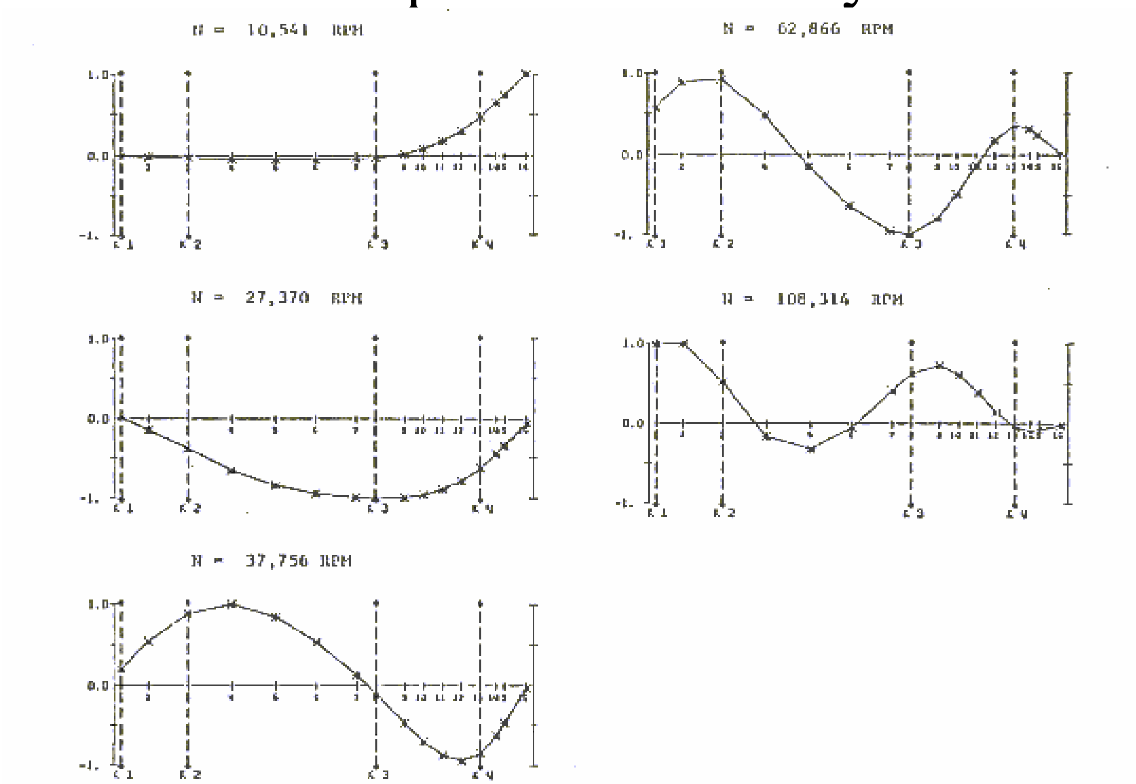

Fig B.3.19 Gas Generator Rotor Undamped Component Mode 1 to 5[12]

12. Li, Dennis, 1978, “Dynamic Analysis of Complex Multi-Level Flexible Rotor Systems”, University of Virginia

Undamped Modal Analysis

N = 10421 CPM

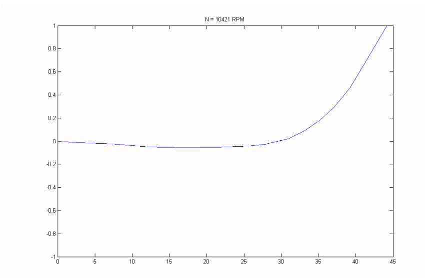

N = 25902 CPM

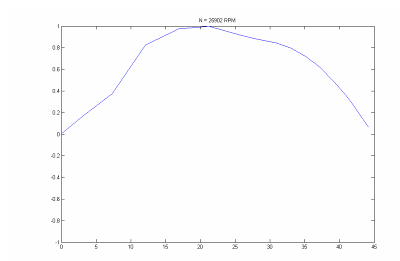

N = 34685 CPM

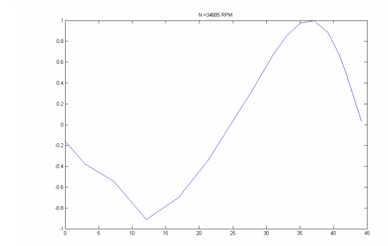

N = 58570 CPM

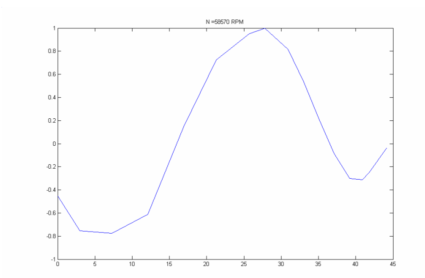

N = 92049 CPM

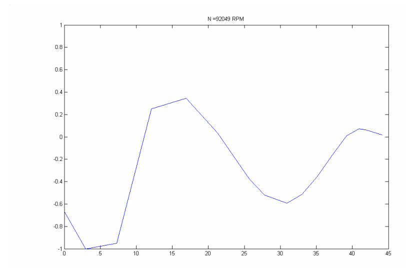

Fig B.3.20 Gas Generator Rotor Undamped Component Mode 1 to 5

Gyroscopic Damped Mode Shapes

- The mode shapes are generated considering the effect of the gyroscopic and damping matrices. This is done using the equation:

$$[\Lambda][\Phi] = [\Phi]\,[\lambda]$$

$[\Lambda] = \begin{bmatrix} -M^{-1}C & -M^{-1}K \\ I & O \end{bmatrix}$

[C] = System damping matrix including gyroscopic terms

[I] = Identity matrix

[O] = Zero Matrix

[λ] = Eigen values matrix (diagonal matrix)

- The 2D mode shapes show the displacement in the y direction against the shaft length.

Gyroscopic Damped Mode Shapes

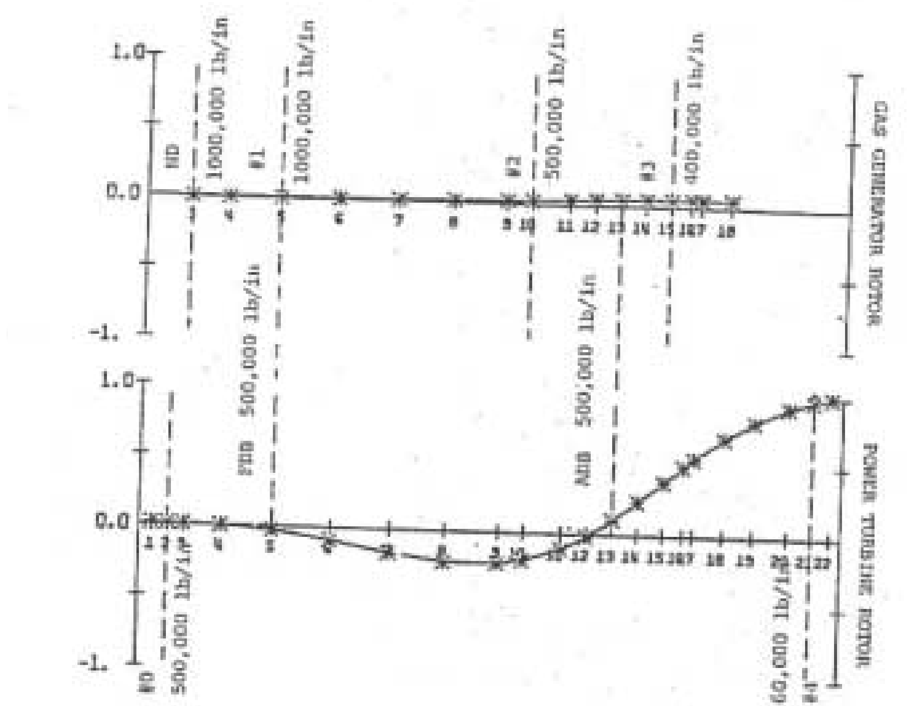

Fig B.3.21 First Power Turbine Critical Speed N = 6936 RPM[13]

13. Li, Dennis, 1978, “Dynamic Analysis of Complex Multi-Level Flexible Rotor Systems”, University of Virginia

Gyroscopic Damped Mode Shapes

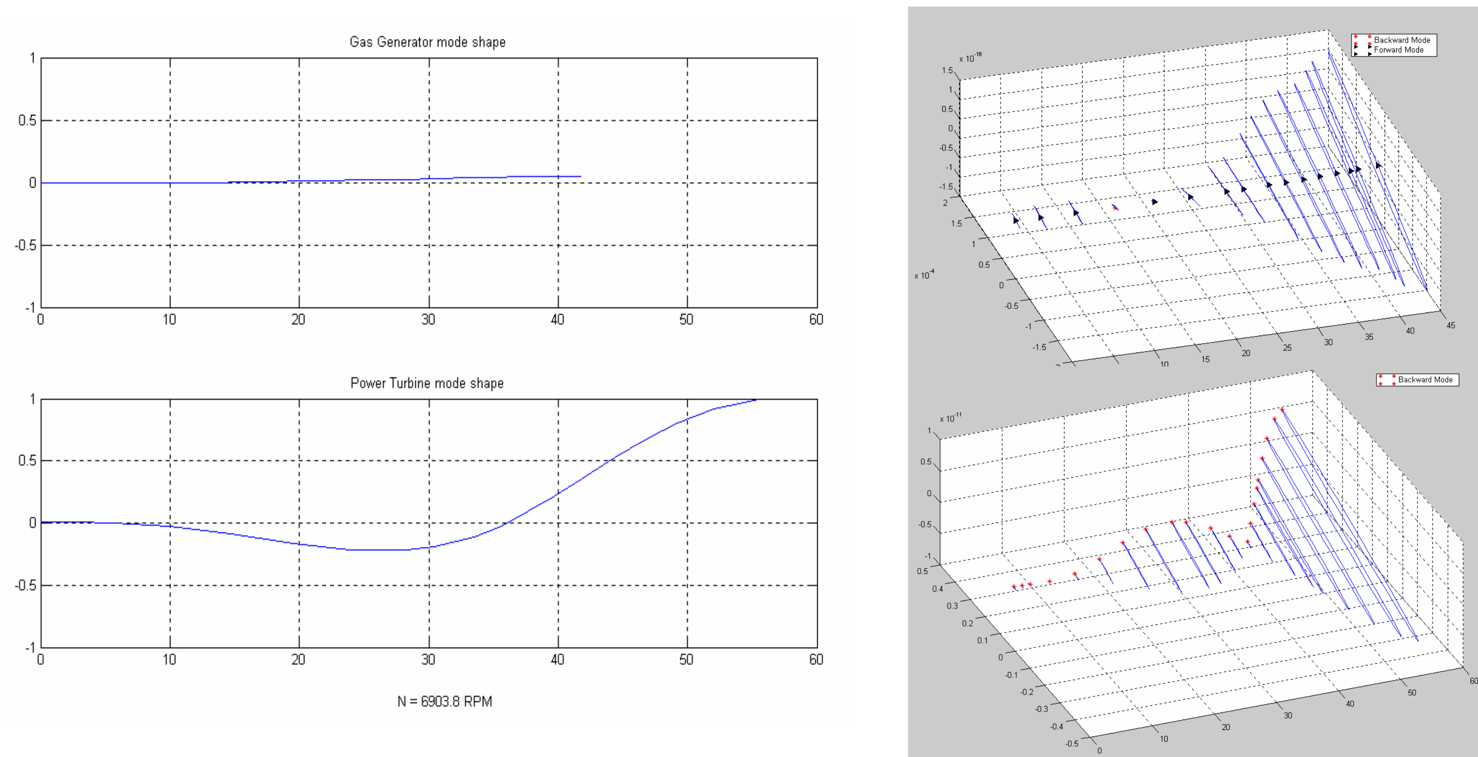

Fig B.3.22 2D and 3D Mode Shapes(with whirl direction) at N=6903.8 RPM

Gyroscopic Damped Mode Shapes

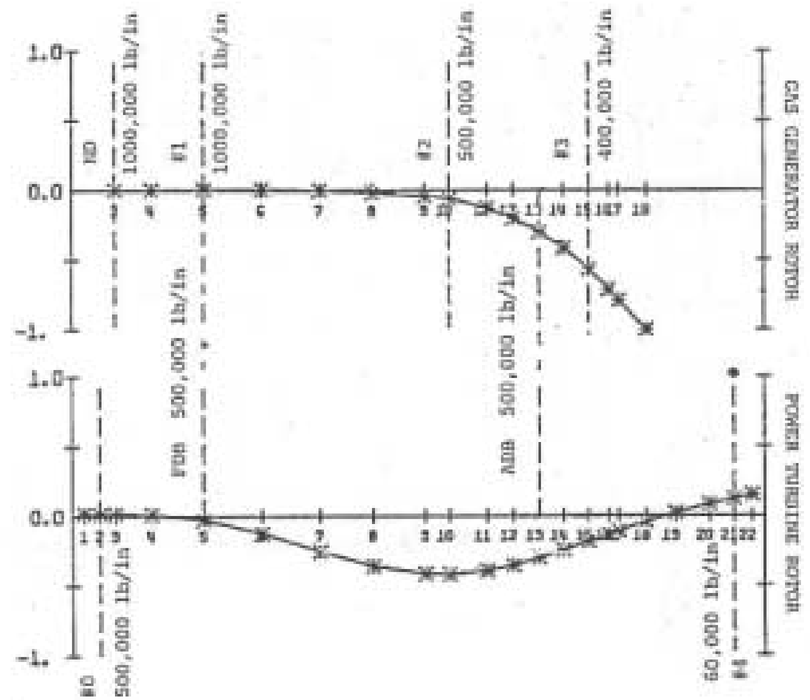

Fig B.3.23 First Power Turbine Critical Speed N = 12555 RPM[14]

14. Li, Dennis, 1978, "Dynamic Analysis of Complex Multi-Level Flexible Rotor Systems", University of Virginia

Gyroscopic Damped Mode Shapes

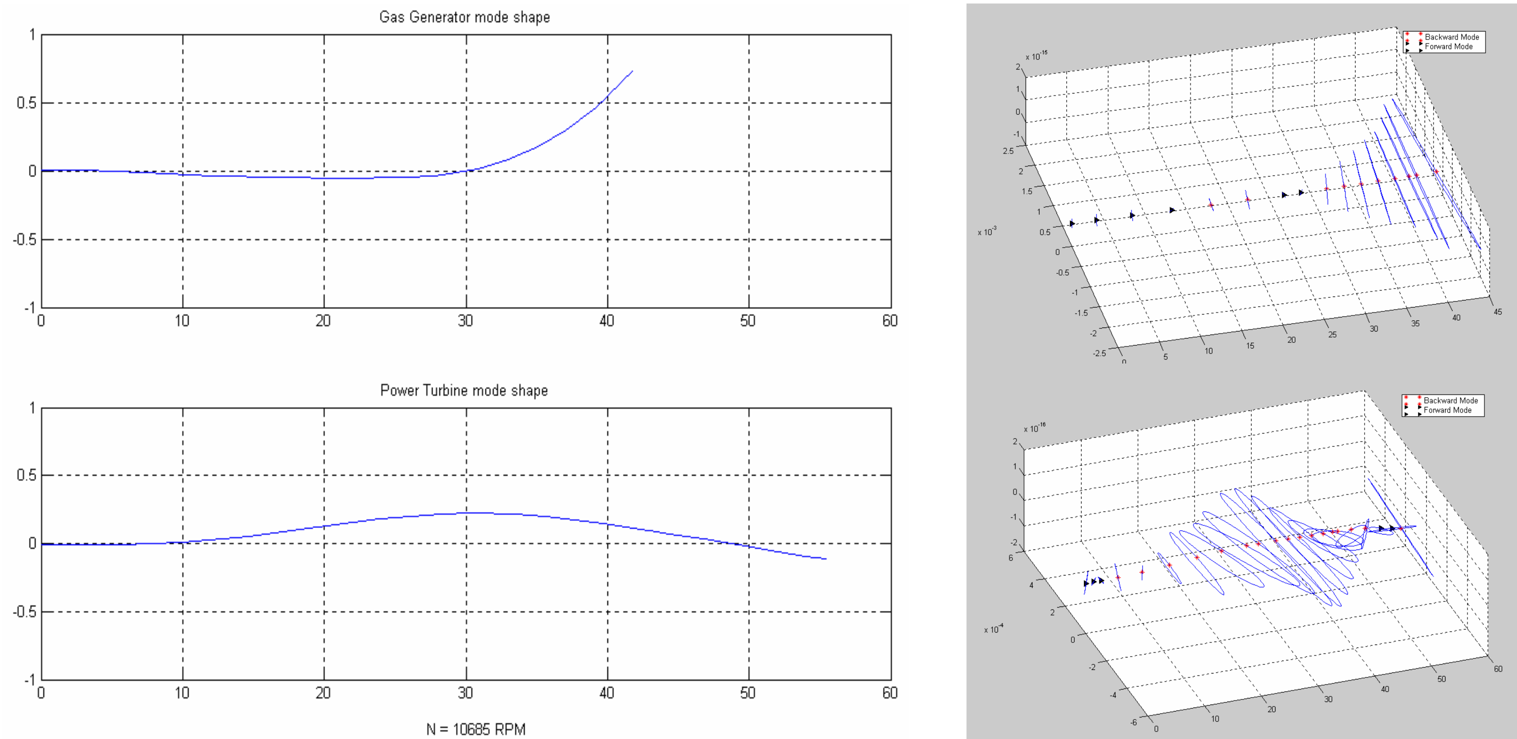

Fig B.3.24 2D and 3D Mode Shapes(with whirl direction) at N=10397 RPM

Gyroscopic Damped Mode Shapes

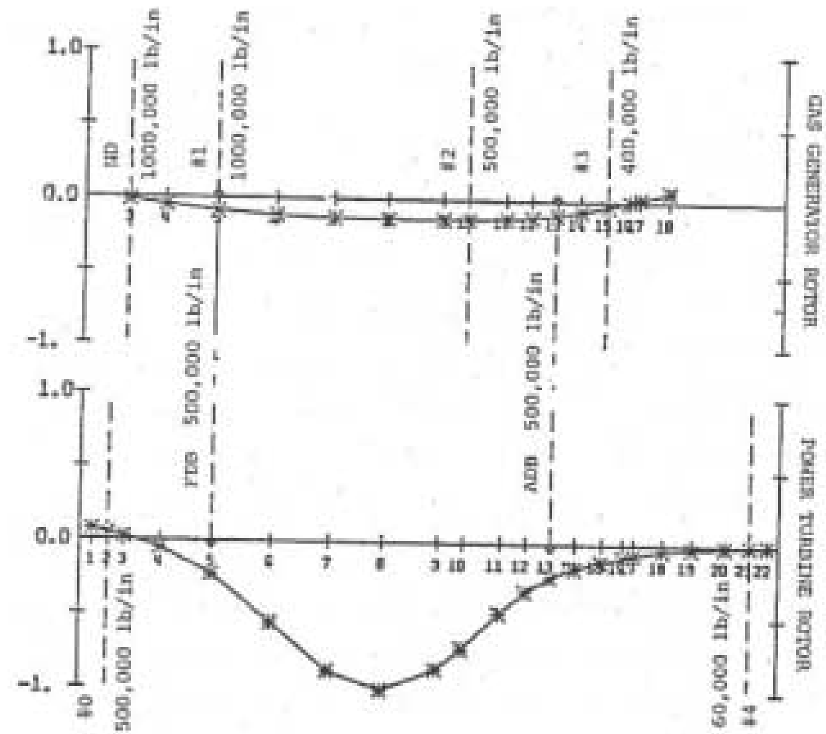

Fig B.3.25 First Power Turbine Critical Speed N = 20792 RPM[15]

15. Li, Dennis, 1978, “Dynamic Analysis of Complex Multi-Level Flexible Rotor Systems”, University of Virginia

Gyroscopic Damped Mode Shapes

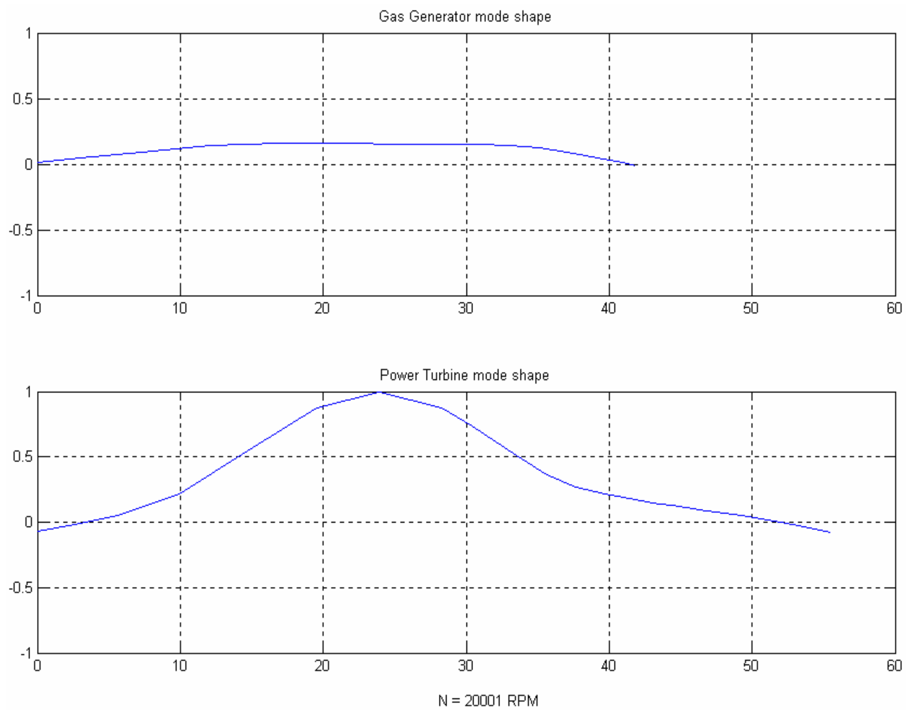

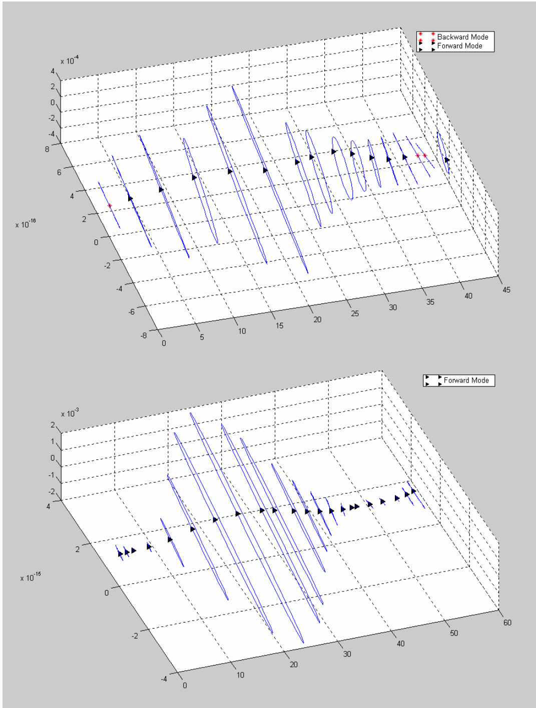

Fig B.3.26 2D and 3D Mode Shapes(with whirl direction) at N=20504 RPM

NASA/CR—2003-212205

Critical Speed Analysis

- Performed similar to the Mode Shape generation, where the reference spin speed is varying.
- Loops through the Power Turbine spin speeds from 0 to 30000 rpm in steps of 500 rpm, calculating the eigenvalues at each step.
- Useful to show the following system properties as a function of shaft speed:
  - Sub/super-synchronous frequencies excitable at a particular operating speed.
  - Confirms single analysis computation of critical speeds with $\lambda = i\omega$ (ω = Spin Speed)
  - Increasing separation of forward and backward whirl modes with shaft speed.

Glenn Research Center

High Temperature Magnetic Bearing - Blade Loss Mitigation
NRA-GRC-99-02 - 1Year Milestone Review
September 27, 2002, NASA Glenn

Texas A&M Vibration Control and Electromechanics Lab

Critical Speed Analysis

Full Model (without reduction)

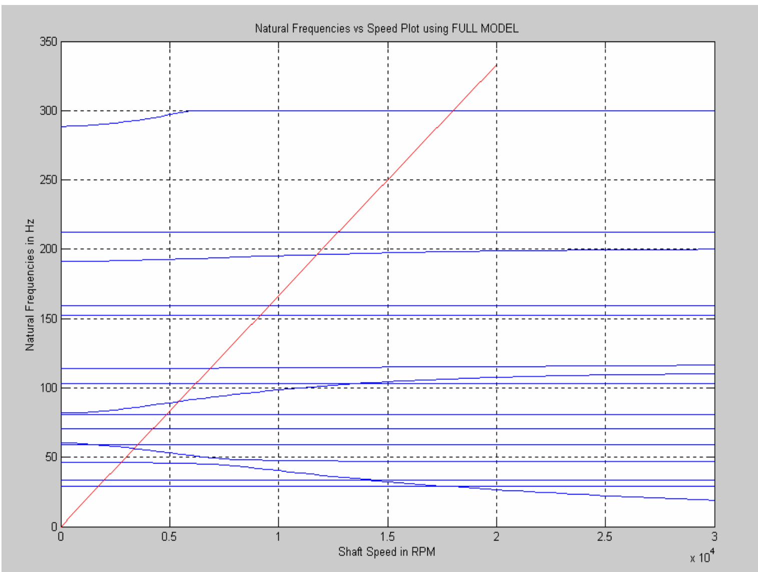

VCEL Model (Component Mode Synthesis)

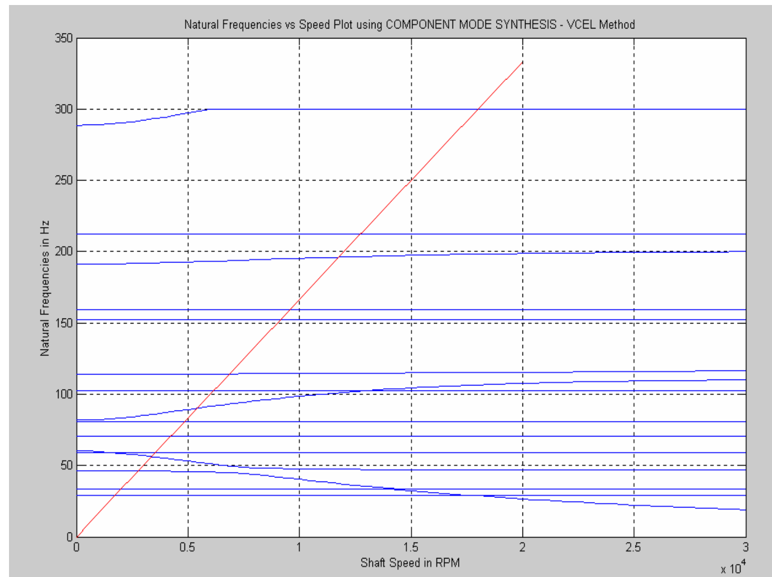

Fig B.3.27 Campbell Diagram - Natural Frequencies vs Speed Plot

Steady State Harmonic Response Analysis

- The general form of the equilibrium equation is written as:

$$(-\omega^2 [M] + i\,\omega [C] + [K])\,\{Q(\omega)\} = \{F(\omega)\}$$

$[C] = [C_b] + [G(\omega)]$

$[C_b]$ = System Damping Matrix

$[G(\omega)]$ = Gyroscopic matrix

$Q(\omega)$ = Steady State Response vector

$F(\omega)$ = Input forcing function

- An imbalance equivalent to 160 lbs force at 16000 RPM was applied to the power turbine mid-span and second stage turbine with a phase difference of Π rads.

Glenn Research Center

High Temperature Magnetic Bearing - Blade Loss Mitigation
NRA-GRC-99-02 - 1Year Milestone Review
September 27, 2002, NASA Glenn

Texas A&M Vibration Control and Electromechanics Lab

Steady State Harmonic Analysis

Full Model (without reduction)

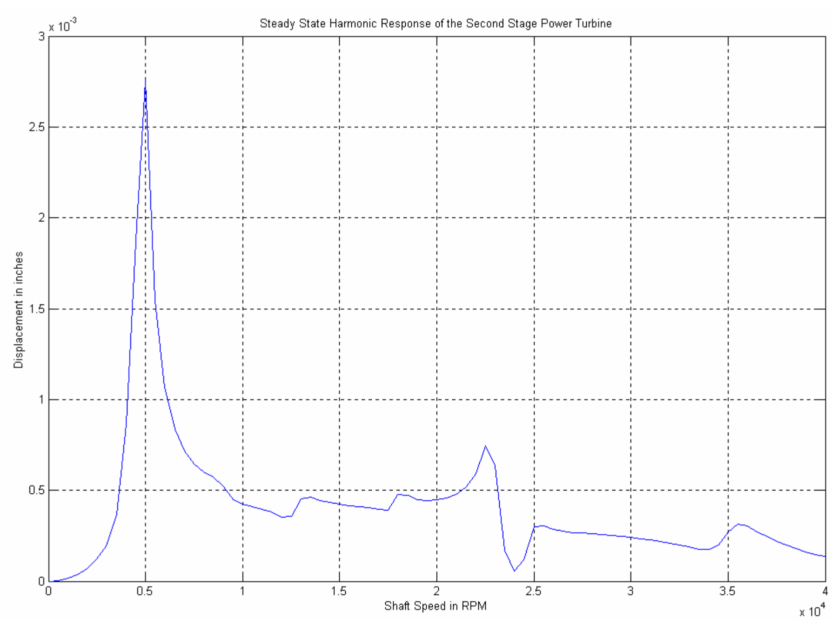

VCEL Model (Component Mode Synthesis)

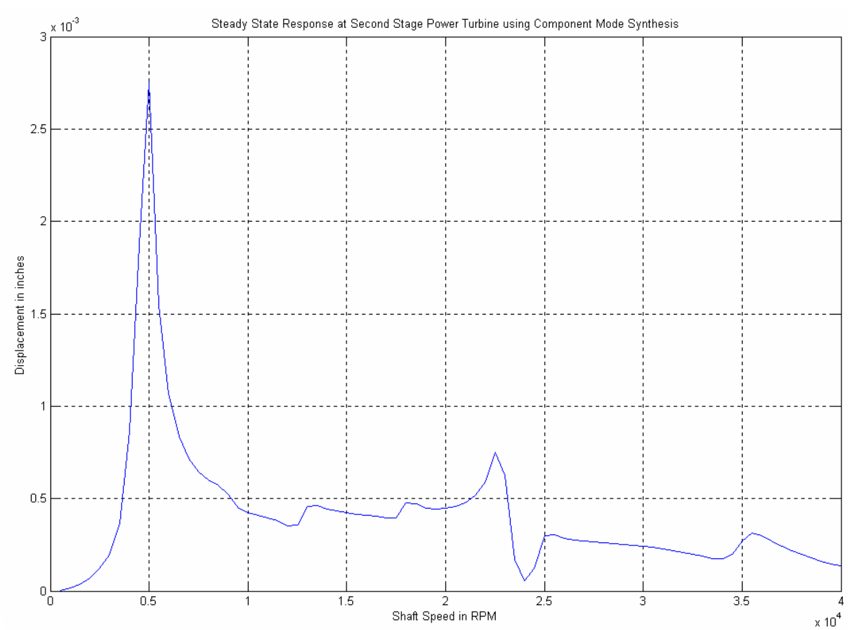

Fig B.3.28 Steady State Harmonic Response of Second Stage Power Turbine

Transient Response Analysis

- The general system equation for the transient response analysis is given by:

$$[M] + [C] + [K] \{Q(t)\} = \{F(t)\} + \{N(t)\}$$

$\{F(t)\}$ = Input forcing function vector (e.g. rotor unbalance)

$\{N(t)\}$ = Non linear force vector (e.g. squeeze film damper)

- An imbalance equivalent to 160 lbs force at 16000 RPM was applied to the power turbine mid-span and second stage turbine with a phase difference of Π rads.
- The gas generator is run at a constant speed of 15000 rpm and the power turbine is run at a speed of 16000 rpm.

Transient Response Analysis - only Linear unbalance force

Full Model (without reduction)

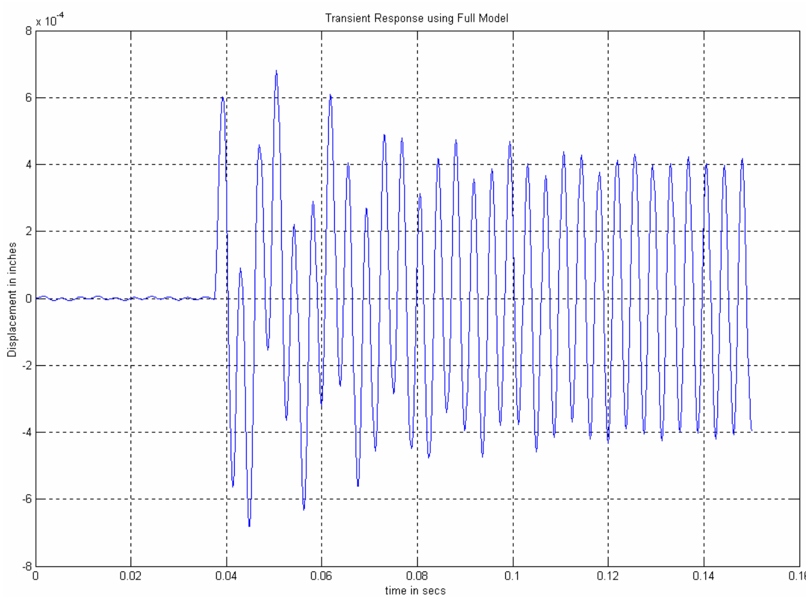

VCEL Model (Component Mode Synthesis)

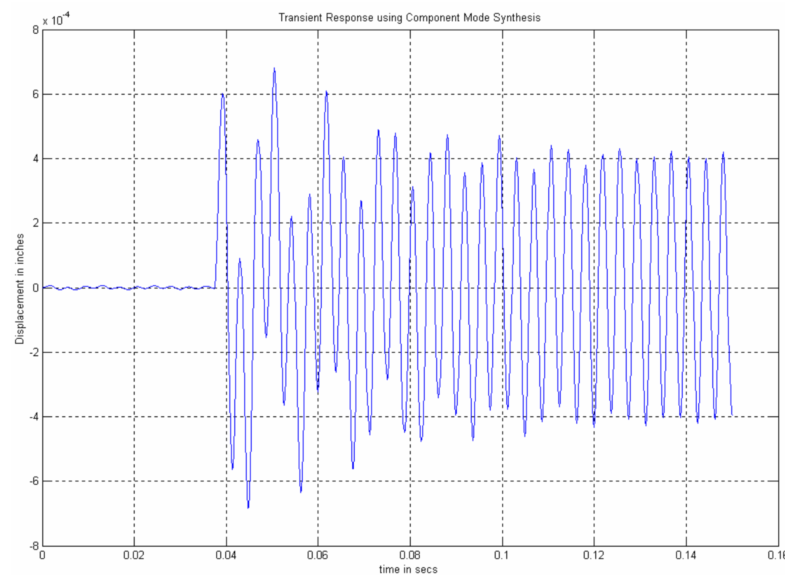

Fig B.3.29 Transient Response of the Second Stage Power Turbine
No of revolutions = 40

Transient Response Analysis - only Linear unbalance force

Problem Dimension	Frequency upto which modes retained	Gas Generator Modes Retained	Power Turbine Modes Retained	Time taken for 40 revolutions	Max Displacement at Power Turbine 2nd Stage (inch)
32	400 Hz	4	5	26.97 secs	6.643E-4
38	600 Hz	6	7	27.02 secs	6.972E-4
54	1000 Hz	10	11	34.11 secs	6.935E-4
74	2000 Hz	15	16	88.48 secs	6.817E-4
456	All*	All*	All*	19.13 hrs	6.816E-4

Table B.3.6 Transient Response Results - Time Savings

* Indicates Physical Co-ordinate Solution

High Temperature Magnetic Bearing - Blade Loss Mitigation
NRA-GRC-99-02 - 1Year Milestone Review
September 27, 2002, NASA Glenn

Glenn Research Center

Texas A&M Vibration Control and Electromechanics Lab

Transient Response Analysis - only Linear unbalance force

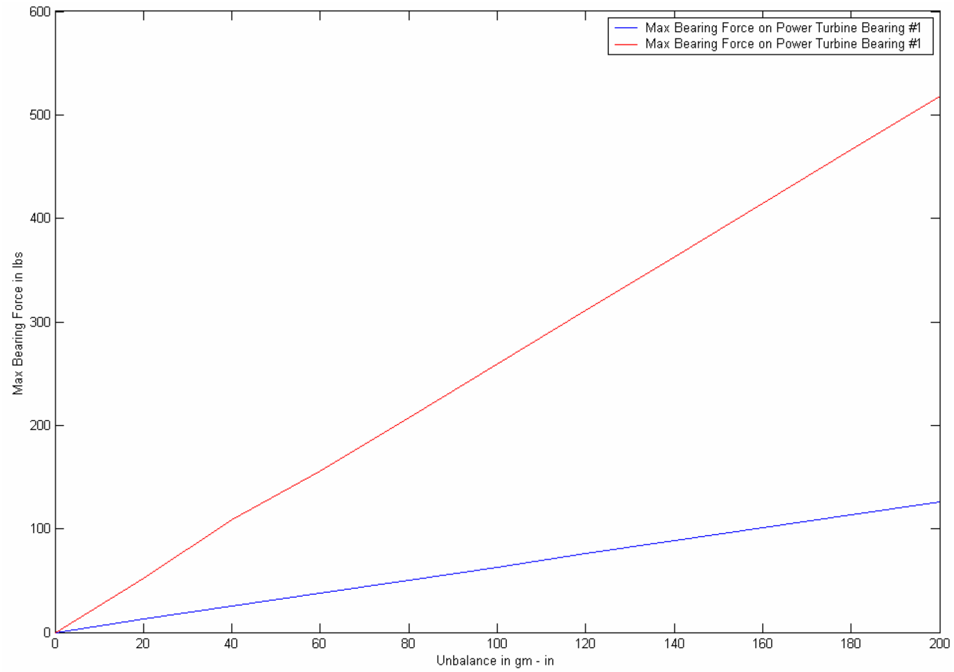

Fig B.3.30 Max Power Turbine Bearing Force vs Unbalance

Transient Response Analysis
Equivalent Imbalance force ~ 3000 lbs @ 16000 RPM

Power Turbine Bearing #1 — Power Turbine Bearing #2

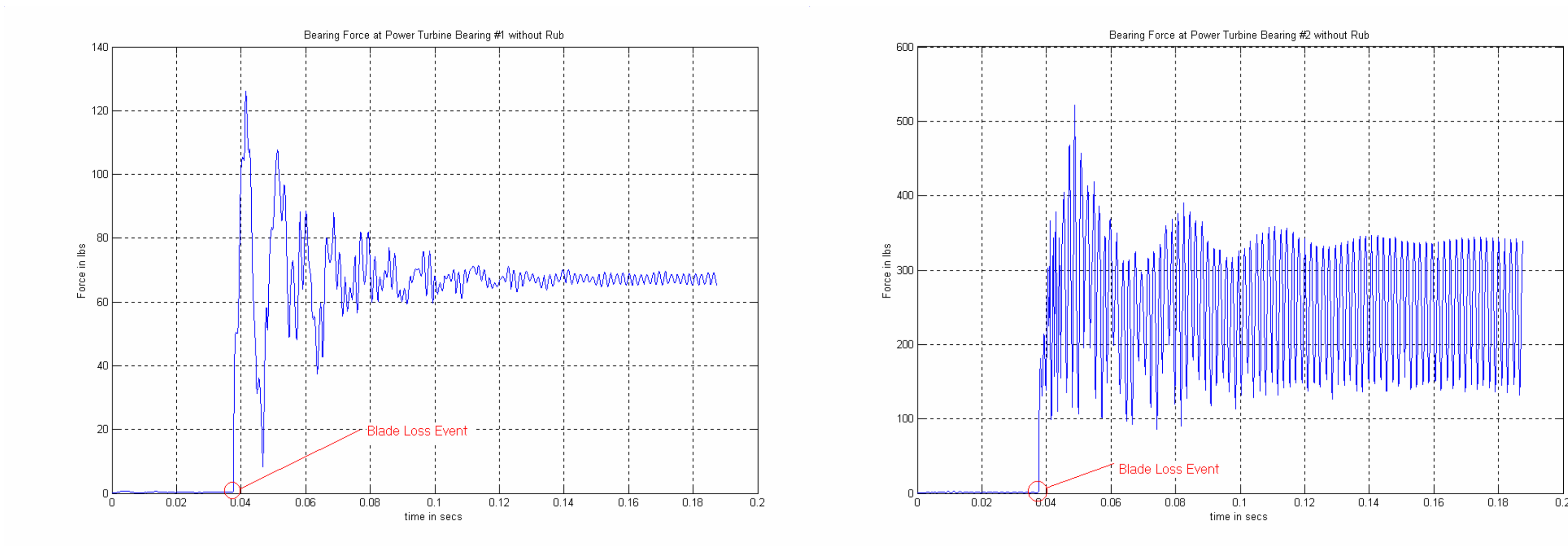

Fig B.3.31 Max Bearing Force vs Time at the Power Turbine Bearings
No of revolutions = 50

Transient Response Analysis - Including Rub

- An imbalance equivalent to 3000 lbs force at 16000 RPM was applied to the power turbine mid-span and second stage turbine with a phase difference of Π rads.
- Rub was included by using a clearance of 0.01” at the rub node.
- Gas generator is run at a constant speed of 15000 rpm and the power turbine is run at a speed of 16000 rpm.
- Contact Stiffness = 250,000 lbs/in
- Coefficient of friction = 0.1

Transient Response Analysis - Including Rub

Displacement vs time

Shaft Orbit Motion

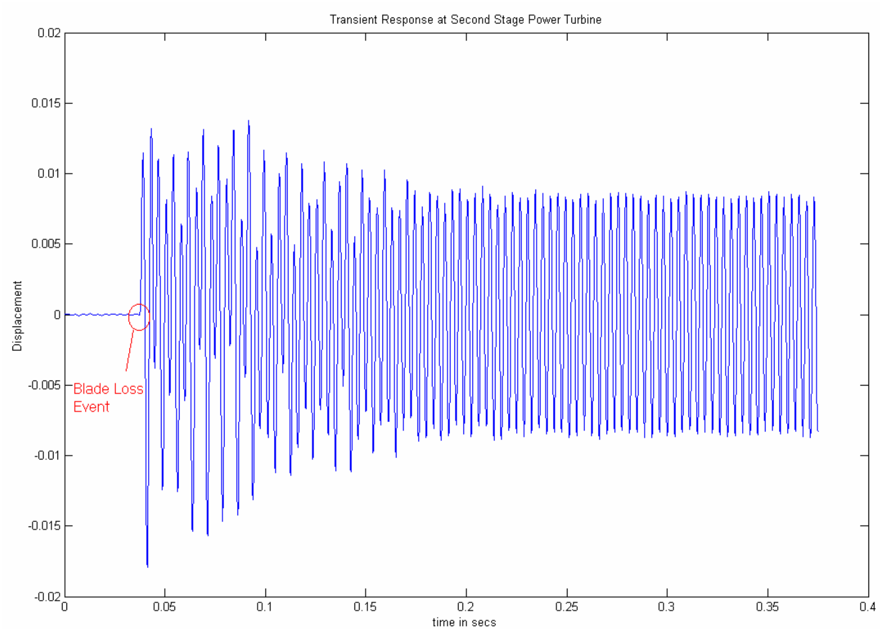

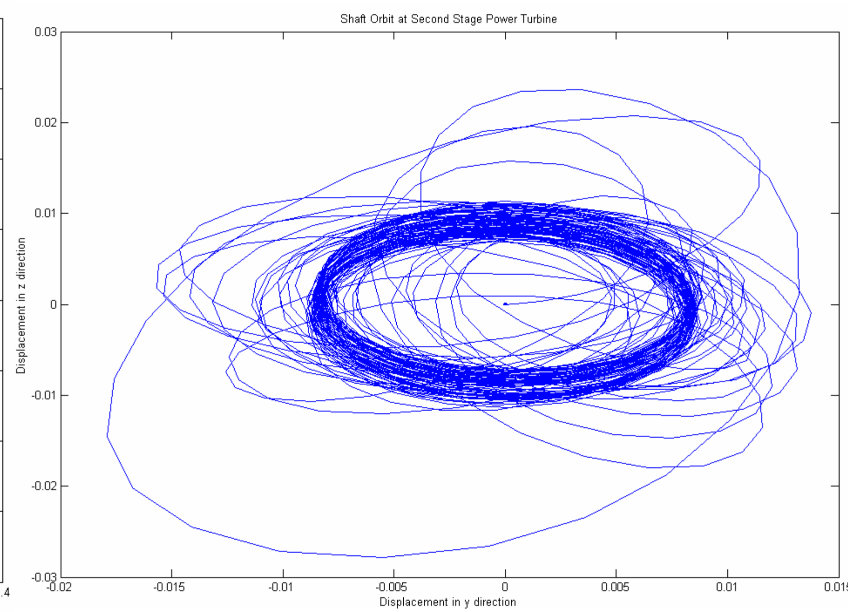

Fig B.3.32 Transient Response Analysis at second stage Power Turbine
No of revolutions = 100

Transient Response Analysis - Including Rub

Power Turbine Bearing #1

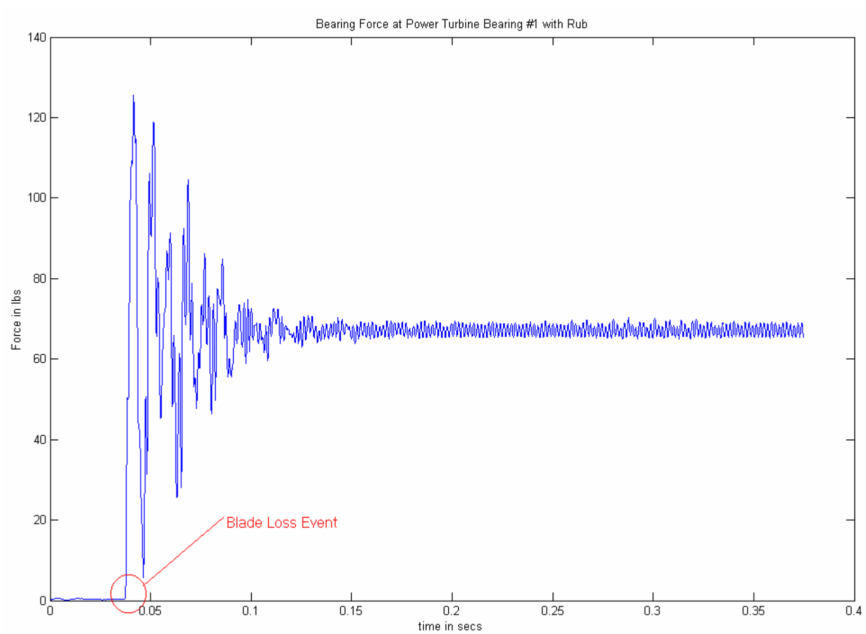

Power Turbine Bearing #2

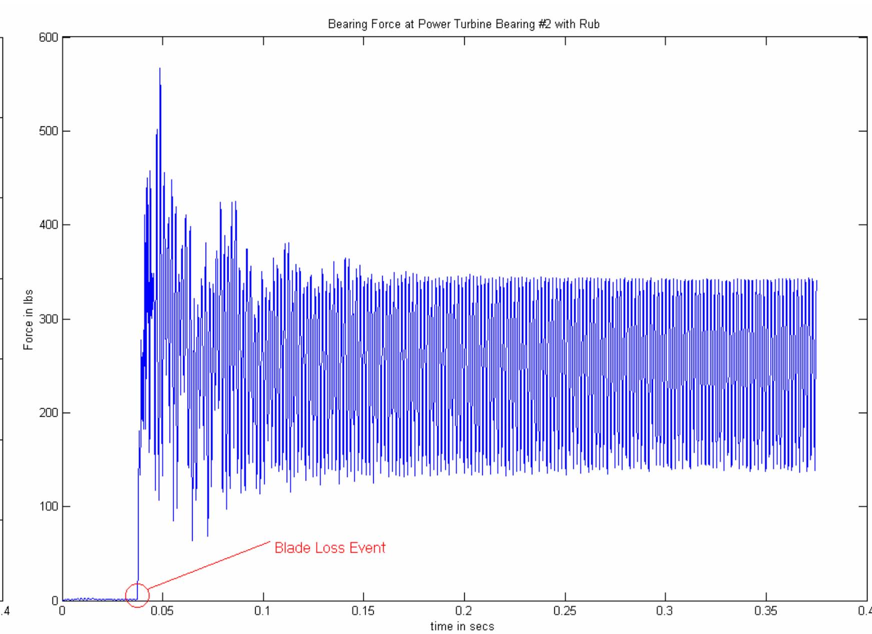

Fig B.3.33Max Bearing Force vs Time at the Power Turbine Bearings
No of revolutions = 100

Transient Response Analysis at 16000 RPM Including Squeeze Film Damper (SFD) Bearing

- The two main Power Turbine Bearings were modeled with detailed squeeze film dampers.
- A comparison is provided between the results obtained using damper formula and numerical finite element model of oil film.
- In the FE model, the coefficient matrix is determined and assembled at staggered intervals of time to improve computational efficiency.
- An imbalance equivalent to 1500 lbs force at 16000 RPM was applied at the power turbine mid span and second stage power turbine.

Transient Response Analysis at 16000 RPM Including Squeeze Film Damper (SFD) Bearing

Using Formula | Using FE Model

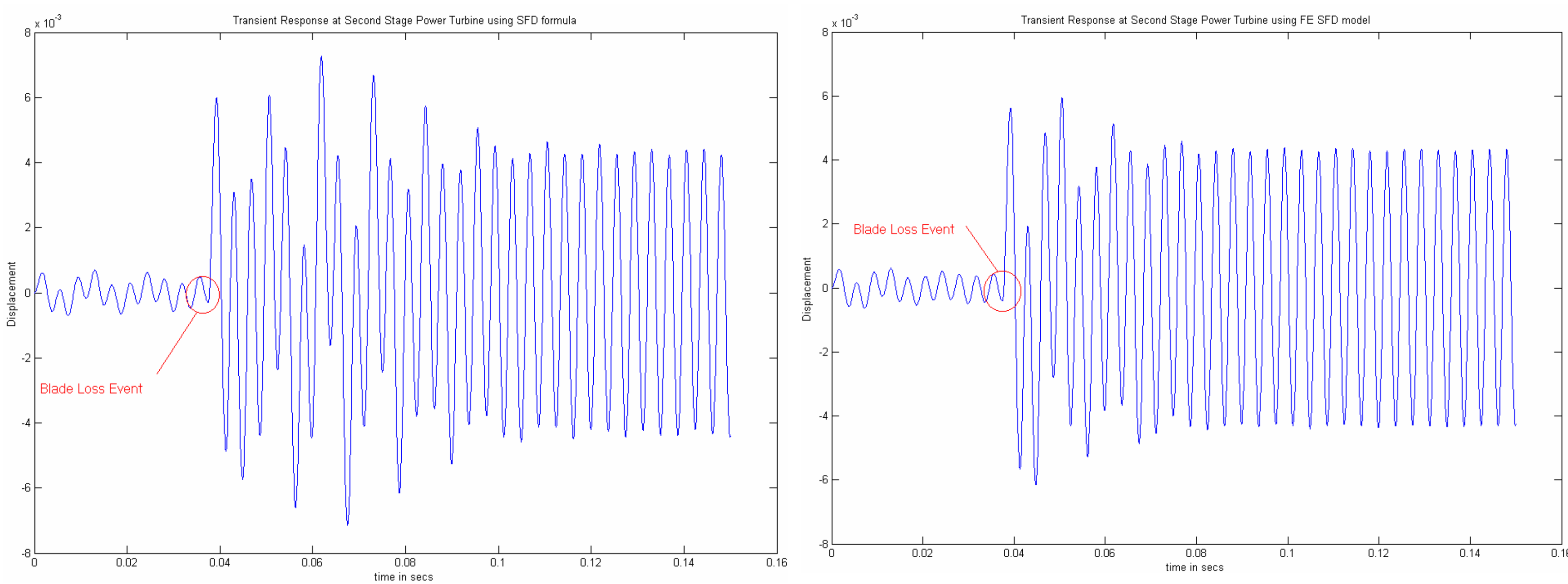

Fig B.3.34 Displacement vs time plots at second stage Power Turbine
No of revolutions = 40

Transient Response Analysis at 16000 RPM Including Squeeze Film Damper (SFD) Bearing

Using Formula

Using FE Model

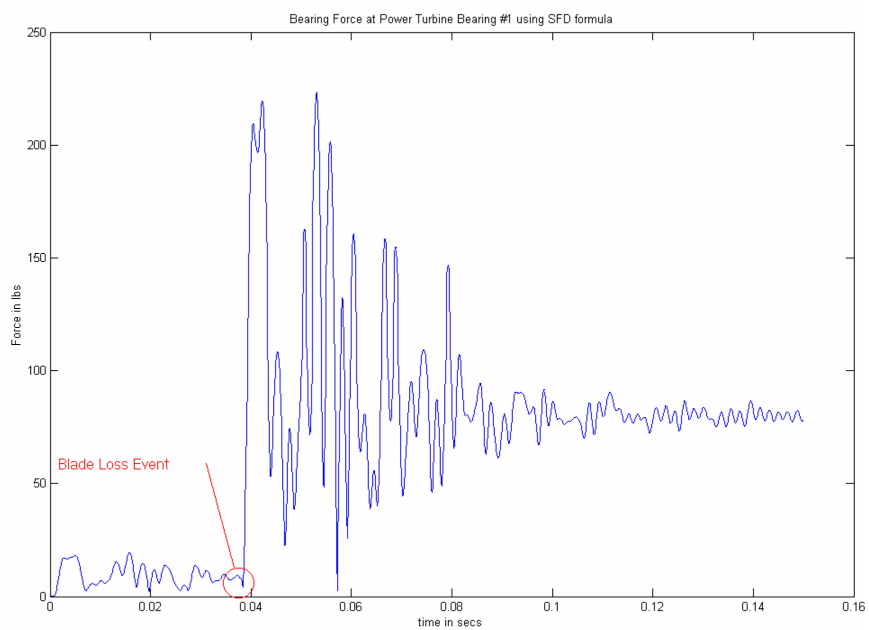

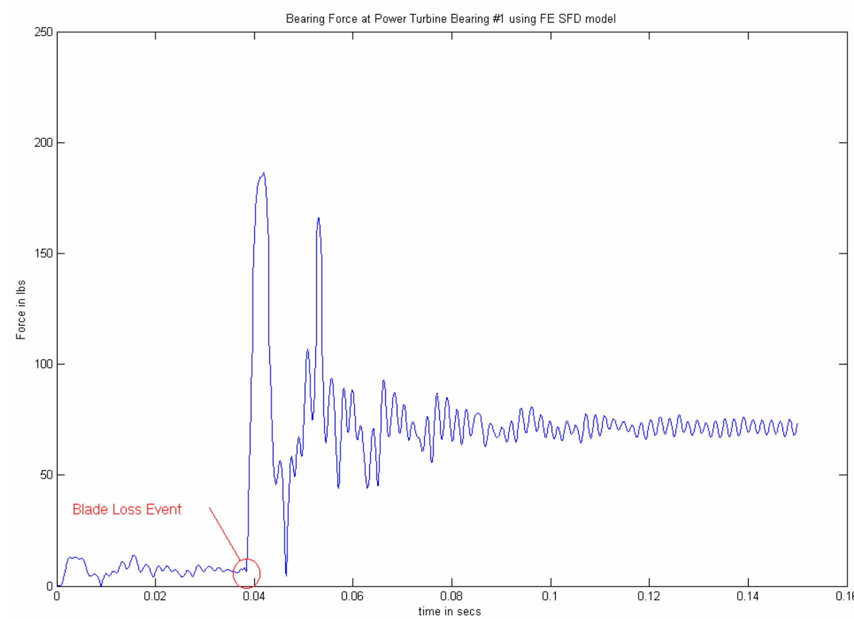

Fig B.3.35 Max Bearing Force Magnitude vs Time at Power Turbine Bearing #1
No of revolutions = 40

Transient Response Analysis at 16000 RPM Including Squeeze Film Damper (SFD) Bearing

Using Formula

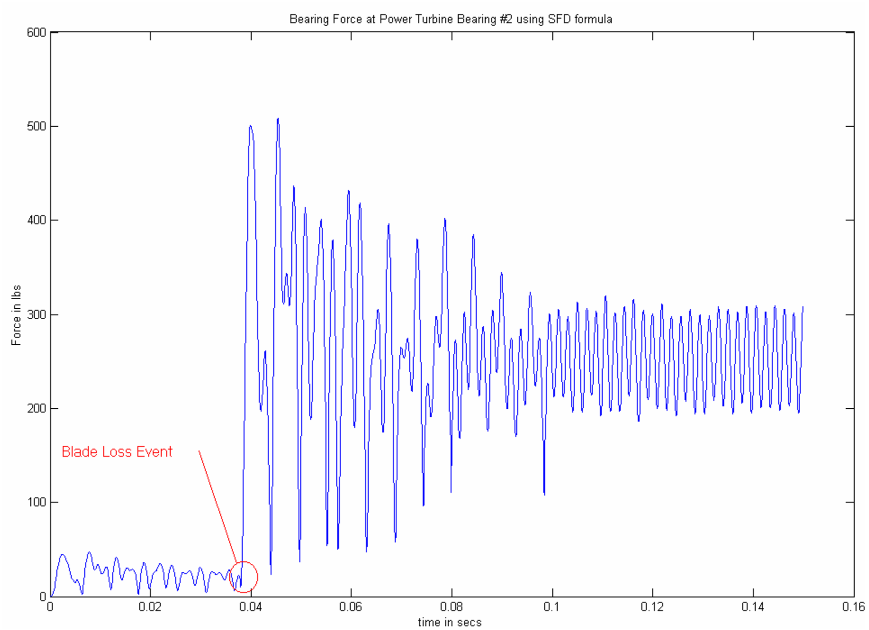

Using FE Model

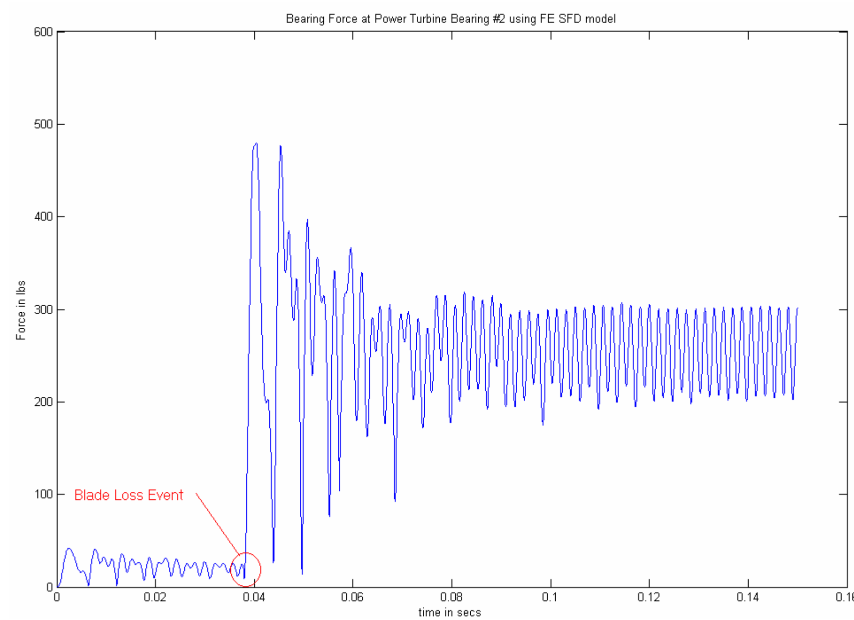

Fig B.3.36 Max Bearing Force Magnitude vs Time at Power Turbine Bearing #2
No of revolutions = 40

NASA/CR—2003-212205

Transient Response Analysis Using High Fidelity 2D Linearized Bearing Model

- Power turbine main bearings replaced by high fidelity models.
- Includes motions of ball and cage, forces, stresses, and thermal expansions into the code.
- Calculates temperature at 6 temperature points at each bearing.
- Ambient temperature of 80 F was used at all points.
- An imbalance equivalent to 1500 lbs force at 16000 RPM was applied at the power turbine mid span and second stage power turbine.

Glenn Research Center

High Temperature Magnetic Bearing - Blade Loss Mitigation
NRA-GRC-99-02 - 1Year Milestone Review
September 27, 2002, NASA Glenn

Texas A&M Vibration Control
and Electromechanics Lab

Transient Response Analysis
Using High Fidelity Linearized 2D Bearing Model

Power Turbine Bearing #1

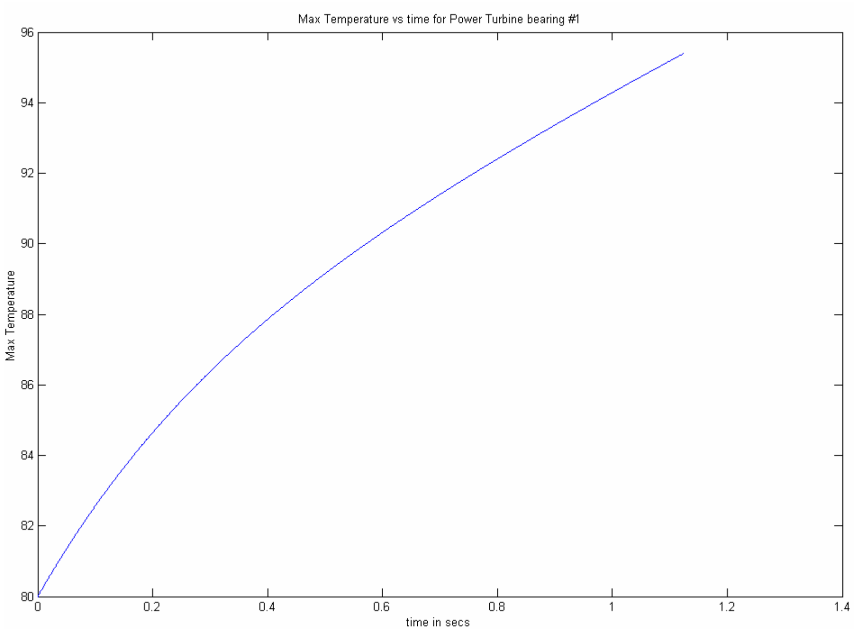

Power Turbine Bearing #2

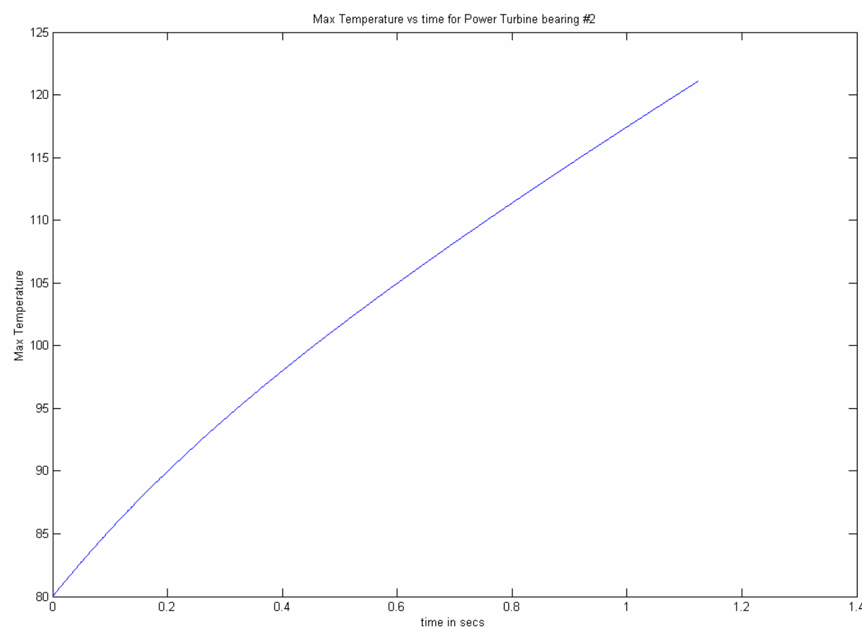

Fig B.3.37 Max Temperature vs Time at the Power Turbine Bearings
No of revolutions = 300

Transient Response Analysis Using High Fidelity Linearized 2D Bearing Model

Power Turbine Bearing #1

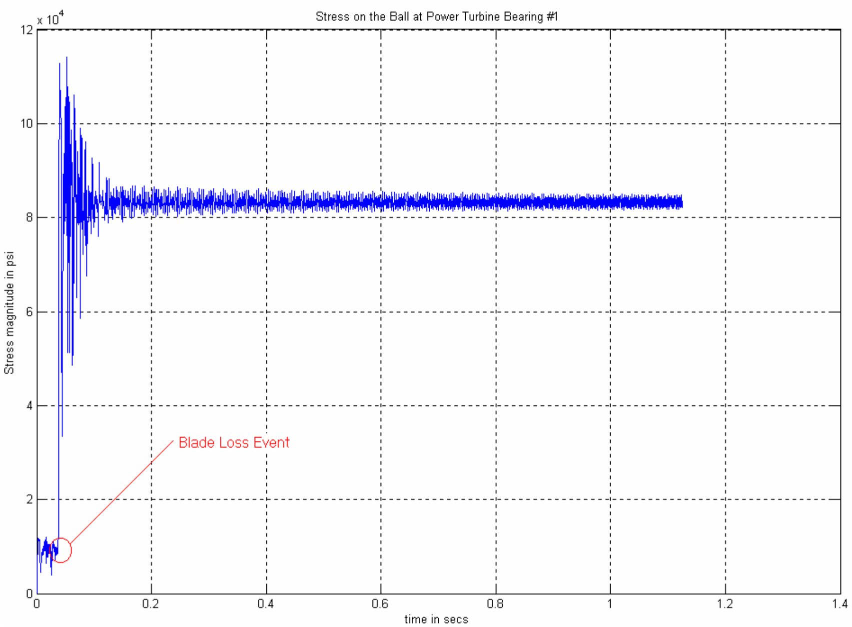

Power Turbine Bearing #2

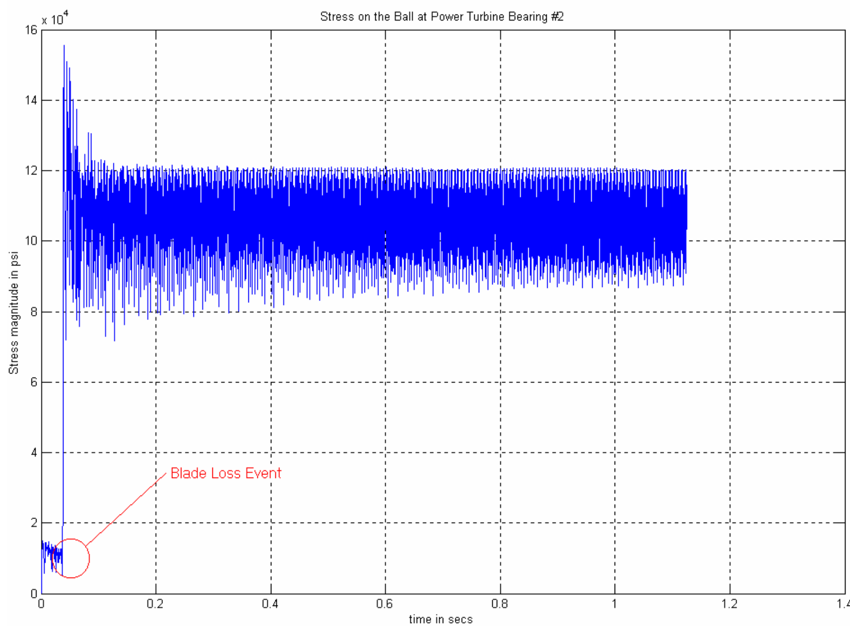

Fig B.3.38 Ball Stresses vs Time at the Power Turbine Bearings
No of revolutions = 300

NASA/CR—2003-212205

Future Work

- Add solid, plate and conical beam elements.
- Develop modal synthesis and modeling capability for N components (levels) including rotors, case, cowl, nozzle, etc. Components defined with super elements, modes or internal element library.
- Update with 3D bearing model incorporating individual ball dynamics and stresses.
- Bearing Life Prediction model.
- Update to include more sophisticated rub models (Need NASA information to define these).
- Update output GUI for animation with hidden surface model motions.
- Build rig in TAMU Spin Pit to measure temperatures during blade out and compare to simulation.

5 KW.Hr Containment Vacuum Spin Pit at TAMU

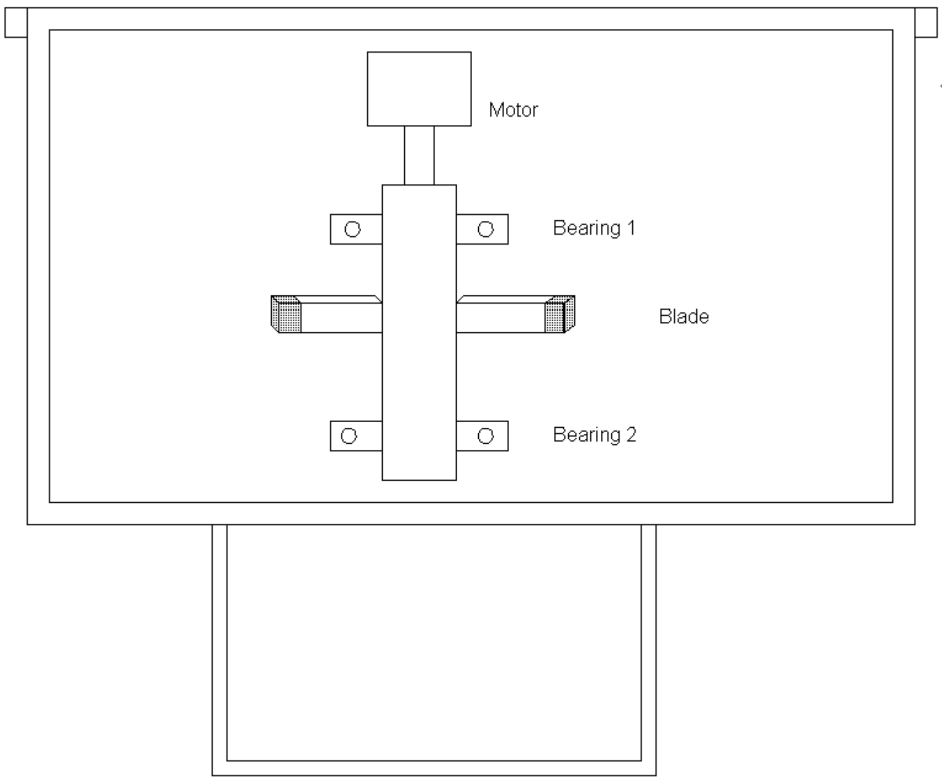

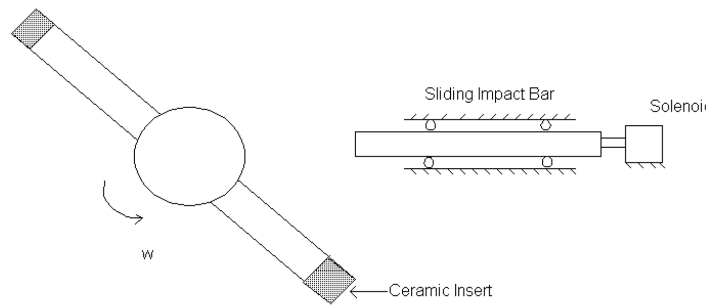

Top View of Rig

Glenn Research Center

Texas A&M Vibration Control and Electromechanics Lab

NASA/CR—2003-212205

TASK B.4 : Dual Rotor - High Fidelity Bearing - Blade Out Simulation Code GUI

By

Karthik Ganesan

&

Lakshmi Subrmaniyam

NASA/CR—2003-212205

EXECUTIVE SUMMARY

- Version 1 of GUI for combined Bearing/ Rotor code is complete.
- The Input data for the thermal option will be added in the next version.
- The example in this GUI uses English system of units and is a dual rotor (Power turbine,Gas generator) model.The model is taken from Li, Dennis, 1978, "Dynamic Analysis of Complex Multi -Level Flexible Rotor systems", University of Virginia.

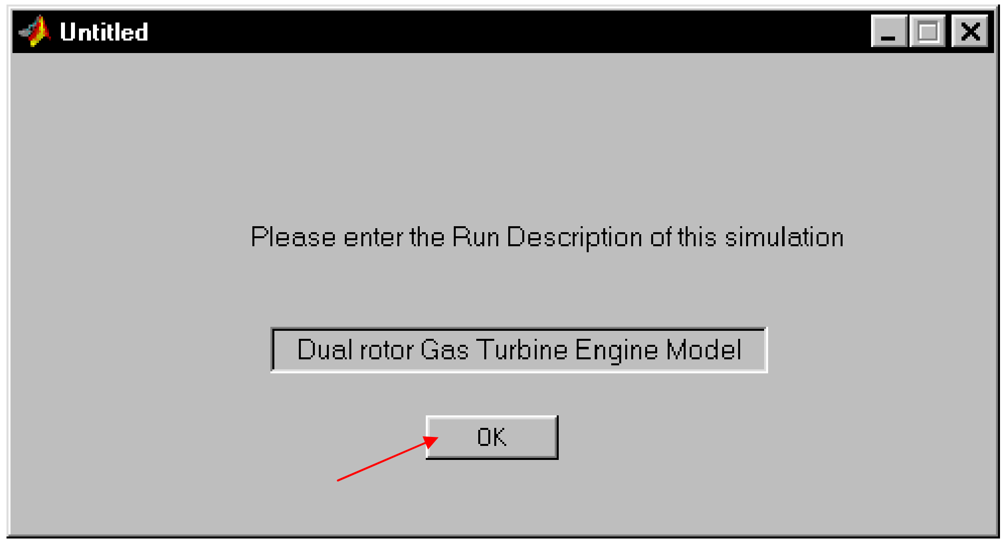

In this section of the GUI all the input data is acquired from the user. In the panel shown above the user enters the run description for the current simulation run.

Glenn Research Center

High Temperature Magnetic Bearing - Blade Loss Mitigation
NRA-GRC-99-02 - 1Year Milestone Review
September 27, 2002, NASA Glenn

Texas A&M Vibration Control and Electromechanics Lab

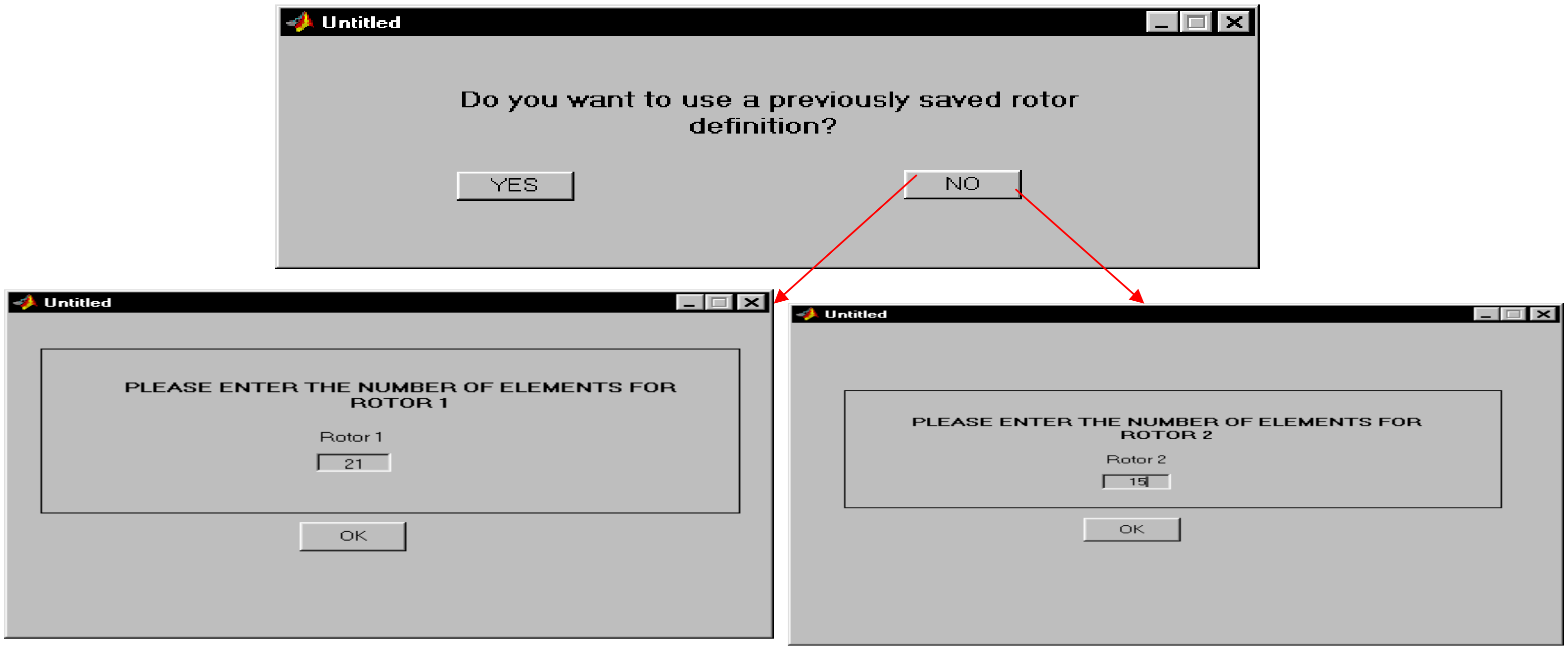

Here the user can select if he wants to use a previously saved rotor definition or define a new set of rotors. If “NO”is clicked then the user is asked for the number of elements on Rotor 1 and Rotor 2.

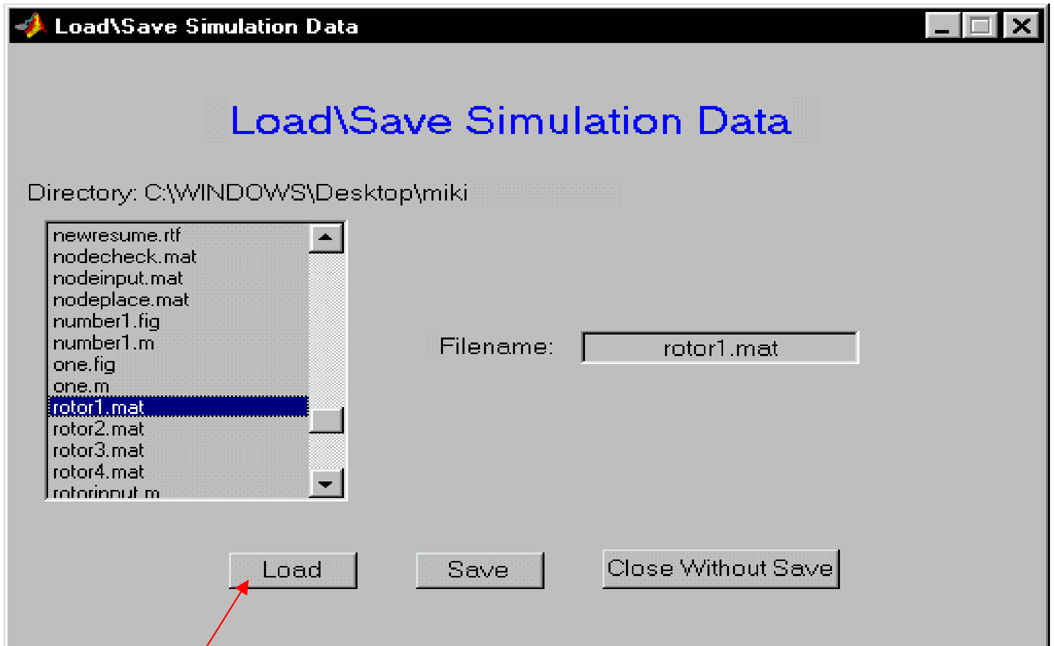

If the user clicks "YES" in the previous panel , a LOAD/SAVE panel pops up which displays a list of all the files in the directory. Here we use the rotor definition "rotor1.mat" for this presentation. After selecting this file, click on LOAD.

Glenn Research Center

High Temperature Magnetic Bearing - Blade Loss Mitigation NRA-GRC-99-02 - 1Year Milestone Review September 27, 2002, NASA Glenn

Texas A&M Vibration Control and Electromechanics Lab

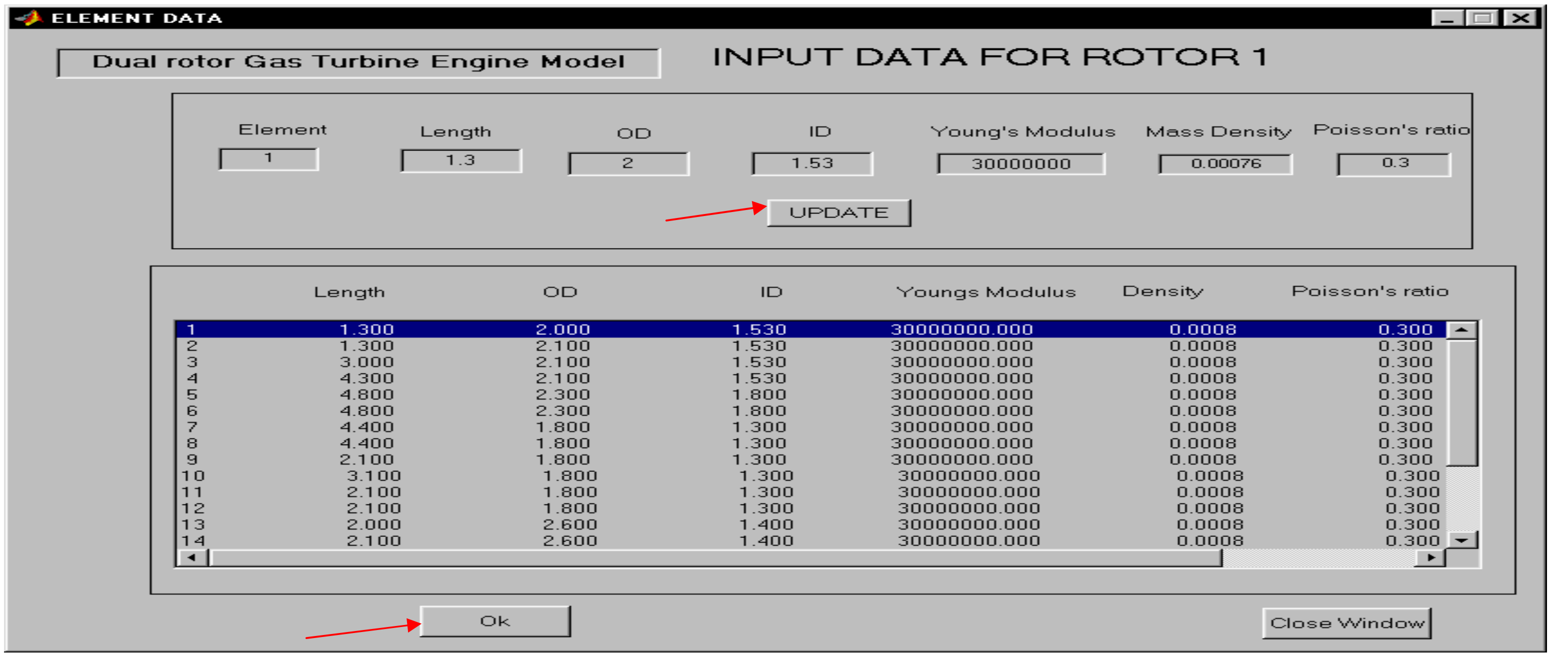

This panel is used to input the rotor definition data like element length, Outside diameter,Young's modulus, Density etc.Here the “rotor.mat” file is shown with the rotor containing 21 elements.We can modify the values by clicking on the element in the list-box and then enter values in the corresponding edit boxes and then hit “UPDATE”

Glenn Research Center

High Temperature Magnetic Bearing - Blade Loss Mitigation
NRA-GRC-99-02 - 1Year Milestone Review
September 27, 2002, NASA Glenn

Texas A&M Vibration Control and Electromechanics Lab

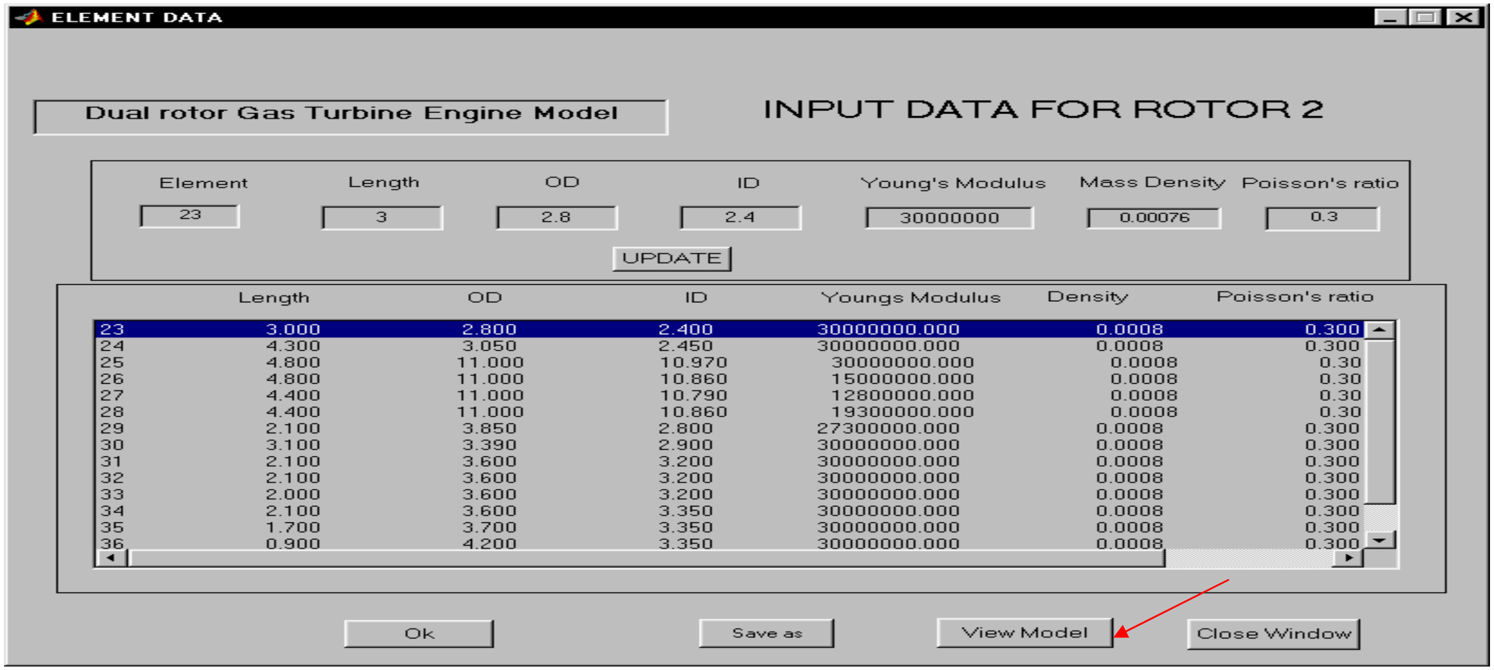

In this panel , as the previous slide, the user inputs second rotor definition .After completing the input, the block diagram of the rotors can be viewed by clicking on “View model”.The user can also save this new definition by clicking “Save as”(Load/ Save panel pops up)

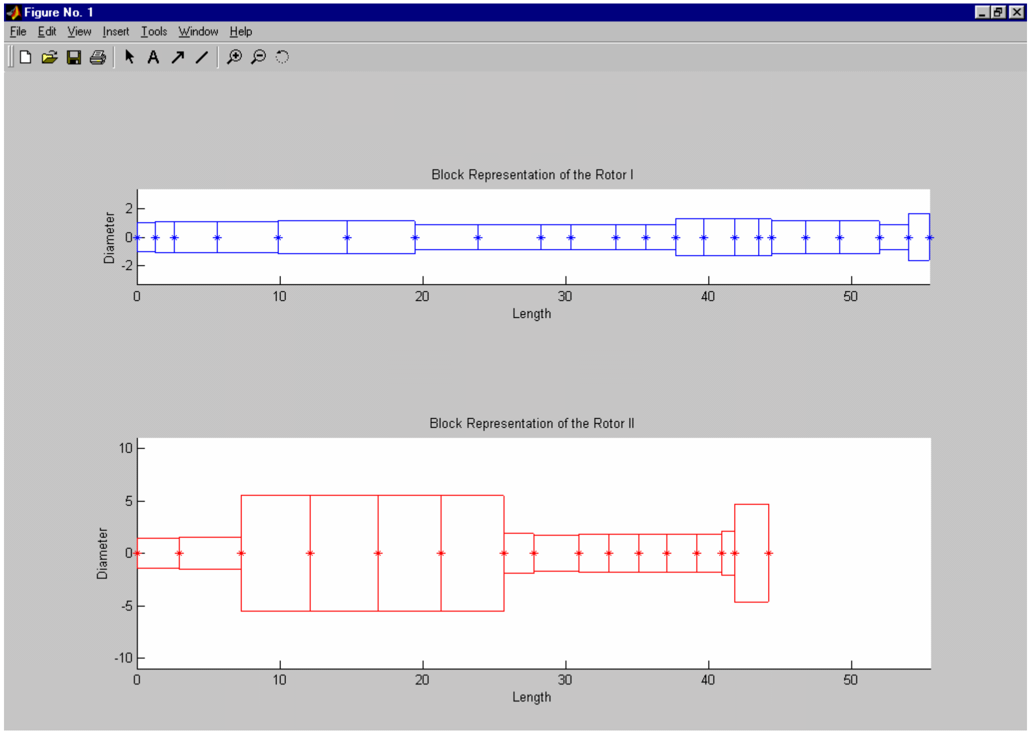

Shown here is the block diagram of the two rotors that the user has defined in the previous panels. This block diagram can viewed dynamically after every time the input data is modified.

Glenn Research Center

High Temperature Magnetic Bearing - Blade Loss Mitigation
NRA-GRC-99-02 - 1Year Milestone Review
September 27, 2002, NASA Glenn

Texas A&M Vibration Control and Electromechanics Lab

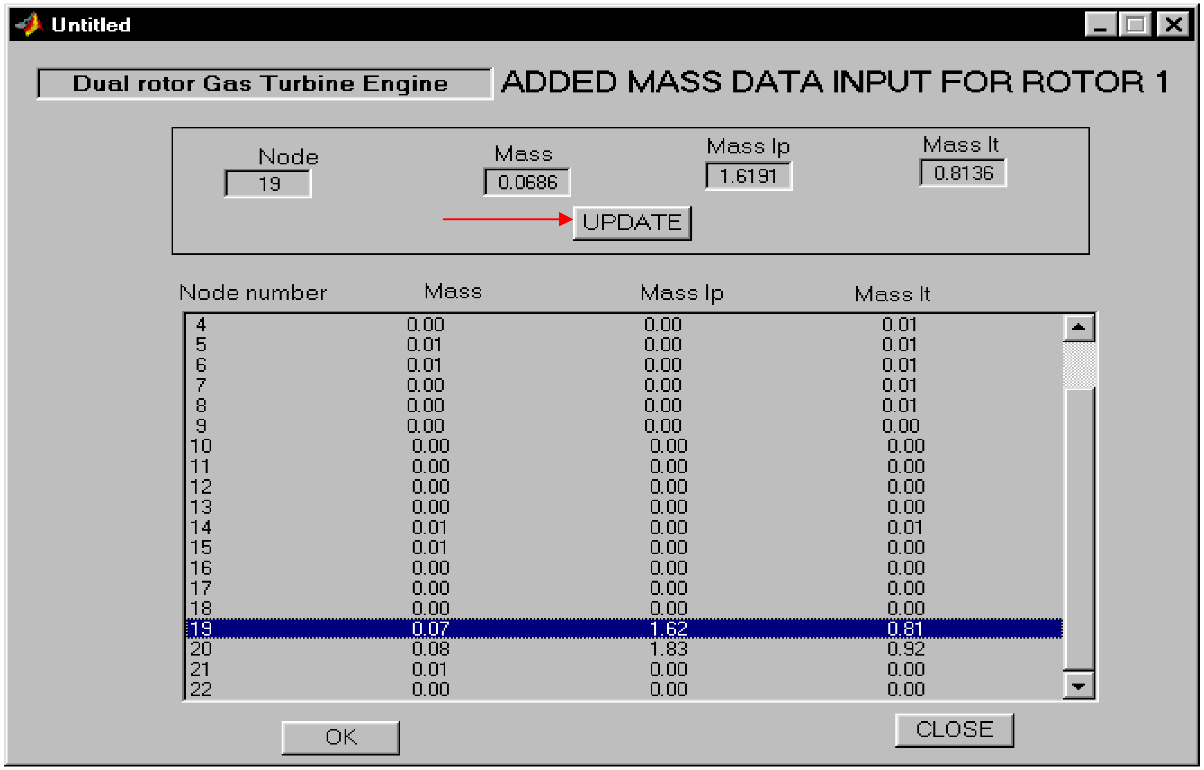

This panel shows the added mass data at different nodes along rotor1. The user can add extra masses at any of the nodes using this panel.

Glenn Research Center

High Temperature Magnetic Bearing - Blade Loss Mitigation
NRA-GRC-99-02 - 1Year Milestone Review
September 27, 2002, NASA Glenn

Texas A&M Vibration Control and Electromechanics Lab

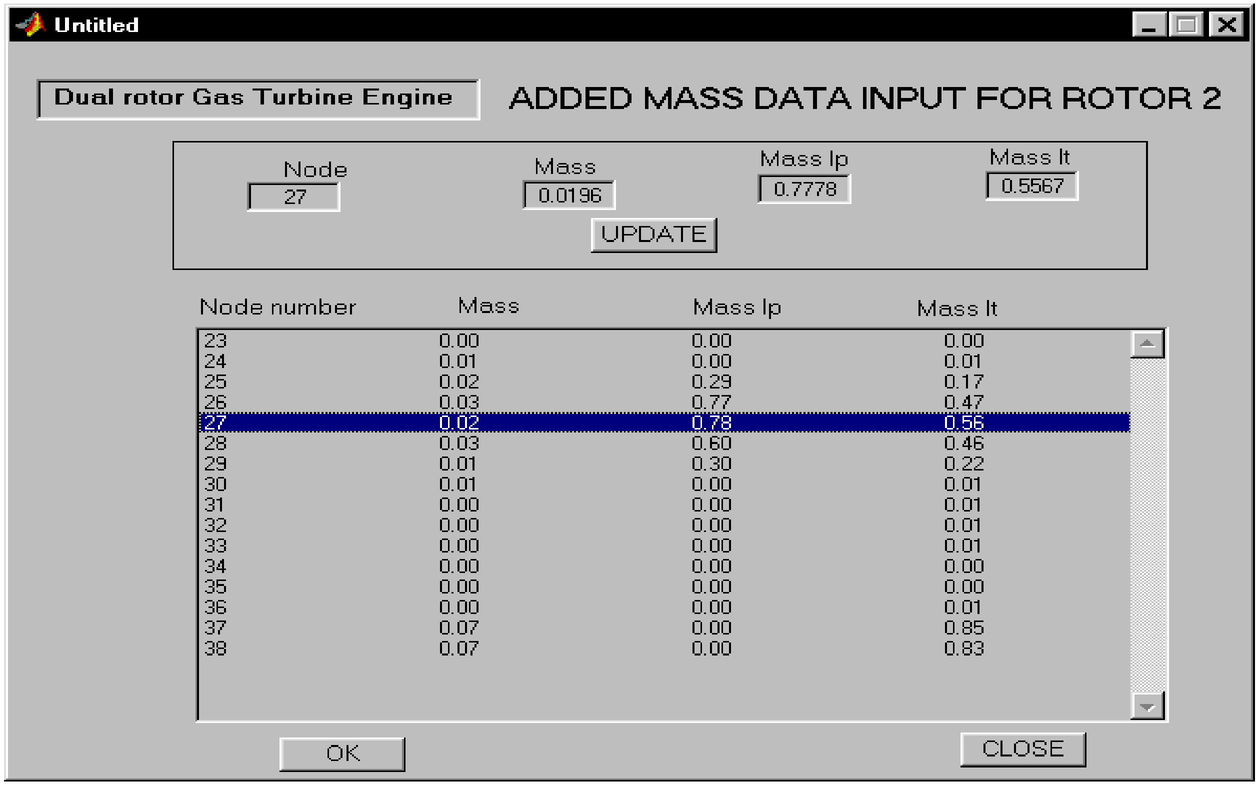

This mass data panel for the second rotor.Here also the user can add masses at any of the nodes along rotor 2.

NASA/CR—2003-212205

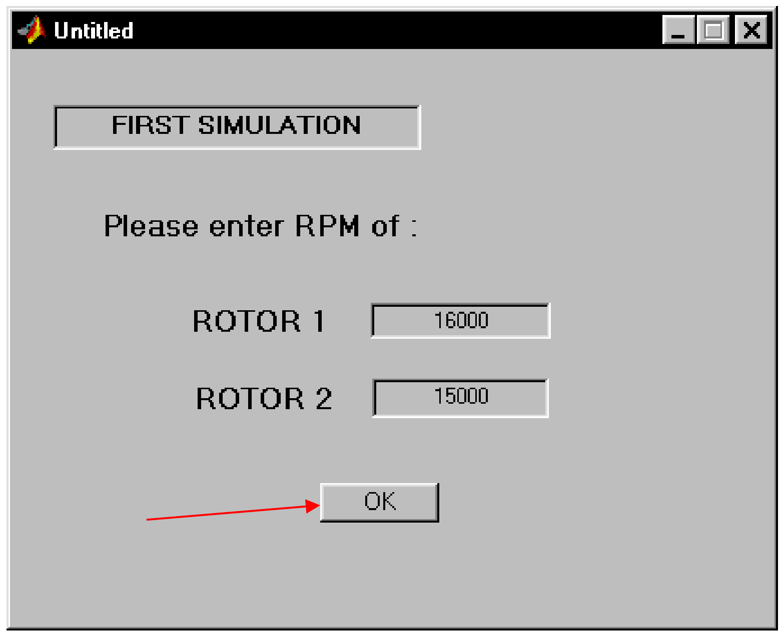

Here the user inputs the RPM of Rotor 1 and Rotor 2

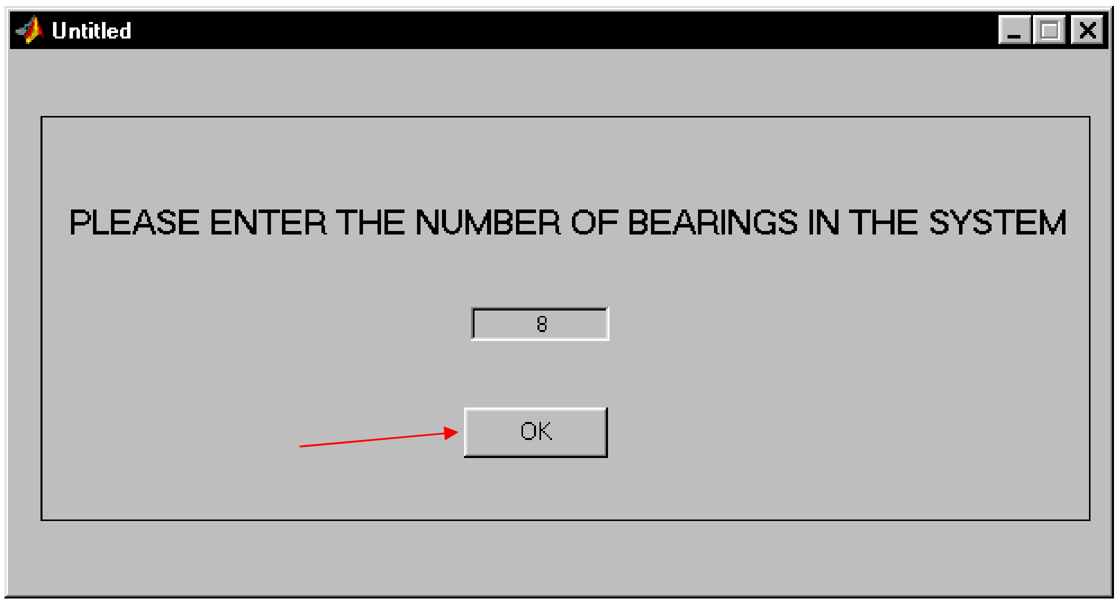

Here the user inputs the number of bearings in the system of rotors.

Glenn Research Center

High Temperature Magnetic Bearing - Blade Loss Mitigation
NRA-GRC-99-02 - 1Year Milestone Review
September 27, 2002, NASA Glenn

Texas A&M Vibration Control and Electromechanics Lab

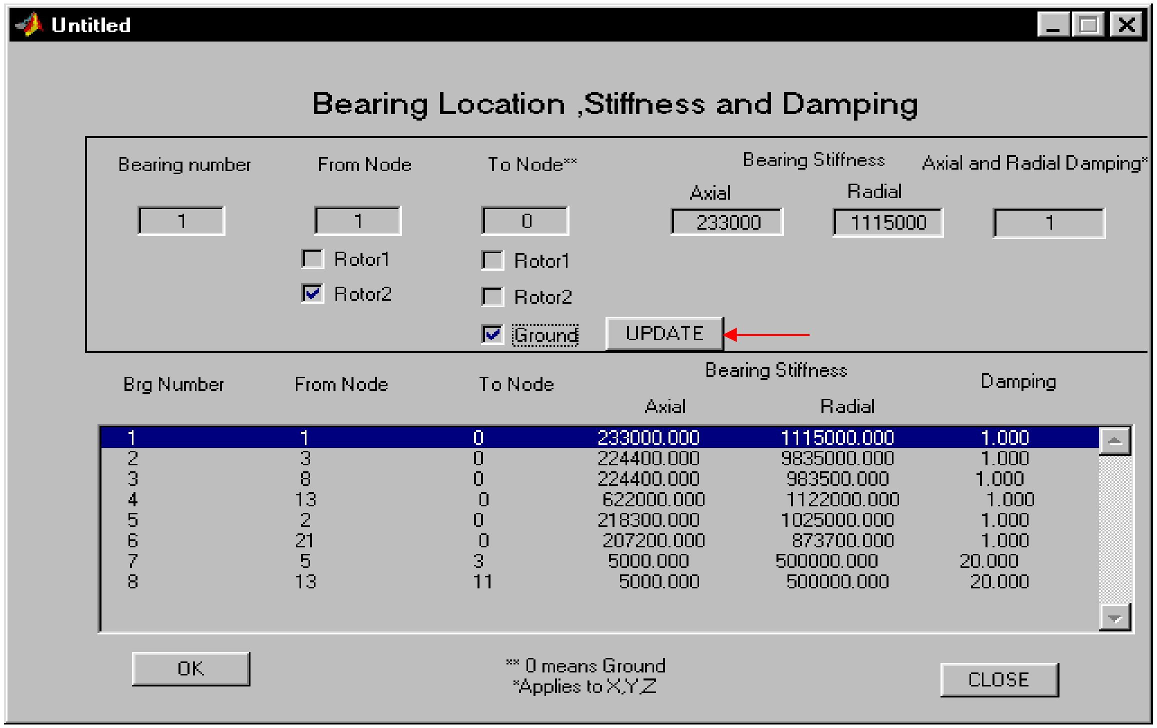

This is the bearing Location , stiffness and damping screen. Here the user inputs the bearing location (From node, To node etc.) ,axial and radial stiffness values and Damping values.

NASA/CR—2003-212205

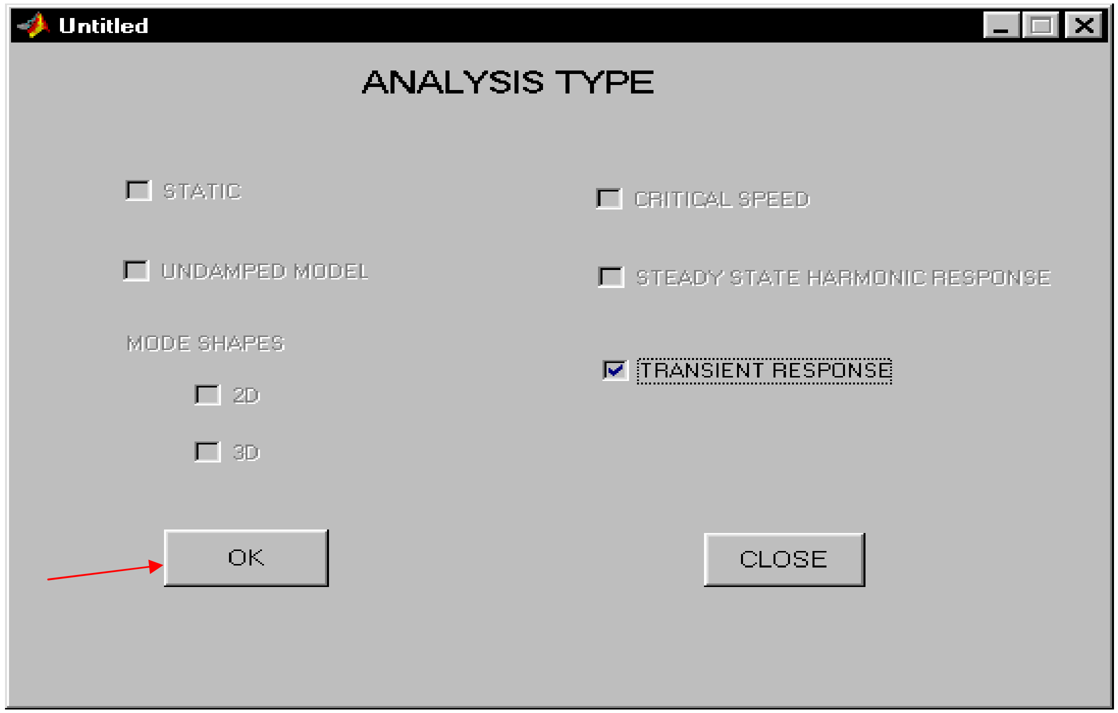

This screen contains the different analysis types.Only Transient Response is enabled at this time.

Glenn Research Center

High Temperature Magnetic Bearing - Blade Loss Mitigation
NRA-GRC-99-02 - 1Year Milestone Review
September 27, 2002, NASA Glenn

Texas A&M Vibration Control and Electromechanics Lab

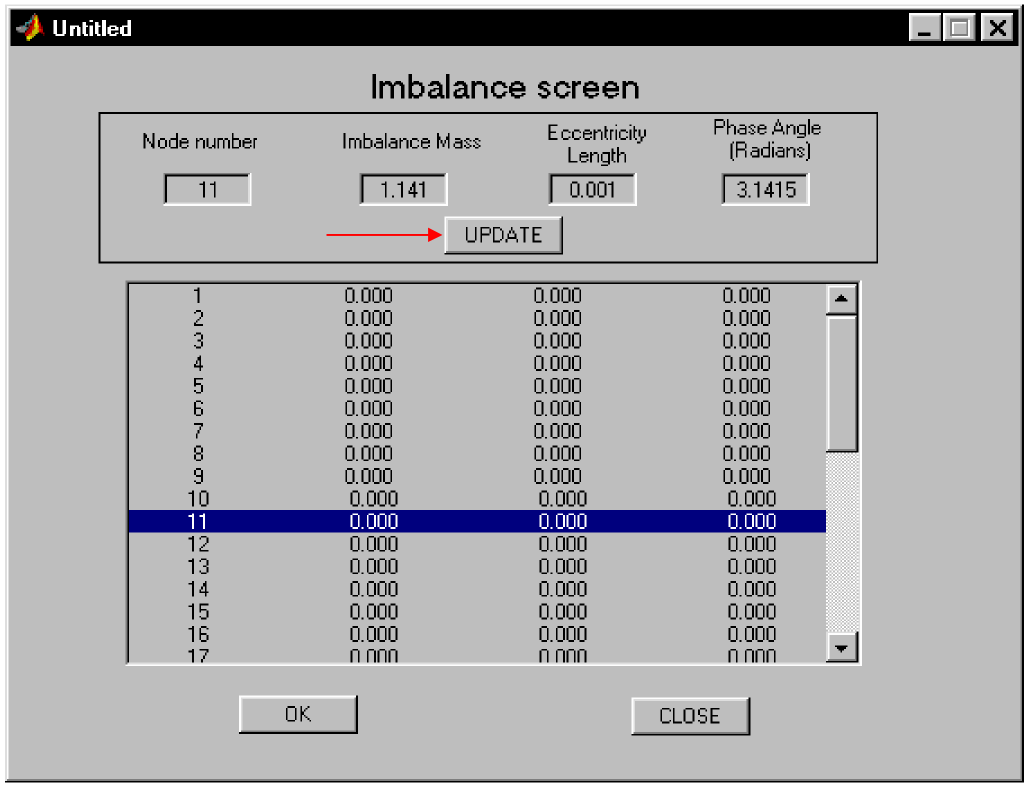

In this screen the user enters the imbalance values(imbalance weight, eccentricity,phase angles) for specific nodes .

Glenn Research Center

High Temperature Magnetic Bearing - Blade Loss Mitigation
NRA-GRC-99-02 - 1Year Milestone Review
September 27, 2002, NASA Glenn

Texas A&M Vibration Control and Electromechanics Lab

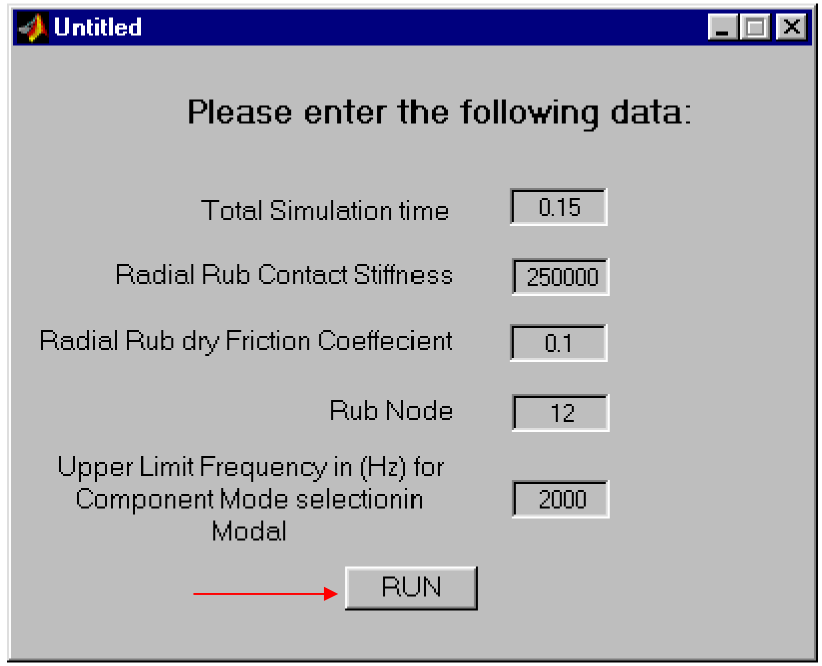

This is the final input screen in which the user inputs Total Simulation time,Radial rub contact stiffness, Rub Node etc. Click on "RUN" to run the simulation.The Post input Screen for Transient Response will open after the simulation is complete.

POST INPUT SCREEN FOR TRANSIENT RESPONSE

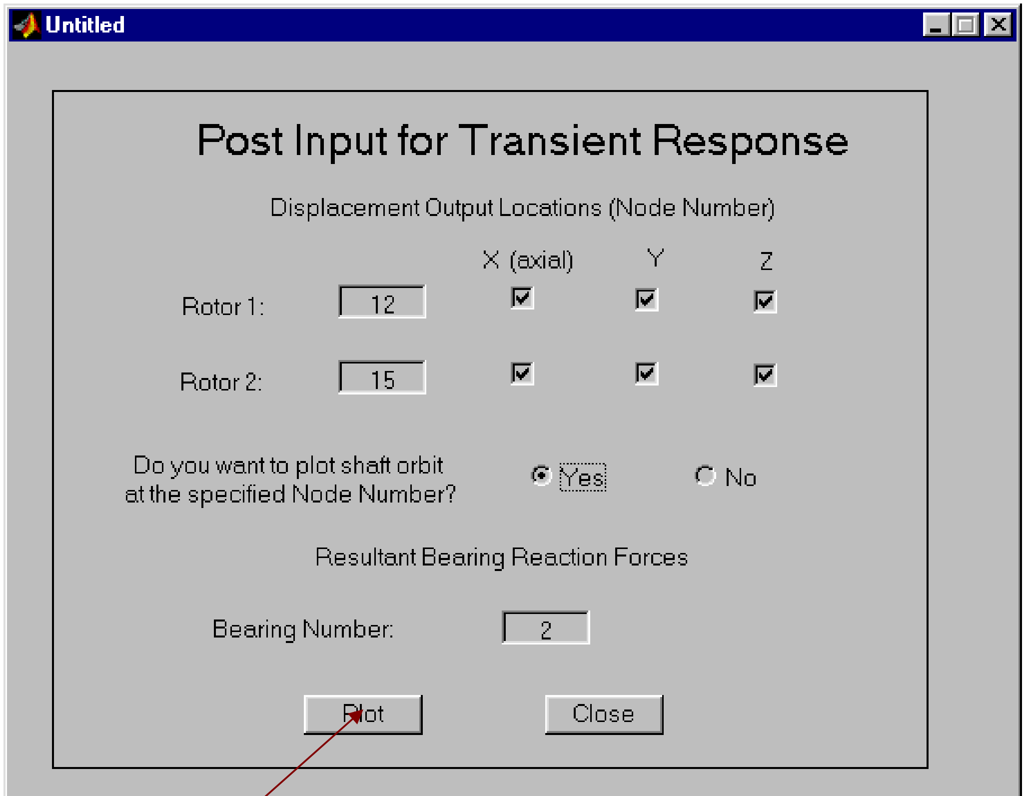

Click here

The User selects various features in this screen to view the various Output characteristics of the two rotors.

Output Characteristics

(Displacement of Rotor 1 in X & Y directions)

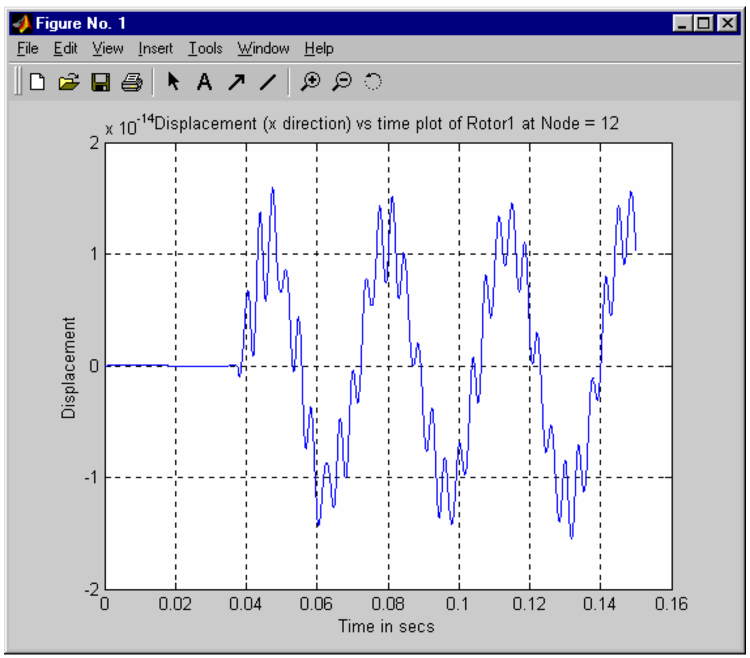

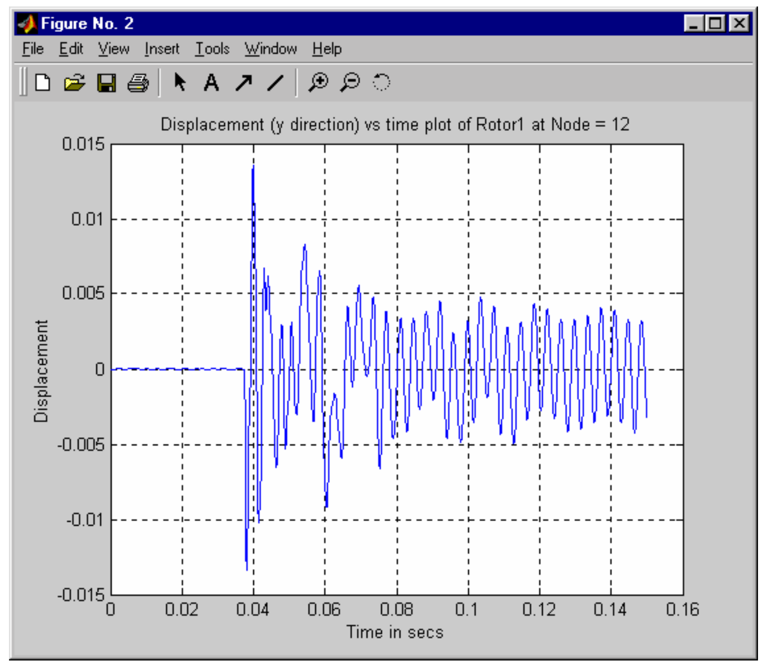

Displacement of Rotor 1 in Z direction & Rotor 2 in X direction

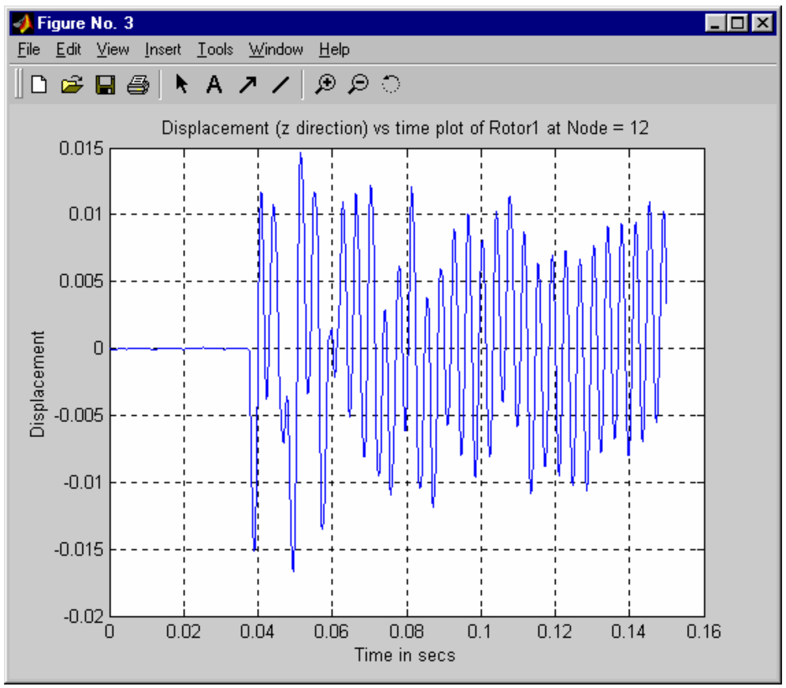

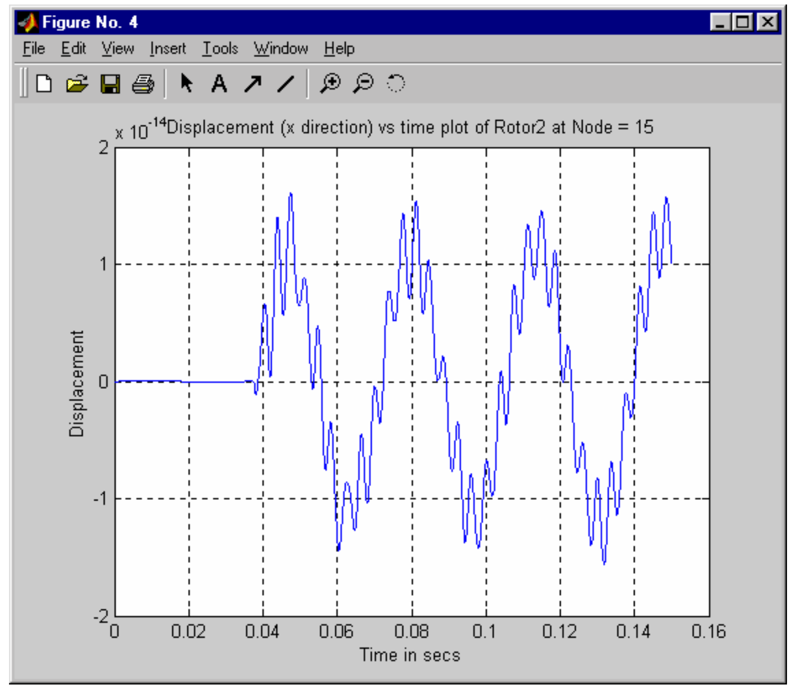

Displacement of Rotor 2 in Y & Z directions

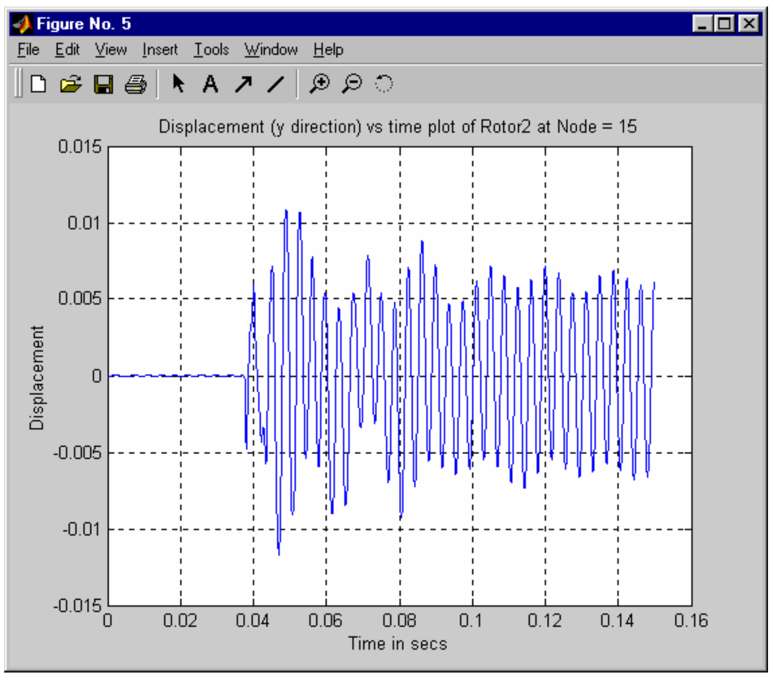

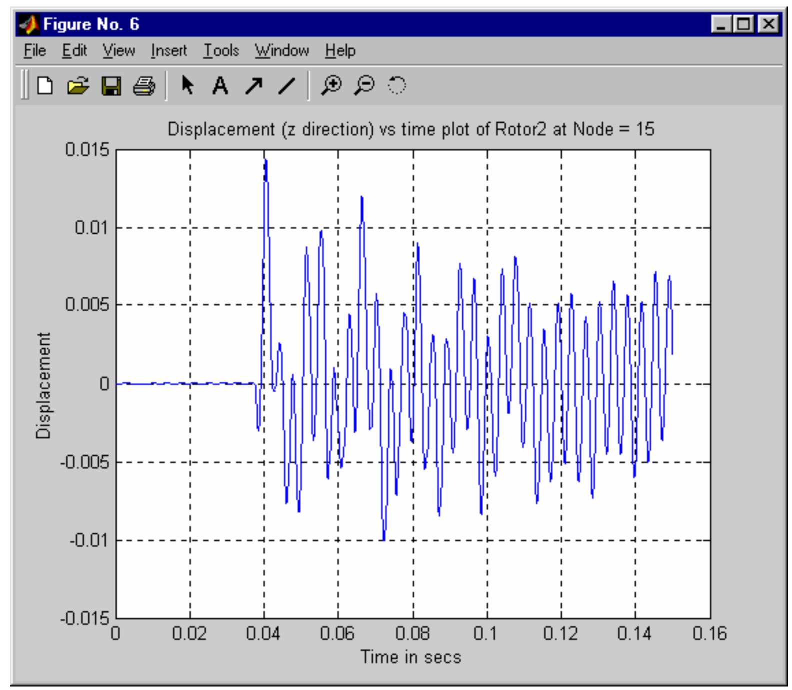

NASA/CR—2003-212205

Shaft Orbits of Rotor 1 & 2 at User specified Nodes (3 & 7)

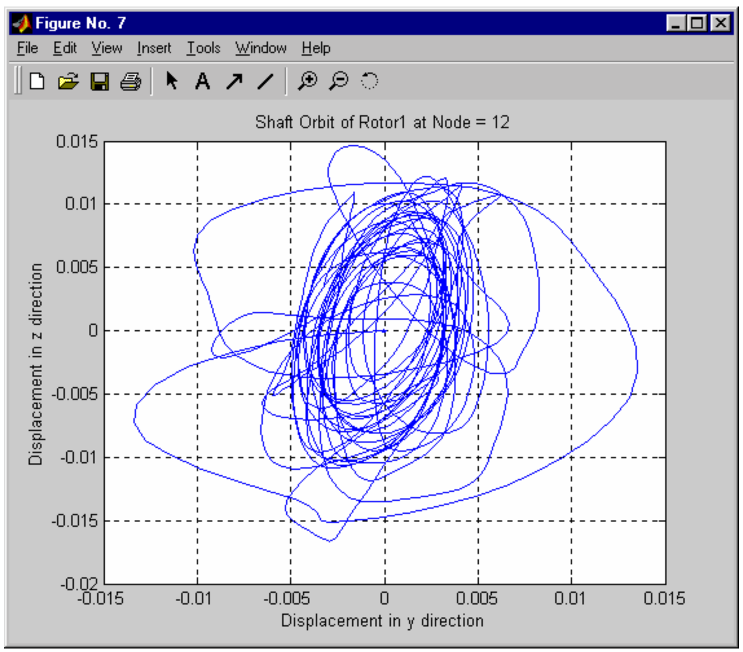

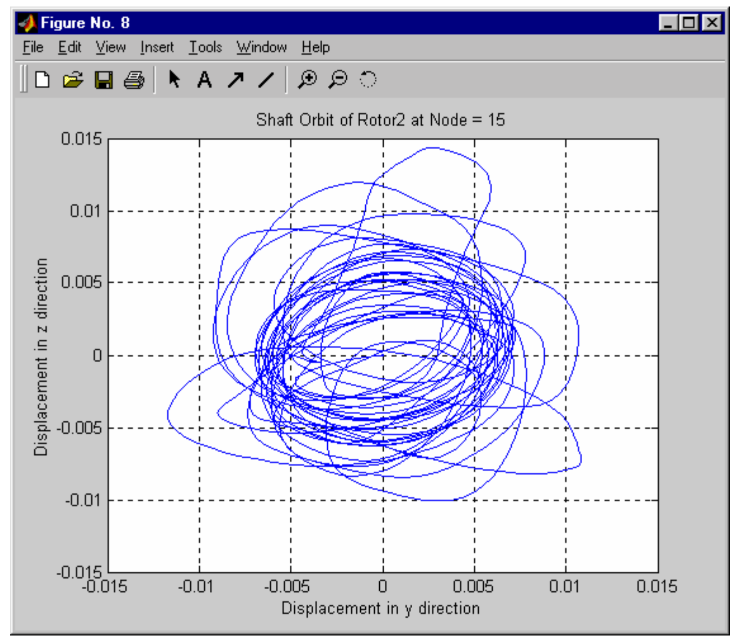

Resultant Bearing Reaction Force at User specified Bearing Number, 2

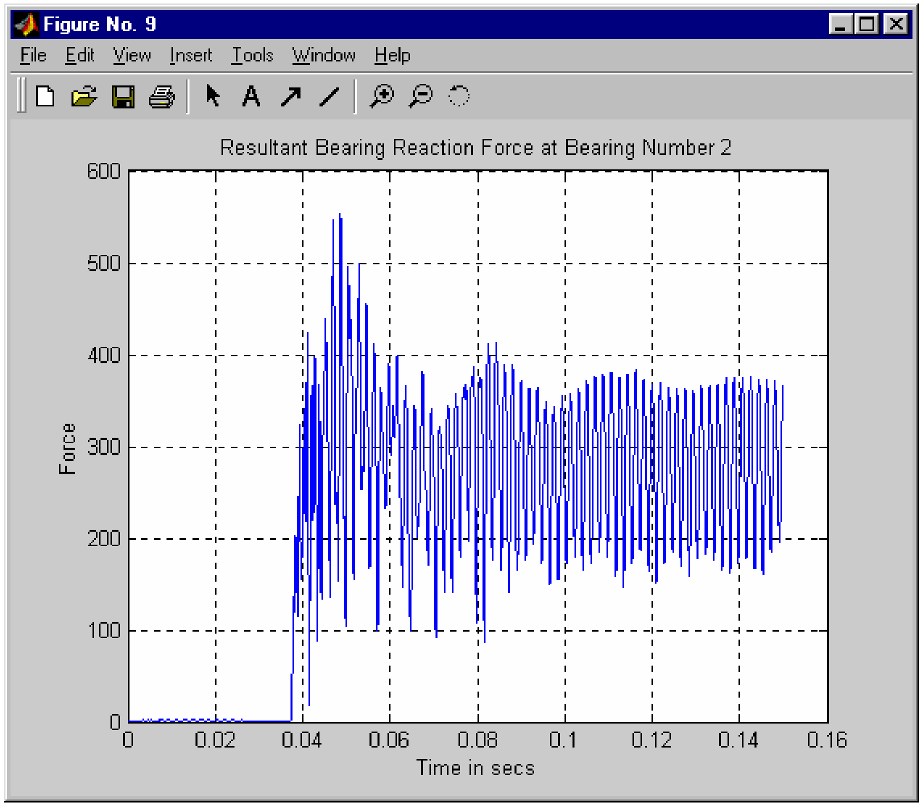

NASA/CR—2003-212205

FUTURE WORK

In this presentation we have seen the working of the GUI panels for the DRBB simulation code.This is the first Version of the GUI and further modifications will be made with new additions to the simulation code like:

- Different Analysis types like Static Analysis, Undamped Modal, Mode shapes, Steady state Harmonic Response etc.
- The 3D Ball Bearing Model and Thermal Model Inputs
- The GUI will be further developed to make it more User friendly with help features for the input and output panels.

NASA/CR—2003-212205

Task B.5: 3D High Fidelity Ball Bearing Simulation Code

By
Guangyoung Sun, Ph.D. Candidate
and
Dr. Alan B. Palazzolo, Professor

Objectives

- Including individual ball motion and nonlinear Hertzian contact load interaction, 3D high fidelity bearing model is developed and applied to rotor-wheels system.
- The simulation code is developed to predict the contact force and stress applied for individual balls, and thermal loads in bearing in the presence of high unbalance force.

NASA/CR—2003-212205

Executive Summary

- The rotor-wheels system dynamic responses including ball motions under high imbalance eccentricity are obtained by the simulation code.
- The simulation code predicts the contact load and stress for individual balls as well as temperature distribution and thermally induced loads.

Summary of Prior Work

Ball Bearing Model

- J. M. de Mul, et al., Jan. 1989, "Equilibrium and Associated Load Distribution in Ball and Roller Bearings Loaded in Five Degrees of Freedom While Neglecting Friction-Part I: General Theory and Application to Ball Bearings", *ASME Journal of Tribology*, Vol. 111, pp. 142 - 148 (Static Ball Bearing Model)
- N. Akturk, et al., Oct. 1997, "The Effects of Number of Balls and Preload on Vibrations Associated with Ball Bearings", *ASME Journal of Tribology*, Vol. 119, pp.747-753 (Dynamics of Rotor on Ball Bearings, no damper used)
- G. H. Jang and S. W. Jeong, Jan. 2002, "Nonlinear Excitation Model of Ball Bearing Waviness in a Rigid Rotor Supported by Two or More Ball Bearings Considering Five Degree of Freedom", (continued)

Summary of Prior Work (continued)

ASME Journal of Tribology, Vol. 124, pp.82 - 90 (Dynamics of Rotor on Ball Bearings Including Geometric Imperfection and Defects, no damper used)

From the literature review, the original points of our bearing model are

- Ball mass is included in the model. In high speed rotor system, the centrifugal force applied to balls is very important factor of determining contact load. It can't be ignored.
- The present model is the first one in the literature that combines 3D ball bearing with squeeze film damper.
- The thermal model is composed of power loss of bearing, heat transfer, thermal expansion and thermally induced load. The thermal expansion influences bearing distorsions and contact loads in the bearing dynamic model.

Simulation Model

Rotor

- Two wheels are connected to rotor by flexible hubs.
- Rotor and two wheels are rigid models.
- Two wheels have unbalance eccentricity and the rotor is assumed to be balanced.
- Axial transverse motion of the rotor is not considered.
- Three bodies are torsionally rigid (spin with same speed).

Bearings

- Barden bearing CZSB103J back to back arrangement is modeled at each end.
- Outer race plus SFD ring are supported by SFD and O-rings.

Fig.B.5.a Rotor-two-wheels system supported on ball bearings (Gs: shaft mass center, Gw1,w2: wheel mass center)

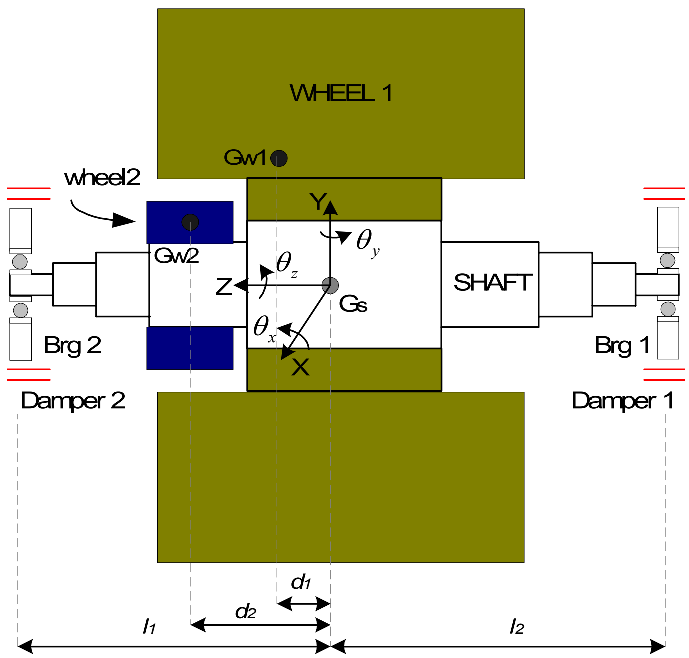

Dimension	Specification
Shaft	
Weight	3.5141 [lb]
Polar MOI	0.006342 [lb-in-sec^2]
Transverse MOI	0.051266 [lb-in-sec^2]
l_1 and l_2	7.63, 6.4766 [in]
Wheel 1	
Weight	73.55 [lb]
Polar MOI	8.0026 [lb-in-sec^2]
Transverse MOI	4.9352 [lb-in-sec^2]
d_1	0.8374 [in]
Wheel 2	
Weight	2.92 [lb]
Polar MOI	0.0264 [lb-in-sec^2]
Transverse MOI	0.0145 [lb-in-sec^2]
d_2	4.1854 [in]
Total	
Weight	79.98 [lb]
Total polar MOI	8.0353 [lb-in-sec^2]

Fig.B.5.b Back to back duplex pair of ball bearing supported on SFD

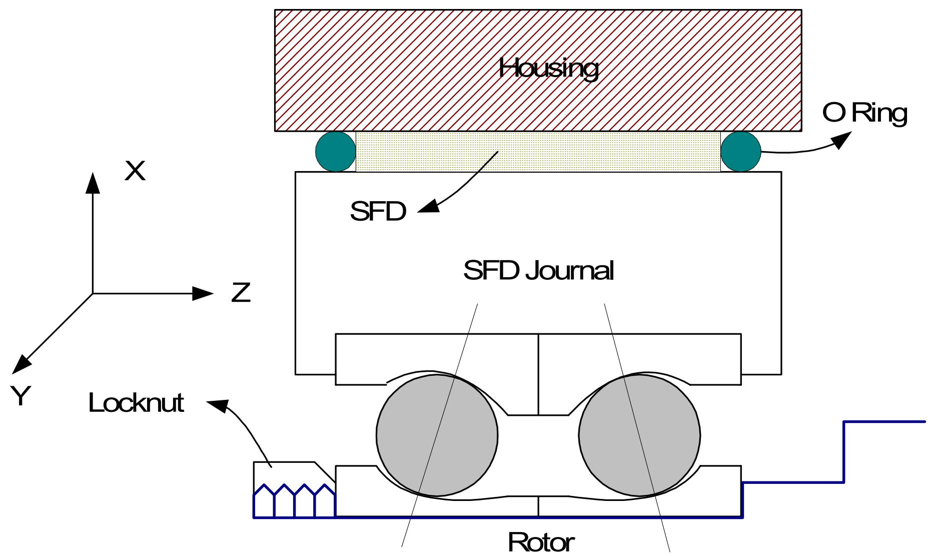

Fig.B.5.c SFD geometry and force direction

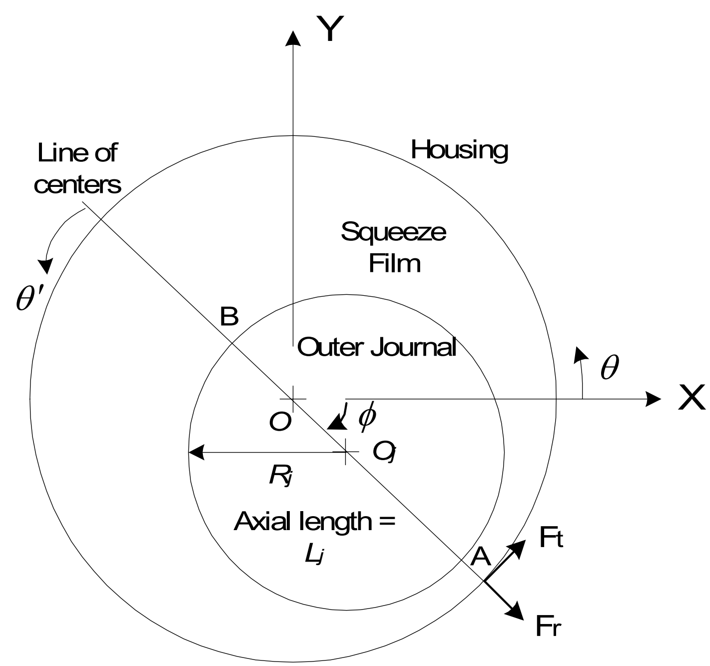

Fig.B.5.d Coordinate transformation for 3D bearing model

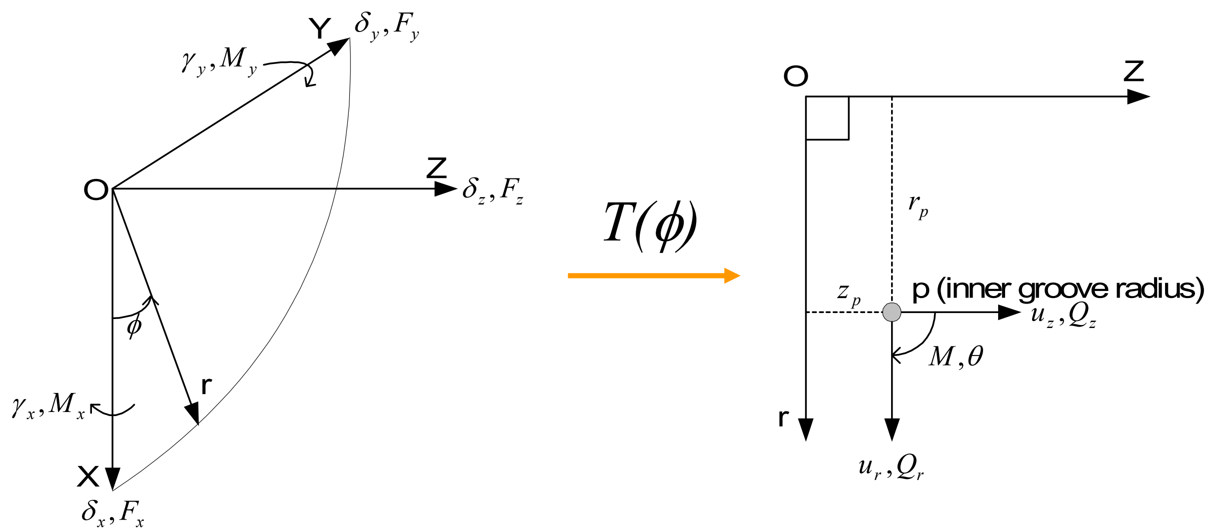

(a) bearing loads and displacements

(b) cross section with contact loads

3D Nonlinear Bearing Model

Assume dry contact load (Hertzian contact load) and small damping force (1 % damping ratio) are applied to bearing internal components,

- Rotor Radial Transverse Motion

$$[M_s]\cdot\{\ddot{X}_s\}=\{F_{ext}\}+\sum_{j=1}^{n}T'_{1j}\{Q_{i1}+f_{di1}\}_j+\sum_{j=1}^{n}T'_{2j}\{Q_{i2}+f_{di2}\}_j$$

where $\{X_s\}^T=[x_s \quad y_s]$, $\{Q_{i1,2}\}$ and $\{f_{di1,2}\}$ are Hertzian contact load vector and contact damping force vector applied to inner race, $\{F_{ext}\}$ is external force vector, and n is number of balls. 1, 2 represent bearing number in Fig.B.5.1.

- Rotor Rotational Motion

$$\begin{bmatrix} I_{tx} & 0 \\ 0 & I_{ty} \end{bmatrix}\cdot\begin{Bmatrix}\ddot{\theta}_x \\ \ddot{\theta}_y\end{Bmatrix}=\{M_{ext}\}+\begin{Bmatrix} f_{By1}\cdot l_2-f_{By2}\cdot l_1 \\ f_{Bx2}\cdot l_1-f_{Bx1}\cdot l_2\end{Bmatrix}$$

3D Nonlinear Bearing Model (continued)

where $f_{Bx,y}$ are nonlinear bearing forces in x and y axes, l_1 and l_2 are distances from rotor center in Fig.B.5.1, $\{M_{ext}\}$ is external moment vector.

- Ball transverse motion

$$m_b \begin{Bmatrix} \ddot{v}_r \\ \ddot{v}_z \end{Bmatrix} = \begin{Bmatrix} F_r \\ F_z \end{Bmatrix} = \begin{Bmatrix} (Q_i + f_{di})\cos\alpha_i - (Q_e + f_{de})\cos\alpha_e + F_c \\ (Q_i + f_{di})\sin\alpha_i - (Q_e + f_{de})\sin\alpha_e \end{Bmatrix}$$

where F_c is centrifugal force.

- Outer Race Radial Transverse Motion

$$[M_o]\cdot\{\ddot{X}_o\} = \{F_{sfd}\} + \sum_{j=1}^{n} T_j'\{Q_e + f_{de}\}_j$$

where $\{X_o\}^T = [x_o \quad y_o]$, $\{F_{sfd}\}$ is the SFD force including O-ring support force.

NASA/CR—2003-212205

Comparison of 2D and 3D Bearing Models

- 2D bearing model is linear stiffness as a function of inner race speed and preload, which is obtained from linearized static load equilibrium equations for balls and rings, while 3D model allows the bearing components to interact with Hertzian nonlinear contact loads.
- 2D model assumes every ball experiences same contact load regardless of inner race motion, while 3D model considers contact load applied to individual ball depending on inner race motion. The figure in the next page illustrates this point.
- 3D model can predict peak stress at every ball and rings and bearing life.

NASA/CR—2003-212205

Fig.B.5.e Different contact loads applied to balls

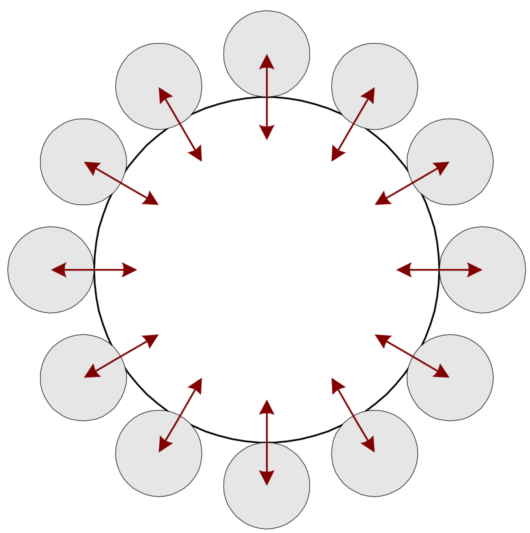

(a) Inner race (IR) located at bearing center

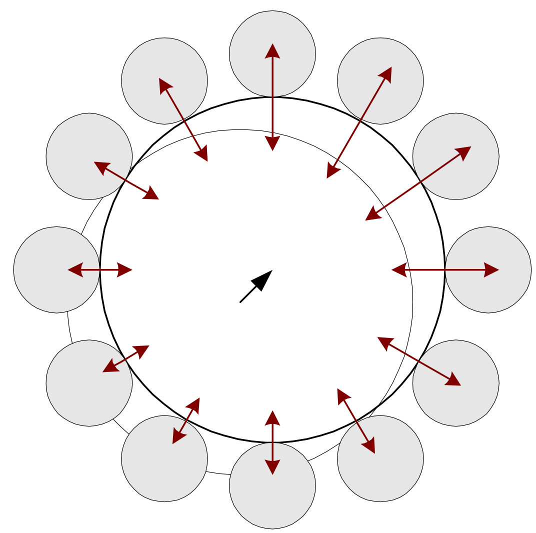

(b) Inner race moves

Fig.B.5.f Ball location in bearing

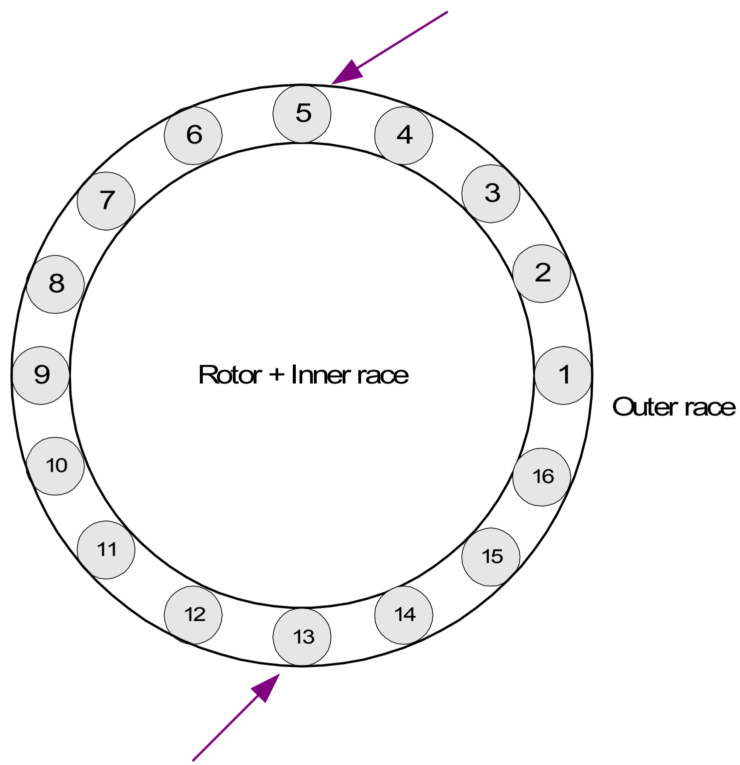

FE SFD & Thermally Induced Bearing Load Models

- Finite element based SFD model is used in conjunction with 3D bearing model.
- The thermally induced bearing load model consists of power loss in bearing, heat transfer, thermal expansion, and thermally induced load.
- The theoretical backgrounds for the above models are explained in detail in Task B.3.

Fig.B.5.g Temperature nodes of cross-sectioned bearing

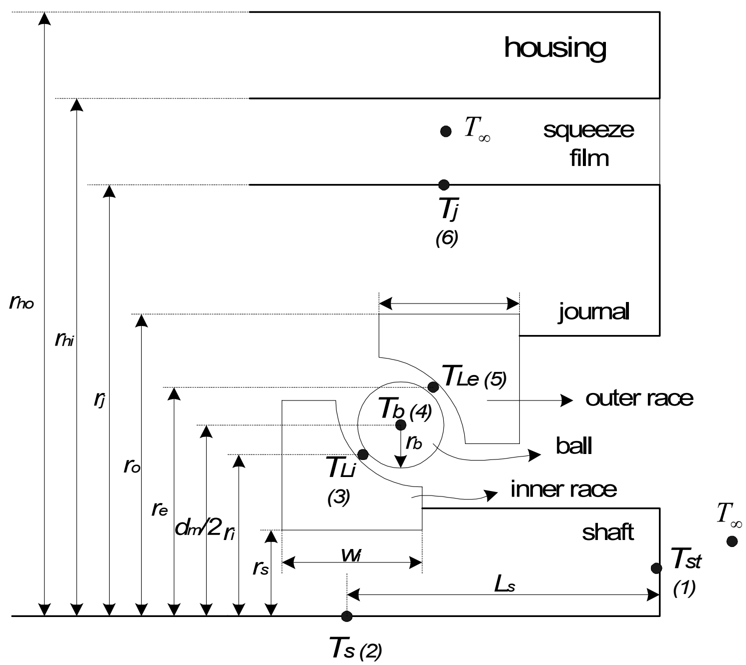

Fig.B.5.h Temperature effect1[1] on rolling element fatigue life of hot-pressured alumina balls in five ball fatigue tester

(Maximum Hertz stress, 3.79 Gpa (550 ksi); contact angle 20°)

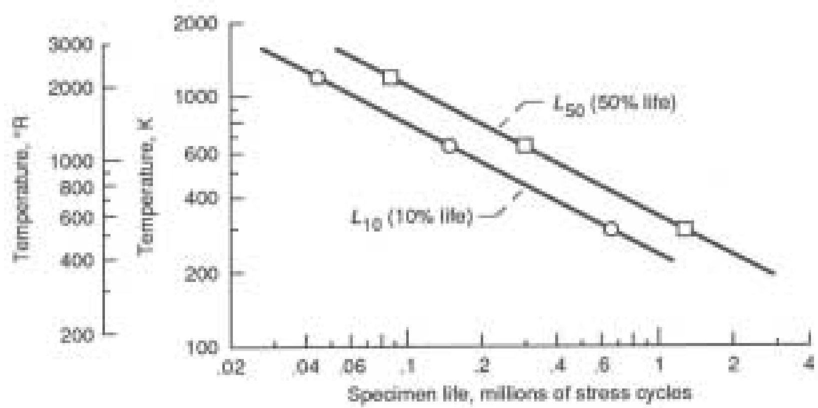

1. Erwin V. Zaretsky, 1992, “STLE Life Factors for Rolling Bearings”, STLE Publication

Simulation Conditions

- Wheel 1, 2: spin speed = 30,000 rpm, low (20 lb), high (4,000 lb) unbalance forces, 90° phase difference between two unbalance masses
- Rotor: spin speed = 30,000 rpm
- Bearing: Barden bearing CZSB103J duplex pair (2D and 3D models), detailed specs are in the next page, ceramic balls, 20 lb preloaded, lubricant viscosity = 50 [cST]
- FE SFD: 10 mil radial clearance, number of elements = 64×20, O-ring stiffness = 20,000 [lb/in], ambient pressure = 30 [psi]
  fluid viscosity = 30 [cP] for 20 lb case, 70 [cP] for 4,000 lb case
  fluid density = 12 [lb/in^3], housing contact stiffness = 10^6 [lb/in]
- Simulation time: 0.1 sec for 20 lb case, 0.02 sec for 4,000 lb case
- Initial and ambient temperature = 80 [°F]

Table B.5.1 Bearing specifications

Geometric Specification: CZSB103J	
Bore diameter	0.6693 [in]
Outside diameter	1.3780 [in]
Width	0.3937 [in]
Inner and outer race groove radius	0.082 and 0.0844 [in]
Number of balls	16
Diameter of a ball	5/32 [in]
Initial contact angle	15 [degree]
Axial preload	20 [lb]
Material specification	
Density of ball (ceramic ball)	0.11553 [lb/in^3]
Density of inner and outer race	0.2816 [lb/in^3]
Elastic modulus of ball	45E+6 [psi]
Poisson's ratio of ball	0.26
Elastic modulus of inner and outer race	30E+6 [psi]
Poisson's ratio of inner and outer race	0.3

Fig.B.5.1 Dynamic response of Wheel 2: 3D Brg, 20 lb unbalance

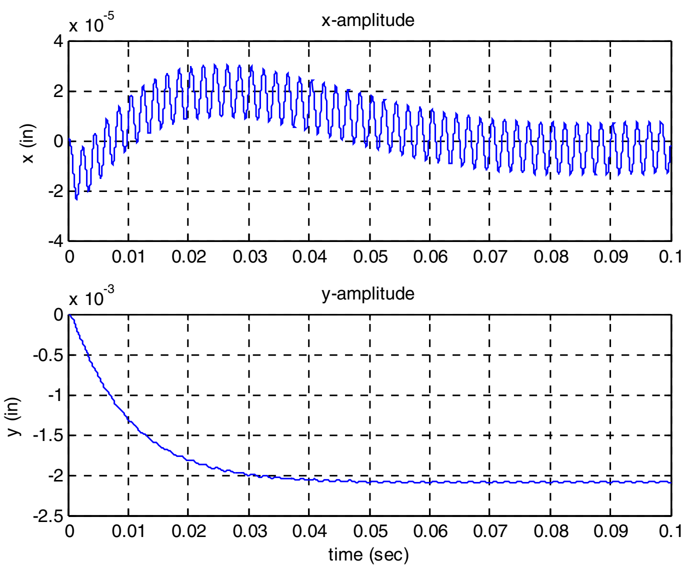

(a) Dynamic responses

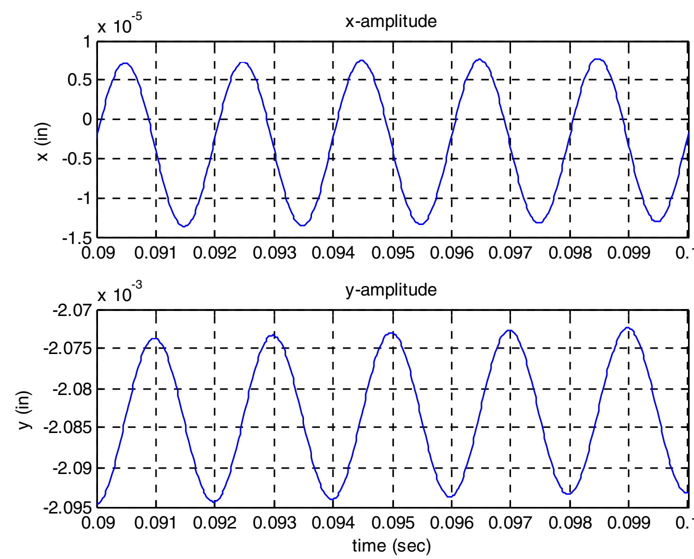

(b) Scaled plot from 0.19 to 0.2 sec

Fig.B.5.2 Dynamic response of Wheel 1: 3D Brg, 20 lb unbalance

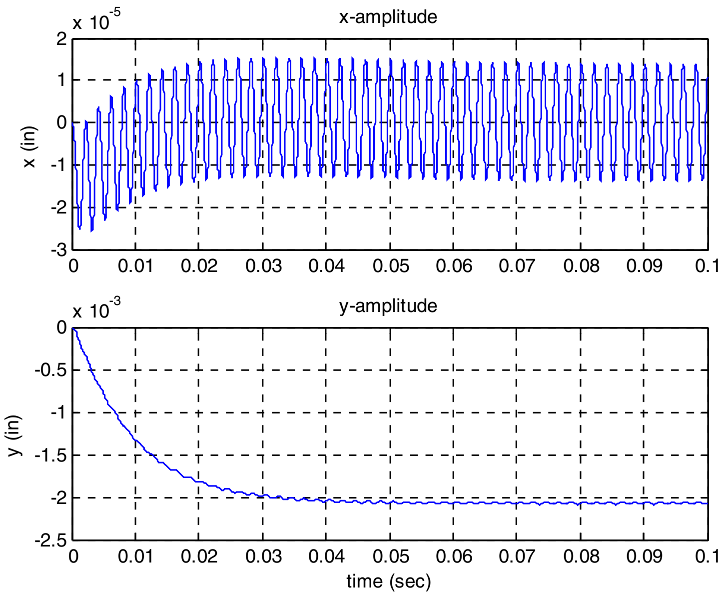

(a) Dynamic responses

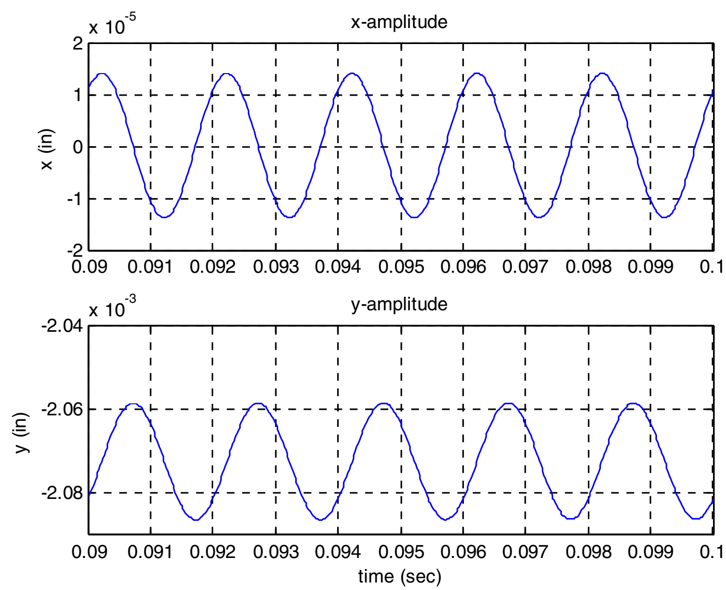

(b) Scaled plot from 0.19 to 0.2 sec

Fig.B.5.2 Dynamic response of Wheel 1: 3D Brg, 20 lb unbalance

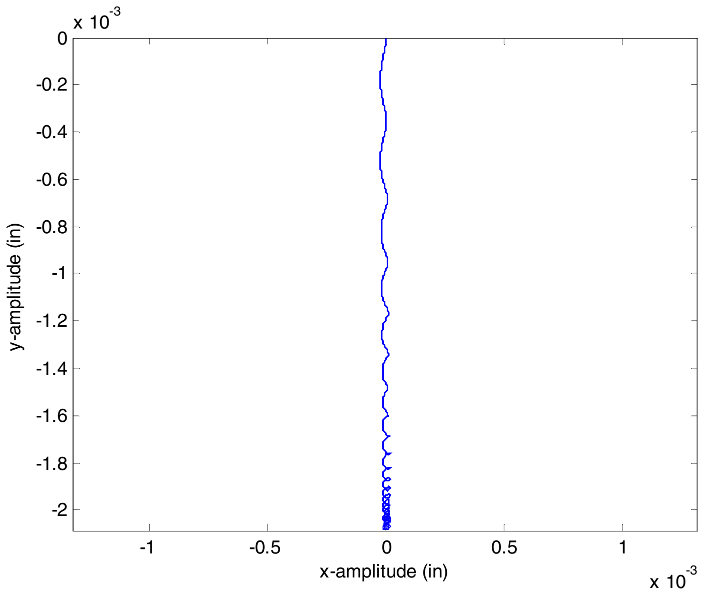

(c) Orbit plot

Glenn Research Center

High Temperature Magnetic Bearing - Blade Loss Mitigation
NRA-GRC- 99-02 - 1 Year Milestone Review
September 27, 2002, NASA Glenn

Texas A&M Vibration Control and Electromechanics Lab

Fig.B.5.3 Rotor motions at bearing 1 and 2: 3D Brg, 20 lb unbalance

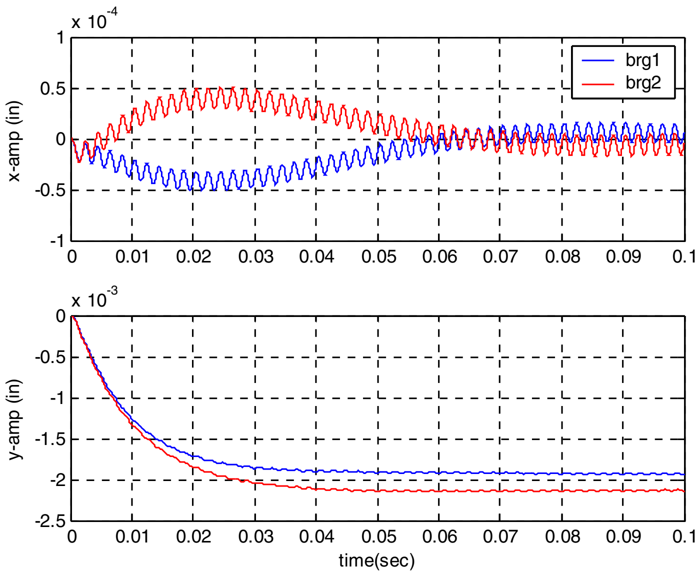

(a) Dynamic responses

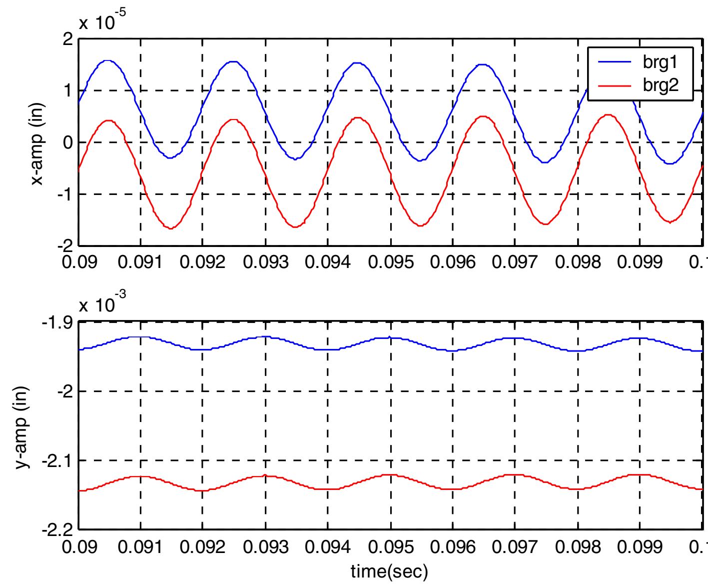

(b) Scaled plot from 0.19 to 0.2 sec

Fig.B.5.3 Rotor motions at bearing 1 and 2: 3D Brg, 20 lb unbalance

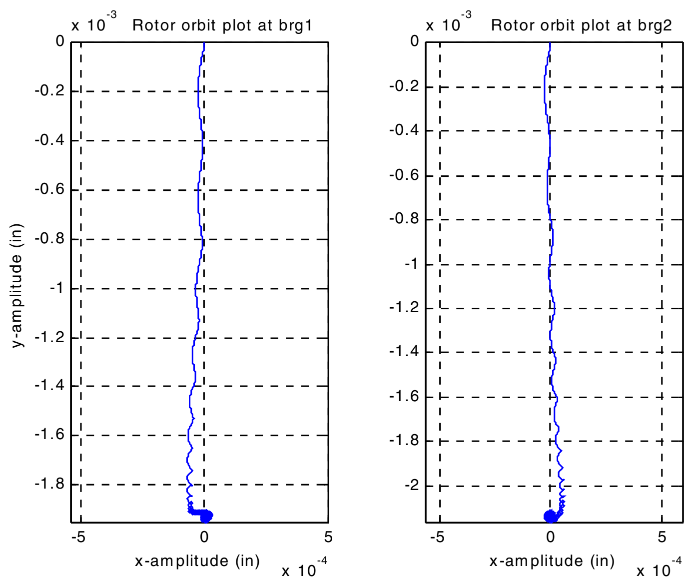

(c) Orbit plot

Fig.B.5.4 Outer ring plus SFD journal motions at bearing 1 and 2: 3D Brg, 20 lb unbalance

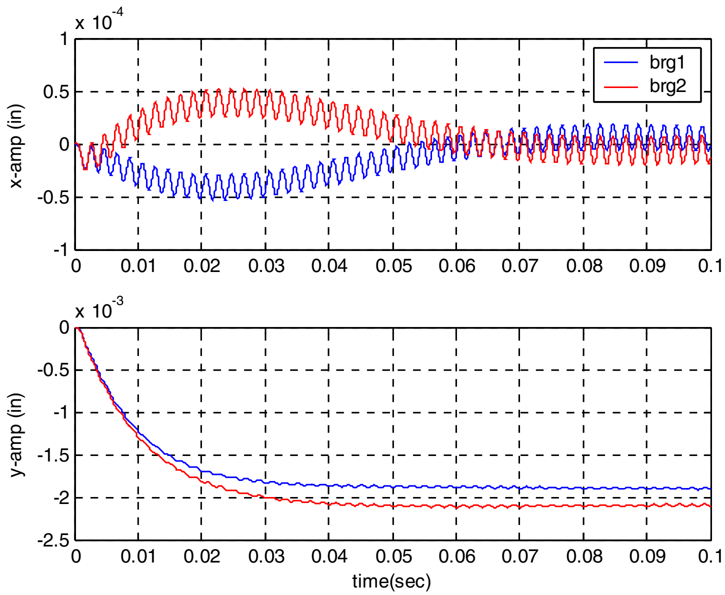

(a) Dynamic responses

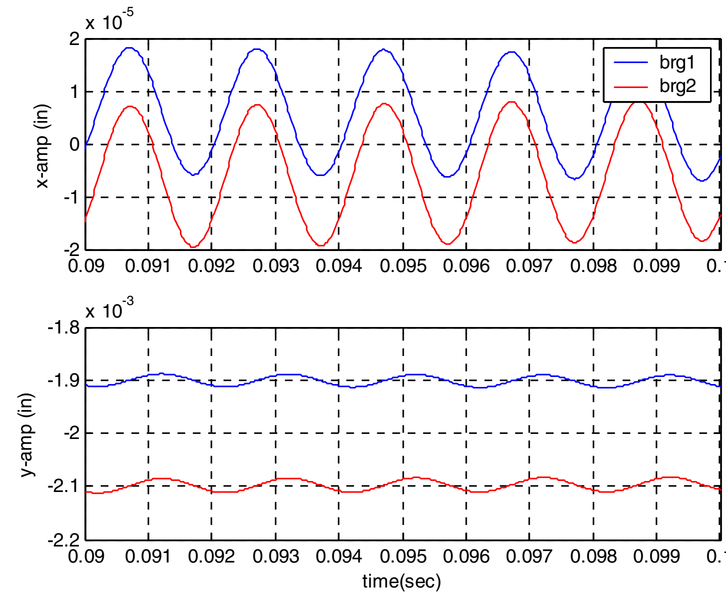

(b) Scaled plot from 0.19 to 0.2 sec

Fig.B.5.4 Outer ring plus SFD journal motions at bearing 1 and 2: 3D Brg, 20 lb unbalance

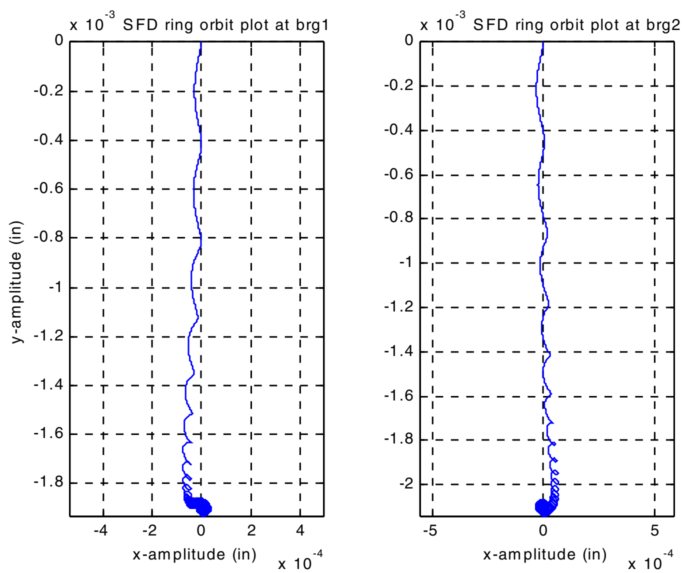

(c) Orbit plot

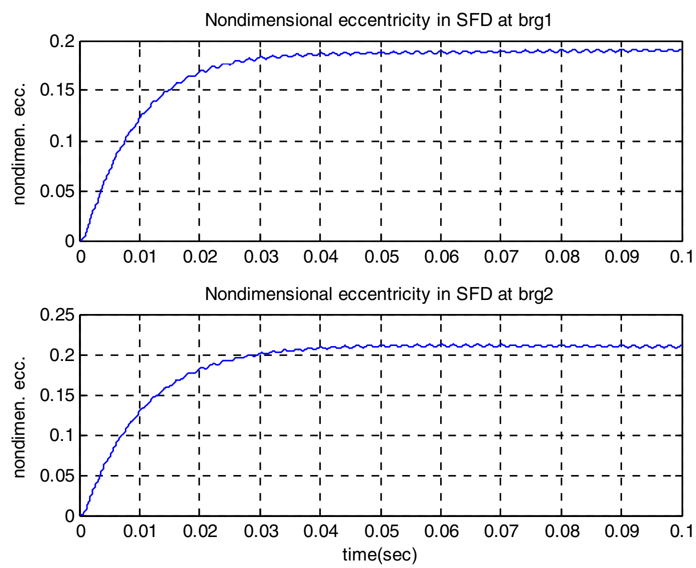

(d) Nondimensional eccentricity

Fig.B.5.5 Contact loads at 5th and 13th balls: 3D Brg, 20 lb unbalance

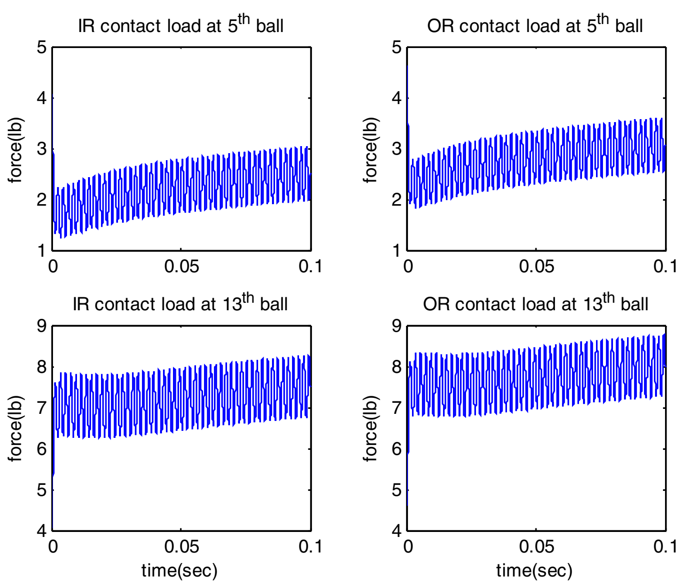

(a) Bearing 1

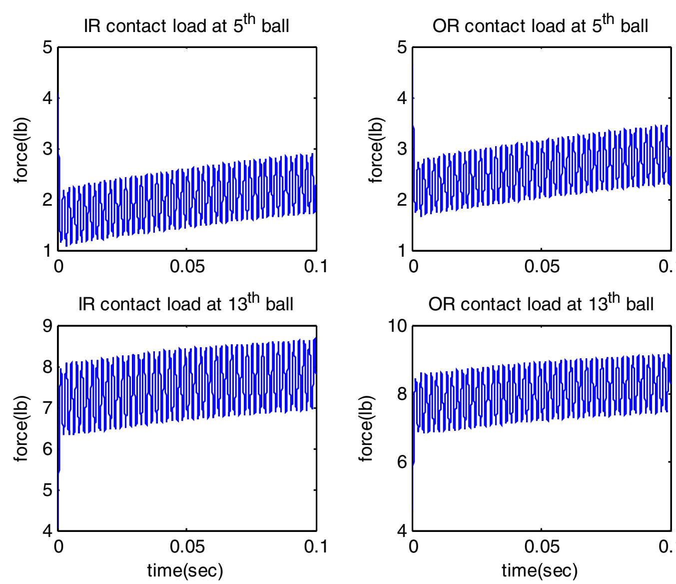

(b) Bearing 2

High Temperature Magnetic Bearing - Blade Loss Mitigation
NRA-GRC- 99-02 - 1 Year Milestone Review
September 27, 2002, NASA Glenn

Glenn Research Center

Texas A&M Vibration Control and Electromechanics Lab

Fig.B.5.6 Contact stress at 5th and 13th balls: 3D Brg, 20 lb unbalance

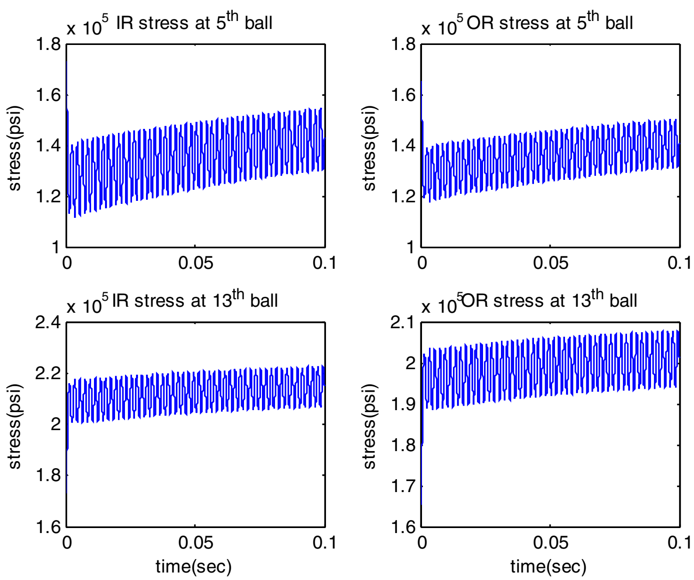

(a) Bearing 1

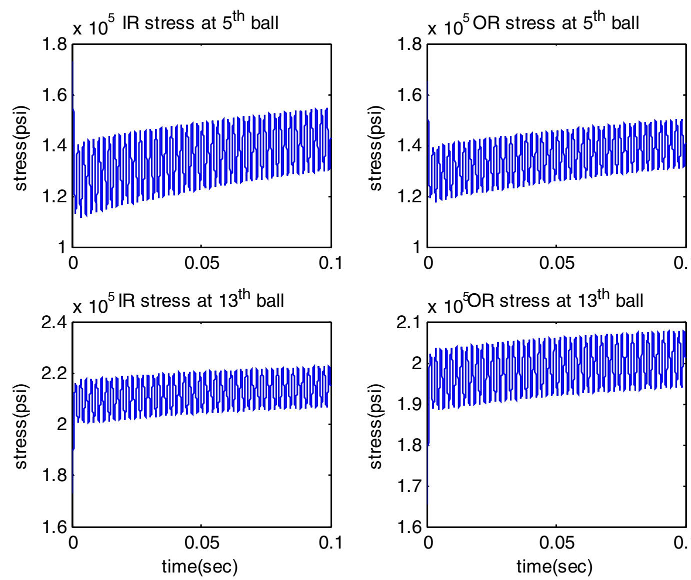

(b) Bearing 2

Fig.B.5.7 Squeeze film damping force: 3D Brg, 20 lb unbalance

(Radial force Fr is to the outward direction to min film thickness, Ft is perpendicular to Fr)

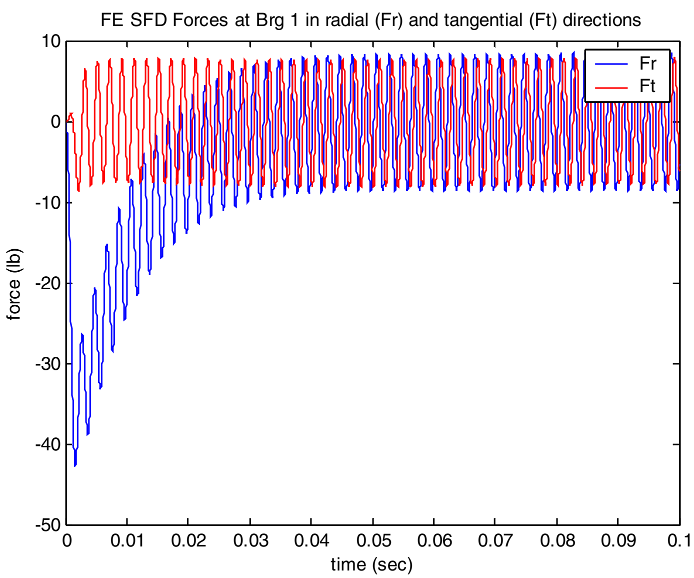

(a) Bearing 1

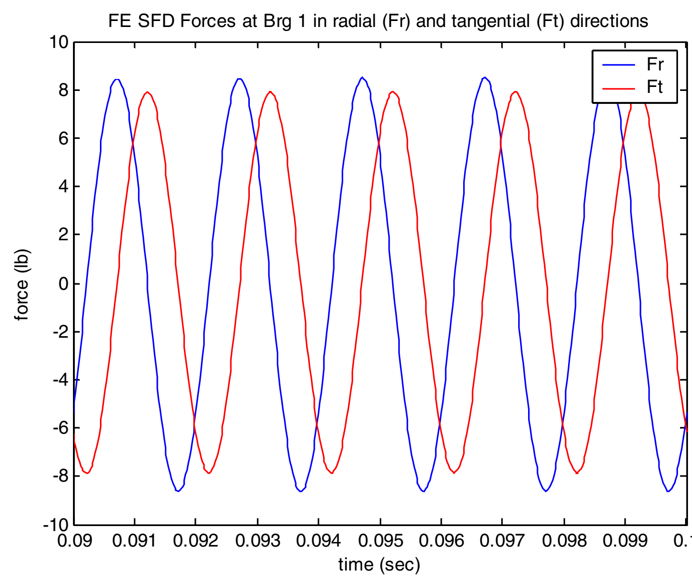

(b) Scaled plot for (a) from 0.19 to 0.2 sec

Fig.B.5.7 Squeeze film damping force: 3D Brg, 20 lb unbalance

(Radial force Fr is to the outward direction to min film thickness, Ft is perpendicular to Fr)

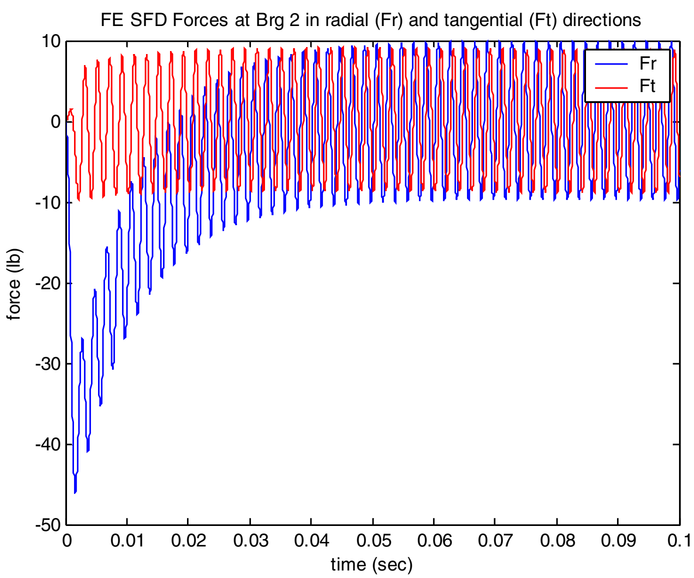

(c) Bearing 2

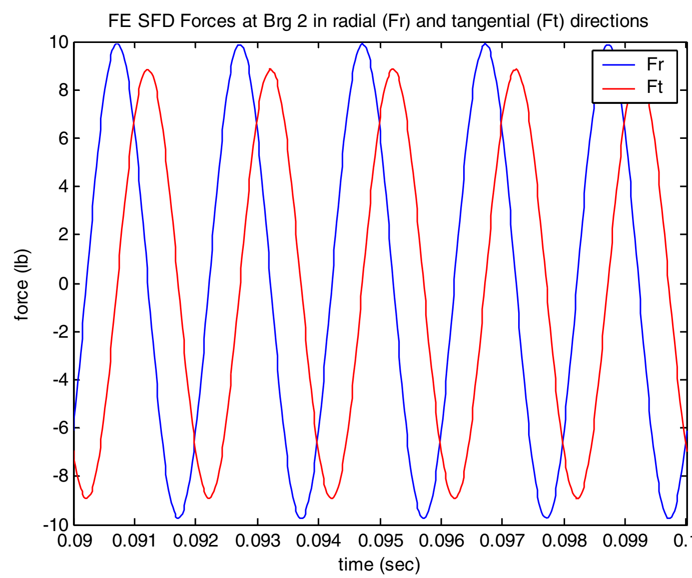

(d) Scaled plot for (c) from 0.19 to 0.2 sec

Fig.B.5.8 Max and min fluid film pressures in FE SFD: 3D Brg, 20 lb unbalance (Ambient pressure is 30 psi)

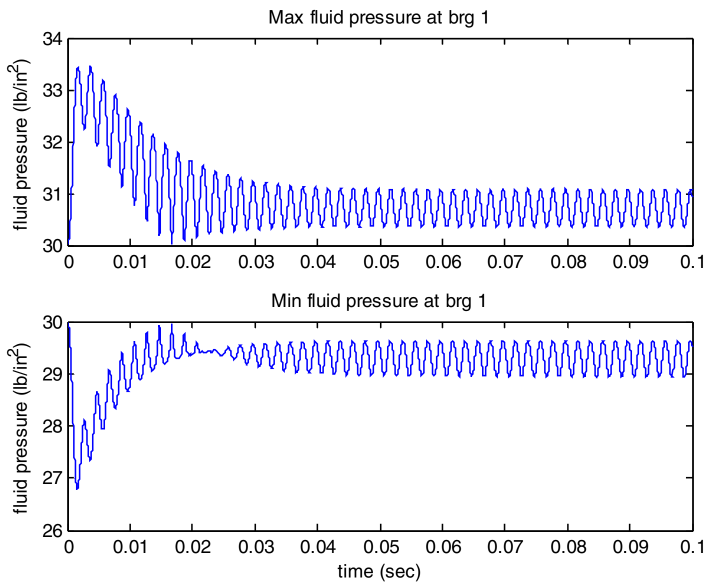

(a) Bearing 1

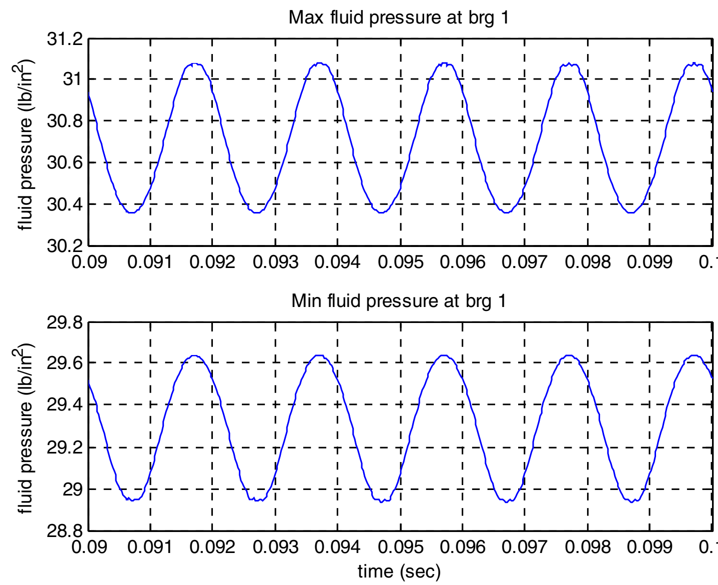

(b) Scaled plot for (a) from 0.19 to 0.2 sec

Fig.B.5.8 Max and min fluid film pressures in FE SFD: 3D Brg, 20 lb unbalance (Ambient pressure is 30 psi)

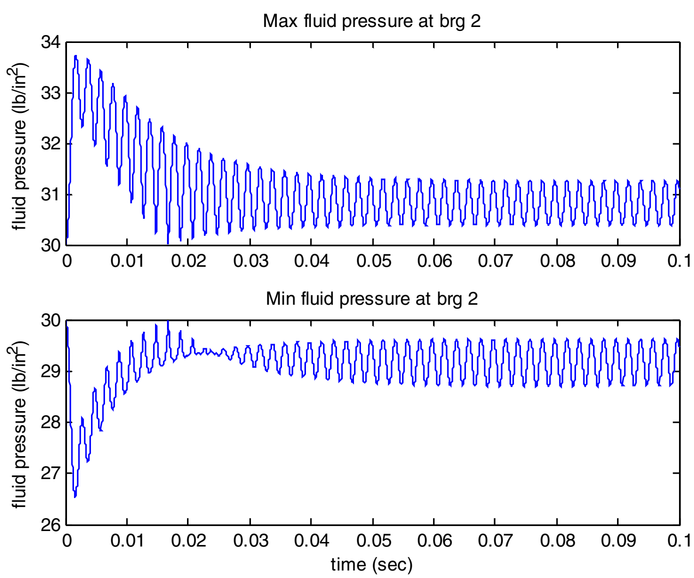

(c) Bearing 2

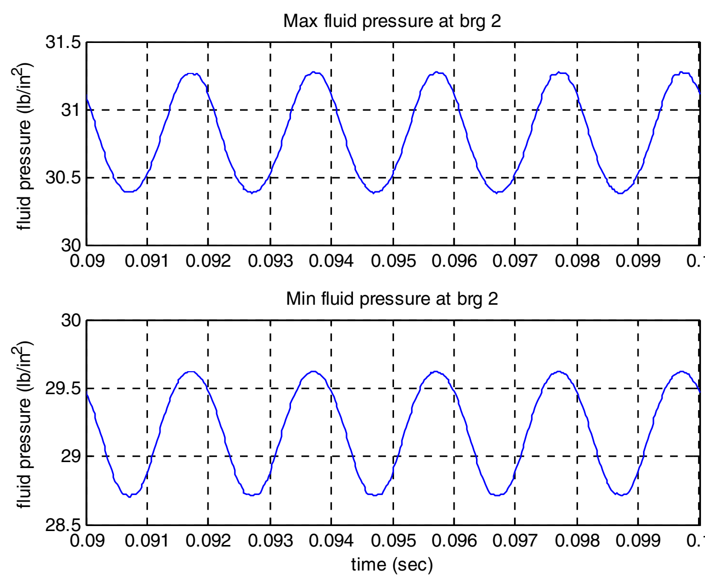

(d) Scaled plot for (c) from 0.19 to 0.2 sec

Fig.B.5.9 Temperature growth and induced thermal load in bearings: 3D Brg, 20 lb unbalance (Initial temp is 80 °F)

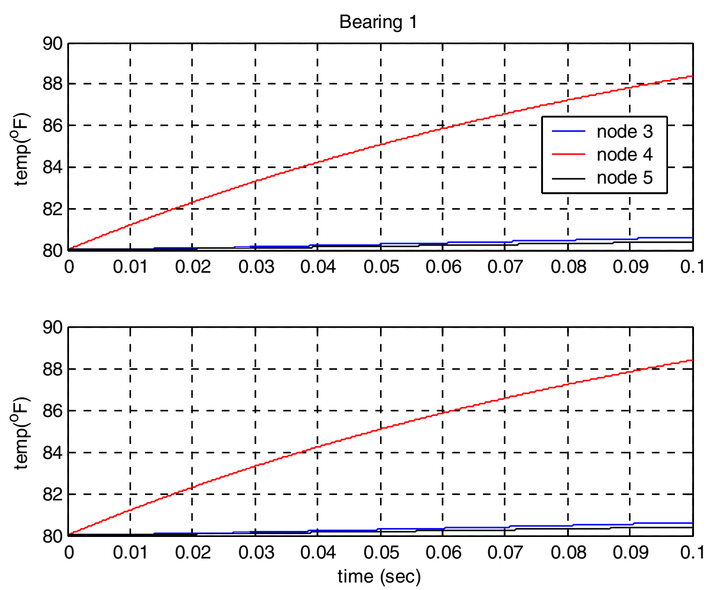

(a) Temperature growth

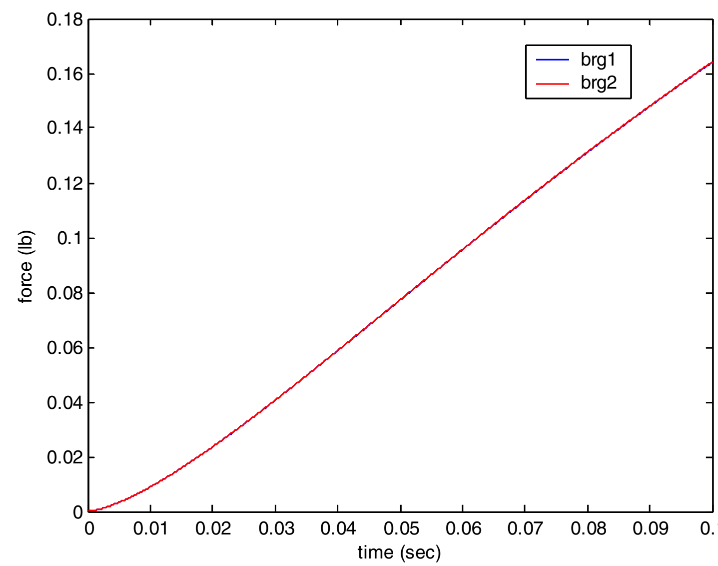

(b) Thermally induced bearing load at IR

Glenn Research Center

High Temperature Magnetic Bearing - Blade Loss Mitigation
NRA-GRC- 99-02 - 1 Year Milestone Review
September 27, 2002, NASA Glenn

Texas A&M Vibration Control and Electromechanics Lab

Fig.B.5.10 Dynamic response of Wheel 2: 2D Brg, 20 lb unbalance

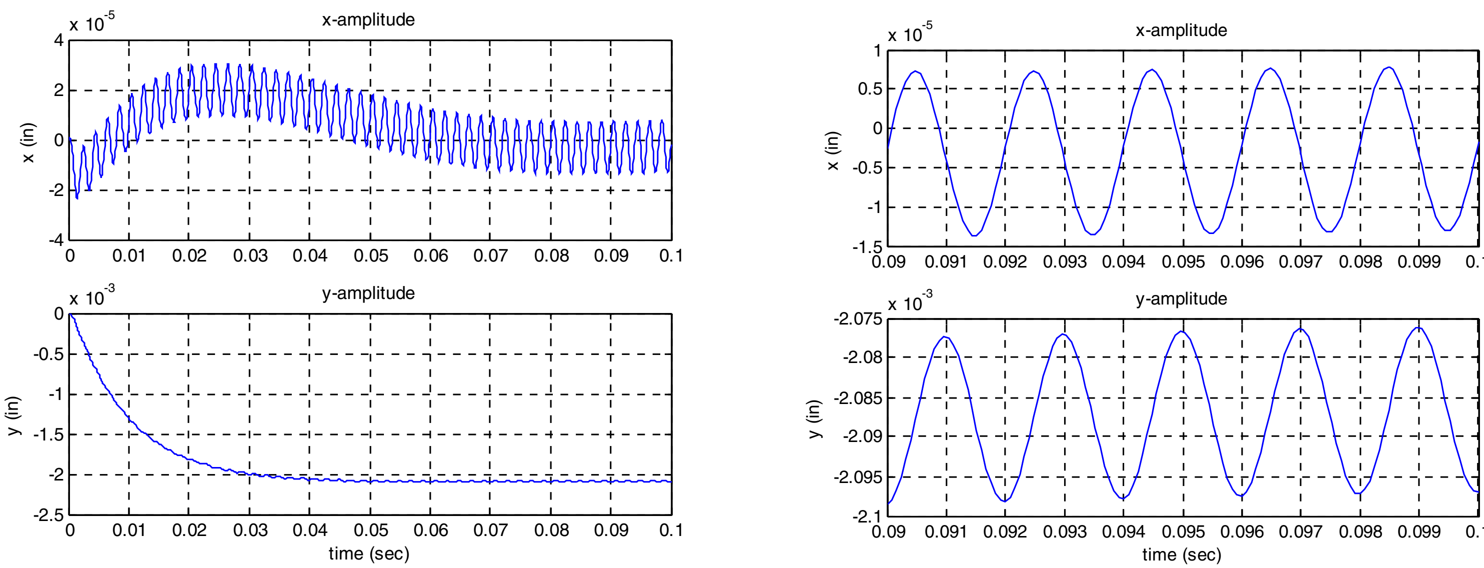

(a) Dynamic responses

(b) Scaled plot from 0.19 to 0.2 sec

Fig.B.5.10 Dynamic response of Wheel 2: 2D Brg, 20 lb unbalance

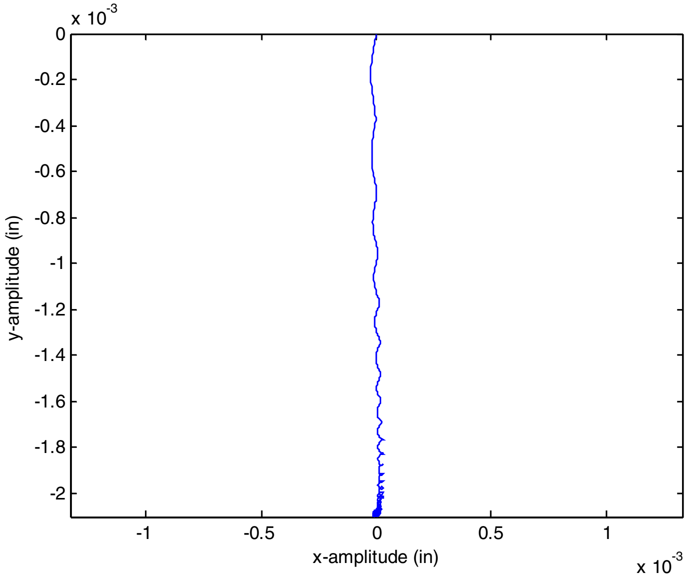

(c) Orbit plot

High Temperature Magnetic Bearing - Blade Loss Mitigation
NRA-GRC- 99-02 - 1 Year Milestone Review
September 27, 2002, NASA Glenn

Glenn Research Center

Texas A&M Vibration Control and Electromechanics Lab

Fig.B.5.11 Dynamic response of Wheel 1: 2D Brg, 20 lb unbalance

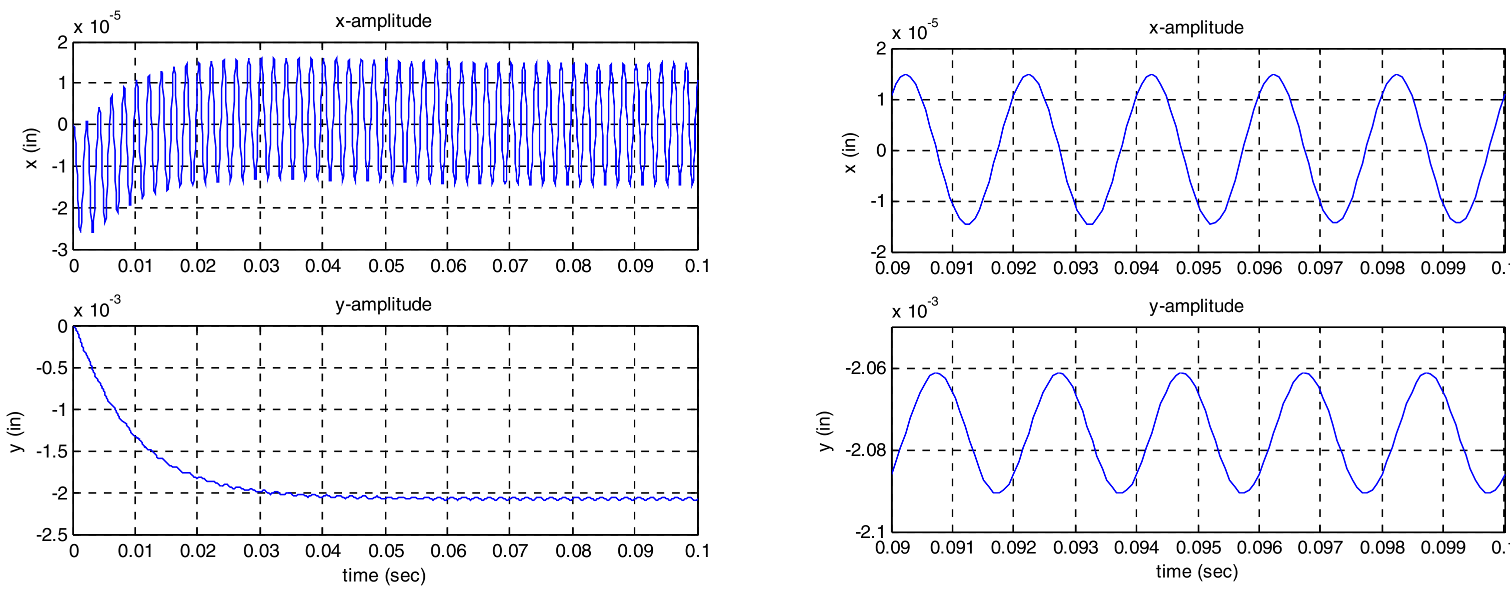

(a) Dynamic responses

(b) Scaled plot from 0.19 to 0.2 sec

Fig.B.5.11 Dynamic response of Wheel 1: 2D Brg, 20 lb unbalance

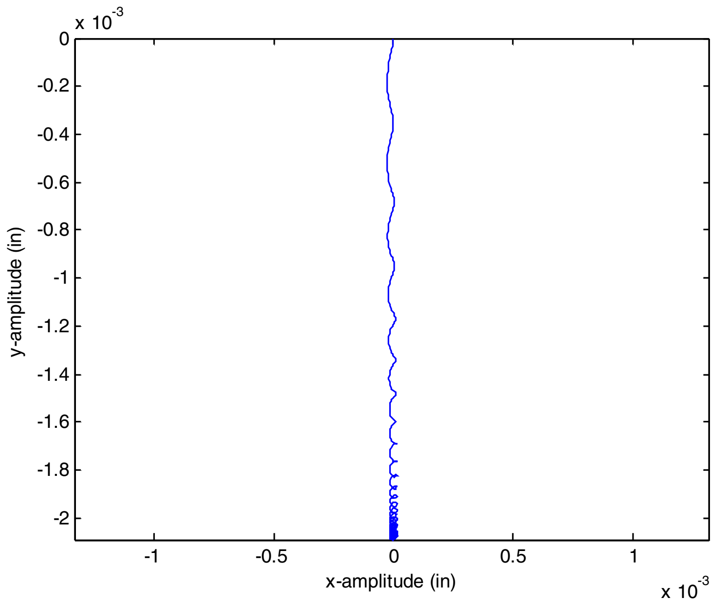

(c) Orbit plot

Fig.B.5.12 Rotor motions at bearing 1 and 2: 2D Brg, 20 lb unbalance

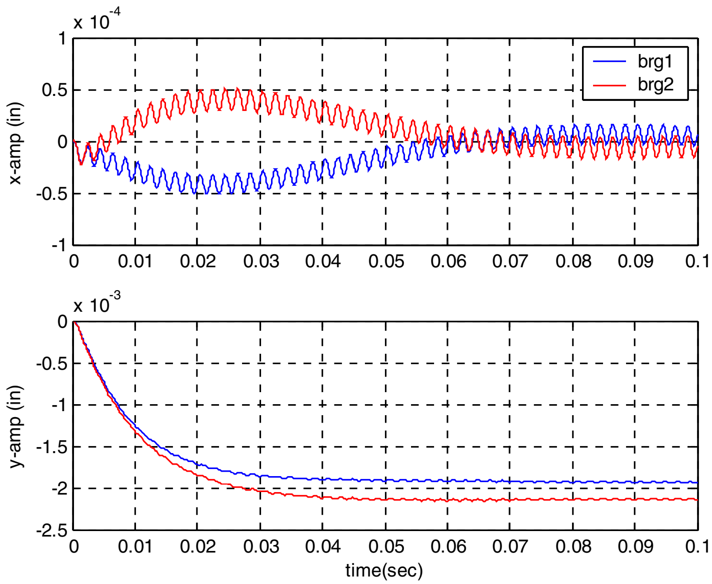

(a) Dynamic responses

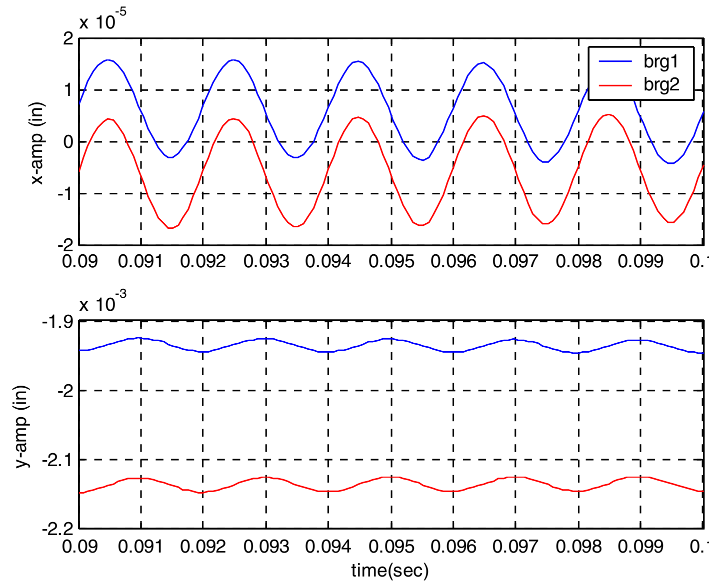

(b) Scaled plot from 0.19 to 0.2 sec

Fig.B.5.12 Rotor motions at bearing 1 and 2: 2D Brg, 20 lb unbalance

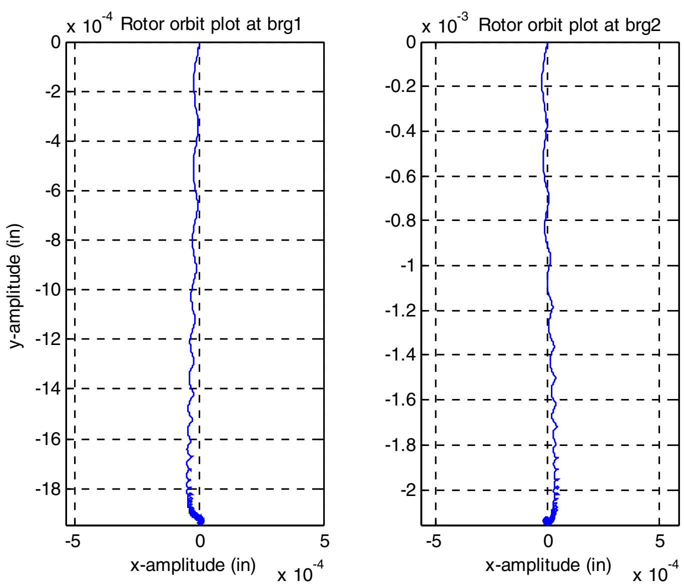

(c) Orbit plot

Fig.B.5.13 Outer ring plus SFD journal motions at bearing 1 and 2: 2D Brg, 20 lb unbalance

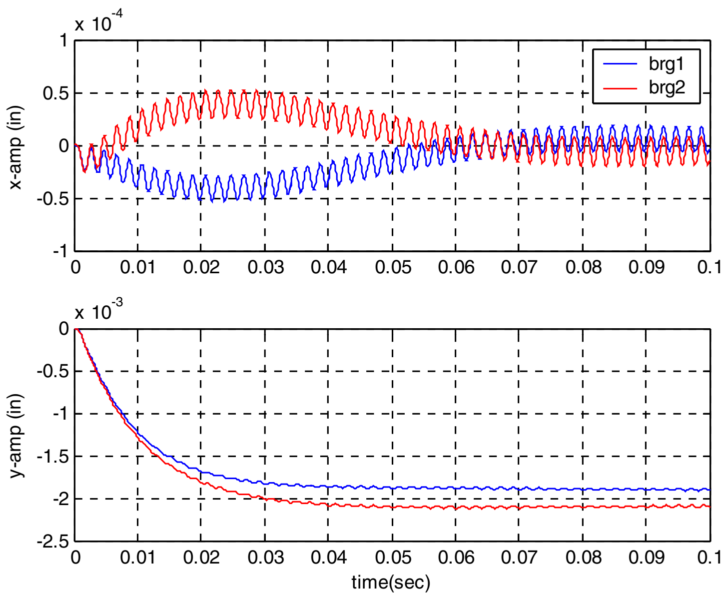

(a) Dynamic responses

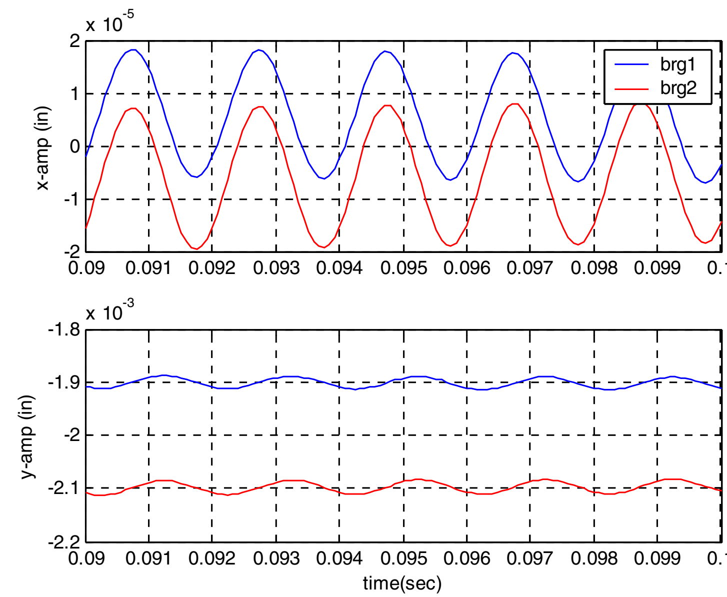

(b) Scaled plot from 0.19 to 0.2 sec

Glenn Research Center

High Temperature Magnetic Bearing - Blade Loss Mitigation
NRA-GRC- 99-02 - 1 Year Milestone Review
September 27, 2002, NASA Glenn

Texas A&M Vibration Control and Electromechanics Lab

Fig.B.5.13 Outer ring plus SFD journal motions at bearing 1 and 2: 2D Brg, 20 lb unbalance

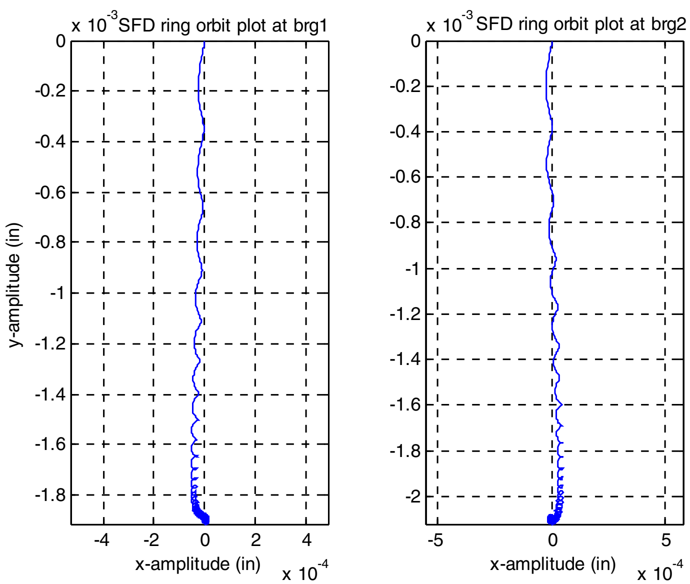

(c) Orbit plot

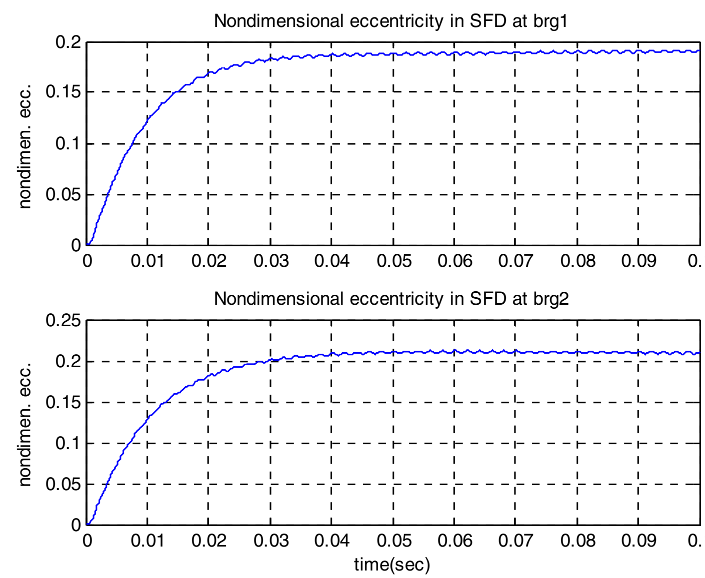

(d) Nondimensional eccentricity

Fig.B.5.14 Squeeze film damping force: 2D Brg, 20 lb unbalance

(Radial force Fr is to the outward direction to min film thickness, Ft is perpendicular to Fr)

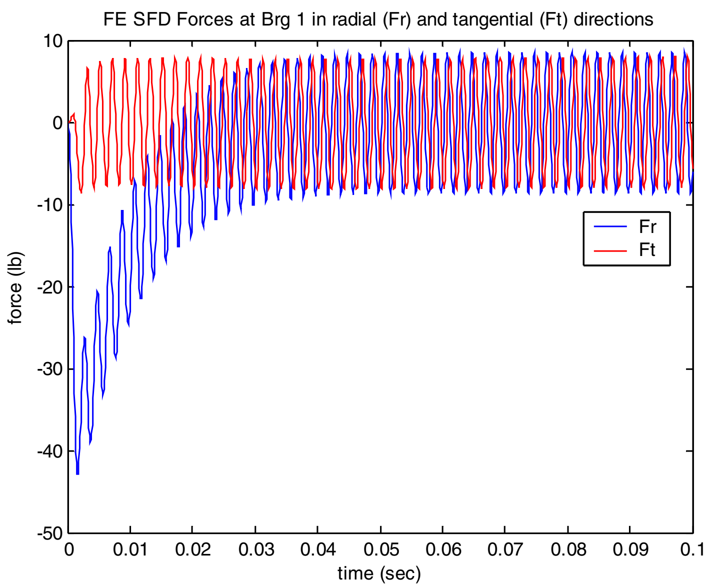

(a) Bearing 1

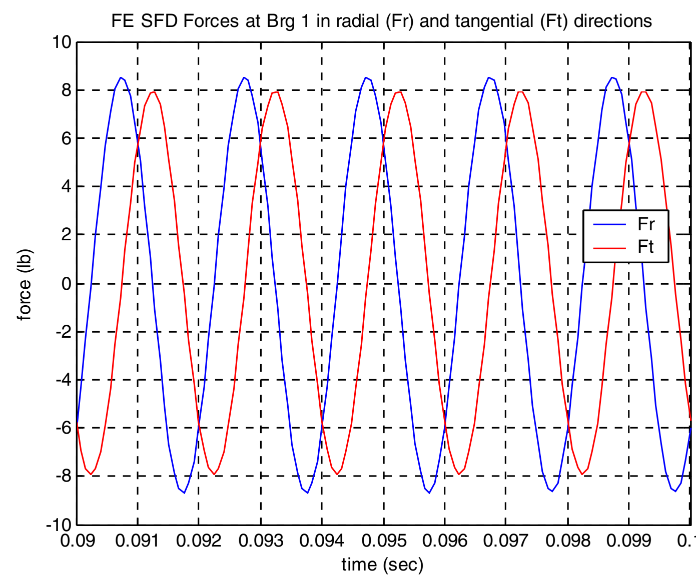

(b) Scaled plot for (a) from 0.19 to 0.2 sec

High Temperature Magnetic Bearing - Blade Loss Mitigation
NRA-GRC- 99-02 - 1 Year Milestone Review
September 27, 2002, NASA Glenn

Glenn Research Center

Texas A&M Vibration Control and Electromechanics Lab

Fig.B.5.14 Squeeze film damping force: 2D Brg, 20 lb unbalance

(Radial force Fr is to the outward direction to min film thickness, Ft is perpendicular to Fr)

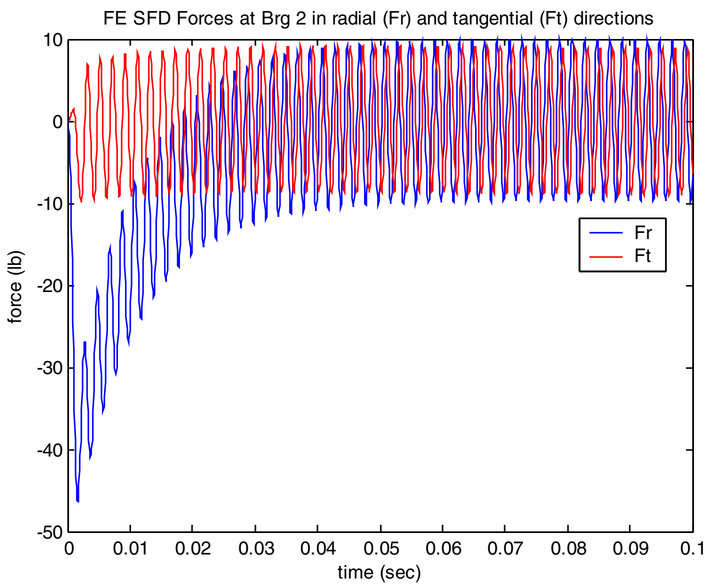

(c) Bearing 2

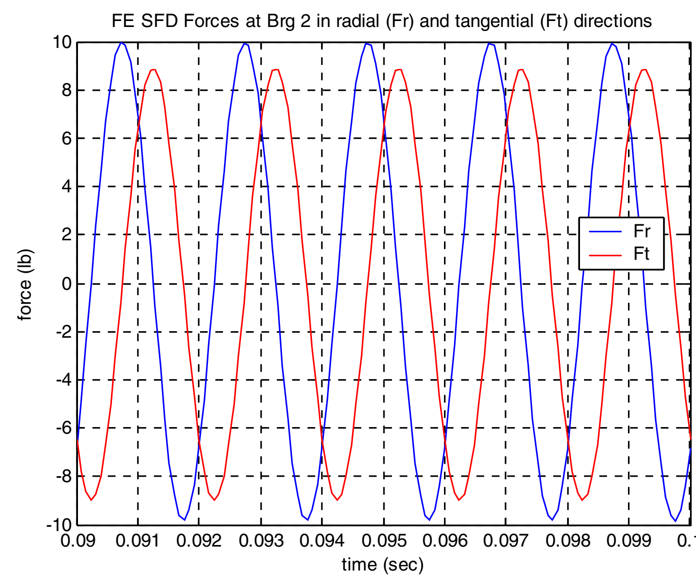

(d) Scaled plot for (c) from 0.19 to 0.2 sec

Fig.B.5.15 Max and min fluid film pressures in FE SFD: 2D Brg, 20 lb unbalance (Ambient pressure is 30 psi)

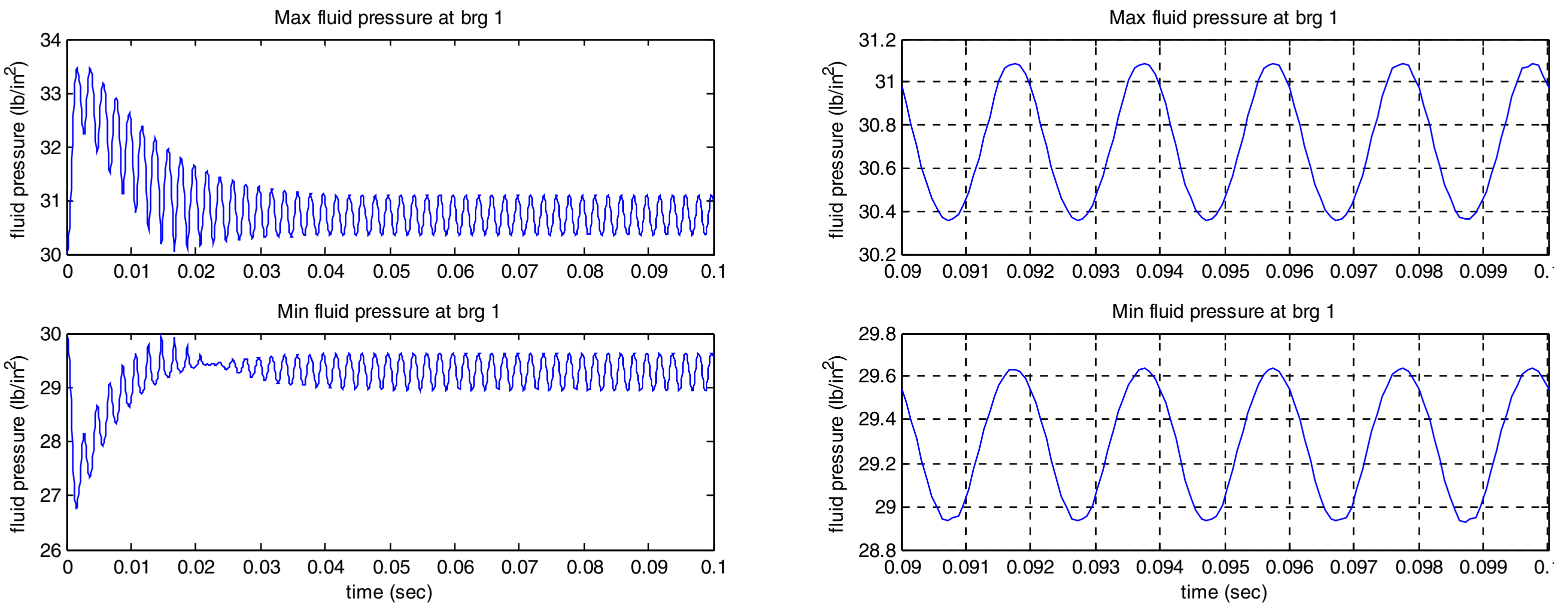

(a) Bearing 1

(b) Scaled plot for (a) from 0.19 to 0.2 sec

Fig.B.5.15 Max and min fluid film pressures in FE SFD: 2D Brg, 20 lb unbalance (Ambient pressure is 30 psi)

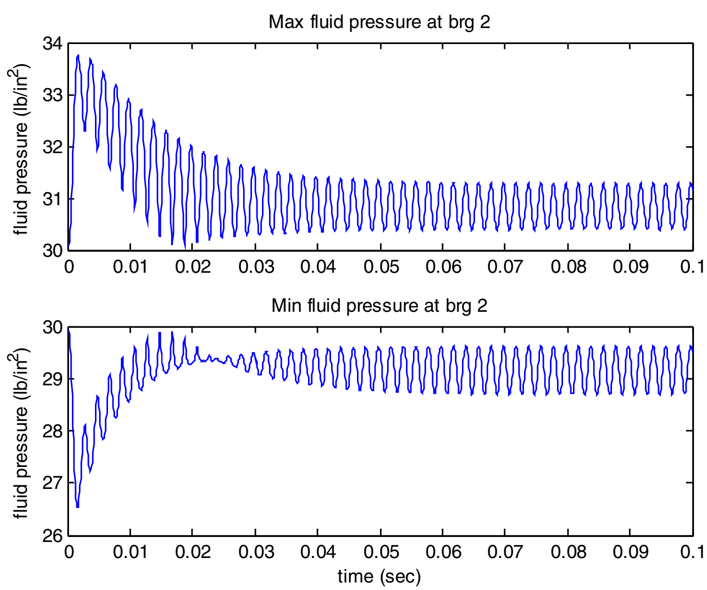

(c) Bearing 2

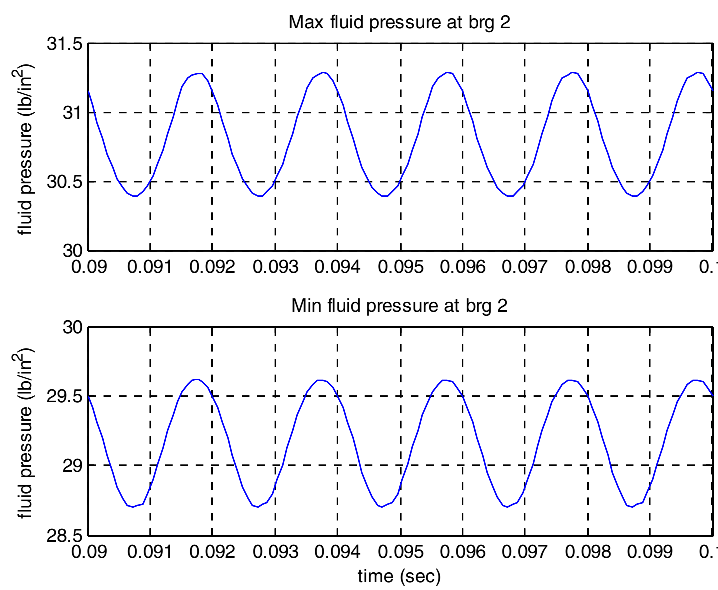

(d) Scaled plot for (c) from 0.19 to 0.2 sec

Fig.B.5.16 Temperature growth and induced thermal load in bearings: 2D Brg, 20 lb unbalance (Initial temp is 80 °F)

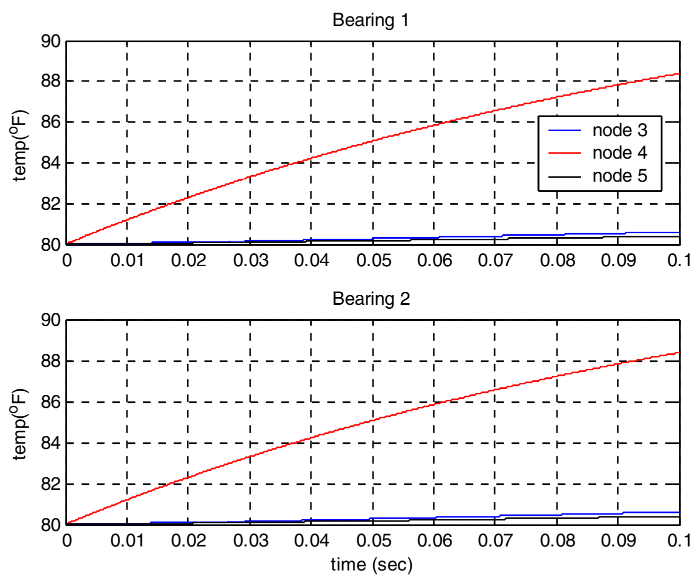

(a) Temperature growth

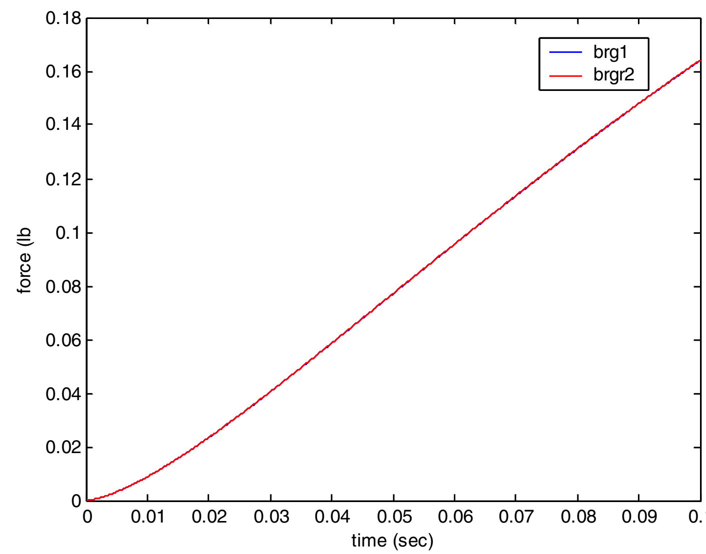

(b) Thermally induced bearing load at IR

Fig.B.5.17 Dynamic response of Wheel 2: 3D Brg, 4,000 lb unbalance

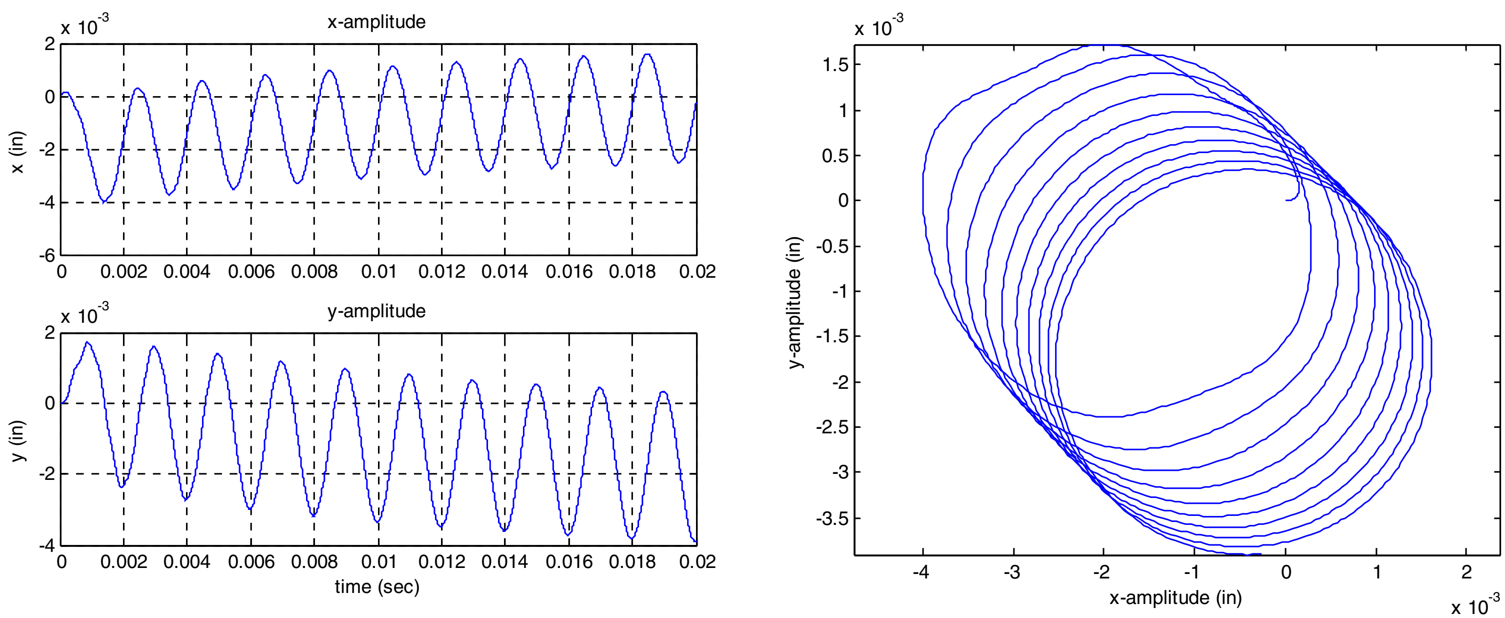

(a) Dynamic responses

(b) Orbit plot

Fig.B.5.18 Dynamic response of Wheel 1: 3D Brg, 4,000 lb unbalance

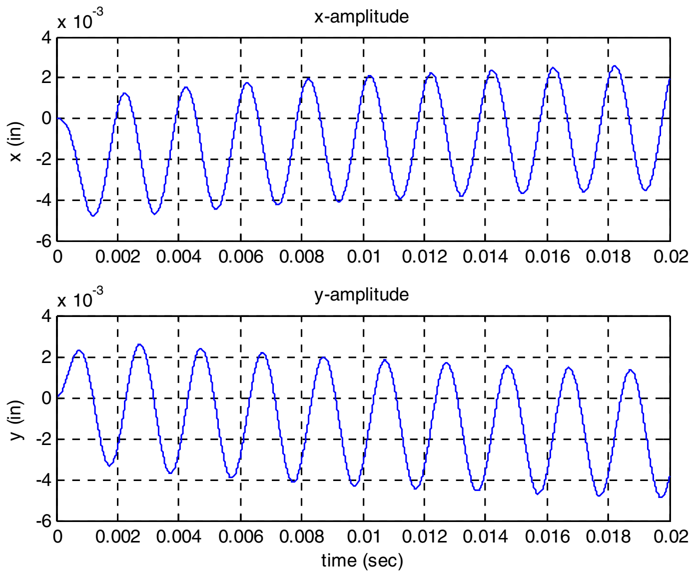

(a) Dynamic responses

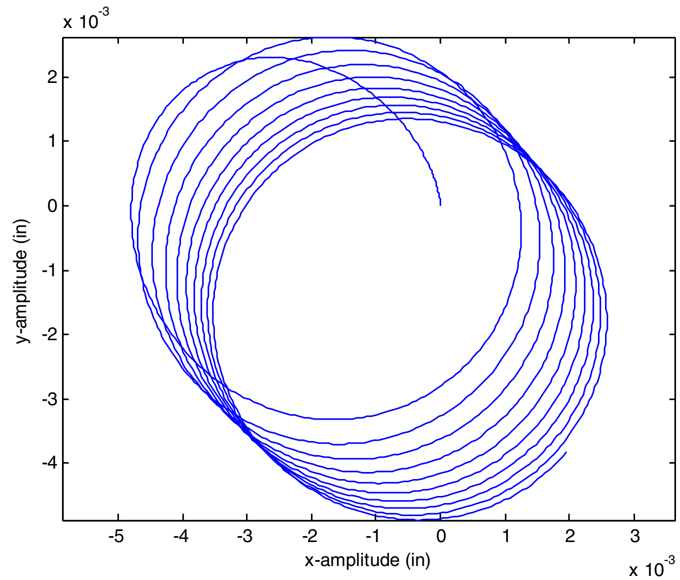

(b) Orbit plot

Fig.B.5.19 Rotor motions at bearing 1 and 2: 3D Brg, 4,000 lb unbalance

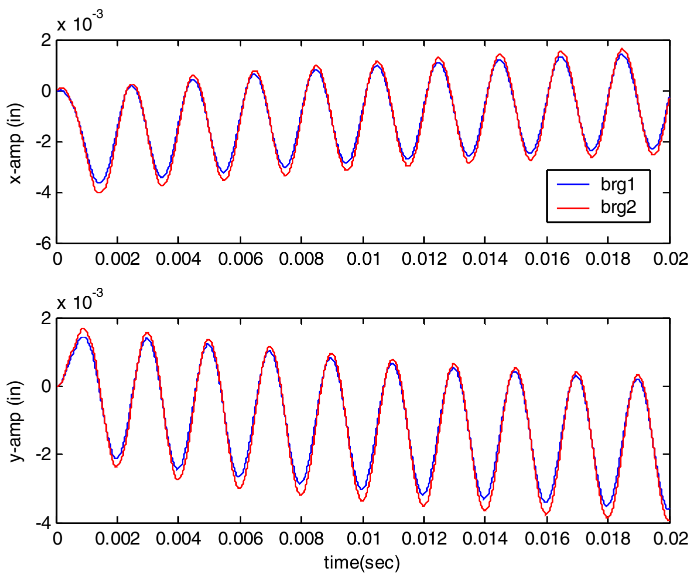

(a) Dynamic responses

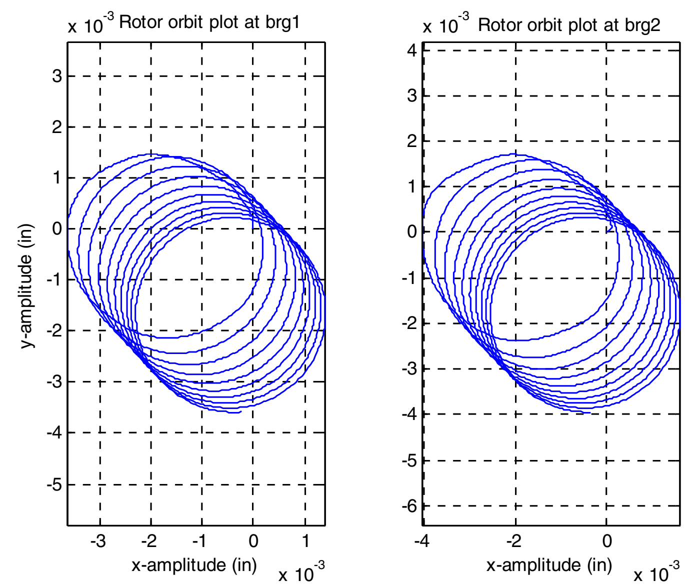

(b) Orbit plot

Glenn Research Center

High Temperature Magnetic Bearing - Blade Loss Mitigation
NRA-GRC- 99-02 - 1 Year Milestone Review
September 27, 2002, NASA Glenn

Texas A&M Vibration Control and Electromechanics Lab

Fig.B.5.20 Outer ring plus SFD journal motions at bearing 1 and 2: 3D Brg, 4,000 lb unbalance

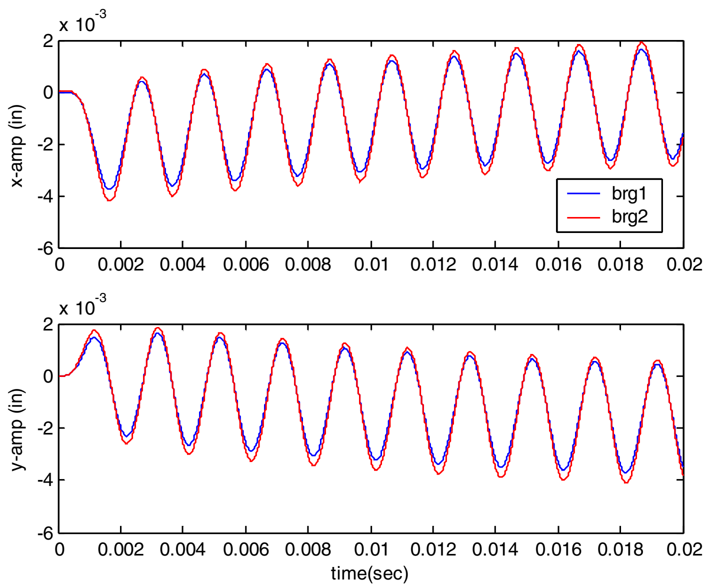

(a) Dynamic responses

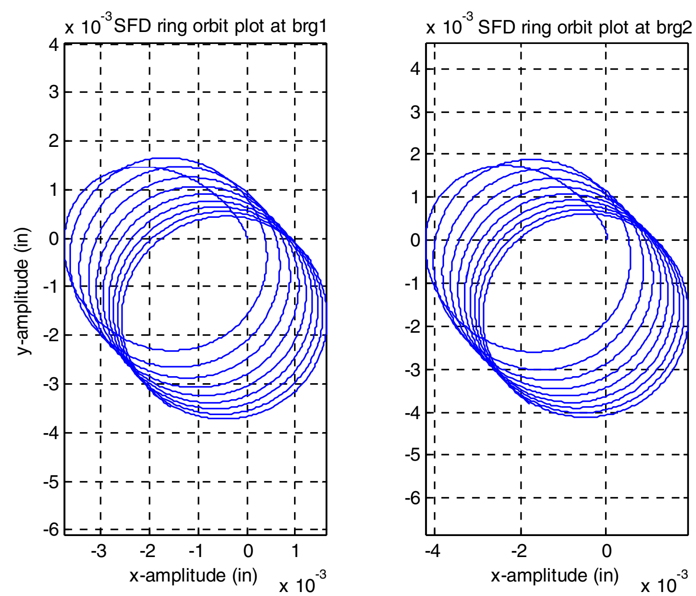

(b) Orbit plot

Fig.B.5.20 Outer ring plus SFD journal motions at bearing 1 and 2: 3D Brg, 4,000 lb unbalance

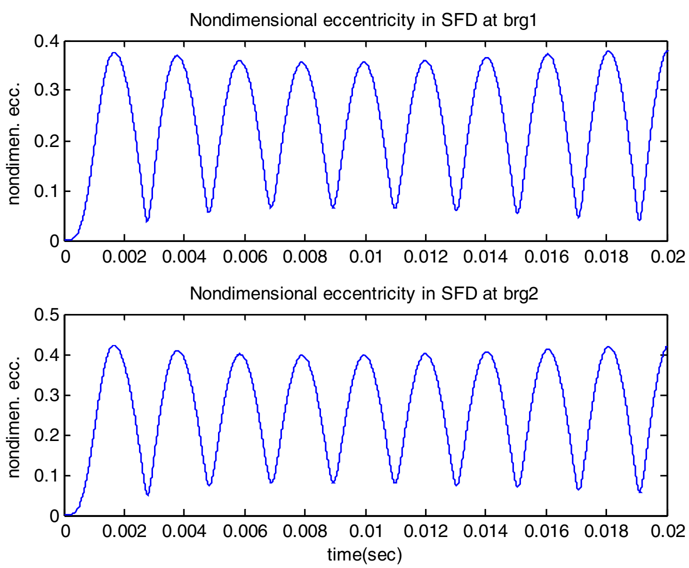

(c) Nondimensional eccentricity

Fig.B.5.21 Contact loads at 5th and 13th balls: 3D Brg, 4,000 lb unbalance

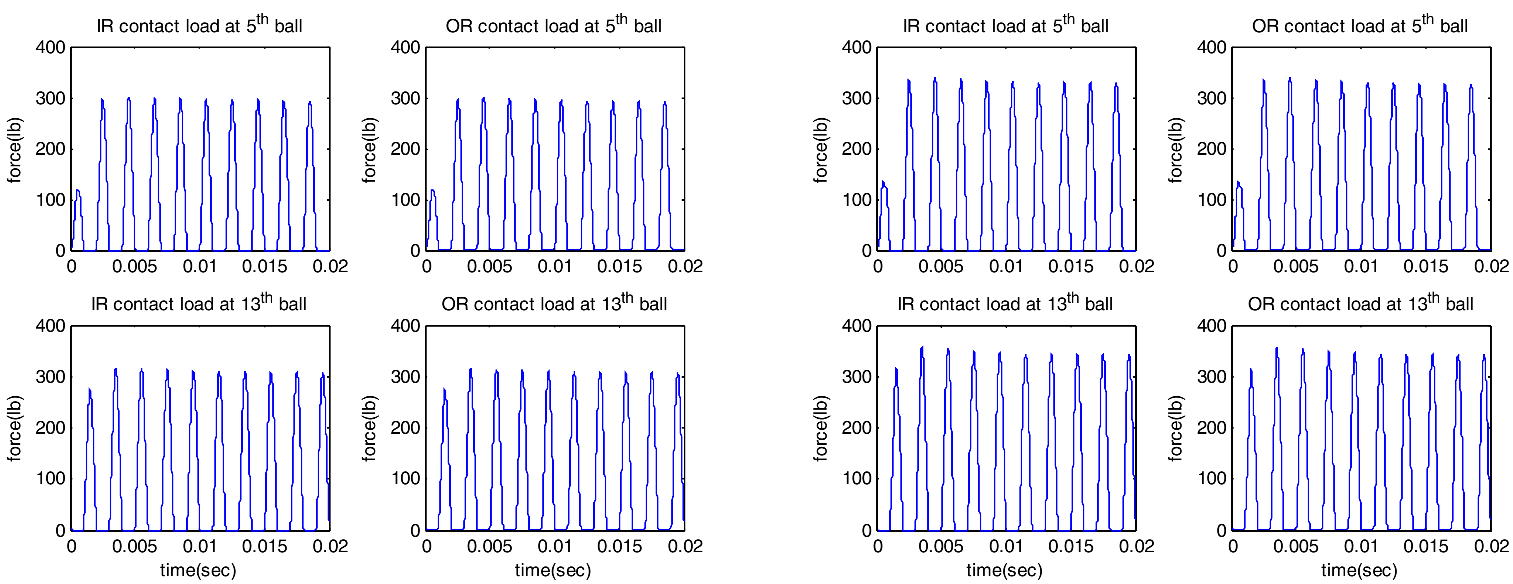

(a) Bearing 1

(b) Bearing 2

Fig.B.5.22 Contact stress at 5th and 13th balls: 3D Brg, 4,000 lb unbalance

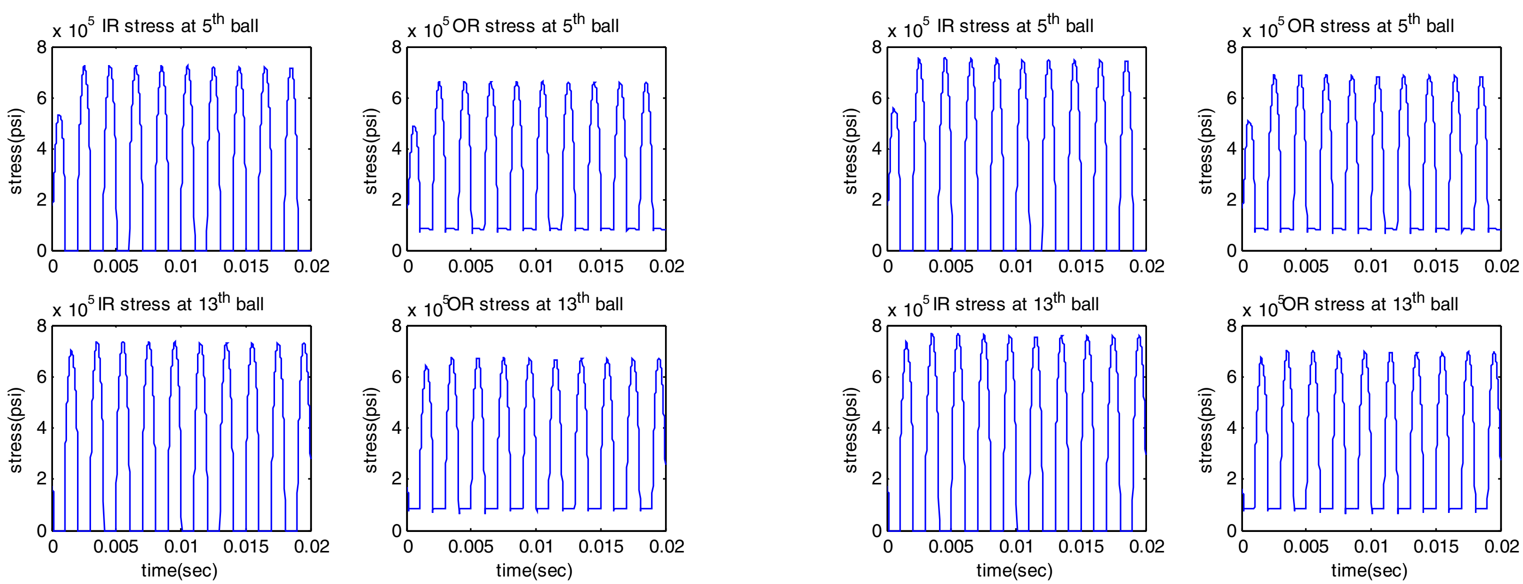

(a) Bearing 1   (b) Bearing 2

Fig.B.5.23 Squeeze film damping force: 3D Brg, 4,000 lb unbalance

(Radial force Fr is to the outward direction to min film thickness, Ft is perpendicular to Fr)

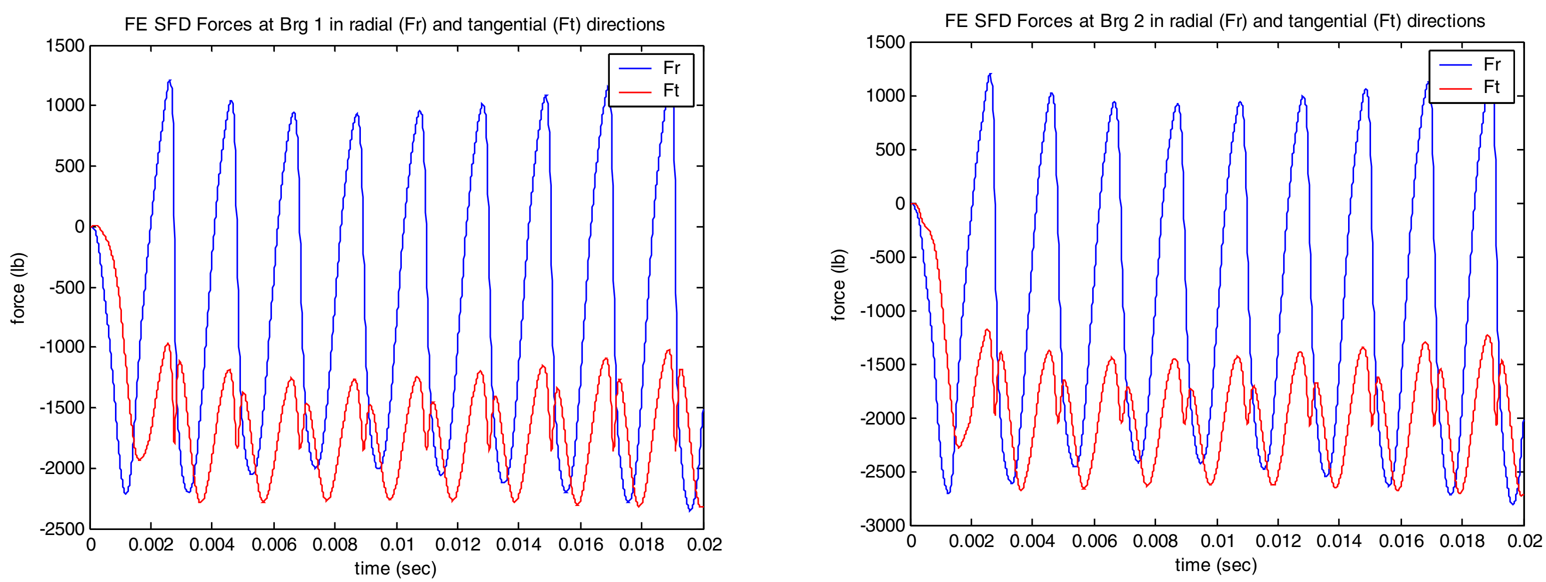

(a) Bearing 1 (b) Bearing 2

Glenn Research Center

High Temperature Magnetic Bearing - Blade Loss Mitigation
NRA-GRC- 99-02 - 1 Year Milestone Review
September 27, 2002, NASA Glenn

Texas A&M Vibration Control and Electromechanics Lab

Fig.B.5.24 Max and min fluid film pressures in FE SFD: 3D Brg, 4,000 lb unbalance (Ambient pressure is 30 psi)

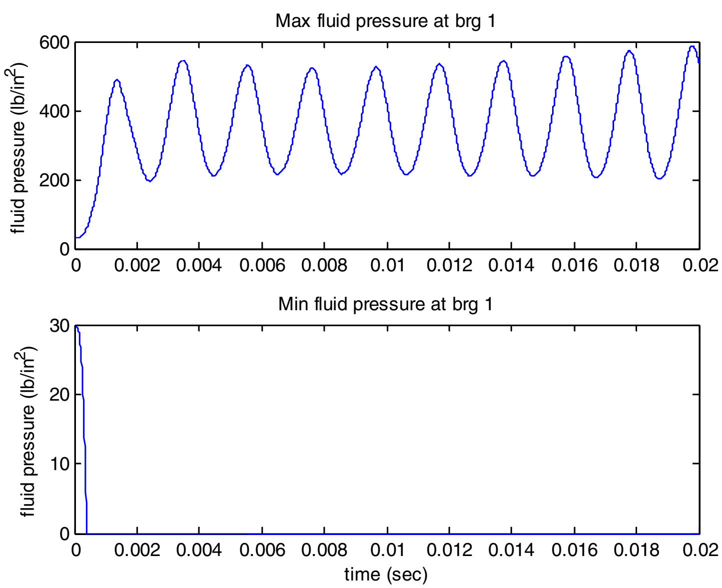

(a) Bearing 1

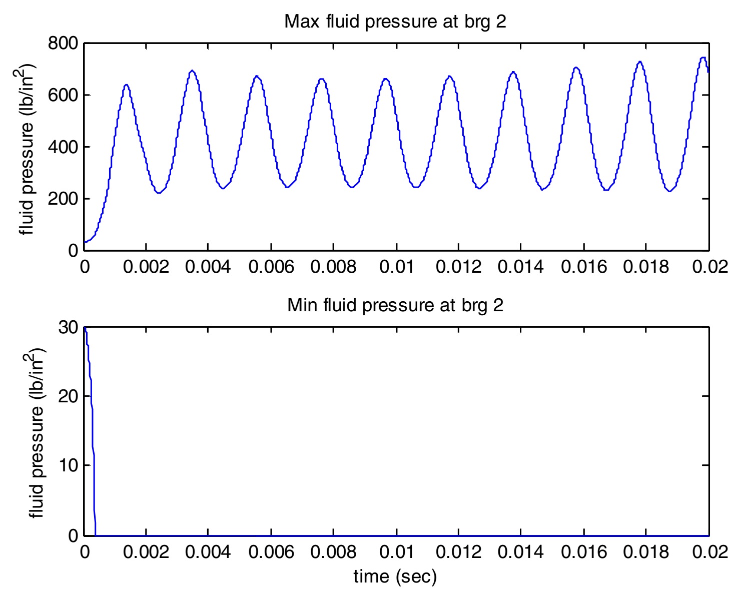

(b) Bearing 2

Fig.B.5.25 Temperature growth and induced thermal load in bearings: 3D Brg, 4,000 lb unbalance (Initial temp is 80 °F)

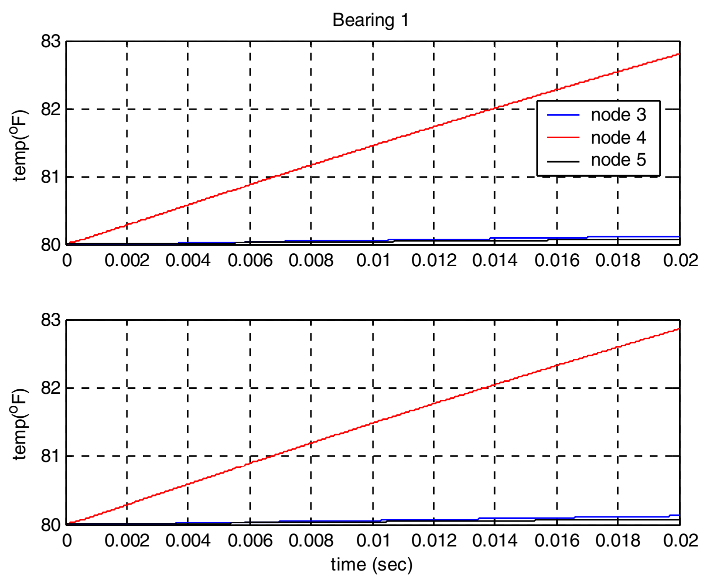

(a) Temperature growth

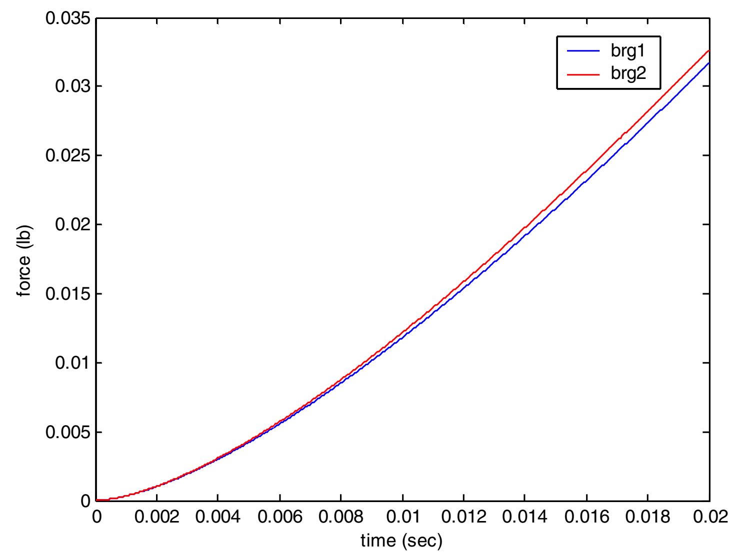

(b) Thermally induced bearing load at IR

Fig.B.5.26 Dynamic response of Wheel 2: 2D Brg, 4,000 lb unbalance

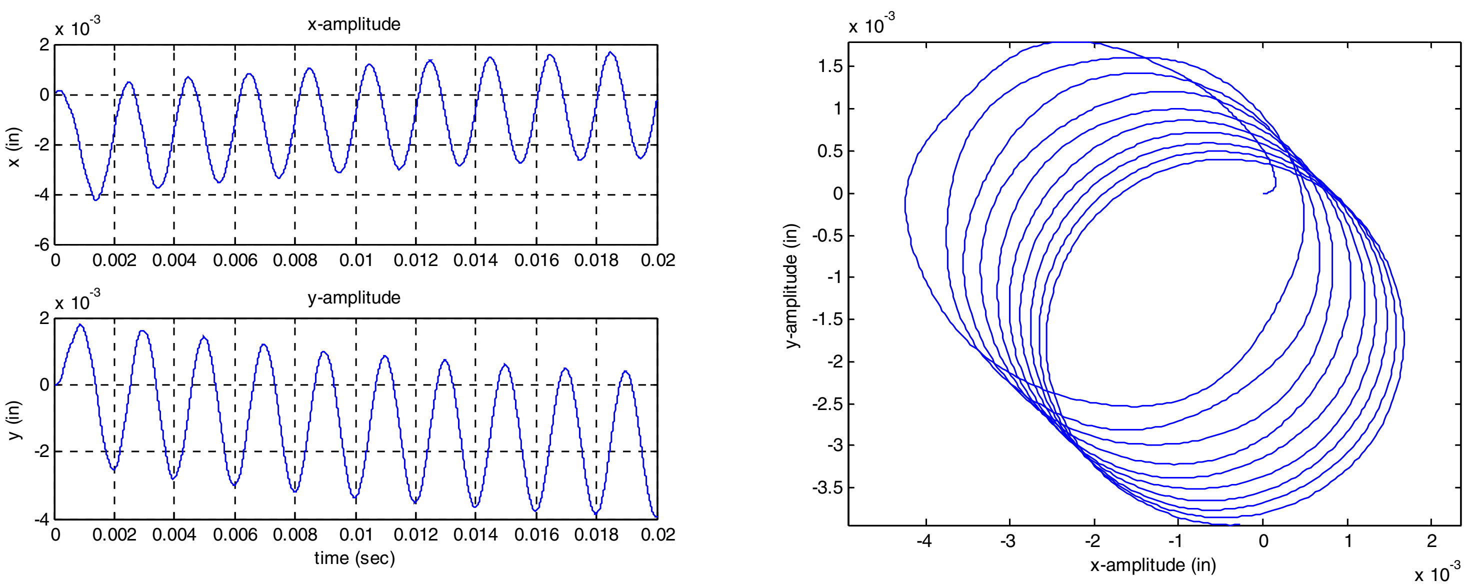

(a) Dynamic responses

(b) Orbit plot

Fig.B.5.27 Dynamic response of Wheel 1: 2D Brg, 4,000 lb unbalance

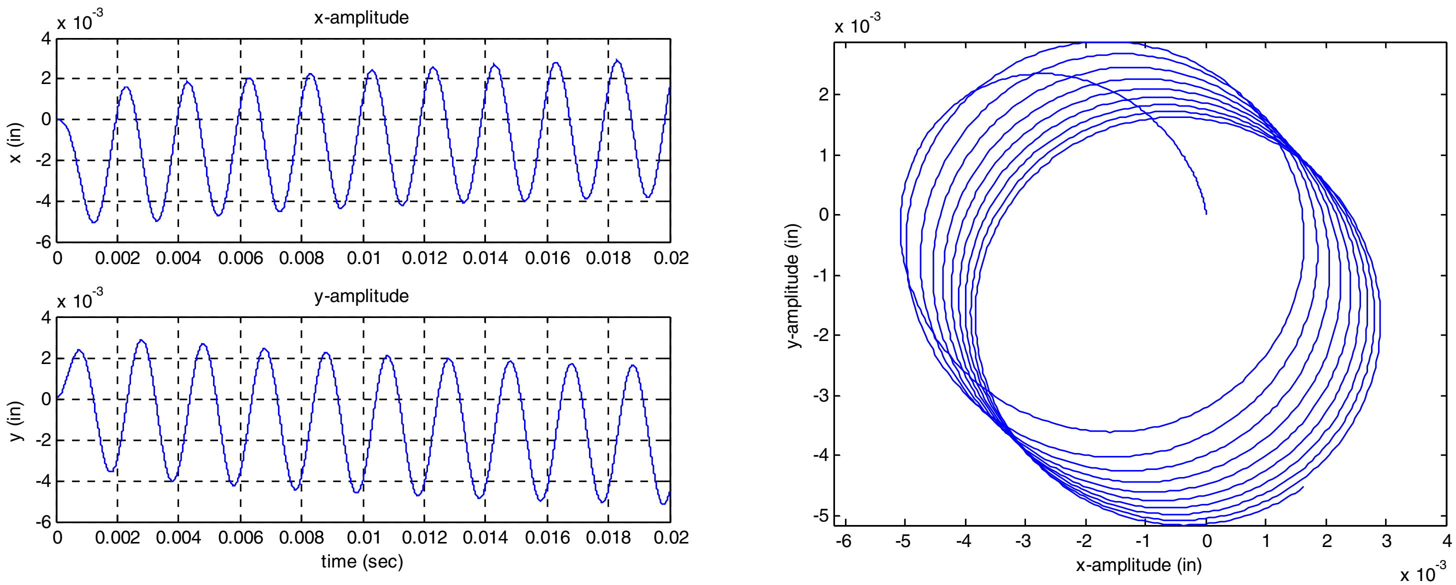

(a) Dynamic responses

(b) Orbit plot

Fig.B.5.28 Rotor motions at bearing 1 and 2: 2D Brg, 4,000 lb unbalance

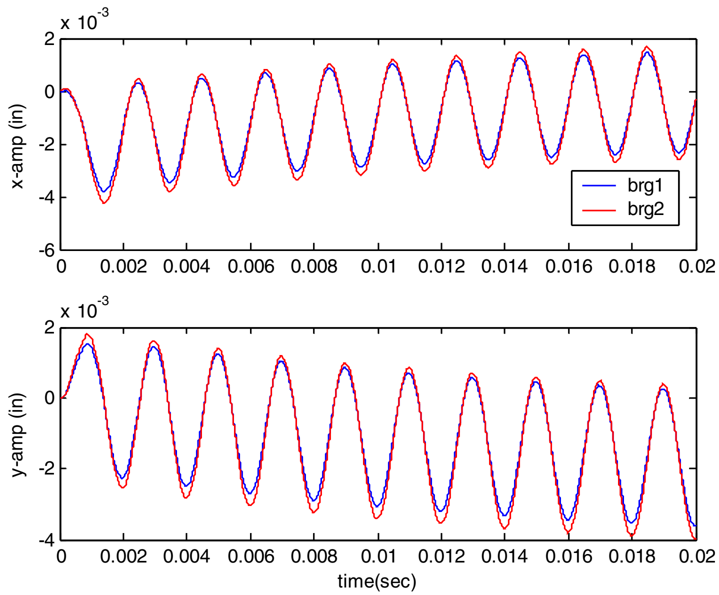

(a) Dynamic responses

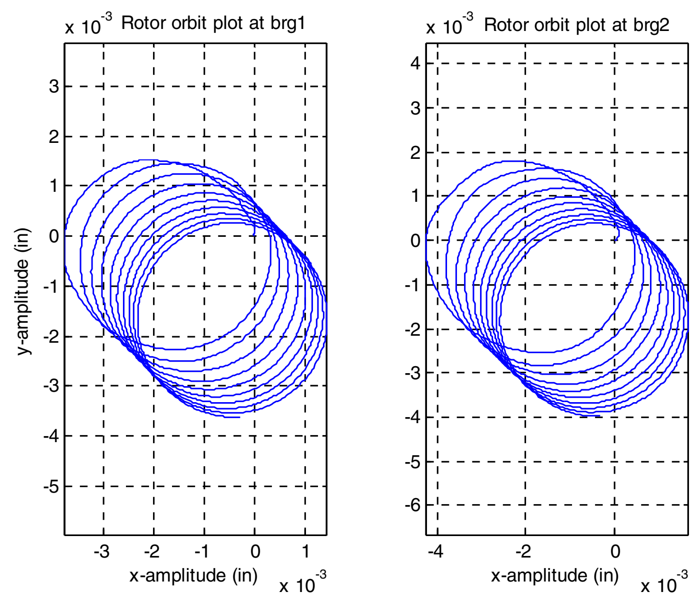

(b) Orbit plot

Fig.B.5.29 Outer ring plus SFD journal motions at bearing 1 and 2: 2D Brg, 4,000 lb unbalance

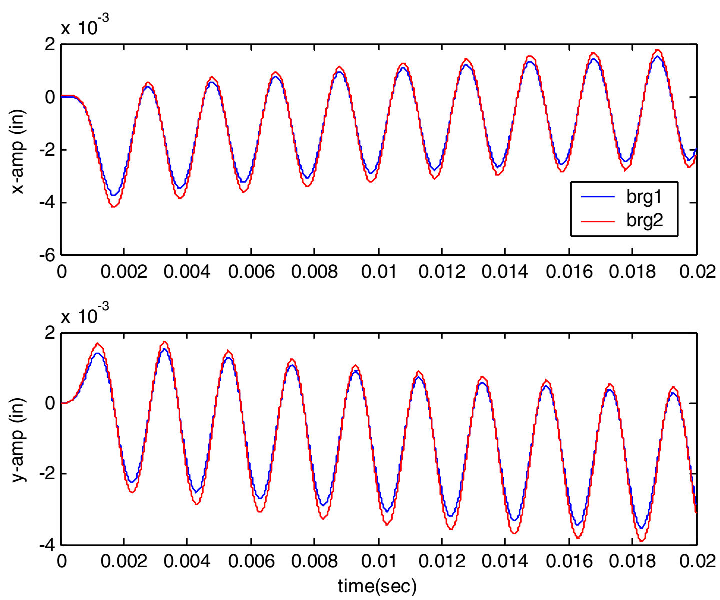

(a) Dynamic responses

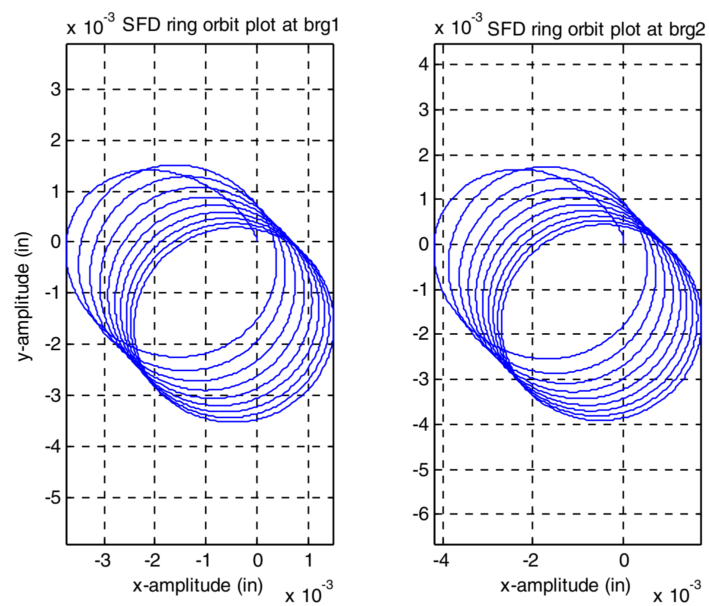

(b) Orbit Plot

NASA/CR—2003-212205

Fig.B.5.29 Outer ring plus SFD journal motions at bearing 1 and 2: 2D Brg, 4,000 lb unbalance

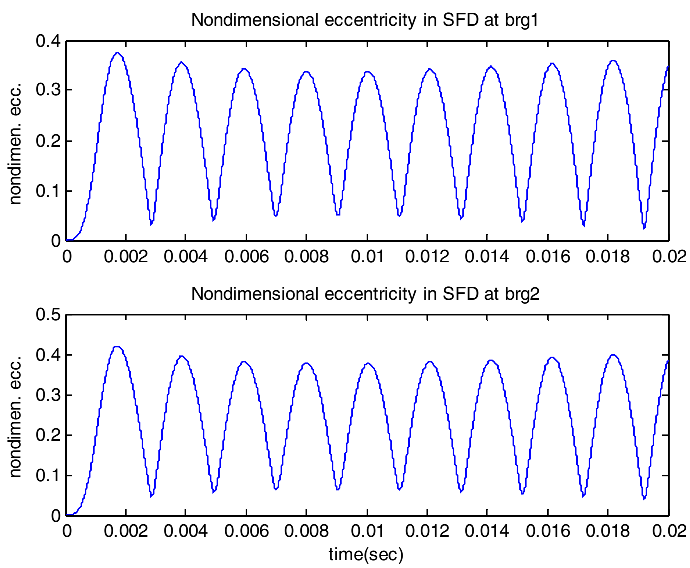

(c) Nondimensional eccentricity

Fig.B.5.30 Squeeze film damping force: 2D Brg, 4,000 lb unbalance

(Radial force Fr is to the outward direction to min film thickness, Ft is perpendicular to Fr)

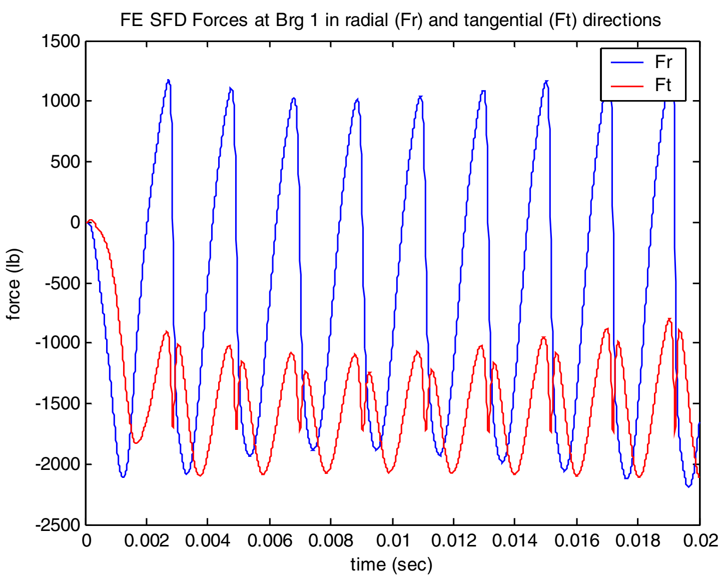

(a) Bearing 1

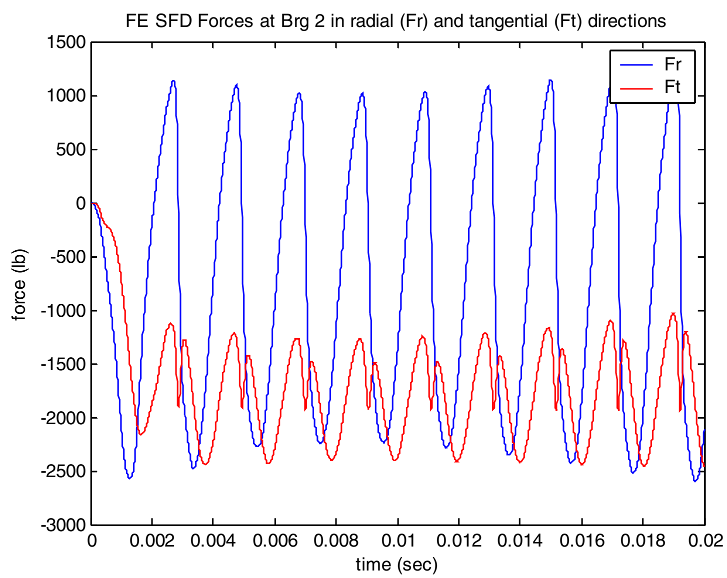

(b) Bearing 2

Fig.B.5.31 Max and min fluid film pressures in FE SFD: 2D Brg, 4,000 lb unbalance (Ambient pressure is 30 psi)

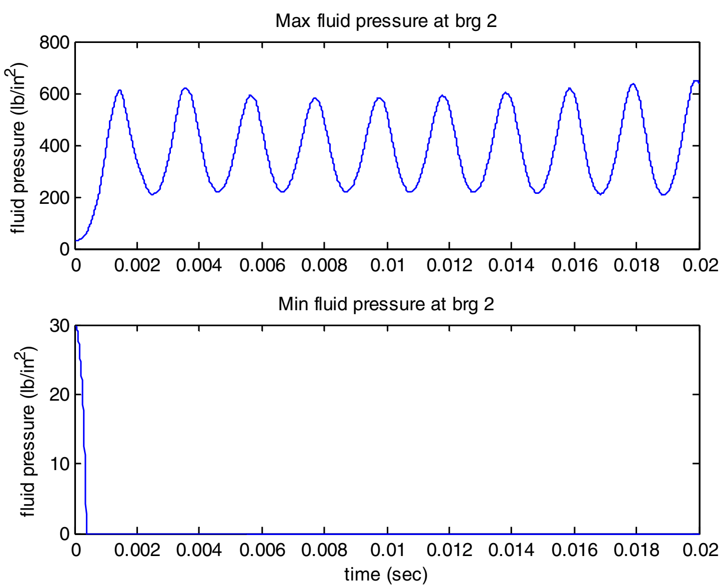

(a) Bearing 1

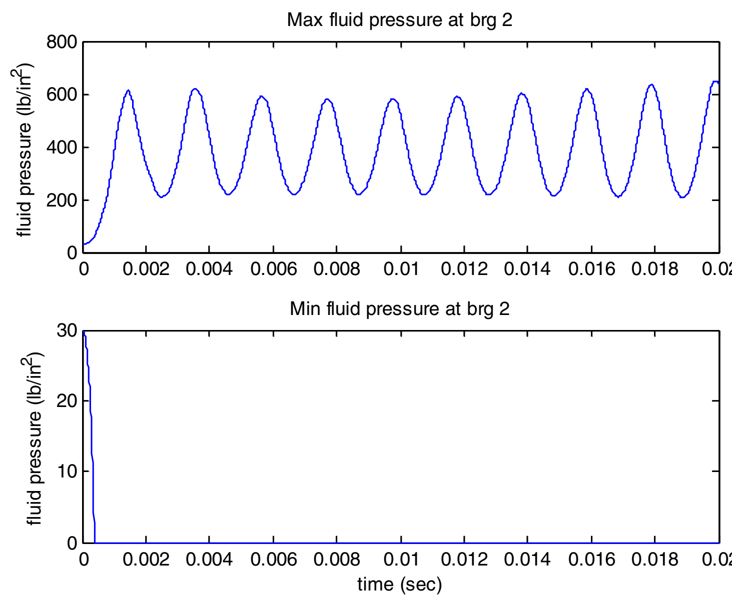

(b) Bearing 2

Fig.B.5.32 Temperature growth and induced thermal load in bearings: 2D Brg, 4,000 lb unbalance (Initial temp is 80 °F)

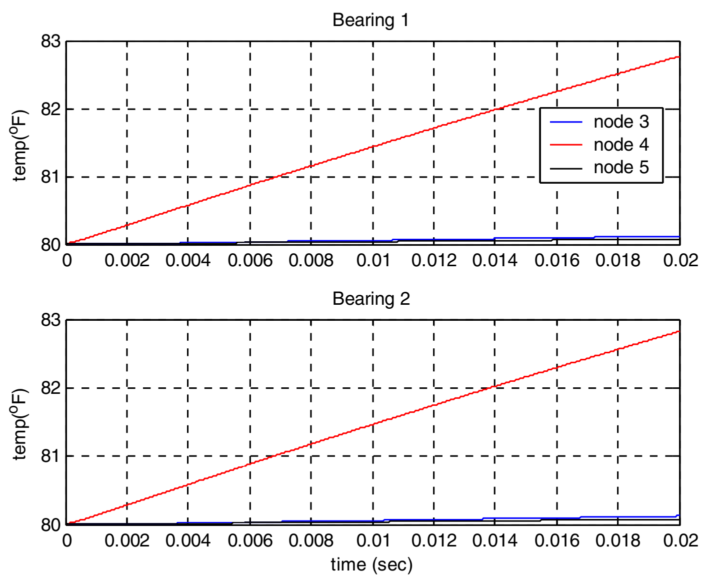

(a) Temperature growth

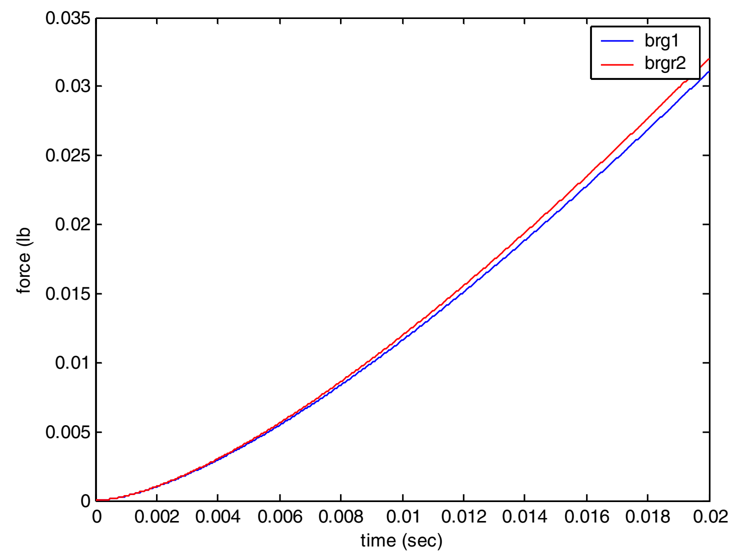

(b) Thermally induced bearing load at IR

Summary

- The 2D and 3D bearing model are developed and applied to rotor-two-wheels system with unbalance load.
- The numerical results for 4,000 unbalance load case show 500 Hz oscillating frequency, which is exactly the spinning frequency of the rotor.
- The simulation code successfully predicts the contact load and stress applied for individual ball, temperature distribution and thermally induced load in the bearing as well as dynamic responses of rotor-two-wheels system.

Planned Work

- Variant SFD viscosity depending on temperature
- Predict bearing life based on stress distribution in bearing
- Replace the rigid rotor into a flexible rotor.
- Develop graphic user interface (GUI) for rigid rotor-wheels system with 3D high fidelity ball bearing, FE SFD, and thermal bearing load models
- Integrate bearing model into system rotordynamic simulation

SMART STRUCTURAL COMPONENTS AND SIMULATION TOOLS FOR INCREASED ENGINE EFFICIENCY, FLIGHT RANGE AND SAFETY
ID: SA- 04-25
NRA-01-GRC-02 (Phase 2)

The proposer has received 15 years of continuous funding from NASA GRC in the areas of rotodynamics, active vibration control, magnetic bearings, and expert systems. This work has been monitored by the Machinery Dynamics Branch of the Structures Division and the Space Power Division. The proposed tasks seek to extend previous accomplishments in theses areas by developing innovative and effective means to:

(A) provide high performance, reliable and practical high temperature magnetic bearings for gas turbine aircraft engines, and
(B) provide high fidelity component models, novel approaches and system simulation code enhancements in the area of blade loss mitigation

Specific areas for development and implementation in task A include:

- Design, build and performance testing of an innovative, redundant high temperature (HT) thrust bearing,
- Inexpensive HT eddy current position sensor development,
- PWM servo power amplifier development with built in power monitoring capability,

- Flight ready controller design, prototype and testing,
- HT catcher bearing development and implementation
- HT magnetic bearing expert system development and implementation for anomaly detection/correction and enhanced performance,
- Hybrid high temperature magnetic bearing with built in foil bearing

Specific areas for development and implementation in task B include:

- higher fidelity, mechanical component simulation models,
- increased computational efficiency for repeated simulations of system dynamics,
- providing benchmark cases for the Boeing/NASA blade loss, system simulation code,
- providing feasibility studies and implementation plans for blade loss mitigation with active magnetic bearings (smart structural components).

The deliverables include component and full-up system test results, and hardware, and simulation software along with parametric study results, and user's manuals.

High Temperature Magnetic Bearing - Blade Loss Mitigation
NRA-GRC- 99-02 - 1Year Milestone Review
September 27, 2002, NASA Glenn

Glenn Research Center

Texas A&M Vibration Control and Electromechanics Lab

SMART STRUCTURAL COMPONENTS AND SIMULATION TOOLS FOR INCREASED ENGINE EFFICIENCY, FLIGHT RANGE AND SAFETY
ID: SA- 04-25
NRA-01-GRC-02 (Phase 2)

PROJECT DESCRIPTION AND PLAN

A. HIGH TEMPERATURE MAGNETIC BEARINGS FOR AIRCRAFT ENGINES

Description

The proposers have delivered 2 high temperature magnetic bearings (HTMB) to Gerald Montague and Al Kascak of GRC under NRA-99-GRC-2 and prior grants. The most recent HTMB has been tested to 150 lb. load capacity at 1000°F, and 10,000 rpm at 1000°F. The 12-pole geometry of this radial bearing allows redundant operation which was successfully confirmed at 13000 rpm and 750°F when any one of the 3 control aces was allowed to fail and suspension was maintained by the two remaining control axes. The control objectives of the proposed work are to develop and test a high temperature thrust (axial) magnetic bearing and to develop high temperature (HT) position sensors and catcher bearings. This work is required to realize the large gains in efficiency made available by HT operation of the engine and by adaptive (smart) operation of its components.

Glenn Research Center

High Temperature Magnetic Bearing - Blade Loss Mitigation
NRA-GRC- 99-02 - 1Year Milestone Review
September 27, 2002, NASA Glenn

Texas A&M Vibration Control and Electromechanics Lab

The Potential Impact and Benefits for Task A (High Temperature Magnetic Bearings) are:

Goal 1 Revolutionize Aviation

- Objective 1: Increase safety with redundant magnetic bearings and fault diagnosis/correction expert system.
- Objectives 4 and 5: Increase capacity and speed utilizing magnetic bearings that allow ultra high temperature (high efficiency) operation, very low power loss (bearing drag), and very high engine shaft speed (high DN operation).
- Objective 2: Protect the environment with oil free operation.

Goal 2 Advance Space Transportation

- Objective 3: Advancement of magnetic shaft suspension technology has tremendous spin-off potential for satellite/space travel advancement via highly efficient energy storage/attitude control flywheels utilizing magnetic suspensions.
- Objectives 6 and 7: Redundant magnetic bearings on flywheels will increase their safety and flywheels will reduce cost relative to electrochemical batteries.

Goal 3 Pioneer Technology Innovation

- Objectives 9 and 10: High temperature magnetic bearings (HTMB) present a significant advance in technology relative to conventional rolling element bearings. The analysis tools for designing the HTMB's are also revolutionary relative to passive shaft bearings.

The Potential Applications for **Task A (High Temperature Magnetic Bearings)** are:

- Revolutionary Aeropropulsion Concepts (L. Burkardt)
- Intelligent and/or adaptive structural components
- Smart Efficient Components (R. Corrigan)
- Ultra-Safe Propulsion (S. Johnson)
    - FailSafe magnetic bearings and fault diagnosis expert system
    - High temperature backup bearings
- Higher Operating Temperature Propulsion Components (C. Ginty)

The technology readiness level for this task is:

- TRL-5 (based on proposer's present NRA progress)

<u>Plan</u>

The new proposed work in this area includes the following tasks:
Design, build and test a thrust magnetic bearing (TMB) with capability to provide 10,000lb. load capacity at 1,000°F and 20,000 rpm. Testing of the bearing will be conducted as an isolated component at Texas A&M, and as part of a rotating assembly on the dedicated test rig designed by the proposer, and presently installed and operating at GRC-ERB. A concept drawing for the rig modified for TMB testing is shown in Fig. 1. **Use of the existing rig will significantly reduce test cost requirements.**

High Temperature Magnetic Bearing - Blade Loss Mitigation
NRA-GRC- 99-02 - 1Year Milestone Review
September 27, 2002, NASA Glenn

Glenn Research Center

Texas A&M Vibration Control and Electromechanics Lab

- Two ball bearings with radial dampers are used to support the weight of the rotor and provide damping at its critical speeds. Both bearings are mounted on thin plates that are very compliant in the thrust direction, which insures that the thrust magnetic actuator carries the full axial load. Electromagnetic external load actuators (EELA) are included at both for and aft locations to apply simulated engine thrust loads up to 10,000 lbs, while the rotor is spinning at up to 20,000 rpm. Air-cooled ball bearings will be used as axial catcher bearings to protect the thrust magnetic bearing. In addition electronic circuitry will be provided that will shutdown both the TMB and the EELA's if rotor thrust motion exceeds some pre-set limit. Some novel features of the TMB include:
  - (a) Tapered, slightly conical profile to decrease stresses due to centrifugal and magnetic force loadings,
  - (b) High temperature position sensors embedded in the TMB stators to provide collocated control,
  - (c) Ceramic potting of ribbon, round or square coils with s-glass wrapping for insulation,
  - (d) Hiperco 27 or HS material for rotor material,
  - (e) Redundancy will be built into the TMB actuator by use of multiple coils and a special control algorithm.

Design, build and test low cost, high temperature (1200^{o}F) shaft position sensors (HTSPS) and drive circuitry for magnetic suspension application. This work will compliment and extend the proposer's present NRA-99-GRC-2 task for furnace testing of COTS HTSPS, the proposer's present NASA Center for Space Power Task (monitor Raymond Beach) of shaft position sensor development, and the proposer's previous development of a HTSPS for GRC program manager Albert Kascak.

NASA/CR—2003-212205

- An innovative aspect of the proposed effort will be to deliver sensor arrays that compensate for shaft runout along with position sensing. Present COTS HTSPS costs are about $8K per channel, which are prohibitively expensive for 8 Channel arrays at both radial bearings. Thus the proposed work will provide sensors at much lower cost to make these arrays practical
- Implementation of HTMB's will require high temperature catcher bearings (HTCB), since the HTCB's and HTMB's should be closely located for shaft bending and thermal expansion reasons. The proposed work in this area will include:
  - Retrofitting the GRC HTMB test rig for HTCB testing
  - Testing of rolling element and sleeve HTCB concepts with dry (powder) or solid (coating) lubricants
  - By test and simulation optimize the HTCB flexible support and pre-load designs for long term, high load, high temperature, 6-12 hr. operation. The catcher bearing design software being developed by the proposer on NRA-GRC-99-02 (Gerald Montague) will be invaluable for the proposed HTCB development effort.
  - Design and install foil bearing as catcher bearing adjacent to the high temperature magnetic bearing

Design, build and test PWM power amplifiers (PWMPA) magnetic bearing current sources. COTS PWMPA's afford little flexibility for optimizing efficiency, power measurement, miniaturization, direct digital control, etc. The proposed effort will supply PCB mounted PWMPA's with surface mount electronics, onboard power monitoring and edge filtering (EMI reduction). **Accurate power monitoring will be a high priority development area for this effort**.

- The potential for using the PWM voltage pulses as a carrier for magnetic actuator, self-position sensing will also be developed. The PWMPA's developed by this effort will be component tested at Texas A&M and then installed in the High Temperature Magnetic Bearing, Fail Safe Magnetic Bearing or Flywheel Module Test Rigs at GRC, for actual system levitation and spin testing at GRC.
- Implementation of magnetic bearings in aircraft engines will require flight ready hardware. This task will identify acceptable platforms for magnetic suspension controller implementation. A controller will be designed and tested to meet these requirements in microprocessor, DSP, FPGA, analog or hybrid form. The proposer has significant experience for magnetic bearing controller development with controller deliveries to NASA, GRC, NAVY-ONR and University of Texas Austin--Center for Electromechanics.
- To enable the magnetic suspension to act more fully as a smart, structural component, it will be implemented with an expert system which optimizes the control law with temperature, speed and load, and detects and corrects anomalies (when possible). This task will benefit from related work in the proposers NRA-GRC-99-02 grant.

- To improve flight safety, redundant, fail safe control algorithms will be employed such as developed in:

  Na, U.J. and Palazzolo, A.B., "Fault Tolerance of a Magnetic Bearing Including Material Path Reluctances and Fringe Factors", IEEE Journal of Magnetics, Nov. 2000, Vol. 36, No. 6

High Temperature Magnetic Bearing - Blade Loss Mitigation
NRA-GRC- 99-02 - 1Year Milestone Review
September 27, 2002, NASA Glenn

Glenn Research Center

Texas A&M Vibration Control and Electromechanics Lab

The significant milestone list is:

- Year 1:
  - Design and Fabricate High Temp Thrust Mag Brg
  - Develop position Sensor hardware and drive electronics
  - Identify Flight Controller Components
  - Test Expert System on High Temp Mag. Brg. Test Rig at GRC (HTMBTR)
- Year 2:
  - Test High Temp Thrust Mag. Brg. At Temp and Speed in HTMBTR
  - Design PWM power amplifier
  - Identify components and perform component testing for high temp. catcher brgs.
  - Test position sensors in HTMBTR
  - Construct flight ready magnetic suspension controller at GRC
- Year 3:
  - Test PWM power amplifier in HTMBTR
  - Test high temp. catcher bearings in HTMBTR

Timeline / Cost Estimate / Milestones

Timeline

TASK	Year 1 Qtr. 1 2 3 4	Year 2 Qtr. 1 2 3 4	Year 3 Qtr. 1 2 3 4
A			
• High Temp. Thrust Mag. Brg.			
• High Temp. Position Sensor			
• PWM Power Amplifier			
• Flight Ready Controller			
• High Temp Catcher Brgs.			
• Expert System and Redundant Mag. Brgs			

NASA/CR—2003-212205

A. BLADE LOSS MITIGATION

Description

Significant progress has been made in blade loss mitigation and containment by a NASA/Industry Team including Dr. C. Lawrence and Kelly Carney. The team's objectives are reductions in weight and design an testing times, and improved quality and safety. Utilizing a super-element assembly approach, their work has yielded high fidelity structural simulation models for the engine/nacelle/wing portion of the aircraft, and consequent improvement in blade out margin of safety predictions. For high fidelity simulation, their engine model itself consists of a fan cowl and case, strut, nozzle, fan, and high/low/fan rotors with bearings. The corresponding code is hereinafter called the Boeing/NASA code.

The Potential Impact and Benefits for **Task B (Blade Loss Mitigation)** are:

Goal 1 Revolutionize Aviation

- Objective 1: The simulation tool enhancements contained in this proposal will aid in reducing the deleterious side effects of blade loss, which is a significant hazard to aviation.

Goal 2 Advance Space Transportation

Objective 6: The simulation tool enhancements contained in this proposal will aid in reducing the deleterious side effects of blade loss, which is a significant hazard to the space shuttle main engines.

Goal 3 Pioneer Technology Innovation

- Objective 9: The proposed code modeling enhancements and veracity tests will advance the fidelity and reliability of the NASA/Boeing blade loss mitigation engineering design tools.

The Potential Applications for **Task B (Blade Loss Mitigation)** are:

- Ultra-Safe Propulsion (S. Johnson)
  - Magnetic suspensions for blade loss mitigation
- Smart Efficient Components (R. Corrigan)

The technology readiness level for this task is:

- TRL-2 (based on proposer's present and past grant work)

Plan

The proposers seek to achieve the goals of the Ultra-Safe Propulsion Program via contributions to the task for numerical simulation of aircraft engine blade out structural dynamics. The four areas proposed include:

(a) Improved Component Modeling
(b) Increased Computational Efficiency
(c) Boeing Code Veracity Check
(d) Active (Smart) rotor suspension for blade loss mitigation

In category (a) it is proposed to integrate a detailed force-motion model of the engine's squeeze film damper bearing supports into the Boeing/NASA simulation code by solving Reynold's equation for damper pressures at each time step. The proposers have developed efficient algorithms to implement this as applied to fluid film bearings supporting a flexible shaft with thermohydrodynamics, gyroscopics and blade loss, i.e. reference:

Gadangi, R. and Palazzolo, A., "Transient Analysis of Tilt Pad Journal Bearings Including Effects of Pad Flexibility and Fluid Film Temperature", ASME/STLE Joint Conf., Oct. 1994, 94-TRIB-47, ASME Journal of Tribology, April 1995, Vol. 117, pp. 302-307.

Gadangi, R., Palazzolo, A., and Kim, J., "Transient Analysis of Plain and Tilt Pad Journal Bearings Including Fluid Film Temperature Effects", ASME/STLE Joint Conf., Oct., 1994, 94-TRIB-30, ASME Journal of Tribology, April 1996, Vol. 118, pp. 423-430.

The algorithm consists of a numerical finite element based, solution of Reynold's equation including cavitation effects. The coefficient matrix is determined and assembled at staggered intervals in time, whereas the source term vectors are updated at each time step, to improve computational efficiency. In addition it is proposed to integrate high fidelity models of ball bearings including ball and cage motions, forces, stresses and thermal expansions into the Boeing/NASA code at the Component Analysis and/or Back Substitution stages.

High Temperature Magnetic Bearing - Blade Loss Mitigation
NRA-GRC- 99-02 - 1Year Milestone Review
September 27, 2002, NASA Glenn

The proposers are presently developing high fidelity ball bearing models for magnetic bearing/auxiliary (catcher) bearings under the direction of Gerald Montague at NASA/GRC, on their NRA-99-GRC-2 Grant, and under direction of Andy Provenza, on their NRA-99-0SS-05 Cooperative Agreement. The benefit of the high fidelity bearing models is the capability they provide for bearing failure, nonlinear load/deflection and bearing drag torque prediction. It is notable that the NRA-99-GRC-02 and NRA-99-OSS-05 work of the proposer is presently developing high fidelity ball bearing models with squeeze film damper supports to reduce shock loads on the bearings during magnetic bearing power outages.

In category (b) it is proposed to apply reanalysis algorithms to reduce the computation time for evaluating system stability and steady state imbalance response for a range of parameter values. The "design for blade loss mitigation" process will require repetitive simulation for perhaps many values of localized structural components such as a strut, plug or bearing. Methods used and developed by the proposer accelerate solution of "modified' system models by utilizing results from "baseline" model simulations, i.e. reference:

Wang, B.P., Palazzolo, A.B. and Pilkey, U.D. "Reanalysis, Modal Synthesis and Dynamic Design", State of the Art Surveys on Finite Element Technology, edited by A.K. Noor and W.D. Pilkey, ASME Book No. H00290.

Palazzolo, A.B., Wang, B.P. and Pilkey, W.D., "Static Reanalysis Methods", Structural Mechanics Software, Vol. IV, edited by Perrone and Pilkey, University Press of Virginia, 1982.

In some instances, with reanalysis, computational savings are significant enough to enable probabilistic design approaches, i.e. ref.:

Barrett, T., Palazzolo, A., and Kascak, A., "Probabilistic Critical Speed Determination by Receptance Based Reanalysis", Proc. of the 6th International Symposium on Transport Phenomena and Dynamics of Rotating Machinery, pp. 272-288, Honolulu, 3/96.

In category (c) it is proposed to provide NASA with an alternate transient blade loss simulation code to be used for:

(i) Benchmarking the Boeing/NASA high fidelity super-element based code, i.e. provide an ISO 9000 check case that may be used to periodically test the Boeing/NASA code

(ii) Serve as a platform for developing and system integration of the component models described in (a)

This code will trade off fidelity for simplicity and reliability. Three dimensional beam elements will be utilized for all structural components with the inclusion of imbalance, inertial loading and gyroscopics for the rotating elements. Subspace condensation methods on the component and system levels will be employed akin to the Boeing/NASA code. In addition direct, full space analyses will also be included. Benchmark cases will be developed for subsequent comparison between the benchmark and Boeing/NASA code. The proposed code is not intended to replace the higher fidelity code, but only to provide benchmark, check cases for it.

The proposers are currently developing magnetic bearing hardware and control algorithms to integrate into commercial and military aircraft, gas turbine engines. This work is managed by Gerald Montague of GRC on NRA-99-GRC-2. Precursor research by the proposer, and funded by GRC, yielded development and hardware testing of control algorithms for blade loss mitigation, i.e. ref.:

> Manchala, D., Palazzolo, A., Kascak, A., and Montague, G., "Constrained Quadratic Programming, Active Control of Rotating Mass Imbalance", Journal of Sound and Vibration, Vol. 205(5), 4 Sept. 1997, pp. 561-580.

In category (d), it is proposed to integrate a feedback control magnetic bearing model into the code in (c) and into the Boeing/NASA code. The approach developed in the above paper provides the optimum level of magnetic counter force to blade loss, within the realistic saturation constraints of the magnetic bearing system. An alternate approach of allowing zero synchronous force transmission via the bearing, and orbiting about the new principal axis of inertia (after blade loss) will also be developed. In order to demonstrate the benefit of this latter approach, consider the 3 disk, 425 lb. simulation rotor model in Figure 2. A study was conducted to predict transmitted bearing loads and vibration due to a sudden mass imbalance of 0.25 lbs. at a radius of 3.6 inches, and at 30,000 rpm. This creates a rotating load of approximately 23,000 lbs. that conventional bearings would be required to react. Alternatively, Figs. 3 and 4 show the vibration and transmitted magnetic bearing forces during a blade loss event using a zero synchronous force control approach. The magnetic bearings are only required to sustain a large load (2500 lbs.) for a very short duration of time (less that 0.25 seconds).

High Temperature Magnetic Bearing - Blade Loss Mitigation
NRA-GRC- 99-02 - 1Year Milestone Review
September 27, 2002, NASA Glenn

Glenn Research Center

Texas A&M Vibration Control and Electromechanics Lab

It is noteworthy that this simulation includes the realistic effects of force limitation (2500 lbs.), current limitation (25 amps), voltage limitation (300 V), and catcher (backup) bearing impact. These simulations show that the maximum rotor excursion at the magnetic bearings is ________ inches and the steady state motion is ______ inches. The steady state magnetic bearing forces are seen to be less than _____ lbs. Figure 5 shows catcher bearing forces vs. time containing several very short duration impacts. The main objective of this task will be to evaluate the merits of a magnetic bearing suspension of the rotor(s) for mitigating blade loss response and damage. The authors plan to implement a full magnetic bearing component model into the high fidelity NASA/Boeing system model (in modal form) and simulate blade loss with zero synchronous force control, on a realistic gas turbine engine model. The authors have extensive experience with magnetic bearing actuator and feedback control system design in the satellite flywheel area as funded by GRC through the Texas A&M Center for Space Power (ref. Raymond Beach of GRC).

The significant milestone list is:
- Year 1: Complete Squeeze film damper and rolling element bearing modules and install in NASA/Boeing code
- Year 2: Finish and test benchmark code
- Year 3: Finish magnetic suspension module and install in NASA/Boeing code.

Timeline / Cost Estimate / Milestones

Timeline

TASK	Year 1 Qtr. 1 2 3 4	Year 2 Qtr. 1 2 3 4	Year 3 Qtr. 1 2 3 4
B			
• Component Models	←→		
• Veracity Benchmark Code		←→	
• Active Shaft Suspension			←→

SMART STRUCTURAL COMPONENTS AND SIMULATION TOOLS FOR INCREASED ENGINE EFFICIENCY, FLIGHT RANGE AND SAFETY
ID: SA- 04-25
NRA-01-GRC-02 (Phase 2)

EQUIPMENT PURCHASE BREAKDOWN

Year 1

• High Speed Shaft	\$2,000
• Thrust Magnetic Actuator	\$10,000
• Catcher Bearing and Supports	\$2,000
• External Load Actuators	\$6,000
• Test Rig Modifications	\$5,000
• High Temp. Sensor Development (Erwin Thomas at TAMU)	\$5,000
Total Year 1 – Task A Equipment Cost	\$30,000

Year 2

• Foil Type – Catcher Bearing Assembly	$12,000
• High Temp. Position Sensor Array	$5,200
• Power Amplifiers with Power Monitoring	$5,000
• Analog Realization Controller	$3,000
Total Year 2 – Task A Equipment Cost	$25,200

Year 3

• Test Rig Modification for Hybrid Foil Catcher Bearing/12 pole Magnetic Bearing	$7,600
• Rugged Flight-ready Controller with Analog and FPGA circuitry	$8,000
• Two High Temp. Position Sensor Arrays With Amplifier Drivers	$6,000
Total Year 3 – Task A Equipment Cost	$21,600

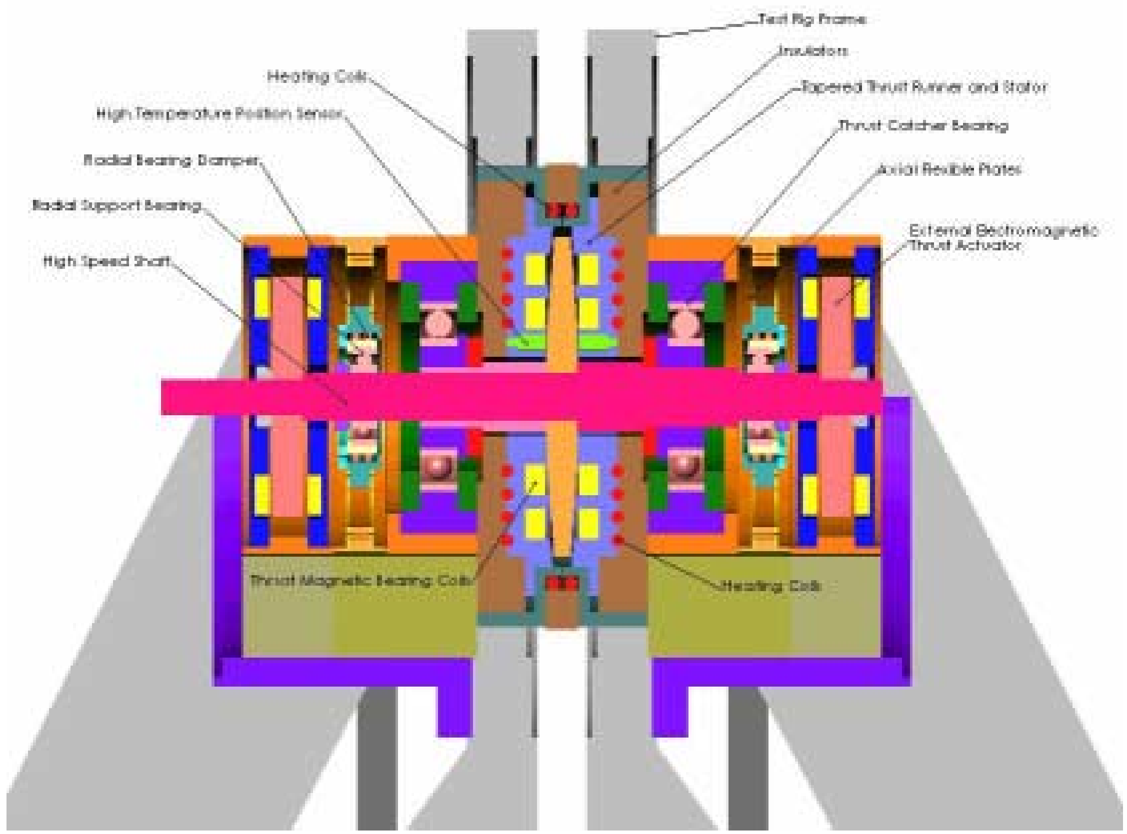

Figure 1a: High Load Thrust Magnetic Bearing Test Rig

High Temperature Magnetic Bearing - Blade Loss Mitigation
NRA-GRC- 99-02 - 1Year Milestone Review
September 27, 2002, NASA Glenn

Glenn Research Center

Texas A&M Vibration Control and Electromechanics Lab

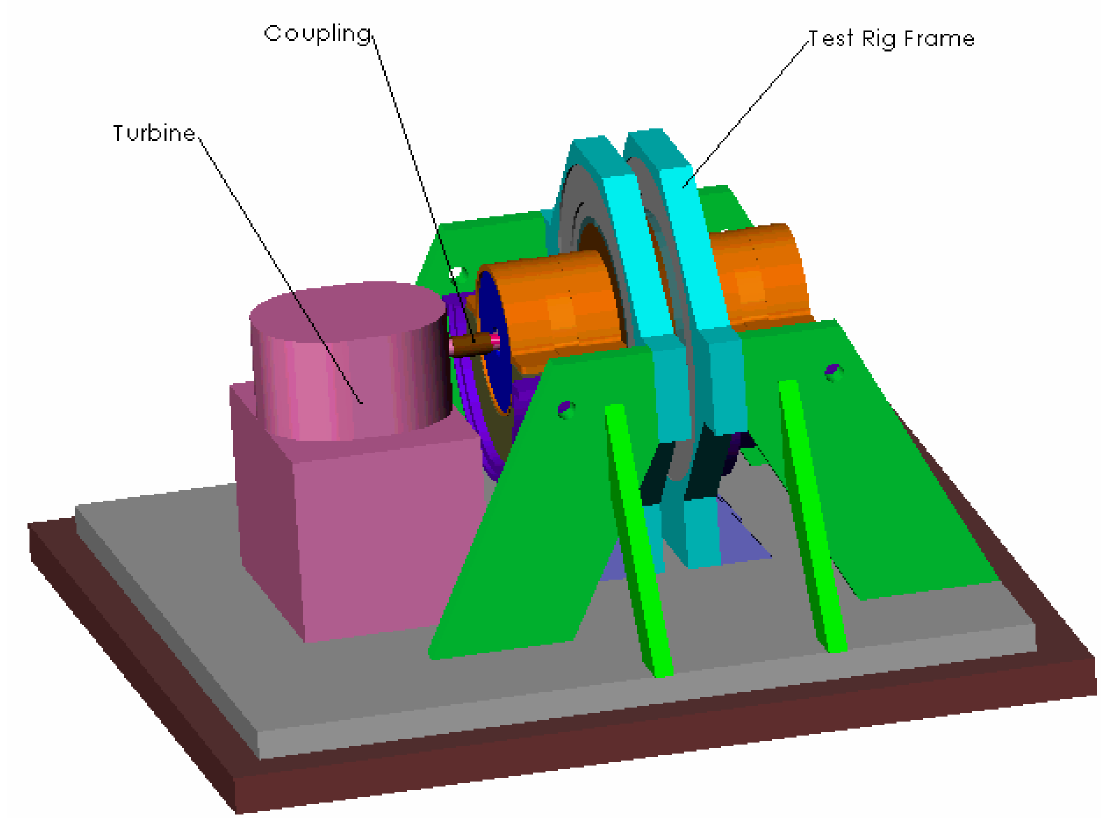

Figure 1b: High Load Thrust Magnetic Bearing Test Rig with Turbine

Glenn Research Center

High Temperature Magnetic Bearing - Blade Loss Mitigation
NRA-GRC- 99-02 - 1Year Milestone Review
September 27, 2002, NASA Glenn

Texas A&M Vibration Control and Electromechanics Lab

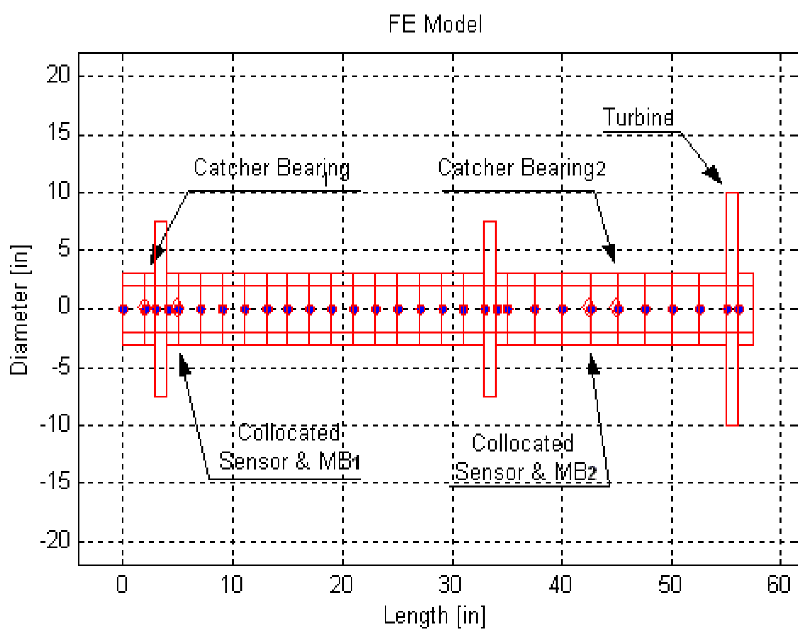

Figure 2: Rotor Simulation Model for Magnetic Bearing Control of Blade Loss

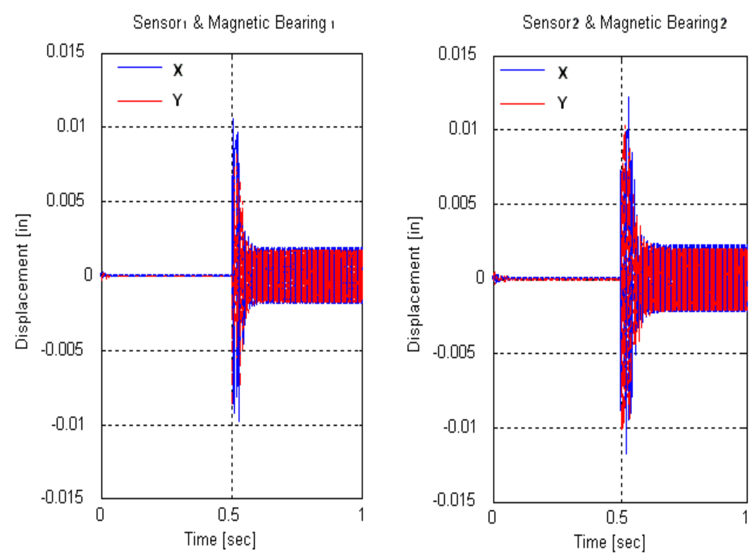

Figure 3: X and Y Positions vs Time at Magnetic Bearings during Blade Loss Event

High Temperature Magnetic Bearing - Blade Loss Mitigation
NRA-GRC- 99-02 - 1Year Milestone Review
September 27, 2002, NASA Glenn

Glenn Research Center

Texas A&M Vibration Control and Electromechanics Lab

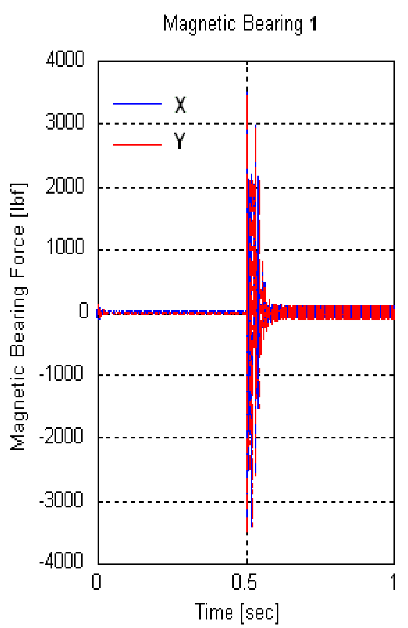

Figure 4: Magnetic Bearing X and Y Forces vs Time during Blade Loss Event

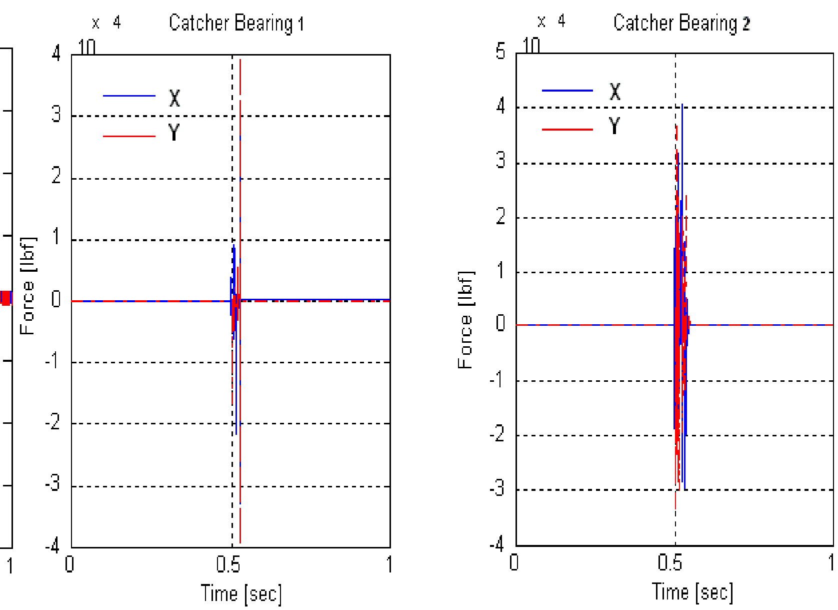

Figure 5: Catcher Bearing Forces vs Time during Blade Loss Event

SMART STRUCTURAL COMPONENTS AND SIMULATION TOOLS FOR INCREASED ENGINE EFFICIENCY, FLIGHT RANGE AND SAFETY
ID: SA- 04-25
NRA-01-GRC-02 (Phase 2)

KEY PERSONNEL

Dr. Palazzolo will lead the proposed research, which will be performed by Dr. Uhn Joo Na and Ph.D., Master, and undergraduate level students. Dr. Na received his Ph.D. M.E. degree from Texas A&M University in 1999 and has published numerous papers on redundant/fail safe magnetic bearings. He has been employed at TAMU, in the Vibration Control and Electromechanics Lab (Director: Palazzolo) for the past 4 years.

FACILITIES AND EQUIPMENT (Capability and Availability)

The task A simulation and component testing will be performed in the Vibration Control and Electromechanics Lab (VCEL) at TAMU. The system tests will be performed in the Magnetic Bearing Research Lab in the NASA-GRC Engine Research Building, under the direction of Mr. Gerald Montague. The P.I. has conducted research in this GRC lab for the past 15 years and is well acquainted with the facility and its operation. The task B simulation work will be conducted in the TAMU-VCEL.

The TAMU-VCEL has 2000 ft^2 of lab space with several workstations for magnetic actuator component testing, coil winding, controller development, and control/power console assembly. Instrumentation in the VCEL includes 2 FFT analyzers, a LABView data acquisition system, numerous scopes function generators and measurement transducers. The VCEL also has numerous high-speed Pentium class computers and SGI workstations. Licensed software includes MATLAB, SIMULINK, VECTORFIELDS, ANSOFT, SOLID WORKS, AutoCAD, and SPICE. A high-speed spin pit for flywheel testing is currently being installed in the lab. There are presently 5 Ph.D. students, 1 Master student, 1 fulltime Research Engineer (Dr. Na) and 6 undergraduate researchers employed in the VCEL.

PARTNERSHIPS

It is anticipated that Gerald Montague of the U.S. Army at NASA GRC (216-433-6252) will provide test support assistance for required system testing at GRC, in Task A, and Task B.

POINTS OF CONTACT

Technical: Dr. Alan Palazzolo, Texas A&M University, Mechanical Engineering,
College Station TX, 77843-3123, 979-548-5280 (3081 fax)
abp8849@acs.tamu.edu

Contractual: Ms. Brett Henry, TEES Research Services, MS 3406,
College Station TX, 77843-3406, 979-845-1264 (9643 fax)
bhenry24@tamu.edu

User Manual

1.1 Installation

1. Copy folder 'DRBB_GUI' from CD into MATLAB R12 or above version work directory on your computer
2. Set path to DRBB_GUI in the work directory in MATLAB
3. Now type "RD" in the command window and enter

1.2 Operation

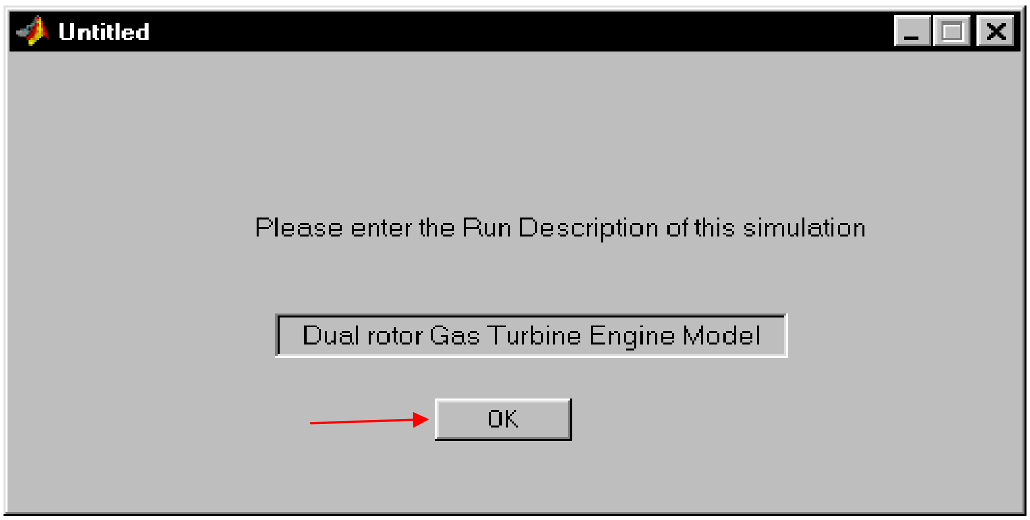

This is this first Panel in the GUI where the user Inputs the Run Description of the simulation .Enter the Text and click 'OK'.

In this GUI Example the input data is taken from the model by Li, Dennis, 1978, "Dynamic Analysis of Complex Multi -Level Flexible Rotor systems," University of Virginia.

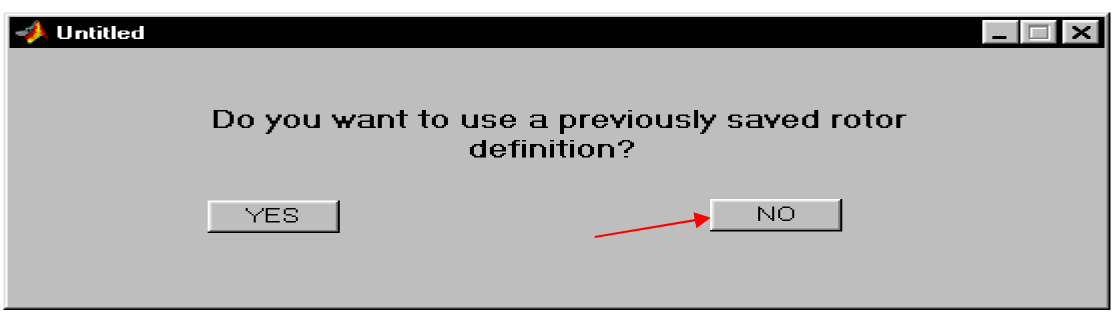

In this window, if the user clicks on 'NO' the GUI asks a new rotor definition for both rotors. The user is now asked for the number of elements in Rotor1 and Rotor2.

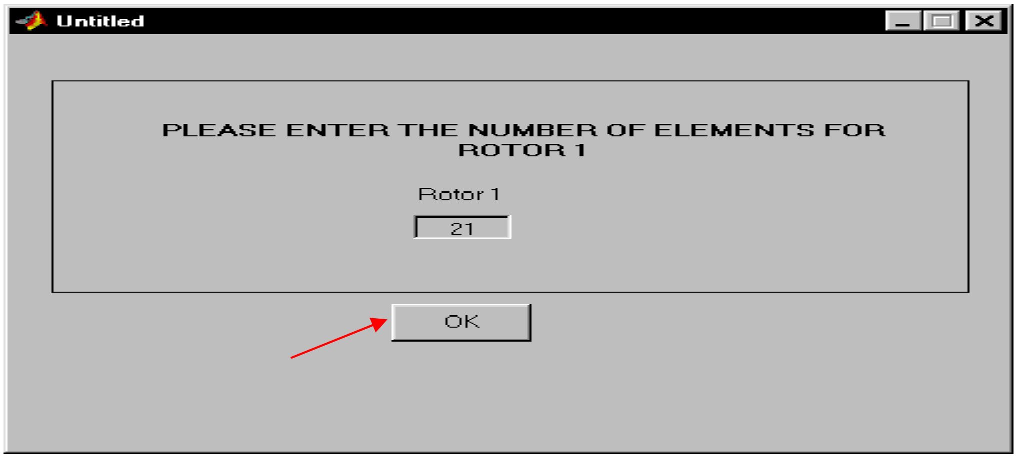

After this the user can input the new rotor data in the corresponding panels that will pop up. However in this example we use Dennis Li`s rotor model. So Click on 'YES'

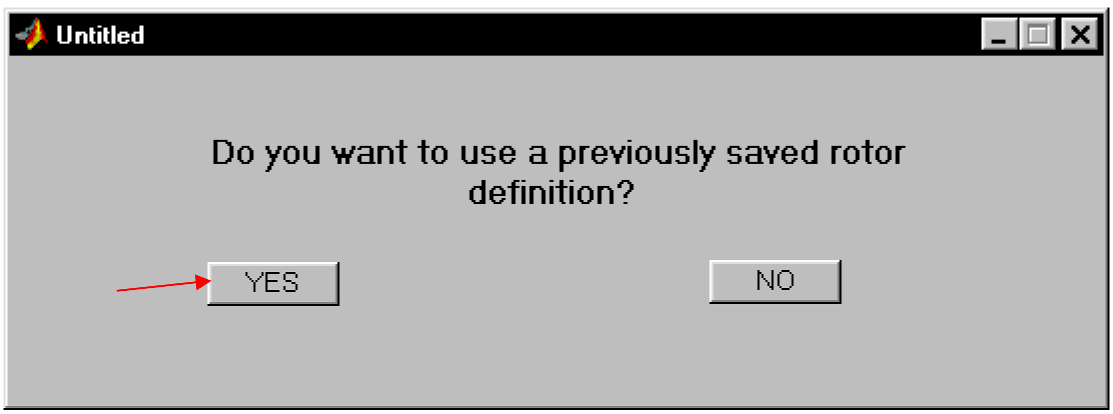

Now the Load save panel opens.Scroll down the list and double-click on 'rotor1.mat'.

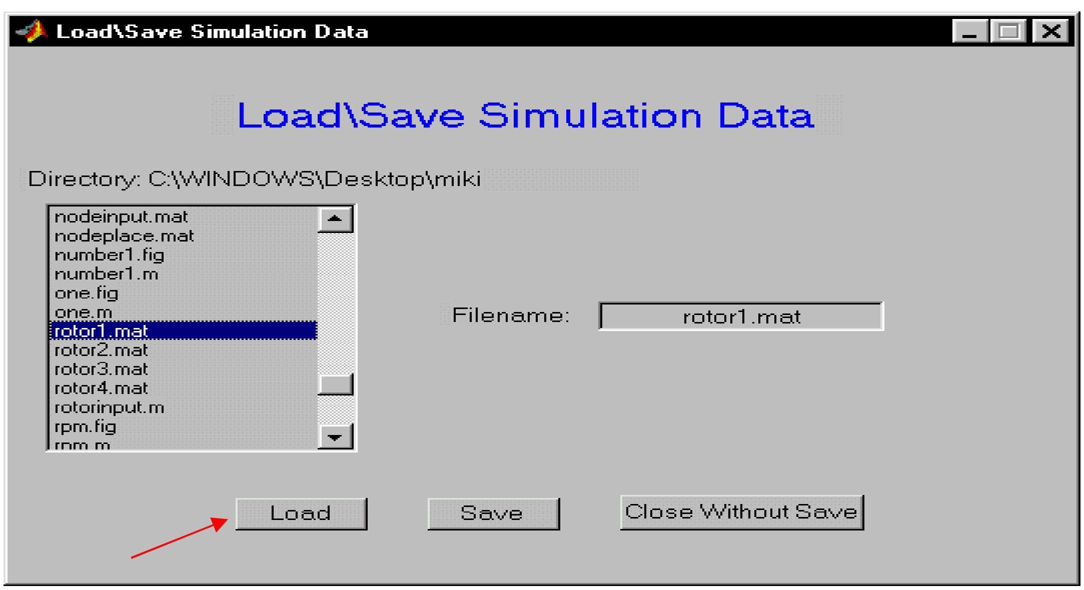

Then click on 'Load'. Now the input data panel for the rotors is opened. The user can use this or modify the model.

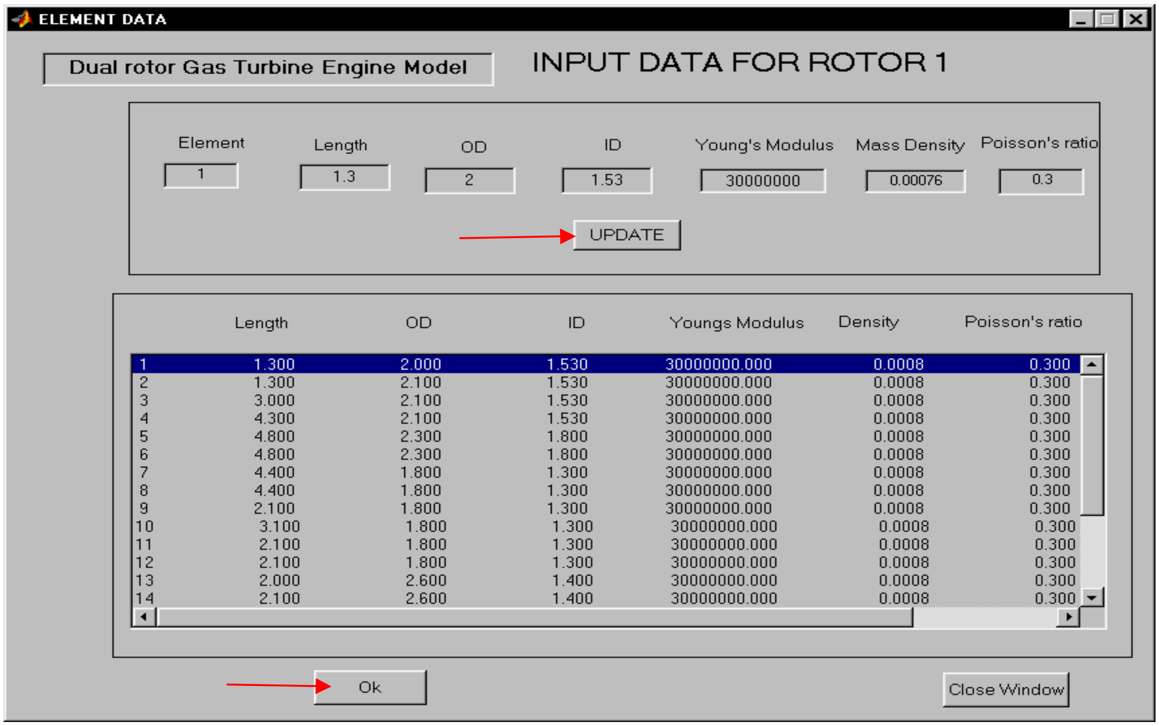

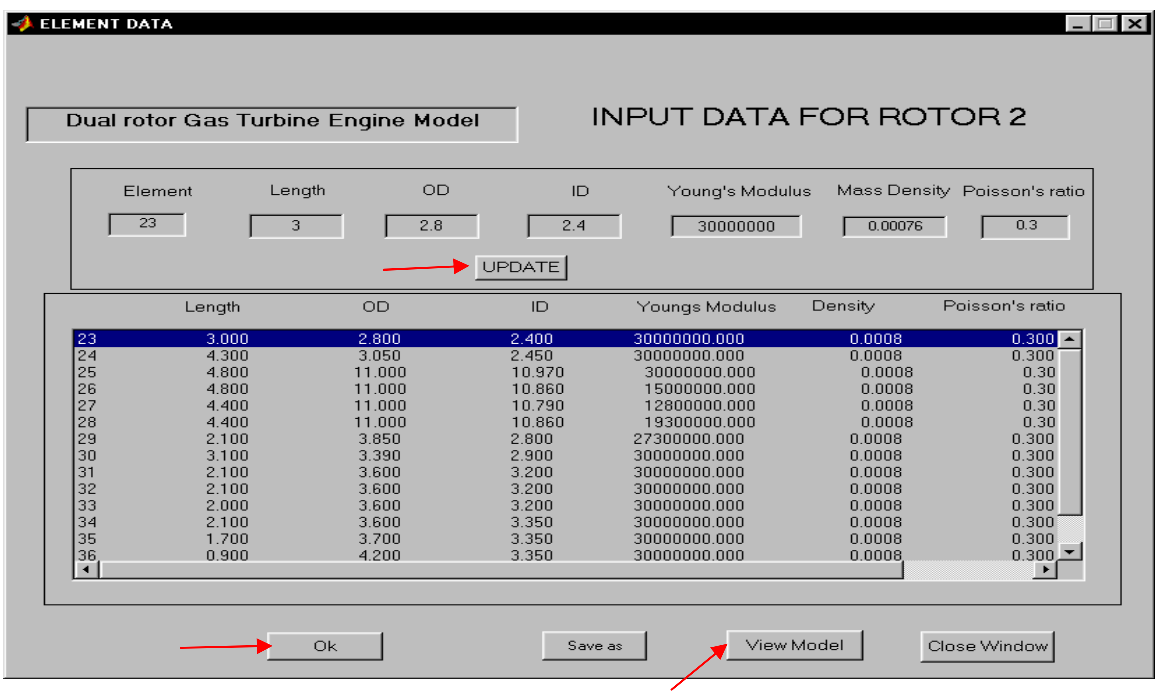

Click on each node shown in the listbox and edit the values in the edit boxes above. After changing each value click on update. Once the Input data is complete, Click on 'View Model ' to view a block diagram of Rotor1 and Rotor2.

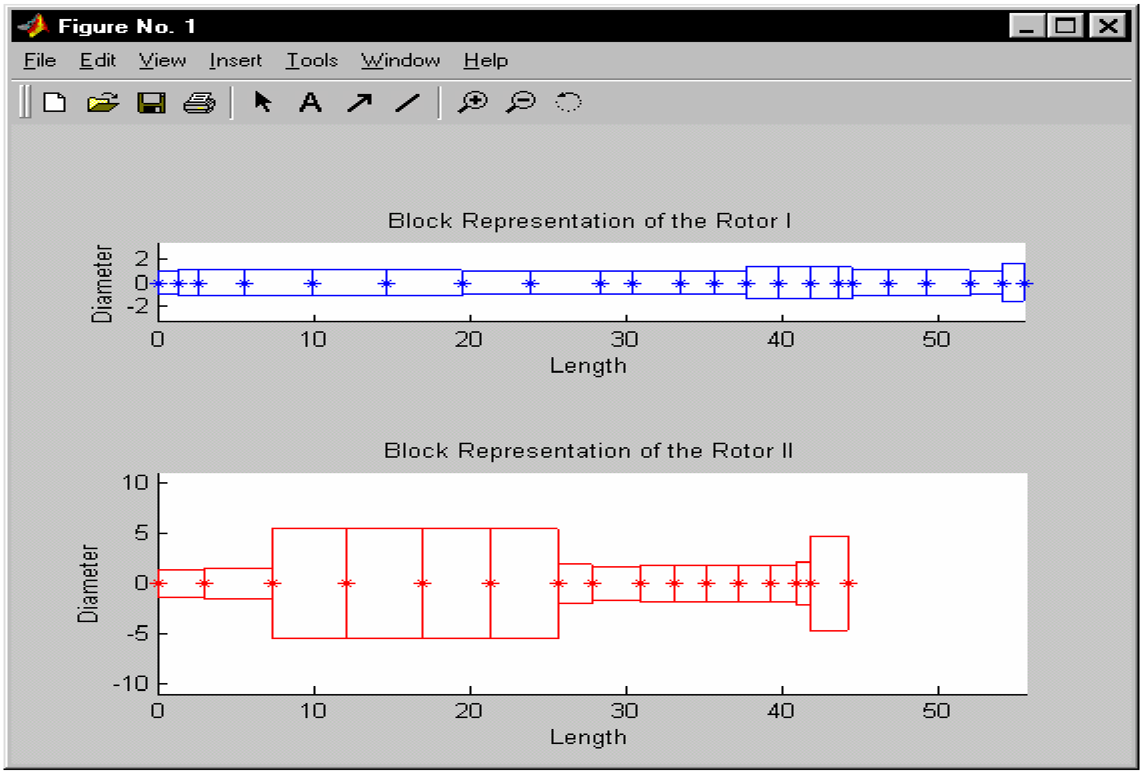

Table 1. Lumped Parameters and cross-sectional properties of the Power Turbine Rotor (Rotor1)

Station No.	Weight (lb)	Length (in)	Shaft dia out	Shaft dia in	I (in^4)	Ip	It	E*10-6
1	0.740	1.3	2.00	1.53	0.52	0.0	0.129	30.0
2	1.539	1.3	2.10	1.53	0.69	0.0	0.297	30.0
3	1.989	3.0	2.10	1.53	0.69	0.0	0.977	30.0
4	1.679	4.3	2.10	1.53	0.69	0.0	2.749	30.0
5	2.082	4.8	2.30	1.80	0.86	0.0	4.623	30.0
6	2.187	4.8	2.30	1.80	0.86	0.0	5.365	30.0
7	1.851	4.4	1.80	1.30	0.38	0.0	4.139	30.0
8	1.516	4.4	1.80	1.30	0.38	0.0	2.913	30.0
9	1.120	2.1	1.80	1.30	0.38	0.0	1.701	30.0
10	0.896	3.1	1.80	1.30	0.38	0.0	0.837	30.0

11	0.896	2.1	1.80	1.30	0.38	0.0	0.837	30.0
12	0.723	2.1	1.80	1.30	0.38	0.0	0.489	30.0
13	1.429	2.0	2.60	1.40	2.05	0.0	1.181	30.0
14	2.187	2.1	2.60	1.40	2.05	0.0	1.959	30.0
15	2.027	1.7	2.60	1.40	2.05	0.0	1.735	30.0
16	1.387	0.9	2.60	1.40	2.05	0.0	1.007	30.0
17	1.173	2.4	2.25	1.57	0.96	0.0	0.953	30.0
18	1.386	2.4	2.25	1.57	0.96	0.0	1.317	30.0
19	26.501	2.8	2.25	1.57	0.96	625.0	314.067	30.0
20	31.028	2.0	1.80	1.50	0.27	704.5	353.257	30.0
21	2.660	1.5	3.30	1.50	5.57	0.0	1.602	30.0
22	1.440	0.0	0.00	0.00	0.00	0.0	1.453	0.0

Table 2. Lumped Parameters and cross – sectional properties of the Gas Generator Rotor (Rotor2)

Station No.	Weight (lb)	Length (in)	Shaft dia outside	Shaft dia inside	I (in^4)	Ip (lb – in^2)	It (lb-in^2)	E*10-6
23	0.693	3.0	2.80	2.40	1.39	0.0	1.110	30.0
24	2.270	4.3	3.05	2.45	2.48	0.0	5.048	30.0
25	9.389	4.8	11.00	10.97	7.81	111.0	65.417	30.0
26	13.514	4.8	11.00	10.86	35.90	297.5	182.243	15.0
27	7.600	4.4	11.00	10.79	53.33	301.5	215.078	12.8
28	11.404	4.4	11.00	10.66	35.90	232.0	177.576	19.3
29	3.126	2.1	3.85	2.80	7.77	117.0	86.170	27.3
30	2.691	3.1	3.39	2.90	3.01	0.0	5.078	30.0
31	1.697	2.1	3.60	3.20	3.10	0.0	3.325	30.0
32	1.270	2.1	3.60	3.20	3.10	0.0	2.307	30.0
33	1.239	2.0	3.60	3.20	3.10	0.0	2.232	30.0
34	1.010	2.1	3.60	3.35	2.08	0.0	1.840	30.0
35	0.872	1.7	3.70	3.35	3.02	0.0	1.600	30.0
36	1.108	0.9	4.20	3.35	9.09	0.0	2.039	30.0
37	27.605	2.4	9.40	9.00	61.19	612.5	329.123	30.0
38	26.963	0.0	0.00	0.00	0.00	600.0	321.721	30.0

Now the input screen for added masses on rotors opens up. Here the user can select the nodes and enter the extra masses.

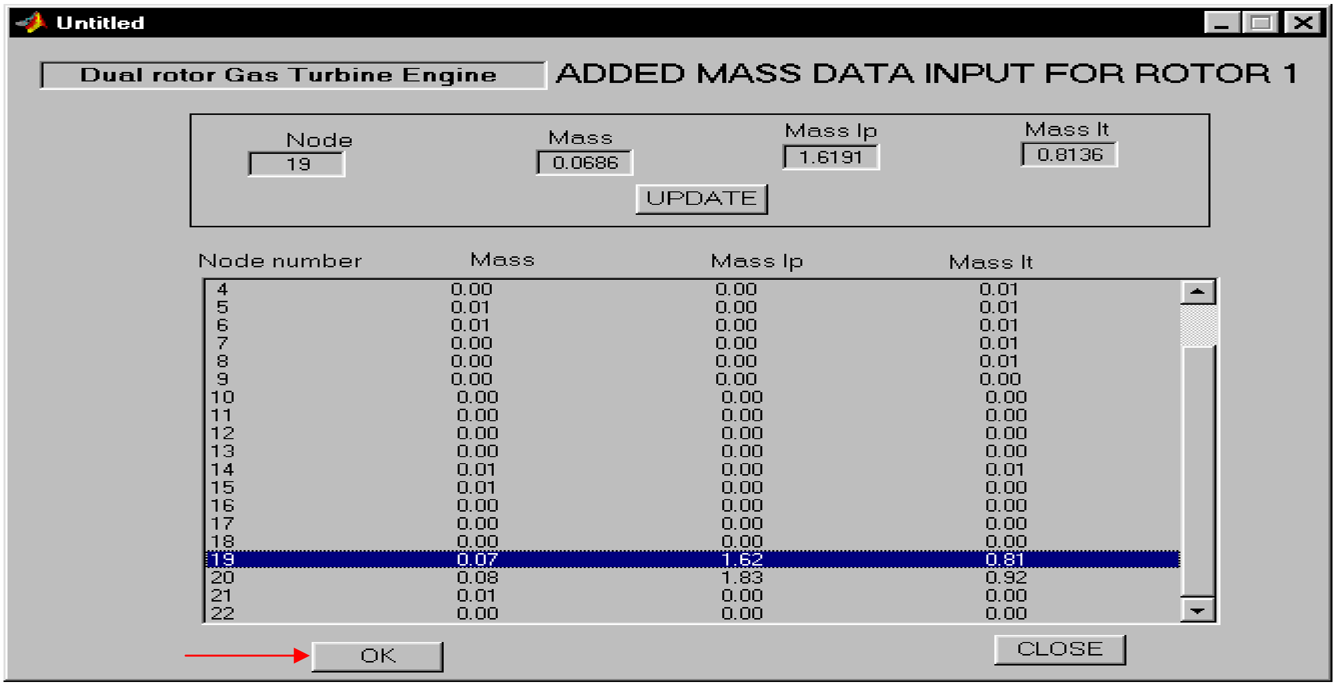

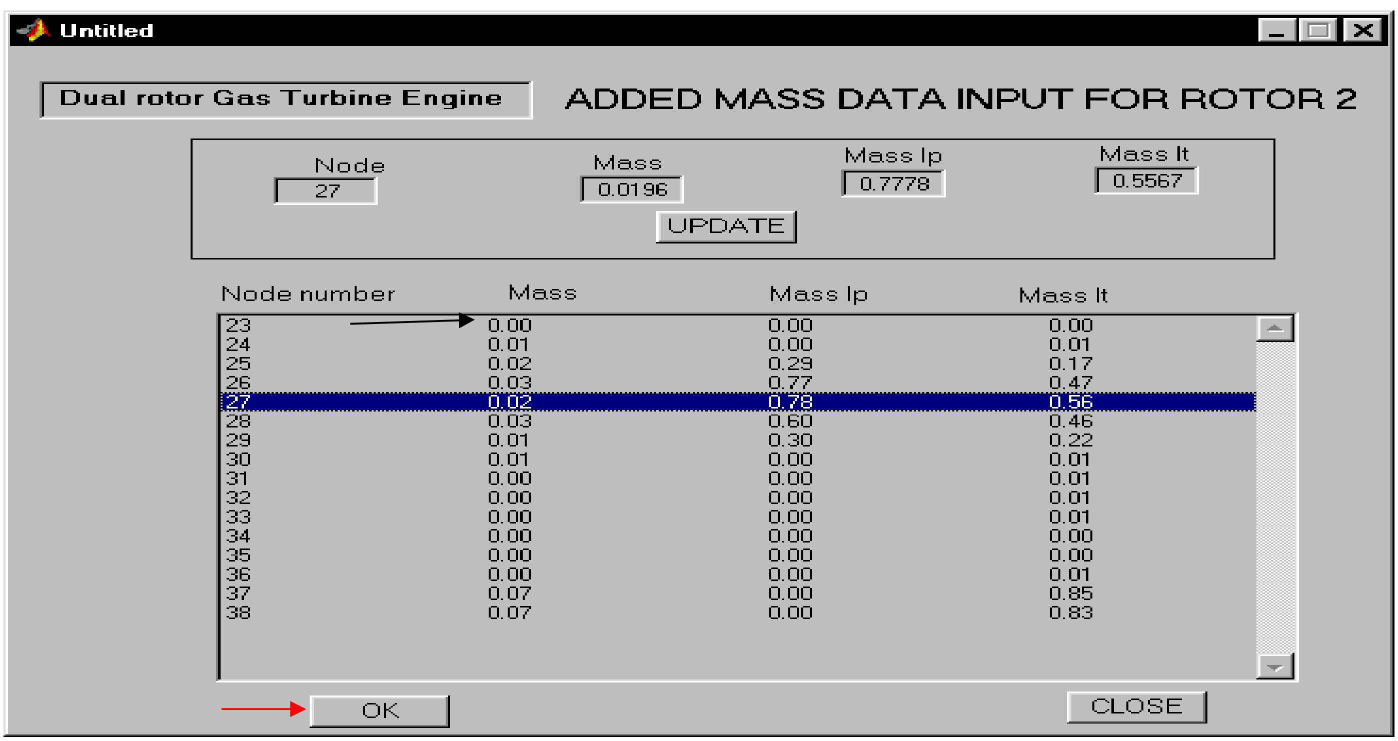

After entering all the input masses for Rotor1 and Rotor 2 Click on 'OK'.

Rotor1 added Mass

Node Number	Mass	Mass Ip	Mass It
19	0	1.6191	0.8136
20	0	1.8251	0.9152

Rotor 2 added Mass

Node Number	Mass	Mass Ip	Mass It
3	0	0.28719	0.16941
4	0	0.76907	0.4719
5	0	0.77788	0.55675
6	0	0.59794	0.45961
7	0	0.30174	0.22305
15	0	0	0.85249
16	0	0	0.83332

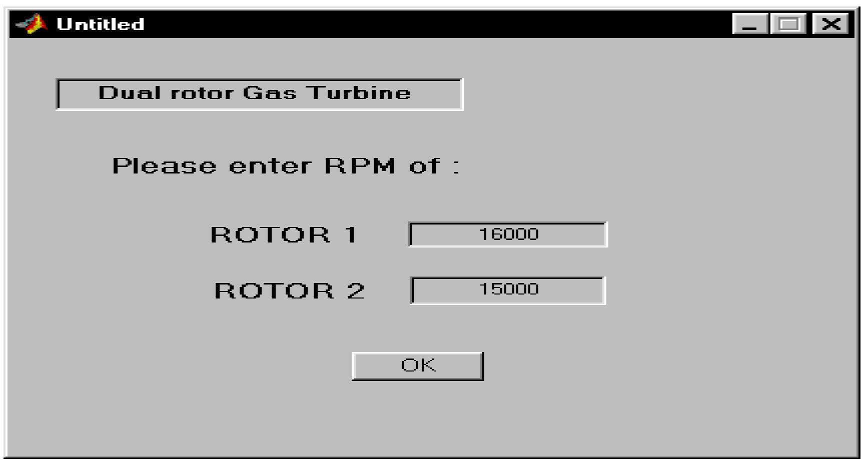

Now enter the RPM for Rotor1 and Rotor2

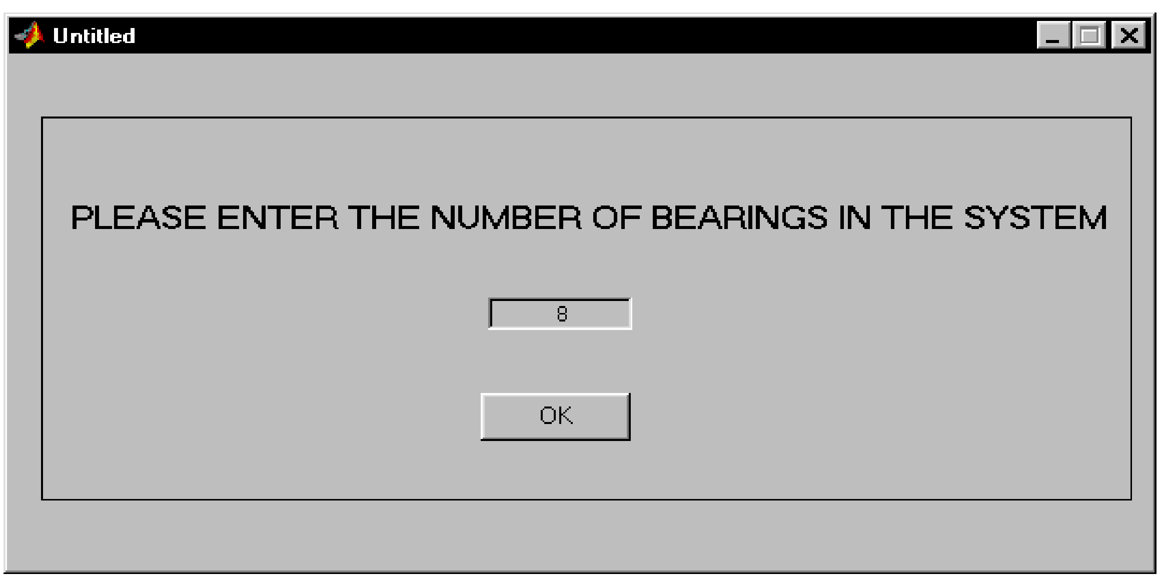

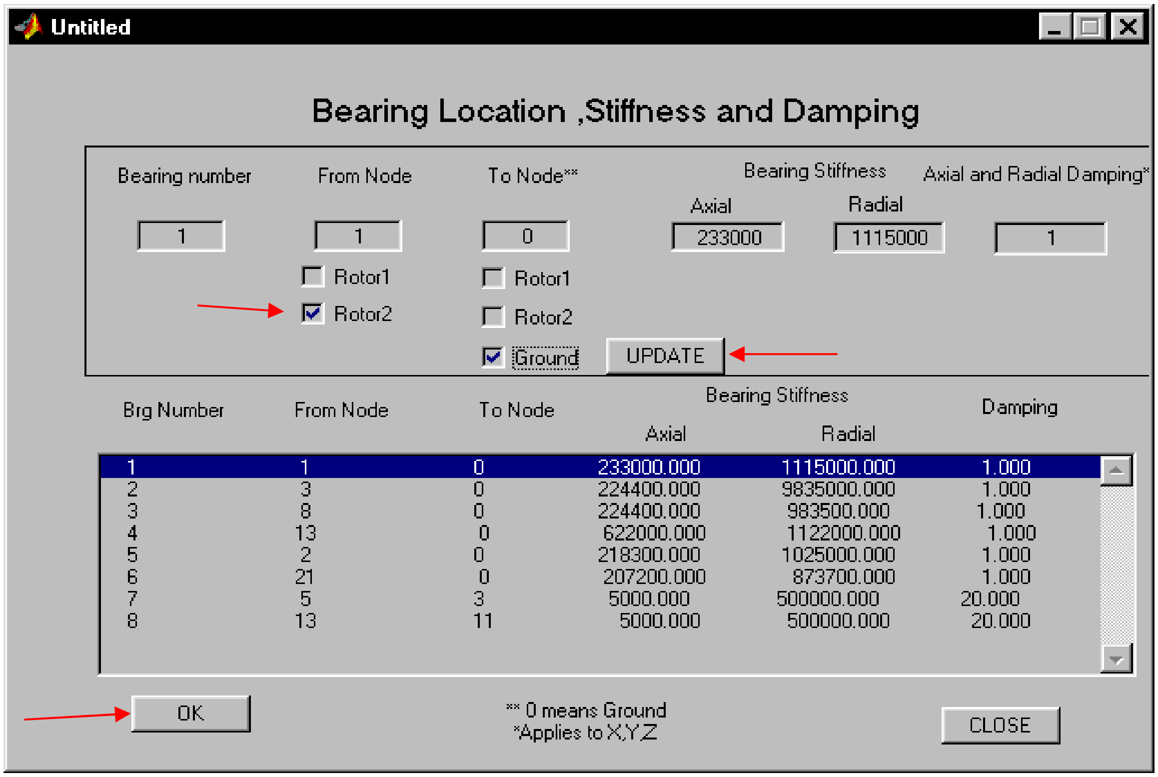

In this panel the User inputs the Bearing Location, Stiffness and Damping. For each bearing the user specifies the from node and a to node. Further the user has to check whether the Node is in Rotor1 or Rotor 2 or the if it is connected to the ground by using the checkboxes. After entering each value Click 'UPDATE'.

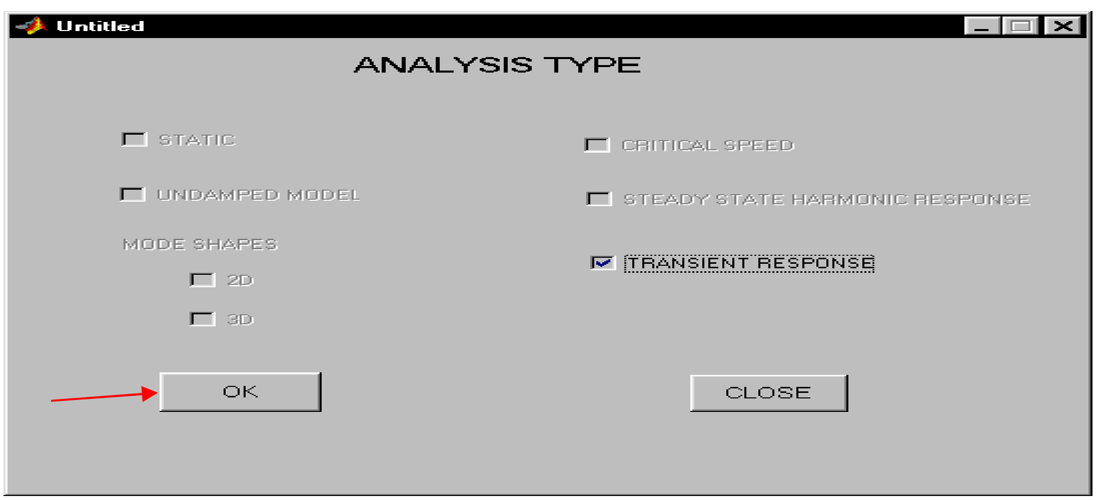

Here the Transient response is selected as the Analysis Type.

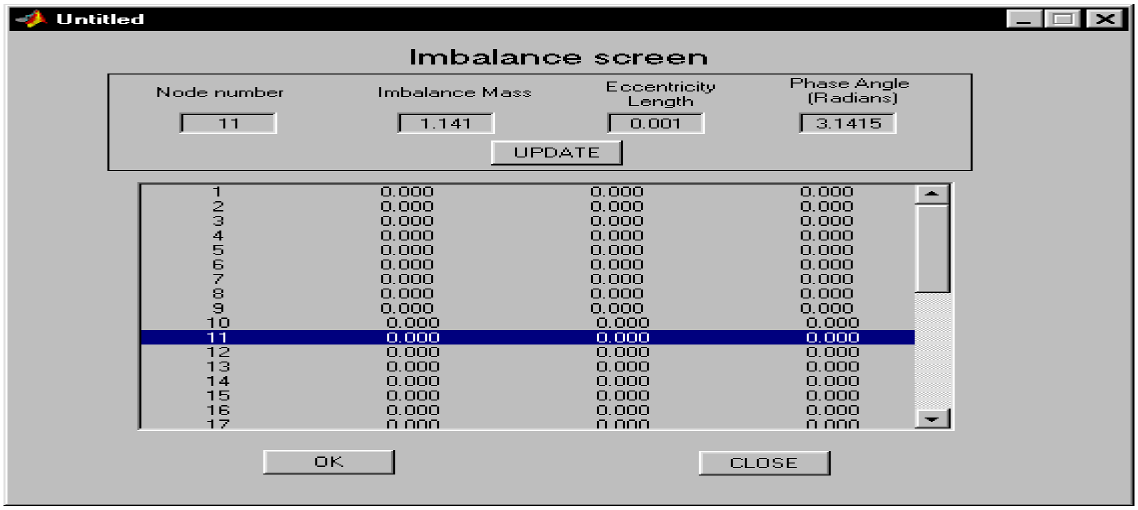

Here the user inputs the unbalance masses at specific nodes. Click on the node number and after entering the values,click on 'UPDATE'.The Imbalance is appied after 0.0375 secs to simulate the Blade loss event.

Node Number	Imbalance Mass	Eccentricity Length	Phase Angle (Radians)
11	1.141	0.001	3.1415
20	1.141	0.001	0

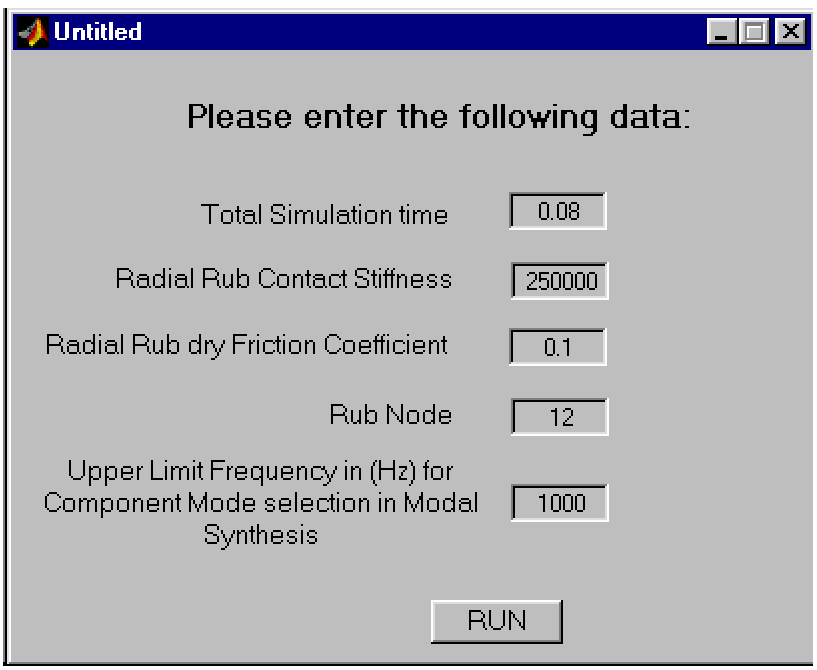

This is the final input screen for the GUI. Enter all the data and click 'RUN' to run The simulation. After the simulation runs,the transient response output screen will show up.Rub can be be implemented only for Rotor1 and a clearance of 0.01” is being used to simulate Rub.

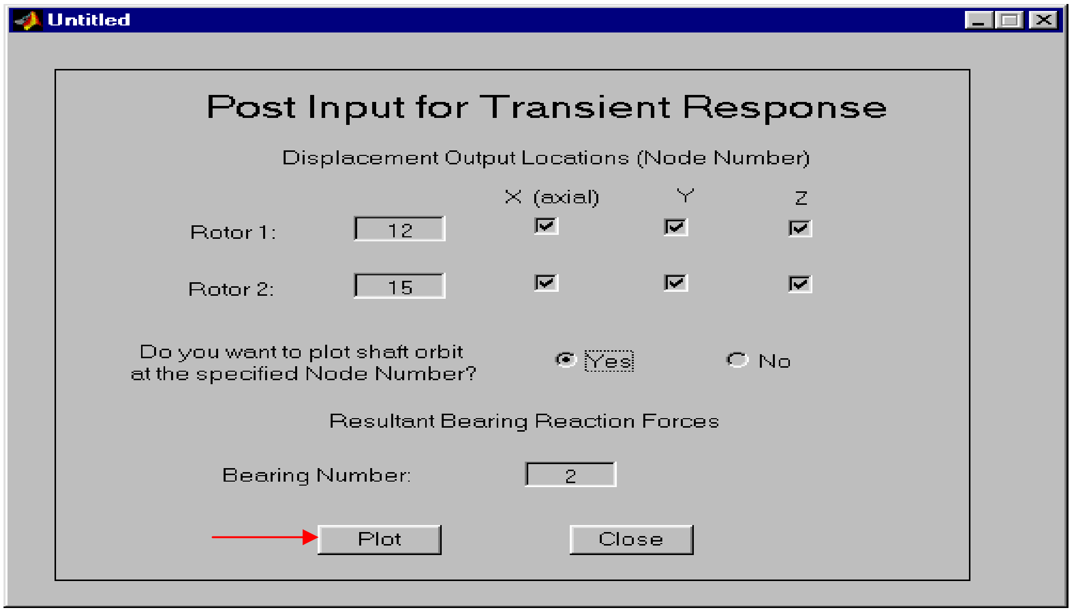

Select the various features in this screen to view the respective output properties of the two rotors and click on 'Plot' .

Output Characteristics

(Displacement of Rotor 1 in X & Y directions)

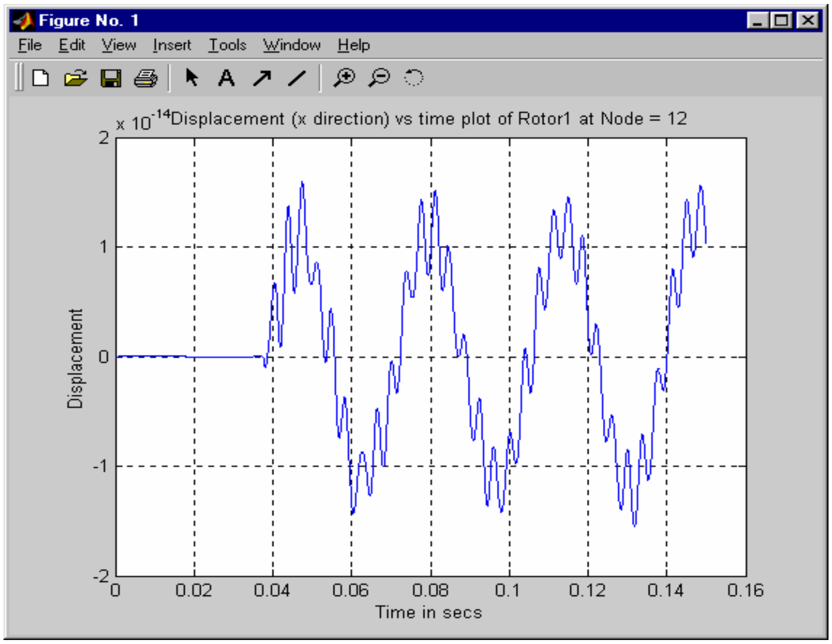

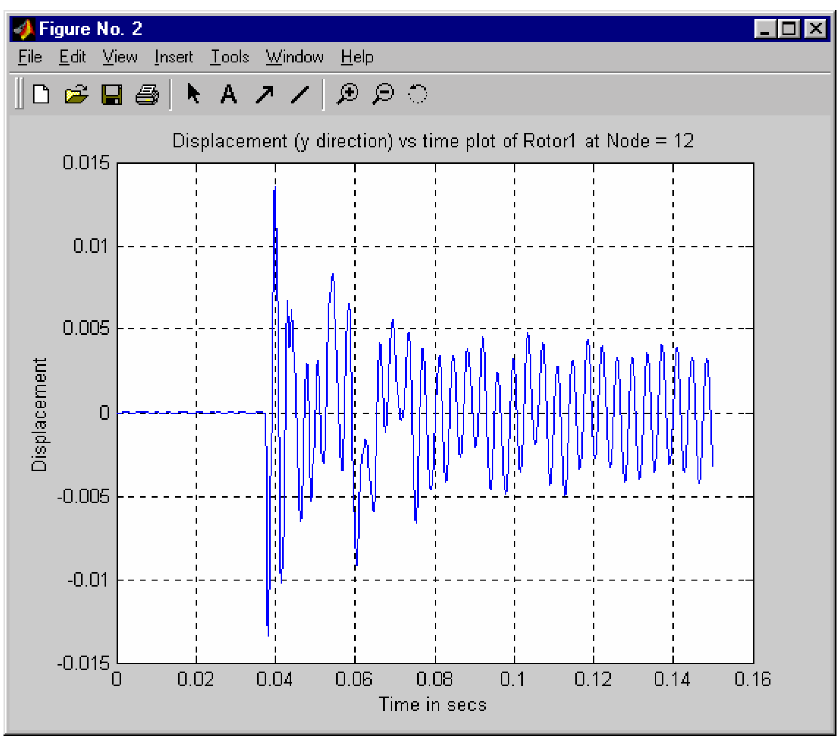

<u>Displacement of Rotor 1 in Z direction & Rotor 2 in X direction</u>

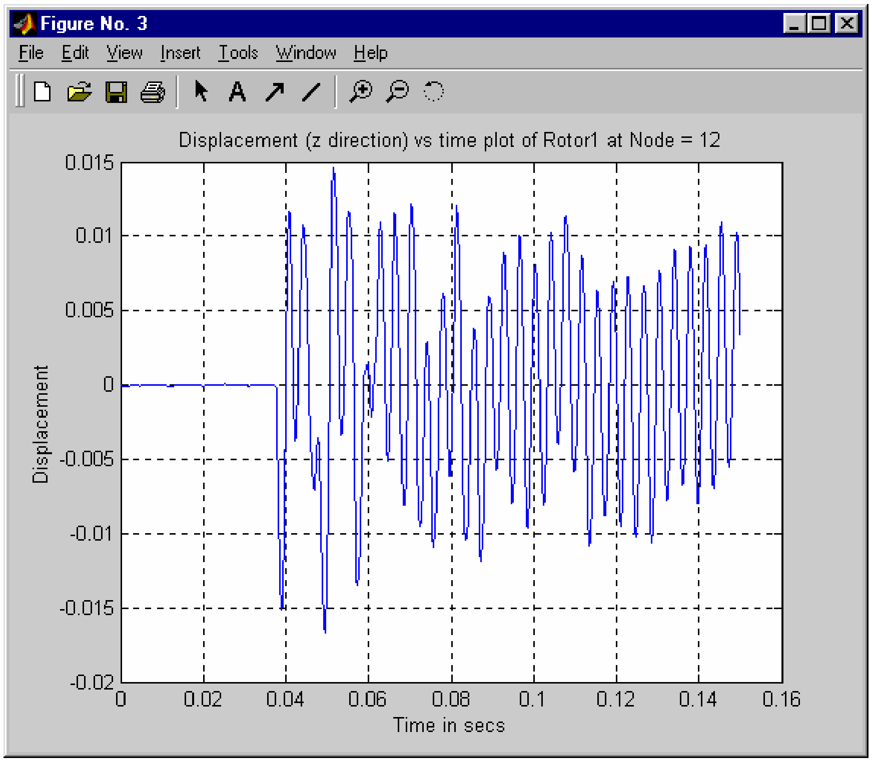

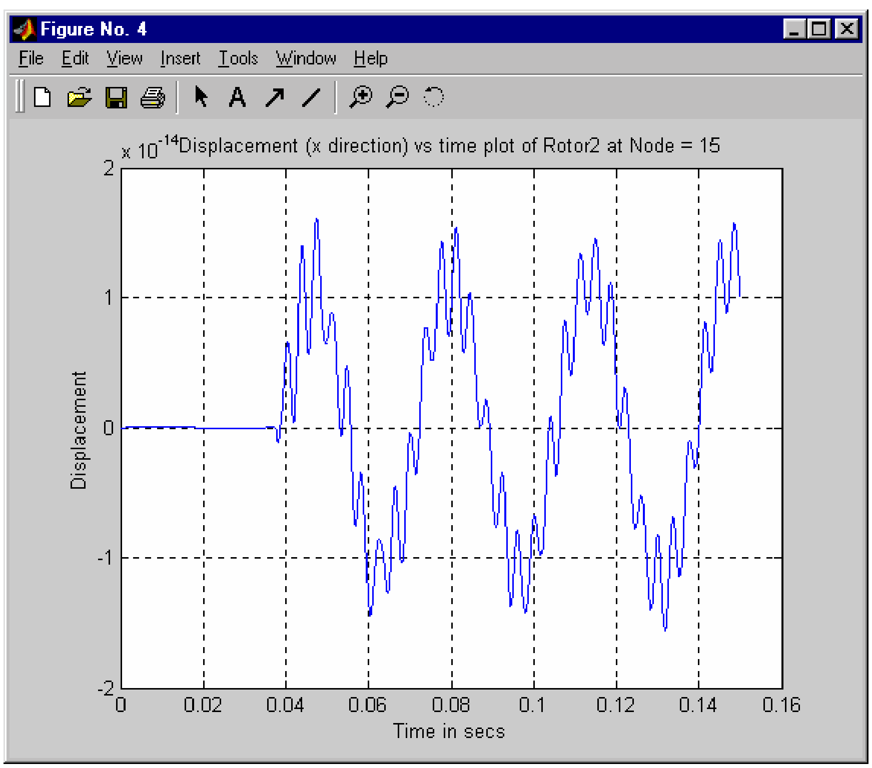

Displacement of Rotor 2 in Y & Z directions

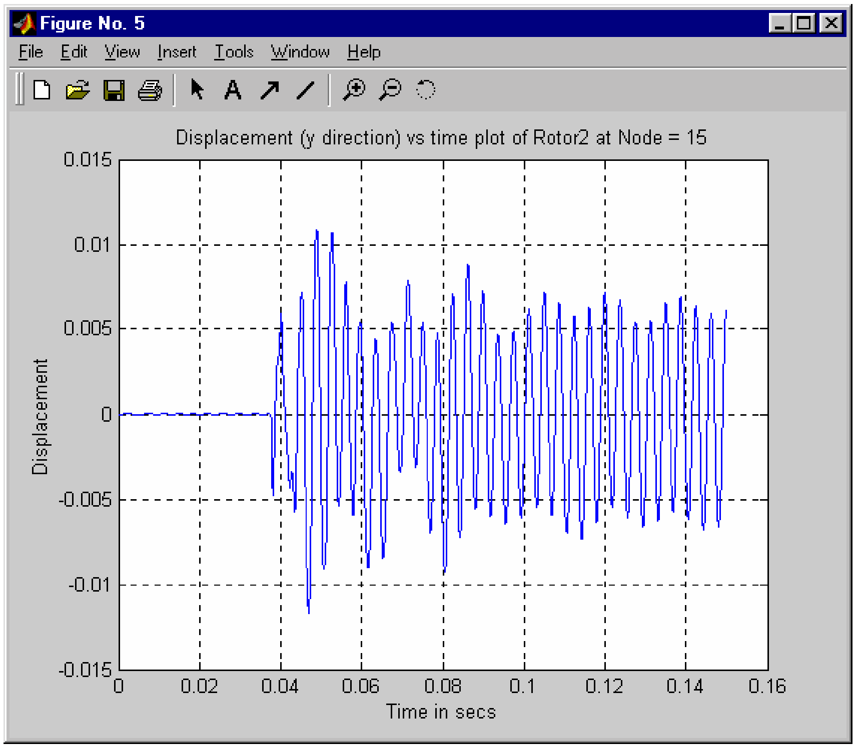

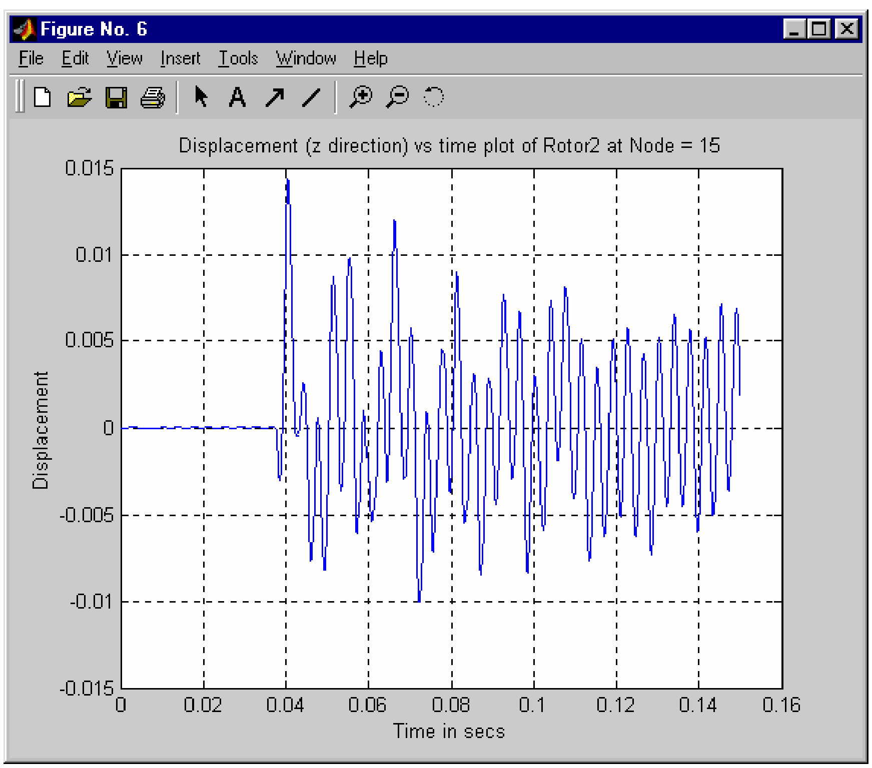

Shaft Orbits of Rotor 1 & 2 at User specified Nodes (3 & 7)

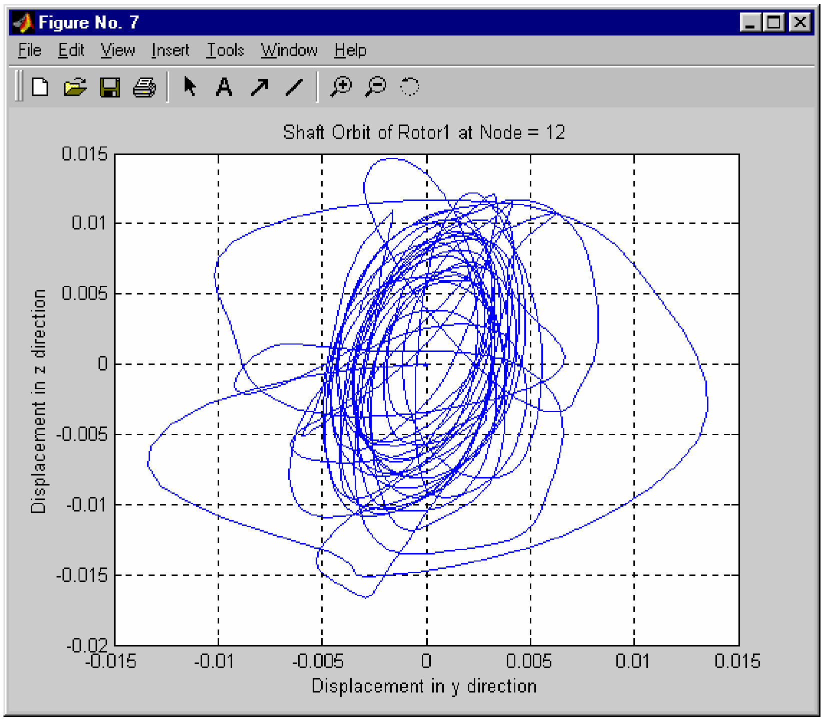

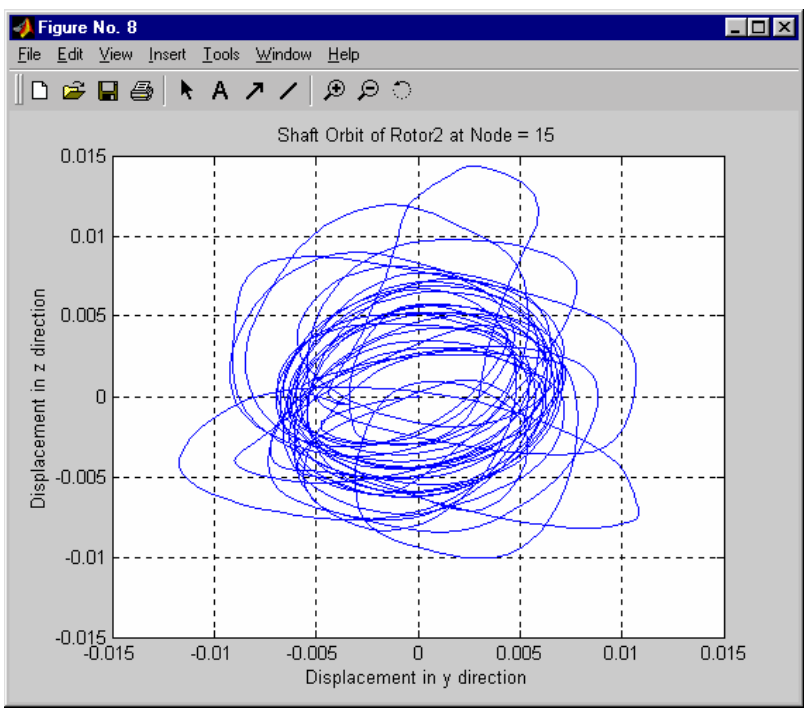

Resultant Bearing Reaction Force at User specified Bearing Number, 2

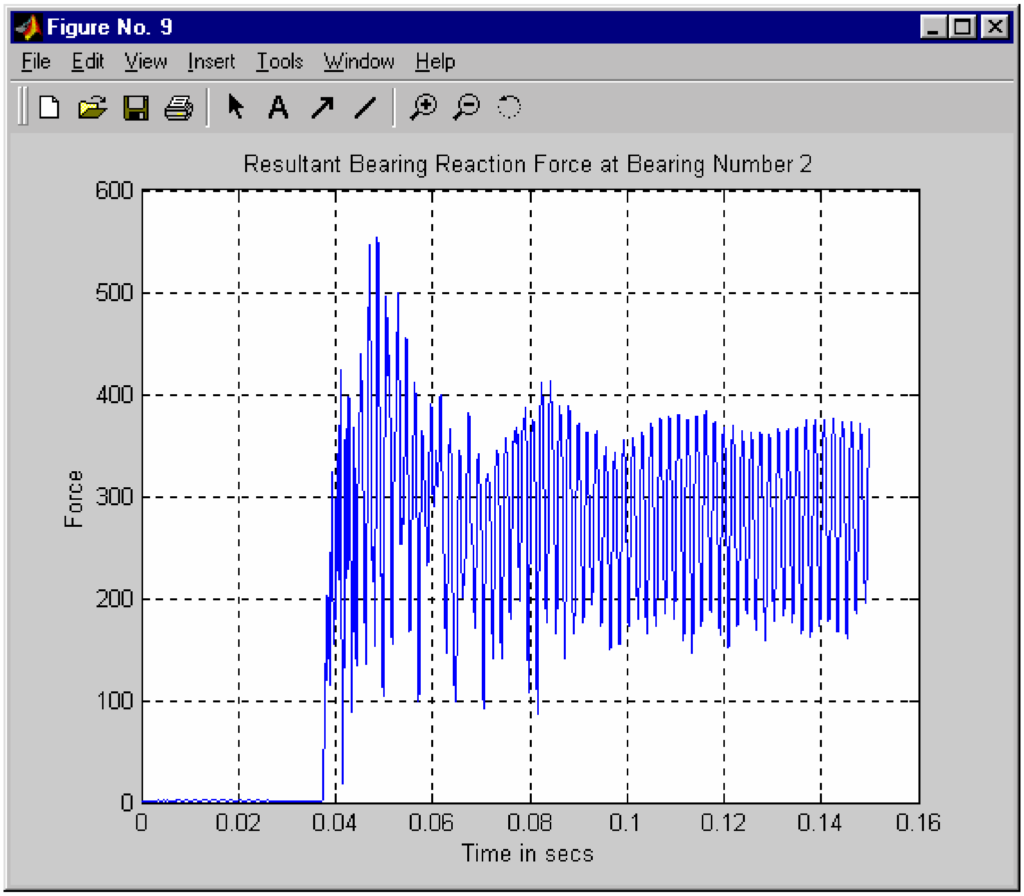

REPORT DOCUMENTATION PAGE

Form Approved
OMB No. 0704-0188

1. AGENCY USE ONLY (*Leave blank*)	2. REPORT DATE	3. REPORT TYPE AND DATES COVERED
	April 2003	Final Contractor Report

4. TITLE AND SUBTITLE

Smart Structural Components and Simulation Tools for Increased Engine Efficiency, Flight Range, and Safety

5. FUNDING NUMBERS

WU–708–87–23–00
NCC3–928

6. AUTHOR(S)

Alan Palazzolo, Guangyoung Sun, Randall Tucker, Nikhil Kaushik, Jason Preuss, Andrew Kenny, Lakshmi Subramaniyam, and Andrew Hunt

7. PERFORMING ORGANIZATION NAME(S) AND ADDRESS(ES)

Texas A&M University
1 Texas A&M University
College Station, Texas 77843

8. PERFORMING ORGANIZATION REPORT NUMBER

E–13809

9. SPONSORING/MONITORING AGENCY NAME(S) AND ADDRESS(ES)

National Aeronautics and Space Administration
Washington, DC 20546–0001

10. SPONSORING/MONITORING AGENCY REPORT NUMBER

NASA CR—2003-212205

11. SUPPLEMENTARY NOTES

Contents were reproduced from author-provided presentation materials. Project Manager, Andrew Provenza, NASA Glenn Research Center, Structures and Acoustics Division, organization code 5930, 216–433–6025.

12a. DISTRIBUTION/AVAILABILITY STATEMENT

Unclassified - Unlimited
Subject Categories: 01 and 07 Distribution: Nonstandard

Available electronically at http://gltrs.grc.nasa.gov

This publication is available from the NASA Center for AeroSpace Information, 301–621–0390.

12b. DISTRIBUTION CODE

13. ABSTRACT ***(Maximum 200 words)***

Summaries of research work for two major topic areas, high temperature magnetic bearings and blade loss mitigation, are presented. Design concepts for a 1000 °F/25000 rpm/1000 lb. force thrust magnetic bearing and accompanying test rig is discussed via detailed Solid Works modeling. Shaft support is supplied by two ball bearings which are flexibly mounted in the axial direction to allow the full force of the magnetic bearing to be applied to a pair of axial load cells. Positioning screws are designed to permit alignment and clearance adjustments for the magnetic bearing. Centrifugally induced stresses are shown to be at acceptable levels with the hyperbolic profile design of the thrust runner. Test results confirm the ability of uniquely designed C cores to withstand a 1000 °F operating environment and to exhibit high (>500V) breakdown voltages. Future work includes completion of the test rig, development of high temperature displacement sensors and catcher bearings, and identification of flight-quality controllers and power amplifiers. Progress in the blade loss mitigation area includes simulations of ball bearing response to high dynamic loading, along with incorporation of a high fidelity bearing model (HFBM) into a flexible shaft, twin-spool gas turbine engine, vibration simulation model. The HFBM includes individual ball dynamics, nonlinear load deflection characteristics plus a squeeze film damper model. A specialized MATLAB code and GUI is provided for obtaining power loss and stiffness of ball bearings. Future work includes efficient simulation capability for an engine model with a HFBM for every bearing and a structural response representation with 300 modes. In addition, the capabilities of magnetic suspensions for mitigating blade loss will also be developed via high fidelity component and large order system simulation.

14. SUBJECT TERMS

Blade loss; Magnetic bearings; High temperature; Vibration sensors

15. NUMBER OF PAGES 334

16. PRICE CODE

17. SECURITY CLASSIFICATION OF REPORT	18. SECURITY CLASSIFICATION OF THIS PAGE	19. SECURITY CLASSIFICATION OF ABSTRACT	20. LIMITATION OF ABSTRACT
Unclassified	Unclassified	Unclassified	